




2020

INVESTIGATION INTO THE ROLES OF HER9 AND CAPN5 DURING RETINAL DEVELOPMENT AND REGENERATION

Cagney Coomer

University of Kentucky, ceco232@g.uky.edu

Author ORCID Identifier:

 <https://orcid.org/0000-0001-5652-1348>

Digital Object Identifier: <https://doi.org/10.13023/etd.2020.477>

[Right click to open a feedback form in a new tab to let us know how this document benefits you.](#)

Recommended Citation

Coomer, Cagney, "INVESTIGATION INTO THE ROLES OF HER9 AND CAPN5 DURING RETINAL DEVELOPMENT AND REGENERATION" (2020). *Theses and Dissertations--Biology*. 69.
https://uknowledge.uky.edu/biology_etds/69

This Doctoral Dissertation is brought to you for free and open access by the Biology at UKnowledge. It has been accepted for inclusion in Theses and Dissertations--Biology by an authorized administrator of UKnowledge. For more information, please contact UKnowledge@lsv.uky.edu.

STUDENT AGREEMENT:

I represent that my thesis or dissertation and abstract are my original work. Proper attribution has been given to all outside sources. I understand that I am solely responsible for obtaining any needed copyright permissions. I have obtained needed written permission statement(s) from the owner(s) of each third-party copyrighted matter to be included in my work, allowing electronic distribution (if such use is not permitted by the fair use doctrine) which will be submitted to UKnowledge as Additional File.

I hereby grant to The University of Kentucky and its agents the irrevocable, non-exclusive, and royalty-free license to archive and make accessible my work in whole or in part in all forms of media, now or hereafter known. I agree that the document mentioned above may be made available immediately for worldwide access unless an embargo applies.

I retain all other ownership rights to the copyright of my work. I also retain the right to use in future works (such as articles or books) all or part of my work. I understand that I am free to register the copyright to my work.

REVIEW, APPROVAL AND ACCEPTANCE

The document mentioned above has been reviewed and accepted by the student's advisor, on behalf of the advisory committee, and by the Director of Graduate Studies (DGS), on behalf of the program; we verify that this is the final, approved version of the student's thesis including all changes required by the advisory committee. The undersigned agree to abide by the statements above.

Cagney Coomer, Student

Dr. Ann C. Morris, Major Professor

Dr. David Weisrock, Director of Graduate Studies

INVESTIGATION INTO THE ROLES OF HER9 AND CAPN5 DURING RETINAL DEVELOPMENT AND
REGENERATION

DISSERTATION

A dissertation submitted in partial fulfillment of the
requirements for the degree of Doctor of Philosophy in the
College of Arts & Sciences
at the University of Kentucky

By
Cagney E. Coomer
Lexington, Kentucky
Director: Dr. Ann C. Morris, Associate Professor of Biology
Lexington, Kentucky
2020

Copyright © Cagney E. Coomer 2020
<https://orcid.org/0000-0001-5652-1348>

ABSTRACT OF DISSERTATION

INVESTIGATION INTO THE ROLES OF HER9 AND CAPN5 DURING RETINAL DEVELOPMENT AND REGENERATION

The formation of a healthy and functioning eye requires coordinated interactions between numerous signaling pathways and gene regulatory networks within the developing neural retina. Tight regulation of gene expression is required for cell specification and differentiation in this multilayered, light sensitive tissue. The photoreceptors are the light detecting cells of the retina, capable of functioning in both intense sunlight and dim light at night. When pigment cells of the photoreceptor outer segment are activated by light, a complex chain of events called phototransduction leads to the electrical signal cascade that is transmitted through the retina and ultimately to the brain to be interpreted as a visual image. Defects in expression of the genes involved in retinal and photoreceptor development have been implicated in many eye diseases, often leading to vision loss. The development, maintenance and function of photoreceptors has been studied in a wide range of model organisms, including the zebrafish. Uniquely, the adult zebrafish is capable of regenerating the photoreceptors and other retinal cells types in response to injury. While immense work has been done to understand the function of genes involved in retinal development, regeneration, and blinding eye diseases, our understanding about many of these genes is still incomplete.

The two genes studied in this dissertation have been either implicated in retinal development, degeneration, or regeneration. Calpain-5 (*capn5*) is a member of a family of calcium-dependent, non-lysosomal cysteine proteases. A mutation in *CAPN5* has been shown to cause autosomal dominant neovascular inflammatory vitreoretinopathy (ADNIV). ADNIV is a devastating inherited autoimmune disease of the eye that displays features commonly seen in other eye diseases, such as retinitis pigmentosa and diabetic retinopathy, and ultimately results in retinal degeneration and blindness. When activated by influxes of calcium, calpains can either degrade their protein substrates or modify the activity of their targets through proteolytic processing. Although *capn5* has been extensively studied in the brain, very little is known about its role during retinal development or in the adult eye. The second gene of interest is Hairy-related (Her) factor Her9, a member of the Hairy/Enhancer of Split (Hes) superfamily of genes. Her9 is a basic-helix-loop-helix-orange (bHLH-O) transcription factor. Her factors have been previously shown to play roles in neural tube closure, floor plate development, and development of various components of the central nervous system as well as the cranial sensory placodes. However, the role of *her9* in retinal development and regeneration is still poorly understood.

Chapter 1 of this dissertation is an overview of retinal development, with an emphasis on photoreceptor development, retinal degenerative diseases, regeneration, and the known roles of *capn5* and *her9* in other tissues. Chapter 2 characterizes the expression of *capn5* during development and the adult retina. Using acute light damage and a zebrafish model for chronic rod degeneration and regeneration, this study provides evidence that *capn5* has a role in photoreceptor maintenance, survival, and regeneration. Chapter 3 characterizes the expression of *her9* during retinal development and uses a combination of molecular and behavioral experiments to characterize the retinal phenotypes present in a *her9* CRISPR/Cas9 knockout. The data presented in this chapter demonstrate that Her9 plays a role in photoreceptor differentiation, maintenance and survival. Chapter 4 examines other phenotypes present in the *her9* knockout. Craniofacial, pigment, and gut defects provide supporting evidence that Her9 is required for the differentiation and survival of neural crest cell lineages. Chapter 5 is a discussion of the conclusions we can draw from these studies, potential future directions for this work, and how these results impact our broader understanding of retinal development and regeneration.

KEYWORDS: zebrafish, Capn5, Her9, retina, development, photoreceptors

Cagney E. Coomer

(Name of Student)

07/17/20

Date

INVESTIGATION INTO THE ROLES OF HER9 AND CAPN5 DURING RETINAL DEVELOPMENT AND
REGENERATION

By
Cagney E. Coomer

Ann C. Morris

Director of Dissertation

David Weisrock

Director of Graduate Studies

07/17/20

Date

DEDICATION

To Mariya Elayna Slaughter

Pinky Promise

ACKNOWLEDGMENTS

I would like to start by expressing my gratitude to my committee, without their guidance I would not have made it to the finish line. To Dr. Harrison, whose developmental biology and advanced genetic classes laid the foundation for the understanding needed to pursue this degree, for always being available to assist me on the microscopes, and for the recommendations and support throughout this journey. To Dr. Falmulski, for first introducing me to confocal microscopy, for taking time to work with me as I learned to use the microscopes in his lab, for making all of his fish lines available for this project and for always asking questions that force me to think outside what is right in my face. To Dr. Geddes, for making all of his resources available for use and for always being available to answer questions and provide suggestions. Their support and assistance have been invaluable to my success.

Next, I would like to thank my advisor, Dr. Ann Morris. When I came to graduate school I would not have defined myself as a scientist, far more than just a lack of confidence. Dr. Morris started by helping me gain the tools necessary to think like a scientist, she gave me the opportunities to make mistakes and learn like a scientist and then held up a mirror to remind me that I was always a scientist. Thank you for taking the time to see me because you helped me see myself. For the celebrations during times of victory and success as well as the empathy during hard times. This journey has not only helped me grow and develop as a scientist but also as a person. Thank you for holding my hand (wink), we made a good team.

To my lab mates, my sisters in science, I could not imagine this journey without each of you. Whether it's my early morning and weekend laughs and conversation with Laura Krueger or my Starbucks runs and microscopy dates with Becky Petersen or dance parties and random concerts with Jessica Bills, you ladies made my day to day life in the lab so full. Thank you for matching my loud with your loud and every hug in the moment, I love each of you. To Lucas

Vieira-Francisco, thank you so much for taking amazing care of our zebrafish. I cannot explain the peace of mind that you brought to each work day. Knowing I could trust my precious fish in your care is something I definitely did not take for granted. Over the years I have had the privilege to mentor many students in the lab and in the classroom. I just wanted to take the time to thank each one of them for the commitment to the work, dedication and time. I am grateful for all the lessons I have learned along this journey with you.

To Kayla Titalii-Torres, yes I had to make a separate paragraph for you. Thank you for being my sister, for teaching me how to talk science in social settings, for being my sounding board, for coming to my house and not being afraid, for showing up, for being a part of NERD SQUAD and for always bringing me snacks. Most importantly, thank you for seeing me without hesitation, without prompting and for always showing me unwavering love and support. I am truly grateful to have shared this journey with you.

#WEGOTUS

This hashtag embodies the sentiment of the village I've built along this journey. I am eternally grateful for the love and support I have received from my village. To Carol Taylor-Shim, Lisa Higgins-Hord and Dr. John Parker, thank you for being anchors of support on this campus. For opening your offices as safe spaces, for showing up and being friendly faces in the crowd, for love and lessons. To Tanya Torp, Sharon Murphy and Tiffany El-Amin, thank you for being my sisters, for always showing up for me and for never missing a moment to remind me who I am. To my NTOO sisters, thank you for always supporting me, for speaking my name at tables and helping me grow. Shelisha, thank you for pushing me and promising to catch me, I will forever be grateful.

To my squad (past, present and future), thank you for allowing me to be your role model, for forcing me to step into my own light and practice what I preach. Thank you for believing in me because you forced me to believe in myself. To my squad parents, Thank you for giving me the opportunity to water your gardens, for believing in my vision and for trusting me. To my Elayna, let this be evidence that anything you want you can have. That you are capable of all things and that where we start does not define the story we decide to write.

To my family, without you who am I? To my sisters (Ree Ree, Larik, Nashayia, Bianca, and Serenity), your support and love is everything. Thank you for being ready to turn up for every milestone, for keeping me grounded and focused, thank you for being the first to look up to me, to believe in me. To my brothers, thank you for being the rational voices, for the strong love and unwavering support. To my aunts and uncles thank you for the support as well. To my parents, it's easy to follow your dreams when your safety net is so solid. To my daddy, thank you for everything, for the pep talks that have gotten me through every milestone in the journey. Thank you for always being the light house when I feel like I've lost my way, for never letting me lose sight of goals and for always reminding me that my first name is Cagney and my last name is Coomer; I love you dearly. To my mother, thank you for being all the empathy and compassion a girl could ever need, for listening to me cry and then reminding me that I am human. Thank you for always lifting my chin; I love you dearly. To my partner, I love you so much. Thank you for creating space for me to accomplish this goal, for loving me, feeding me, and pretty much waiting on me hand and foot while I wrote.

I would like to thank the administrative staff in the Department of Biology; your assistance during every phase of this journey has been greatly appreciated. I also would like to

thank Devin Klaserner for all his assistance during my time as a TA, you were definitely an irreplaceable asset.

Finally, I would like to thank the Department of Biology for their support throughout the years. I am also grateful to have received travel fellowships for NEURAL, the Gordon Conference, and SDB. Financial support provided to Dr. Ann Morris from the National Eye Institute (NIH/R01) and the Lyman T. Johnson fellowship funded the research presented in this dissertation.

TABLE OF CONTENTS

<i>ACKNOWLEDGMENTS</i>	<i>iii</i>
<i>LIST OF TABLES</i>	<i>xi</i>
<i>LIST OF FIGURES</i>	<i>xii</i>
CHAPTER 1. Retinal development, Regeneration, capn5 and her9	1
1.1 Introduction	1
1.2 Vertebrate retinal development	4
1.3 General photoreceptor development	7
1.4 Rod photoreceptors	10
1.5 Cone Photoreceptors.....	12
1.6 Zebrafish as a model organism	14
1.7 Using zebrafish to study retinal degeneration/regeneration	18
1.8 Calpain-5	20
1.9 Hairy-related 9	26
1.10 Specific Aims	30
CHAPTER 2. Capn5 expression in the healthy and regenerating retina	31
2.1 Abstract.....	31
2.2 Introduction	32
2.3 Materials and methods.....	34
2.3.1 Zebrafish lines and maintenance	34
2.3.2 RNA extraction, RT-PCR and Real-time quantitative PCR (qPCR).....	35
2.3.3 Tissue sectioning	35
2.3.4 Riboprobe synthesis	36
2.3.5 Fluorescent in situ hybridization (FISH).....	36
2.3.6 Whole-mount in situ hybridization	37
2.3.7 Immunohistochemistry	37
2.3.8 Light damage experiment.....	37
2.3.9 Quantification and statistical analysis	38
2.4 Results.....	38
2.4.1 Developmental expression of zebrafish capn5 orthologs	38
2.4.2 Capn5 expression is cone specific in the adult zebrafish retina	42
2.4.3 Capn5a expression is increased in response to rod photoreceptor degeneration..	45
2.4.4 Capn5 expression increases in response to acute light damage	46

2.4.5	Expression levels of <i>Capn5</i> correlates with the extent of photoreceptor degeneration	49
2.4.6	Photoreceptor degeneration induces the expression of <i>capn5</i> in the Müller Glia..	51
2.5	Discussion	53
2.6	Chapter 2 tables	57
2.7	Supplemental Figures	59
CHAPTER 3. <i>Her9/Hes4</i> is required for photoreceptor development, maintenance and survival		
60		
3.1	Abstract.....	60
3.2	Introduction	61
3.3	Materials and methods.....	63
3.3.1	Zebrafish line maintenance	63
3.3.2	Generation of <i>her9</i> mutant zebrafish by CRISPR/Cas9.....	64
3.3.3	Restriction fragment length polymorphism (RFLP).....	65
3.3.4	mRNA synthesis and microinjection.....	65
3.3.5	Western blot	65
3.3.6	RNA isolation and riboprobe synthesis	66
3.3.7	RT-PCR and real-time quantitative RT-PCR (qPCR)	66
3.3.8	Visually mediated background adaptation assay (VBA)	67
3.3.9	Optokinetic Response assay (OKR).....	67
3.3.10	Mobility assay	67
3.3.11	Whole-mount and fluorescent in situ hybridization	68
3.3.12	Immunohistochemistry	68
3.3.13	TUNEL staining.....	69
3.3.14	RA treatment	69
3.3.15	Cell counts	70
3.3.16	Statistical analysis	70
3.4	Results.....	71
3.4.1	<i>Her9</i> expression during retinal development.....	71
3.4.2	Generation of <i>her9</i> mutant using CRISPR/Cas9	72
3.4.3	Characterization of <i>her9</i> mutant phenotype	74
3.4.4	<i>Her9</i> mutants lack a visual mediated adaption response and display visual dysfunction.....	76
3.4.5	<i>Her9</i> mutants display a decrease in rod photoreceptors and rod outer segment defects 78	
3.4.6	Cone outer segments are truncated in <i>her9</i> mutants.....	80
3.4.7	<i>Her9</i> mutants display cone subtype-specific phenotypes.....	82
3.4.8	Müller Glia abnormalities in <i>her9</i> mutants.....	84
3.4.9	Loss of <i>Her9</i> has minimal effects on other retinal cell types.....	84
3.4.10	Loss of <i>Her9</i> causes a progressive collapse of the CMZ	87
3.4.11	<i>Her9</i> mutants display abnormal expression of photoreceptor lineage genes	88

3.4.12	Her9 mutant photoreceptors undergo apoptosis.....	91
3.4.13	RA regulates <i>her9</i> expression in the retina but Her9 is not required for RA's effects on opsin expression.....	93
3.5	Discussion	95
3.6	Supplemental Tables	99
3.7	Supplemental figures.....	101
CHAPTER 4. Loss of <i>her9</i> disrupts neural crest cell migration, differentiation and survival..		109
4.1	Abstract.....	109
4.2	Introduction	109
4.3	Materials and methods.....	116
4.3.1	Zebrafish line maintenance	116
4.3.2	Generation of <i>her9</i> mutant zebrafish by CRISPR	117
4.3.3	Genomic DNA (gDNA) extraction and amplification	117
4.3.4	Restriction fragment length polymorphism (RFLP).....	117
4.3.5	RT-PCR and real-time quantitative RT-PCR (qPCR)	118
4.3.6	Immunohistochemistry	119
4.3.7	TUNEL staining	120
4.3.8	H & E staining.....	120
4.3.9	Alcian blue staining	120
4.3.10	Feeding assay.....	121
4.3.11	Statistical analysis	121
4.4	Results.....	121
4.4.1	Her9 mutants display craniofacial defects	121
4.4.2	Loss of Her9 causes a decrease in <i>sox10</i> expression and morphological defects in components of the viserocranium.....	124
4.4.3	Loss of Her9 results in defective segmentation of the branchial arches and an undeveloped ethmoid plate.....	126
4.4.4	Her9 mutants display pigment defects	127
4.4.5	Loss of Her9 results in the increase of xanthophores at the expense of melanophores and iridophores	130
4.4.6	Her9 mutants display morphological defects in the gut	132
4.4.7	Her9 mutants display decreased feeding habits and abnormal gut function	133
4.4.8	Her9 is required for the migration of NCCs into the gut and loss of Her9 results in improper differentiation of the glia and neurons	135
4.4.9	The loss of Her9 has minimal effects on dorsal root ganglia development	137
4.4.10	The loss Her9 during zebrafish development leads to a decrease in Foxd3-positive cells	139
4.4.11	Her9 mutants have an altered <i>Bmp</i> gene expression during significant phases of NCC development.....	141
4.4.12	Loss of Her9 function leads to CNCC and VNCC cell death.....	143
4.5	Discussion	144

4.5.1	Her9/Hes4 during early NCC development	144
4.5.2	Her9 is necessary for the migration and differentiation of NCC lineages	146
4.5.3	Her9 and NCC survival	148
4.5.4	Conclusion.....	149
<i>CHAPTER 5. Capn5 and her9 in the developing and regenerating retina.....</i>		<i>151</i>
5.1	Summary and Discussion	151
5.2	Calpain-5	152
5.3	Hairy-related 9	156
5.4	Conclusion.....	162
<i>APPENDICES.....</i>		<i>164</i>
APPENDIX 1. Progress towards generating a zebrafish Capn5 mutant using CRISPR/Cas9 ..		164
A1.	Introduction	164
A.1.2	Materials and methods.....	168
A.1.2.1	Zebrafish line maintenance.....	168
A.1.2.2	RNA extraction and RT-PCR	168
A.1.2.3	Generation of guide RNA oligonucleotides and Cas9.....	169
<i>REFERENCES.....</i>		<i>176</i>
<i>VITA.....</i>		<i>199</i>

LIST OF TABLES

Table 1. 1 Calpain genes.....	22
Table 1. 2 bHLH-O transcription factors.....	27
Table 2. 1 Primer sequences.....	57
Table 2. 2 IHC antibodies.....	58
Table S3.1 Primer sequences.....	99
Table S3.2 Oligo sequences.....	100
Table 4. 1 Neurocristopathies and implicated genes.....	115
Table 4. 2 Neural crest qPCR primers.....	118

LIST OF FIGURES

Figure 1. 1 Retinal structure and cellular components	3
Figure 1. 2 The order of differentiation of retinal cell types	6
Figure 1. 3 Zebrafish PR mosaic composition and PR structure	9
Figure 1. 4 Model of PR specification	12
Figure 1. 5 The significance of Zf as a model organism.....	16
Figure 1. 6 CAPN5 proteins, ADNIV mutations and the disease stages	25
Figure 1. 7 The zebrafish bHLH-O proteins.....	28
Figure 2. 1 <i>capn5a</i> and <i>capn5b</i> are expressed in the developing CNS of the zebrafish	40
Figure 2. 2 Capn5 is expressed in differentiated PR of the larval zebrafish retina	41
Figure 2. 3 Capn5 is expressed specifically in the cone PR of the adult zebrafish retina.....	44
Figure 2. 4 Expression of Capn5 is elevated in the adult XOPS:mCFP retina.....	45
Figure 2. 5 Capn5a expression is induced in response to acute light damage	48
Figure 2. 6 Increase in Capn5 expression correlates with the magnitude of retinal damage	50
Figure 2. 7 <i>Capn5a</i> is expressed in the Müller Glia in response to acute light damage.....	52
Figure 3. 1 <i>Her9</i> expression in the developing retina	72
Figure 3. 2 <i>Her9</i> mutant phenotype.....	73
Figure 3. 3 <i>Her9</i> mutants lack a VBA response and display abnormal visual behavior (OKR).....	75
Figure 3. 4 <i>Her9</i> mutants have fewer rods with shorter outer segments.....	77
Figure 3. 5 Cone outer segments are truncated in <i>her9</i> mutants.....	79
Figure 3. 6 <i>Her9</i> mutants display cone subtype-specific phenotypes.....	81
Figure 3. 7 Loss of <i>Her9</i> causes a decrease in Müller Glia number and distorts their organization	83
Figure 3. 8 Loss of <i>Her9</i> minimal effects on other retinal cell types.....	86
Figure 3. 9 CMZ defects in <i>her9</i> mutants	88
Figure 3. 10 <i>Her9</i> mutants display abnormal expression of PR lineage genes.....	90
Figure 3. 11 <i>Her9</i> mutant retinas display increased apoptosis beginning at 72 hpf.....	92
Figure 3. 12 RA regulates <i>her9</i> expression but <i>Her9</i> is not required for the effects of RA on opsin expression.....	94

Figure 4. 1 Diagram of the known NCC gene regulatory network	113
Figure 4. 2 Her9 mutants lack a swim bladder and display craniofacial defects	123
Figure 4. 3 Loss of Her9 causes a decrease in sox10 expression and morphological defects in components of the viscerocranium	125
Figure 4. 4 Loss of Her9 results in defective segmentation and an under-developed ethmoid plate	127
Figure 4. 5 Her9 mutants display pigmentation defects	129
Figure 4. 6 Loss of Her9 results in increased numbers of xanthophores at the expense of melanophores and Iridophores	131
Figure 4. 7 Her9 mutants display morphological defects in the gut	132
Figure 4. 8 Her9 mutants display decreased feeding habits and abnormal gut function	134
Figure 4. 9 Her9 is required for the proper migration and differentiation of NCC in the gut	136
Figure 4. 10 Loss of Her9 has minimal effect of DRG development	138
Figure 4. 11 Loss of Her9 leads to decreased <i>foxd3</i> expression	140
Figure 4. 12 Her9 mutants have increased Bmp ligand expression during migration and differentiation of NCC	142
Figure 4. 13 The Loss of Her9 causes the cell death of CNCC and VNCC.....	143
Figure S2. 1 Expression of <i>capn1</i> and <i>capn2</i> in response to acute light damage	59
Figure S3. 1 Generation of <i>her9</i> mutants using CRISPR/Cas9	101
Figure S3. 2 Mobility assay of 5 dpf larvae.....	102
Figure S3. 3 Injection of <i>her9</i> mRNA rescues the <i>her9</i> mutant phenotype.....	103
Figure S3. 4 <i>Her9</i> mutants display a decrease in glial cells in the brain and gut	104
Figure S3. 5 Expression of <i>crx</i> and <i>Nr2e3</i> at 72 hpf.....	105
Figure S3. 6 Her9 is not required for the effects of RA on opsin expression.....	106
Figure S3. 7 Western blot	107

Cagney E. Coomer

1.1 Introduction

The vertebrate eye is a highly developed sensory organ responsible for vision, the process of collecting visual information from the environment, and sending it to the brain for processing. Vision or sight is our most heavily relied upon sense, we use it to navigate the world around us, avoid danger, function in daily tasks, and find a mate. Our visual system, although not essential to our survival, has proven to be advantageous, so much so that the brain dedicates more space to processing and storing visual information than all other senses combined (Lamb et al., 2007). The structure and development of the vertebrate eye are well conserved across many species including the mouse and zebrafish (Mitchell et al., 2015; Stenkamp, 2015). Within the eye, vision is facilitated by the retina, a tissue responsible for both detection of light and processing of visual information. The retina is also the most accessible part of the central nervous system (CNS). A mature and functioning retina requires the generation of six retinal neurons and a glial cell in precise ratios and spatial patterns. This histogenesis is a series of orchestrated genetic and cellular events that involve a multitude of molecular factors. Given the complexities in the development of the retina and visual process, it's not a surprise that defects in the genetic regulation or cellular interactions of the retina lead to diseases of the eye or blindness. According to the World Health Organization (WHO), about 2.2 billion people suffer from visual impairment or blindness globally and of that 2.2 billion, 1 billion have preventable impairments or ones that have yet to be addressed (<https://www.who.int/>). Visual impairment and blindness largely impact underdeveloped countries and adults 50 years or older. Of note, 55% of the population of visually impaired are women (<https://www.iapb.org/>). Although loss of or reduction in sight is not completely debilitating, it can have major effects on all aspects of life, potentially as the result of many things including trauma to the eyes and retinal degenerative diseases. Examples of such diseases include Age-related Macular Degeneration (AMD), Retinitis Pigmentosa (RP), and diabetic retinopathy (Bibliowicz et al., 2011). While research and medical advances have made tremendous headway in identifying genes that contribute to the

pathogenesis of retinal degenerative diseases and targeted therapies, vision loss due to retinal degeneration is currently irreversible and permanent. Further genetic analysis of specific cell types may hold the key to understanding the complexity of retinal degenerative diseases, providing the basis for better therapeutic targets.

The seven major cell types of the vertebrate retina are systematically arranged in three distinct layers, which contain the cell bodies, and two plexiform layers. First is the ganglion cell layer (GCL), occupied by ganglion cells (GC) which are responsible for processing visual information and transmitting it to the brain. The second layer is the inner nuclear layer (INL) and is occupied by amacrine (AC), bipolar (BPC), and horizontal cells (HC) as well as the cell bodies of Müller Glia (MG). Cells of the INL are responsible for modulating the visual signal sent from photoreceptors. The third layer, known as the outer nuclear layer (ONL), is where light-sensing photoreceptors are found. Between each of those nuclear layers, in the inner and outer plexiform layers (IPL, OPL), are the synapses between retinal neurons (**Figure 1.1**).

Figure 1. 1 Retinal structure and cellular components

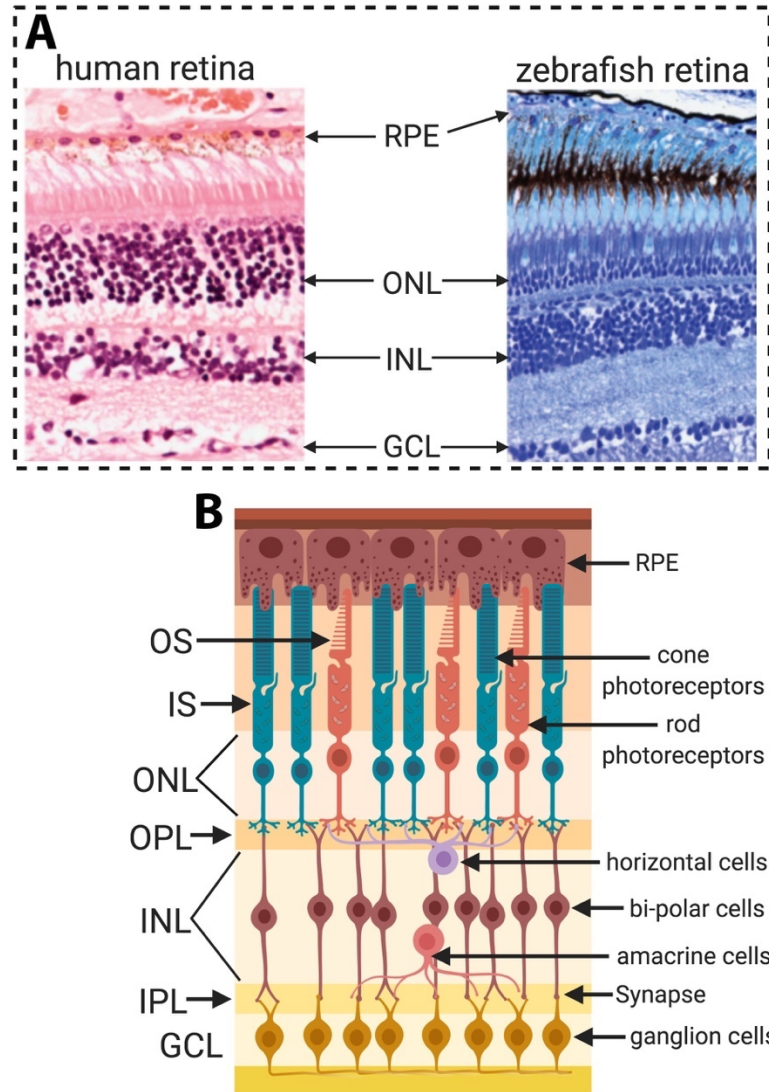


Figure 1.1 Retinal structure and cellular components. A.) Comparison of human and zebrafish retina. The structure and cell populations are highly conserved amongst vertebrates. **B.) Schematic of the vertebrate retina.** The vertebrate retina is composed of three nuclear layers and two plexiform layers: the Outer Nuclear Layer (ONL), the Inner Nuclear Layer (INL), and the Ganglion Cell Layer (GCL). The Outer Plexiform Layer (OPL) contains synapses of photoreceptors, horizontal cells, and bipolar cells, and the Inner Plexiform Layer (IPL) contains synapses of amacrine, bipolar, and ganglion cells. The Retinal pigment epithelium (RPE) envelops the photoreceptor outer segments, and the choroid contains blood vessels that

Although the structure and cell of populations of the retina are relatively conserved between mammals and teleost fish, one major difference is that mammals cannot regenerate any of the retinal cell types. As stated above, damage to the mammalian retina is permanent, whereas the retina of teleost fish, such as zebrafish, is capable of persistent retinal neurogenesis and regeneration in response to acute and chronic retinal damage (Goldman, 2014; Gorsuch and Hyde, 2014; Morris et al., 2005; Vihtelic and Hyde, 2000a). Using zebrafish as a model organism to investigate the underlying mechanisms of the developmental and regenerative process could move us forward in the ultimate goal of restoring human vision.

This chapter will provide an overview of retinal development with an emphasis on photoreceptors, including necessary signaling pathways and transcription factors involved in both development and retinal regeneration. I will further elaborate on using zebrafish as a model organism for these studies, and review the known functions of Hairy-related transcription factors and Calpains. Throughout this text, I will follow established nomenclature, designating human genes in all capital letters, rodent genes with the first letter capitalized, and lower case letters for all other vertebrates; italics indicate genes, whereas non-italicized names refer to proteins.

1.2 Vertebrate retinal development

Utilizing zebrafish as a model organism for retinal development has become a decades long trend owing to their persistent retinal neurogenesis throughout life and response to retinal damage. Due to the strong tissue conservation among most vertebrates, zebrafish studies have been particularly beneficial in illuminating the mechanisms involved in retinal development. The order of cell signaling, proliferation, cell cycle exit, and differentiation are comparable among zebrafish and mammals, revealing similar structure, lamination, cell types, cell morphology, and function.

Retinal development requires the coordinated interactions between the neuroepithelium, surface ectoderm, extraocular mesenchyme and begins with the evagination of the optic vesicles from the developing forebrain, which occurs around 12 hours post-fertilization (hpf). The optic vesicles make contact with the surface ectoderm, induce lens placode formation and triggers the invagination of optic vesicle to form the bilayered optic cup.

The inner layer of the cup develops into the neural retina while the outer later becomes the retinal pigment epithelium (RPE) and the optic stalk (16-20 hpf).

By 24 hpf, the developing zebrafish retina is a single-layered sheet of neuroepithelial cells consistent with other parts of the central nervous system (CNS). The seven major retinal cell types originate from these neuroepithelial cells, born in a conserved spatiotemporal pattern (Schmitt and Dowling, 1999; Stenkamp, 2007). Ganglion cells are the first to differentiate (RGC; 24 – 36 hpf) and do so in a fan-shaped manner, spreading dorsally from the ventral patch (VP) (**Figure 1.2A-B**). The next set of cells generated are the neurons of the inner nuclear layer (INL), which include bipolar cells that start at 60 hpf as well as amacrine and horizontal cells which start between 36 – 48 hpf. Bipolar, amacrine and horizontal cells differentiate in the same fan-shaped pattern seen with the ganglion cells (Connaughton, 2011; Schmitt and Dowling, 1999) (**Figure 1.2A-B**). Photoreceptors are the next to be born, starting with the cones from 48 to 60 hpf. The rods come from a distinct subset of retinal progenitors; the first rods are detectable in the ventral patch at 50 hpf and differentiation only occurs in this region for several hours. The later born rod photoreceptors are produced from early born Müller Glia derived progenitors. These progenitors originate in the inner nuclear but can be seen slowly migrating throughout the central and dorsal regions of the ONL (Morris and Fadool, 2005; Morris et al., 2008; Raymond, 1985; Raymond and Rivlin, 1987) (**Figure 1.2A-B**). Müller Glia are the final cells to exit the cell cycle and differentiate starting at 60 until 90 hpf (Bernardos et al., 2005b; Jadhav et al., 2009; Turner and Cepko, 1987) (**Figure 1.2A-B**). It is important to note that apart from the RGCs, the generation of the other cells types occurs in overlapping time frames, resulting in more than one cell type differentiating at any given time.

Unique to zebrafish, and a significant component of the developing retina is the ciliary marginal zone (CMZ), established following embryonic retinal neurogenesis. This domain is located at the periphery of the retina and contains the proliferating stem cells and retinal progenitors necessary for the indeterminate growth exhibited throughout the lifetime of zebrafish. As zebrafish mature, the CMZ supplies the retina with the cells needed for the eye to grow simultaneously with the rest of the body. Both neurons and glial cells are constantly produced in the CMZ and incorporated into the growing retina to maintain visual acuity (Raymond et al., 2006; Reinhardt et al., 2015; Stenkamp, 2007).

Figure 1. 2 The order of differentiation of retinal cell types

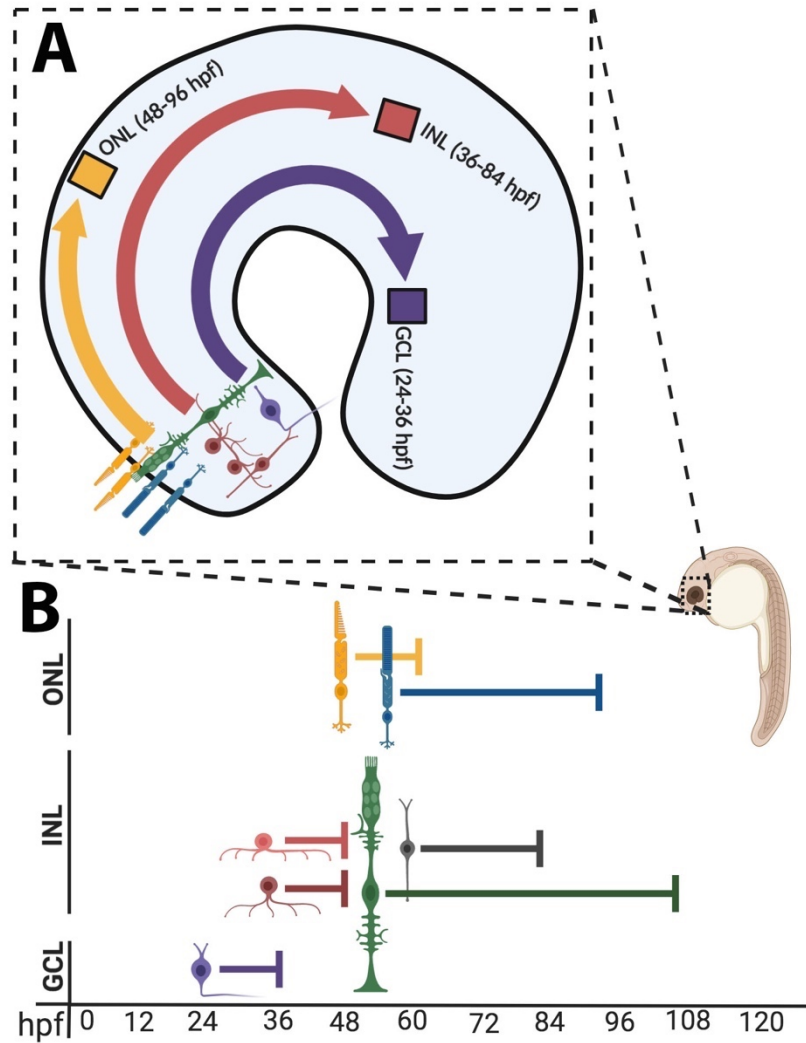


Figure 1.2: The order of differentiation of retinal cell types in vertebrates is highly conserved. **A)** Diagram depicting sequential, fan-shaped waves of differentiation of retinal progenitor cells (RPCs) into retinal neurons starting at the ventral patch. The cells of the GCL are generated from 24-36 hpf, INL neurons (besides BPCs) are generated from 36-48 hpf, and ONL neurons start to differentiate from 48-60 hpf. **B)** Depiction of differentiation sequence of retinal neurons. RGC differentiation begins around 24 hpf and is largely completed by 36 hpf, prior to the onset of AC and HC differentiation at 36 hpf and BPCs begin to differentiate around 60 hpf. In the ONL, cone photoreceptor cells (PRCs) start to differentiate at 48 hpf, and rod PRCs start to appear at 55 hpf. MG, that last retinal cell type to develop, start to differentiate in the INL around 60 hpf.

1.3 General photoreceptor development

Photoreceptor development, function, and maintenance has been studied in many distinct model organisms spanning amphibians to humans (Tsujikawa and Malicki, 2004), zebrafish being an important member of this group. Acting as light sensors, photoreceptor cells (PRCs) are capable of functioning in intense light or near darkness. Cone photoreceptors respond to changes in light intensity and can function at an illumination that is eleven orders of magnitude higher than the rod photoreceptors, which are capable of detecting a single photon in the dim illumination of the night (Lamb et al., 2007; Lamb and Pugh, 2006; Tsujikawa and Malicki, 2004). The morphological structure is key to the function of both photoreceptor types and is highly conserved amongst vertebrates. The distal portion of PRCs are the outer segments, elongated stacks of membrane folds (cones) or disks (rods) containing photopigment molecules (opsins) which are necessary for the detection of light. While both rod and cone photoreceptors possess outer segments, they are longer in rod photoreceptors and interdigitate with the apical processes of the RPE (**Figure 1.3**). Once opsin is activated by light, a change in electrical potential occurs across the cell membrane that is passed through synapses to cells of the INL. This process, phototransduction, is the seminal step in vision.

Vertebrate retinas contain different combinations in the number of rod and cone photoreceptor subtypes. The most commonly observed cone photoreceptor subtypes are: a long singular cone that is sensitive to blue light, and a green /red double cone that is sensitive to green and red wavelengths of light. The zebrafish possess a fourth type of cone PRC, a short, singular cone that is sensitive to ultraviolet (UV) light (Morris and Fadool, 2005). The retinas of rats and mice, which are typically nocturnal, are rod dominated (97% rods and 3% cones;(Carterdawson and Lavail, 1979)) which is complementary to what is found in the peripheral retina of humans. Interestingly, the zebrafish retina is cone dominant (40% rods and 60% cones;(Fadool, 2003) which is similar to what is seen in the central portion of the human retina. Furthermore, cone photoreceptors of the zebrafish retina are arranged in a unique, crystalline mosaic, consisting of rows with double and single cones. The cones are aligned so that the green cone of the double cone pair is always adjacent to a UV cone, while the red cone is always next to a blue cone. The rod photoreceptors also form a unique mosaic, creating a

square surrounding each UV cone ((Fadool, 2003). The determination and arrangement of each of these PRC types is largely dependent upon genetic factors.

Figure 1.3 Zebrafish PR mosaic composition and PR structure

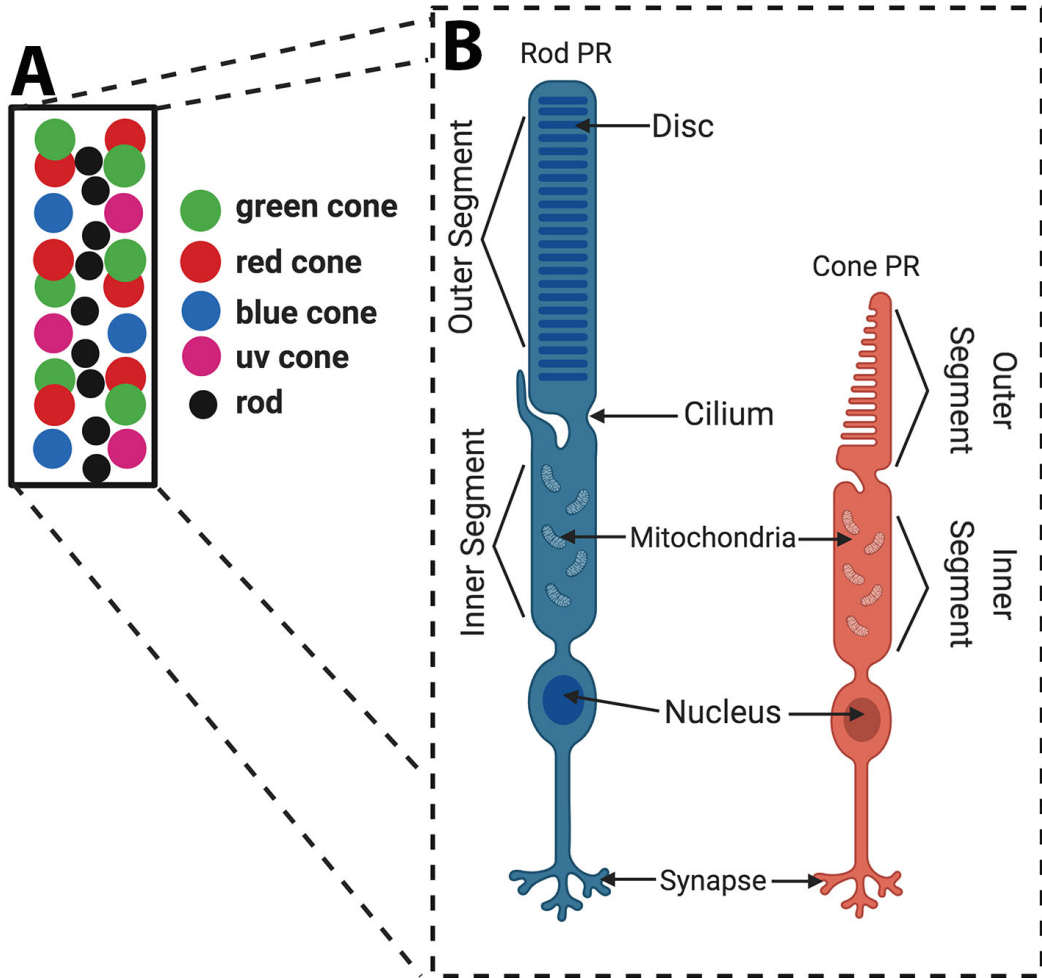


Figure 1.3: Zebrafish photoreceptor mosaic composition and photoreceptor structure. A) schematic showing that zebrafish have a diverse population of photoreceptors across the entire retina. Zebrafish cones are arranged in a row mosaic where rows of ultraviolet and blue cones (colored pink and blue) alternate with rows of red and green cones (red and green, shown in double cone morphology) with the rods (black) dispersed throughout. **B)** Schematic diagram of vertebrate rod and cone photoreceptors. The outer segment is joined to the inner segment by the connecting cilium. Synapses are responsible for the release of neurotransmitters.

There are specific transcription factors that play a role in photoreceptor cell fate determination in retinal progenitor cells. Transcription factor Otx2, and its downstream target Crx, mediate steps in the process of photoreceptor development and play a general role in cell fate determination and differentiation (TsujiKawa and Malicki, 2004). Organisms lacking functional Otx2 have been shown to lack photoreceptor cells while simultaneously developing excess amacrine cells (Nishida et al., 2003). Intriguingly, the loss of Crx does not completely disrupt photoreceptor development. Photoreceptors develop in Crx-deficient mice, but show a significant reduction in visual pigments and eventually degenerate (Furukawa et al., 1999).

1.4 Rod photoreceptors

Following Otx2 and Crx expression, the rod and cone photoreceptors take two distinct paths through development. One major research question is: “How do rod and cone photoreceptors develop their distinct gene expression profiles that lead to separate identities?” The initial steps taken to answer this question have been identifying the genes that control photoreceptor-specific gene expression. Nrl and Nr2e3 are major players when it comes to rod-specific gene expression and rod photoreceptor development (Mears et al., 2001; Peng et al., 2005). The neural retina leucine zipper (Nrl) transcription factor has been experimentally identified as the ‘molecular switch’ for rod development. Nrl acts by mediating rod specific gene expression and inhibiting the development of S-cone photoreceptors (Mears et al., 2001), by activating its downstream target Nr2e3. In mice, lack of Nrl results in the absence of Nr2e3 and non-functional rods in the retina (Kobayashi et al., 1999; Mears et al., 2001). Nr2e3 (nuclear receptor subfamily 2, group E, member 3) is a photoreceptor-specific nuclear receptor that has been shown to repress cone-specific genes in rod photoreceptors (Peng et al., 2005). *NR2E3* mutations in humans lead to an autosomal recessive disorder called enhanced S-cone syndrome; this disease is characterized by the progressive degeneration of rod photoreceptors accompanied with an increase in the number of S-cones and short-wave light sensitivity (Haider et al., 2000; Sharon et al., 2003). In zebrafish, the first rods begin to express rod opsin (rhodopsin) in the ventronasal patch around 50 hpf. Rhodopsin is the visual opsin responsible for the initiation of the phototransduction pathway in rods and acts as a marker for mature rod photoreceptors (Morrow et al., 2017; Nathans, 1992) (Morrow et al., 2017; Nathans, 1992). Although the pathway from retinal progenitor cell to differentiated rod photoreceptor

has been extensively researched, there are still missing components (**Figure 1.4**). Extensive work delving into the various components of rod photoreceptor development has shown developmental differences from other neurons in the retina due to significant regulation by extrinsic and intrinsic factors.

Photoreceptor development is influenced by both intrinsic and extrinsic factors. For example, Vitamin A derived retinoic acid (RA) is an essential extrinsic factor involved in both retinal development and the mature visual system. Dr. John Dowling (1964) laid the foundation for understanding the importance of RA during the development and maintenance of the retina with experiments that identified retinaldehyde as the chromophore for visual pigment. He also characterized retinal degenerative diseases in vitamin A-deprived rats (Dowling and Wald, 1960; Hyatt et al., 1996b; Prabhudesai et al., 2005). Further research has shown that increasing RA in the zebrafish embryo during the formation of the optic primordia results in an increase in cellular proliferation in the ventral portion of the eye that produces a double retina phenotype (Hyatt et al., 1996a). The reverse experiment produced half an eye with no retina (Marsharmstrong et al., 1994) with parallel results demonstrated in mice where RA receptor genes were knocked out (Sanquer and Gilcrest, 1994).

RA has also been shown to play a role later in retinal development. Identification of retinaldehyde dehydrogenases (RALDH2), enzymes that synthesize RA, and their expression patterns implicated RA in the regulation of retinal dorsal-ventral axis specification (Marsharmstrong et al., 1994) This was followed up by cell culture experiments of postnatal retinal cells from rats and chicks that showed RA is important for the differentiation and survival of photoreceptors (Kelley et al., 1994; Stenkamp et al., 1993). Further, when human blastomas were treated with RA, researchers observed a significant upregulation in the expression of multiple photoreceptor-specific genes (Boatright et al., 2002; Li et al., 2003). In vivo experiments in zebrafish showed that treating the embryos with RA between 2 to 5 dpf resulted in retinas that contained a significant increase in rod photoreceptors and red-sensitive cones, a decrease in blue and UV cone photoreceptors, and no effect on green cones. When RA was inhibited, a significant reduction in rods was noted (Hyatt et al., 1996a; Prabhudesai et al., 2005). RA has also been shown to have clinical importance when it comes to treating patients with retinal degenerative diseases such as Retinitis Pigmentosa (Streichert et al., 1999; Xie et al., 2014). Although a great amount of research has been done to understand the mechanisms through

which RA affects retinal and photoreceptor development through the discovery of RALDHs and RAREs (RA response elements), many aspects remain unclear.

Figure 1. 4 Model of PR specification

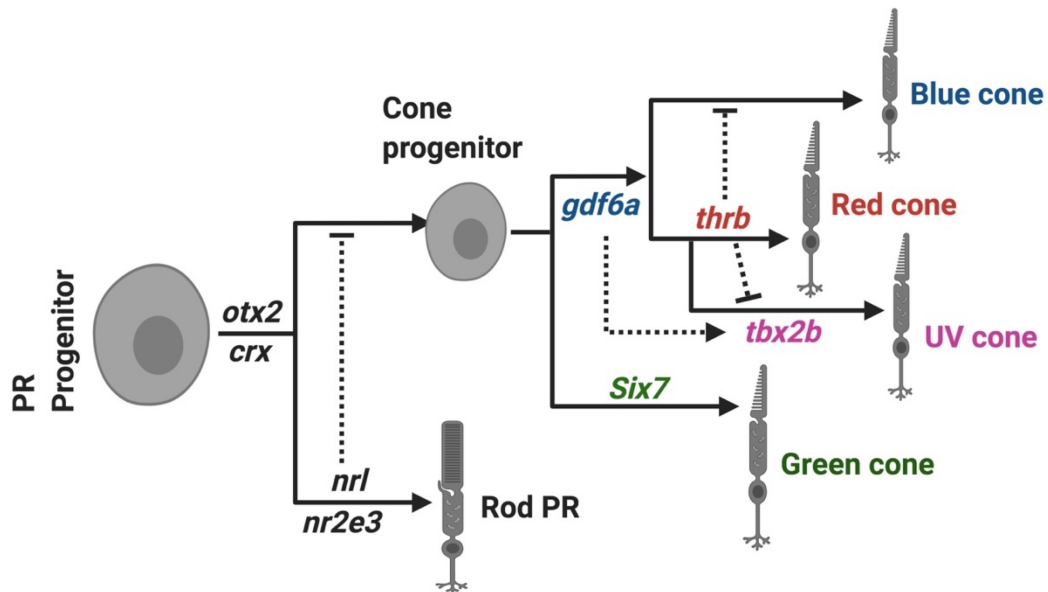


Figure 1.4: Model of photoreceptor specification. *Otx2* influences cell cycle exit; *Crx* drives cells to PR cell fate. *Nrl* and *nr2e3* are expressed in committed rods. Following *crx* expression cone progenitors either express *six7* and become green cones or express *gdf6a*. *Gdf6a* expression triggers *tbx2b* expression and those cells become UV cones, it also triggers *thrb* expression and those cells become red cones, and the cells that only express *gdf6a* become blue cones.

1.5 Cone Photoreceptors

Unlike rod photoreceptors that exist as a single type, there are 3 subtypes of cones in humans and 4 cone subtypes in zebrafish. The perception of color relies on the proper development and signaling from multiple cone photoreceptors (Figure 1.4). Research has shown that Thyroid hormone is one of the major extrinsic factors involved in this process. Thyroid

hormone (TH), tri-iodothyronine (T3) and thyroxine (T4) are critical in orchestrating the development of the central nervous system (CNS) by regulating processes such as cell proliferation, migration, and differentiation. During CNS development, TH binds to nuclear TH receptors (THRA and THRB) and deiodinase enzymes which leads to subsequent modulation of transcriptional gene expression (Bernal, 2017; Vancamp et al., 2019). Regulated expression of TH is important to development, but there are various diseases in which TH synthesis or signaling is disrupted, resulting in excess TH (hyperthyroidism) or insufficient TH (hypothyroidism). Patients with congenital-neonatal hypothyroidism present with CNS developmental abnormalities, as well as aberrant cephalic and facial development (Bierich et al., 1991). TH has also been shown to partially regulate eye development. Treatment of embryos with thyroid hormone disruptors and knockdown of genes that regulate thyroid hormone synthesis result in a reduction in the size of the eye, malformations in eye morphology and defects in the RPE (Baumann et al., 2016; Reider and Connaughton, 2014). A study showed that TH-deficient rat embryos displayed various eye-specific phenotypes including significantly reduced size and thickness as well as developmental delay (Gamborino et al., 2001).

Several studies have provided supporting evidence that TH is essential for retinal development in general. Focusing on photoreceptors specifically, TH is necessary for the regulation of cone photoreceptor differentiation and maturation as well as adult cone opsin expression. These dual roles of TH in retinal development are mediated by the differential expression of two receptors. The chick retina was used to show the contribution of these receptors. Using in situ hybridization for the TH receptor gene, TRa expression was observed in all post-mitotic retinal progenitor cells (Sjoberg et al., 1992), while TRb was expressed in post-mitotic retinal progenitors that later differentiated to become photoreceptors (Trimarchi et al., 2008). Morpholino knockdown of *thrb* in zebrafish produced hypopigmented eyes, retinas that lack lamination, and an absence in differentiated photoreceptors (Marelli et al., 2016). TRb2 deficient mice display a total loss of green opsin expressing cones and an increase in blue/violet opsin expressing cones (Applebury et al., 2007; Ng et al., 2001), suggesting that TRb2 mediates M-opsin cone commitment. The Wong group used loss and gain of function experiments to show that red cones are dependent on the expression of *thrb2* (Suzuki et al., 2013). To follow up, the Allison group conducted experiments that implicated *Thrb* in specification of red, blue, and UV cones and that *Thrb* interacts with *Gdf6a* to regulate retinal lamination (DuVal et al., 2014). A great deal of work and focus has gone into understanding the function of TH,

identifying its downstream targets, and determining how those downstream targets influence retinal and photoreceptor development. However, picture remains incomplete and there is more to uncover.

Cone photoreceptors originate from the same progenitor pool as rods and development is also initiated by the expression of Otx2 and Crx. After initiation, the data above indicates that TH receptors drive the differentiation of cone photoreceptors. How these cones and their subtypes are produced though is still poorly understood. Growth and differentiation factor 6 (Gdf6), a BMP ligand, is required for the regulation of retinal cell proliferation, and promotes blue and red cone development (DuVal and Allison, 2018). *Gdf6a* mutants display microphthalmia and have a reduction in cone photoreceptors. Another gene implicated in cone photoreceptor development, *sine oculis* homeobox homolog 7 (*six7*), was previously knocked out via TALEN which induced the loss of expression of green opsin and impaired the development of green cones (Ogawa et al., 2015). The Fadool lab identified and characterized the *lots-of-rods* mutant (*lor^{p25bbl}*) and observed *tbx2b* is expressed during photoreceptor differentiation and drives the cell towards a UV cone cell fate (Alvarez-Delfin et al., 2009). The *lor* mutant retinas had no UV cones and a significant increase in the amount of rod photoreceptors. Taken together, these data indicate that photoreceptor development is regulated by a variety of extrinsic and intrinsic factors. The genes and signaling molecules discussed so far in this chapter are important, but are certainly not the only factors involved. Even with the extensive amount of research dedicated to retinal development and more specifically photoreceptor development there are still missing pieces to the puzzle, which may be uncovered using zebrafish as a model.

1.6 Zebrafish as a model organism

The zebrafish is a diurnal teleost, native to southeast Asia, that has been used as a model organism since the 1970s when George Streisinger and his colleagues at the University of Oregon uncovered many qualities which made them an ideal study system (Streisinger et al.,

1981) . Zebrafish are a valuable model for studying biological processes, understanding the mechanisms of development and diseases, including (in our case) retinal development and retinal degenerative diseases. As visually oriented organisms, zebrafish retinas show many common morphological features compared to other vertebrates including humans (Glass and Dahm, 2004). Adult zebrafish generally do not exceed a body length of 5–6 cm, meaning these small, robust organisms require a relatively small amount of space and are cheaper to maintain than mice (Ward and Lieschke, 2002).

Figure 1. 5 The significance of Zf as a model organism

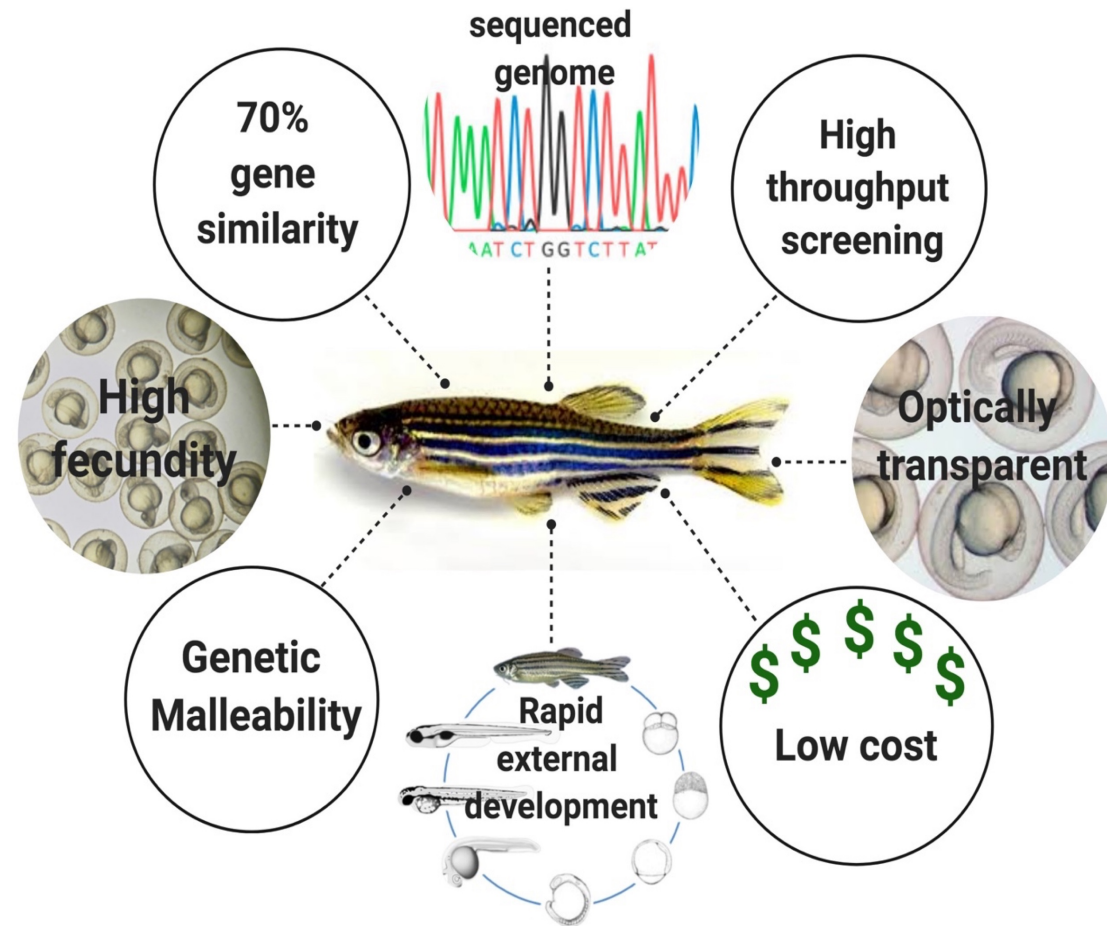


Figure 1.5: The significance of zebrafish as a model organism.

The mating process of zebrafish is triggered in the morning at light onset, and a single mating pair can produce hundreds of eggs. These large clutches are ideal for designing and executing experiments with results that yield high statistical power. Zebrafish eggs are fertilized and develop externally, and the embryos remain optically transparent until pigment cells develop around 24 hpf. Pigmentation can be blocked chemically, or albino strains can be used to avoid it altogether, making them good candidates for studying early development. Additionally, every blood vessel in the zebrafish embryo can be observed using a low power microscope. The developmental process of major tissues and organs such as the eyes, blood, and kidneys shares many significant features with human development. Zebrafish embryogenesis is rapid and begins with the first cell division around 30 min post-fertilization and subsequent cell divisions taking place roughly every 30 minutes. By 24 hpf, all major features and organs (head, tail, eye, heart, somites, and yolk sack) are visually recognizable although not fully functional (Glass and Dahm, 2004). Between 24 – 48 hpf, various cell types begin to differentiate as the development of many organs draws to completion. By the time the embryo reaches 72 hpf, it has hatched from the protective chorion and embryonic development is relatively complete with most organs and tissues established and functional. Starting at 5 dpf, the embryo is free swimming, hunting for food and avoiding predation (Kimmel et al., 1995). At this point, larvae respond to touch and have visually evoked responses, referred to as Optokinetic responses, that can be measured using various devices (Mueller and Neuhauss, 2014). Metamorphosis of the zebrafish larvae takes place between 10 – 14 dpf, followed by initial signs of sexual maturity which is usually achieved by 6 weeks post-fertilization (Hsiao and Tsai, 2003). In addition to a well-established timeline of development and maturation, the zebrafish genome has also been fully sequenced and almost fully annotated (Howe et al., 2013), providing further support for its use as an ideal animal model. The zebrafish shares about 70% gene similarity with humans and 84% of known disease-causing genes in humans have a zebrafish counterpart. Accompanied with their small size and ability to produce a large number of embryos, zebrafish have been ideal for large mutagenesis screens using *N*-ethyl-*N*-nitrosourea (ENU) or ethyl methansulfonate (EMS) alkylating agents on sperm, morpholino knockdown experiments (via interference with mRNA splicing or translation), and ectopic expression of specific genes through the microinjection of mRNA or plasmids (Nasevicius and Ekker, 2000; Postlethwait et al., 1998; Schier et al., 1996; Tappeiner et al., 2012). These experiments have provided a collection of mutations in several

hundred genes and new information that is relevant to vertebrate developmental processes and disease pathogenesis. In addition, zebrafish as a model lend themselves well to studying the phenotypic consequences of mutations on a single-cell level, revealing shared functions of a gene across a wide spectrum of vertebrates (FurutaniSeiki et al., 1996; Kimmel et al., 1990). Their conserved vertebrate physiology and gene similarity combined with developed genome editing tools such as transcription activator-like effector nuclease (TALEN) and clustered regularly-interspaced short palindromic repeats with Cas9 nuclease (CRISPR/Cas9) make zebrafish great candidates for studying human genetic diseases and analyzing the function of the vertebrate genome (Herberger and Loretz, 2013; Ma and Wong, 2016). Zebrafish have also been influential in studying potential therapeutic compounds to treat a wide variety of diseases such as cancer and depression. Their small stature, large clutch size, and easily manipulated environment make them ideal for drug screens and drug discovery applications (Fonseka et al., 2016; Miscevic et al., 2012).

1.7 Using zebrafish to study retinal degeneration/regeneration

Forward genetic screens in zebrafish have been used to isolate retinal defects in both morphology and function, then identify genes associated with retinal degeneration (Brocknerhoff and Fadool, 2011; Brocknerhoff et al., 1995; Li and Dowling, 1997). Photoreceptor death and progressive vision loss are characteristics of a group of diseases called retinal degenerations which currently have no cure (Angueyra and Kindt, 2018). Although a great deal of research has been dedicated to understanding photoreceptor degeneration we still have significant gaps in our knowledge about the photoreceptor degeneration and effects on neighboring photoreceptors (bystander effect). For instance, in mice and humans, rod death frequently results in the death of cones. For most retinal degenerative diseases, malfunctions result in the death of only one type of photoreceptor, but in some retinal degenerative disease like retinitis pigmentosa (RP), the death of the rods leads to the subsequent death of healthy cones. Whereas the effects of cone death on rods is more variable, in some cases of cone dystrophy the rods remain healthy (Michaelides et al., 2004) but in other cases cone degeneration causes a loss in scotopic vision as a result of rod degeneration (Polok et al., 2009). Little is also known

about the effects of cone death on other cones. To develop effective therapies to stop or eliminate photoreceptor degeneration we must first begin filling in these gaps in our knowledge.

Many treatments such as neuroprotective agents, gene therapies, and antibody therapies only provide temporary relief or slow the progression of damage ((Allen et al., 2018; Cideciyan, 2010). Alternatively, recent research using stem cells to produce replacement retinal cells have been successful at producing light-sensitive photoreceptors in cup-like structures, but have had little success at integrating them into a host visual network to recover functional vision (Pearson et al., 2016; Santos-Ferreira et al., 2016). Insights gained from these experiments highlight the fact that we do not have a complete understanding of photoreceptor wiring and integration during development. Leveraging the zebrafish's ability to regenerate could help identify genes involved in synaptic development and opens the opportunity for the use of regenerative therapies to produce new photoreceptors and facilitate rewiring.

The survival of zebrafish larvae is dependent on its ability to perform complex visual behaviors early in life. This is supported by the fact that the zebrafish visual system is functional as early as 5 dpf. Accompanying this rapid development, the zebrafish retina experiences continued growth once the larvae transition into adulthood, and new cells are supplied by the CMZ. The cells of the CMZ differentiate, migrate and incorporate into the retinal network when and wherever needed. Not only is the zebrafish retina capable of continued growth, but it is also capable of regeneration in response to insult or injury such as mechanical damage, light damage, pharmacological damage, and ablation of specific cell types (Bernardos et al., 2007; Fausett and Goldman, 2006; Fimbel et al., 2007). This regenerative response is facilitated somewhat in the periphery of the retina by the CMZ, but Müller glia (MG) are mainly responsible for this robust regenerative response (Raymond et al., 2006).

Unlike humans or other mammals, MG of the zebrafish retina are capable of dedifferentiating in response to injury and taking on a multipotent state (**Figure 1.6**). In response to the damage the MG of most species undergo both morphological, biochemical, and physiological changes which is referred to as reactive gliosis and in some species severity of damage triggers proliferative gliosis. During proliferative gliosis the MG produce mitotic cells that begin expressing retinal progenitor markers such as *Ascl1a*, *Pax6*, *Rx1* and *Neurogenin1*. As regeneration progresses the Müller glia derived progenitors migrate to the respective location and begin expressing the genes consistent with the developmental program of the cell being replaced (Brockerhoff and Fadool, 2011; Ramachandran et al., 2015). Unfortunately, the

pathway leading the proliferative gliosis and migration is poorly understood. This ability makes the zebrafish retina capable of regeneration and rewiring in a short time, significantly dependent on the extent of the damage (Hitchcock and Cirenza, 1994; Hitchcock and Raymond, 2004; Raymond and Rivlin, 1987; Stuermer et al., 1992) and requires the activation of multiple signaling pathways including but not limited to the Bmp/Smad and Jak-Stat pathway. A major challenge has been isolating when and where the pathways are activated during the regenerative process (Goldman, 2014). Taking advantage of both the zebrafish's ability to supply the retina with new cells for continued growth and regeneration will allow us the opportunity to gain a deeper understanding of the mechanisms required for regeneration, incorporation, and rewiring. By understanding the key genes involved (Stenkamp and Cameron, 2002; Thomas et al., 2016) we could unlock the regenerative potential in mammalian MG, facilitating the regeneration of loss retinal cells and advancing the field of regenerative medicine. As will be observed throughout this dissertation, my research suggests that Calpain 5 and Her9 may have an important role in zebrafish photoreceptor regeneration.

1.8 Calpain-5

Calpain-5 (*capn5*) belongs to a family of Ca²⁺ dependent, non-lysosomal, cysteine proteases that are involved in many processes such as apoptosis, necrosis, cell division, differentiation, signal transduction, and embryonic development (Dear et al., 1997). Calpains are considered non-lysosomal because they are found in the cytoplasm of the cell instead of the lysosome like other proteases. There have been 15 mammalian calpains (**Table 1.1**) identified and implicated in a wide range of pathological diseases such as muscular dystrophy, cancer, and neurodegeneration (Lepage and Bruce, 2008). Calpains can be found as inactive proenzymes floating in the cytosol where the resting cell concentration of free Ca⁺ is 50-100 nM. Activation is triggered by an increase in free Ca⁺ concentrations in the cytosol and release of the calpain inhibitor, calpastatin (Pietrobon et al., 1990; Wingrave et al., 2003). Calpastatin is a ubiquitously expressed protein that is a specific regulator of calpains (Emori et al., 1987). One of the proposed mechanisms for Calpain activation is an increase in free intracellular Ca⁺ concentration that results in the autolysis of the N-terminal propeptide domain initiating a

conformational change and the separation of a truncated subunit that in turn activates the enzyme (Ray et al., 2003). Another mechanism proposes that high intracellular Ca^+ concentrations cause the translocation of the inactive calpains from the cytosol to the cell membrane, subsequently activated by Ca^{2+} and phospholipids. This results in the autocatalytic hydrolysis of domain I, resulting in the dissociation of the active enzyme (Ono et al., 2004; Suzuki and Sorimachi, 1998). Calpain activation has been associated with mediating both apoptotic and anti-apoptotic pathways (Tan et al., 2006; Wang et al., 2016) which is supported by their implications in both autoimmune and neurodegenerative diseases. Most research on calpains has been focused on the classical calpains Capn1 and Capn2 which require μM and mM Ca^{2+} concentrations to initiate their activity, respectively.

Table 1. 1 Calpain genes

Table 1.1 Calpain genes

Calpain protein	Calpain gene	Other names	Tissue distribution	Species
Calpain 1	<i>capn1</i>	μ-Calpain, CAPN1	Ubiquitous	Human, Rat Mouse, Zebrafish
Calpain 2	<i>capn2</i>	m-Calpain, CAPN2	Ubiquitous	Human, Rat Mouse, Zebrafish
Calpain 3	<i>capn3</i>	nCL-1, p94, Lp82 Lp85, Rt88	Skeletal muscle, lens, retina	Human, Rat Mouse, Zebrafish
Small subunit 1	<i>capn4</i>	N/A	Ubiquitous	Human, Rat Mouse, Zebrafish
Calpain 5	<i>capn5</i>	htra3, nCL-3	Ubiquitous	Human, Rat Mouse, Zebrafish
Calpain 6	<i>capn6</i>	CAPNX, Calpamodulin	Placenta	Human, Rat Mouse, Zebrafish
Calpain 7	<i>capn7</i>	palBH	Ubiquitous	Human, Rat Mouse, Zebrafish
Calpain 8	<i>ncl-2, capn8</i>	nCL-2	Stomach mucosa	Human, Rat Mouse, Zebrafish
Calpain 9	<i>capn9</i>	nCL-4	Digestive track	Human, Rat Mouse, Zebrafish
Calpain 10	<i>capn10</i>	CAPN10	Ubiquitous	Human Mouse, Zebrafish
Calpain 11	<i>capn11</i>	N/A	Testis	Human, Rat Mouse, Zebrafish
Calpain 12	<i>capn12</i>	N/A	Ubiquitous	Human, Rat Mouse, Zebrafish
Calpain 13	<i>capn13</i>	Sol H	Ubiquitous	Human, Rat Mouse, Zebrafish
Small subunit 2	<i>capn14</i>	N/A	N/A	Human, Rat Mouse, Zebrafish
Calpain 15	<i>capn15</i>	N/A	N/A	Human, Rat Mouse, Zebrafish

Calpain expression in the retina was first characterized in 1985 (Tsong and Lombardini, 1985) and the activation of Calpains was implicated in retinal degeneration 15 years later. It was proposed that the high intracellular concentration of Ca⁺ during degeneration leads to the subsequent increased activation of calpain that in turn triggers cell death (Suzuki and Sorimachi, 1998; Wang et al., 2004). Since their discovery CAPN1, CAPN2, CAPN3, CAPN5 and CAPN10 have all been shown to be expressed in the adult retina of many organisms including humans (Ma and Wong, 2016; Nakajima et al., 2001; Tamada et al., 2005; Yoshimura et al., 1984). Calpain activity has been identified in glaucoma, where traumatic injury to the optic nerves results in a significant increase in the activation of calpain in association with axonal degeneration and ganglion cell death (Das et al., 2006; Saatman et al., 2003). To support this analysis, treating injured optic nerves with calpain inhibitor II resulted in a significant decrease in cell death and damage (Couto et al., 2004). Interestingly, calpain activation has also been associated with Retinitis Pigmentosa (RP) in the rd1 mouse model (Doonan et al., 2005; Paquet-Durand et al., 2006), where calpain activation was associated with photoreceptor cell death (Paquet-Durand et al., 2006). Yet, treating these mice with calpain inhibitors did not affect degeneration. Altogether calpains have been shown to play some role in retinal degeneration, but there is still much work needed to directly link calpains to mediation of cell death during retinal degeneration. Moreover, CAPN5 is the only calpain directly associated with a retinal disease in humans, and much less is known about the function of CAPN5 regarding retinal development and degeneration (Dear et al., 1997).

Capn5 is categorized as a non-classical calpain because it lacks the EF-hand motif. Instead, it has a calcium-binding domain, catalytic domain, and unique C-terminus domain or C2-like domain (Singh et al., 2014). Based on its sequence and structure, *Capn5* is considered an ortholog of *TRA-3* in *C. elegans*, which is thought to play a role in sex determination and mediating a necrotic pathway during neurodegeneration (Aggad et al., 2014; Sorimachi et al., 2011). Additionally, it is the second most abundantly expressed Calpain within the vertebrate central nervous system (Singh et al., 2014). Dominant-negative mutations in *CAPN5* are linked with autosomal dominant neovascular inflammatory vitreoretinopathy (ADNIV), a progressive autoimmune disease of the eye. ADNIV is characterized by retinal and iris neovascularization, abnormal retinal pigmentation, cystoid macular edema, vitreous hemorrhage, vitreous

inflammation, and tractional retinal detachment. The disease shares several features with more common retinal diseases such as retinitis pigmentosa, diabetic retinopathy, uveitis, and cataracts.

Figure 1. 6 CAPN5 proteins, ADNIV mutations and the disease stages

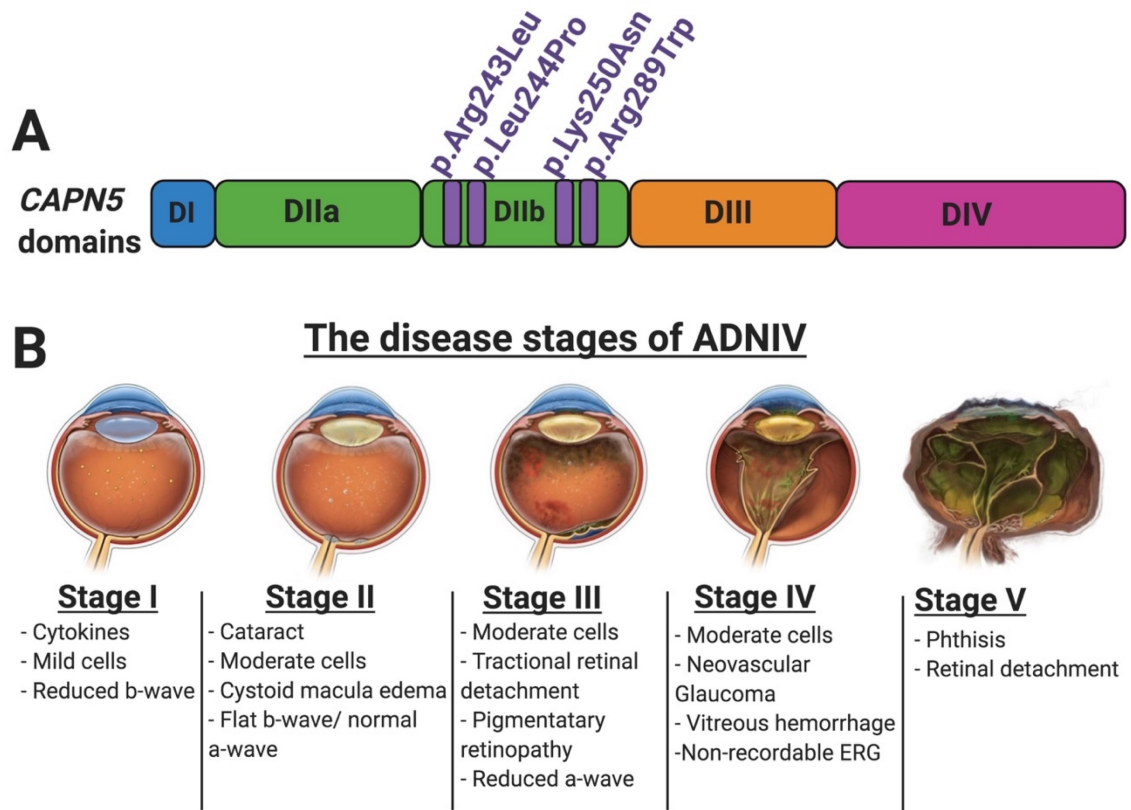


Figure 1.6: CAPN5 protein, ADNIV mutations and the disease stages of ADNIV. A) CAPN5 is composed of four domains, and the ADNIV mutations (p.Arg243Leu, p.Leu244Pro, p.Lys250Asn, p.Arg289Trp; Purple) are in located in catalytic domain II (Green). **B)** The disease stages of ADNIV phenocopy common retinopathies. In Stage I disease, there are mild cells in the vitreous (orange) and a reduced b-wave on electroretinography (ERG). In Stage II disease, the anterior chamber (blue) shows mild inflammatory cells and there is early development of cataract. The posterior segment shows moderate cells, retinal pigmentary changes, and some edema in the macula or optic nerve head. There is selective loss of the b-wave in the scotopic bright flash ERG. In Stage III disease, the anterior segment shows moderate cells, progressive cataract, and iris synechiae. Progressive inflammation in the posterior segment shows development of vitreous bands and epiretinal membranes, and more posterior retinal pigmentary changes. There is reduction of the a-wave on ERG. In Stage IV disease, inflammation in the anterior segment causes neovascular and angle closure glaucoma. Neovascularization develops in the retina with vitreous hemorrhage and progressive retinal detachment that may include features of anterior or posterior proliferative vitreoretinopathy. The ERG becomes non-recordable. In Stage V disease, the eye becomes non-functional. Figure modified from <https://mahajanlab.stanford.edu/> with permission.

The missense mutations (p. Arg243Leu, p. Leu244Pro, p. Lys750Asn) in CAPN5 (**Figure 1.7**) that are linked to ADNIV have been shown to cause hyperactivity of the protein by lowering its threshold for calcium activation (Bassuk et al., 2015). However, the precise mechanism whereby mutant Capn5 causes ADNIV is not well understood. Therefore, elucidating the role of Capn5 in photoreceptor degeneration could reveal the underlying pathogenetic mechanisms of ADNIV as well as other retinal degenerative diseases that display similarities to ADNIV. Chapter 2 of this dissertation will describe the studies I performed to characterize the expression of *capn5* during zebrafish retinal development and regeneration and to determine its function during retinal neurogenesis. The data presented in this dissertation will add some insight into the potential roles of Capn5 in retinal development and regeneration.

1.9 Hairy-related 9

Hairy-related (Her) genes are members of the basic-Helix-Loop-Helix-Orange (bHLH-O) family of transcription factors that both actively and passively repress target gene transcription (Kageyama et al., 2007). Evolutionarily conserved, the bHLH-O family of transcription factors exist as four groups within the animal kingdom (Stra13, Hey, (Stra13, Hey, E(spl), and Hairy;(Davis and Turner, 2001; Muller et al., 1996). bHLH-O transcriptions factors have been shown to act downstream of Notch-Delta, FGF, Hh, Nodal and RA signaling, and are implicated in many cellular processes such as differentiation, cell cycle arrest, self-renewal and apoptosis (Holzschuh et al., 2005a; Latimer et al., 2005; Liu et al., 2015; Radosevic et al., 2011b). Additionally, bHLH-O transcription factors have been shown to play a critical role in developmental processes like segmentation, floor plate development, CNS development and neural tube closure (Takke et al., 1999) as well as regeneration of tissue in the CNS (Zupanc and Sirbulescu, 2011).

Table 1. 2 bHLH-O transcription factors

Table 1.2 The zebrafish bHLH-O superfamily of transcription factors

Gene	Human ortholog	Regulatory pathway (s)	References
<i>hes2.1</i> (hairy/enhancer of split 2.1)	<i>HES2</i>	Notch	(Zhou et al., 2012)
<i>hes2.2</i> (hairy/enhancer of split 2.2)	<i>HES2</i>	Notch	(Zhou et al., 2012)
<i>hes6</i> (hairy/enhancer of split 6)	<i>HES6</i>	FGF	(Kawamura et al., 2005)
<i>hey1</i> (hairy/enhancer of split -related with YRPW motif 1)	<i>HEY1</i>	Notch	(Fischer et al., 2004)
<i>hey2</i> (hairy/enhancer of split -related with YRPW motif 2)	<i>HEY2</i>	Hh, VegF	(Rowlinson and Gering, 2010)
<i>hey1</i> (hairy/enhancer of split -related with YRPW motif-like)	<i>HEYL</i>	Notch	(Zhou et al., 2015)
<i>hey4</i> (hairy/enhancer of split -related with YRPW motif 4)	<i>HELT</i>	unknown	(Peukert et al., 2011)
<i>her1</i> (hairy/enhancer of split-related 1)	<i>HES7</i>	Notch	(Takke and Campos-Ortega, 1999)
<i>her2</i> (hairy/enhancer of split-related 2)	<i>HES5</i>	Notch	(Cheng et al., 2015)
<i>her3</i> (hairy/enhancer of split-related 3)	<i>HES3</i>	Negatively regulated by Notch	(Hans et al., 2004)
<i>her4.1</i> (hairy/enhancer of split-related 4.1)	<i>HES5</i>	Notch	(Takke et al., 1999)
<i>her4.2</i> (hairy/enhancer of split-related 4.2)	<i>HES5</i>	Notch	(Takke et al., 1999)
<i>her4.3</i> (hairy/enhancer of split-related 4.3)	<i>HES5</i>	Notch	(Takke et al., 1999)
<i>her4.4</i> (hairy/enhancer of split-related 4.4)	<i>HES5</i>	Notch	(Takke et al., 1999)
<i>her4.5</i> (hairy/enhancer of split-related 4.5)	<i>HES5</i>	Notch	(Takke et al., 1999)
<i>her5</i> (hairy/enhancer of split-related 5)	<i>HES7</i>	FGF, negatively regulated by Notch	(Dyer et al., 2014)
<i>her6</i> (hairy/enhancer of split-related 6)	<i>HES1</i>	Notch	(Pasini et al., 2004)
<i>her7</i> (hairy/enhancer of split-related 7)	<i>HES7</i>	Notch	(Oates et al., 2005)
<i>her8a</i> (hairy/enhancer of split-related 8a)	<i>HES6</i>	Notch	(Chung et al., 2011)
<i>her8.2</i> (hairy/enhancer of split-related 8.2)	<i>HES6</i>	Unknown	(Wang et al., 2009)
<i>her9</i> (hairy/enhancer of split-related 9)	<i>HES1, HES4</i>	Nodal, BMP, RA	Bae et al., 2005, Latimer et al., 2005, Radosevic et al., 2011)
<i>her11</i> (hairy/enhancer of split-related 11)	<i>HES7</i>	Negatively regulated by Notch	(Sieger et al., 2004)
<i>her12</i> (hairy/enhancer of split-related 12)	<i>HES5</i>	Notch	(Shankaran et al., 2007)
<i>her13</i> (hairy/enhancer of split-related 13)	<i>HES7</i>	Notch	(Dias et al., 2012)
<i>her15.1</i> (hairy/enhancer of split-related 15.1)	<i>HES5</i>	Notch	(Shankaran et al., 2007)
<i>her15.2</i> (hairy/enhancer of split-related 15.2)	<i>HES5</i>	Notch	(Shankaran et al., 2007)

** Table modified from Dr. Stephen Wilson's dissertation (2016) with permission

The zebrafish genome contains 26 members of the hairy/enhancer of split gene superfamily with 19 of those being hairy-related (her) class bHLH-O genes (**Table 1.2**). There are three conserved domains in members of this family, the bHLH, the orange and the WRPW domains (Sasai et al., 1994). The bHLH domain contains the basic region for DNA binding to the E box (CANNTG) consensus sequence that is present in its target genes. The Orange domain is responsible for regulating the selection of bHLH heterodimer partners and the WRPW domain contains the tetrapeptide Trp-Arg-Pro-Trp which represses transcription (Dawson et al., 1995; Ohsako et al., 1994). This domain has been shown to recruit *transducin-like enhancer of split (tle)* co-repressors (orthologs of Groucho in *Drosophila*) and histone deacetylases. By binding to the WRPW tetrapeptide, the ability of Her proteins to repress transcription is repressor (Fischer and Gessler, 2007).

Figure 1. 7 The zebrafish bHLH-O proteins

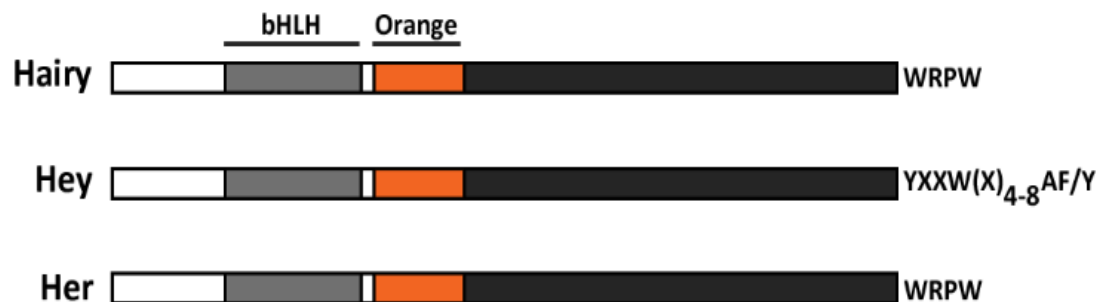


Figure 1.7: The zebrafish bHLH-O proteins. The zebrafish genome contains 3 classes of bHLH-O transcription factors; 3 Hairy (Hes), 4 Hairy/Enhancer of Split-Related with YRPW motif (Hey), and 19 Hairy/Enhancer of Split-Related (Her). The HLH domain is composed of two amphipathic α -helices (H) separated by a loop (L) that serve as a dimerization domain as well as an interface for additional protein-protein interactions. The Orange domain (O) is composed of two additional α -helical structures that bind to DNA to inhibit binding of pro-neural bHLH genes and also serves as a site for additional protein interaction. The WRPW tetrapeptide motif (in Hes and Her proteins) and YXXW motif (in Hey proteins) associates with co-repressors and HDACs which lead to strong repression of target genes. This figure modified from Dr. Stephen G. Wilson's Dissertation with permission.

Members of the Hairy/Hes family are expressed in various tissues including the developing and adult retina. Hes1, Hes5, and Hey2 proteins have been identified as key players in progenitors deciding between glial versus neuronal cell fate. For example, Hes5 deficient mice show a significant decrease in MG in the retina while exogenous expression of Hes5 directs cells toward becoming MG (Hojo et al., 2000). Hey2 is also expressed in the developing retina and ectopic expression results in increased MG (Satow et al., 2001). Previous work in our lab showed that zebrafish *her4* is expressed in the CMZ and MG of the retina during chronic rod degeneration, suggesting that Her4 is involved in maintaining the stem cell populations of the retina (Wilson et al., 2016). In another study, when retinal progenitors were infected with HES1-transducing retrovirus, they were inhibited from differentiating into mature retinal neurons, effectively blocking retinal development. In contrast, *Hes1*-null mice experienced accelerated differentiation with the premature appearance of the rods and horizontal cells, suggesting that Hes1 may regulate the differentiation of retinal neurons (Tomita et al., 1996). Of all the Hairy-related (*her*) genes, *her9* is the least explored, chiefly due to its absence in mice and rats.

Hairy-related 9 or hairy/enhancer of split-related 9 (her9), is a basic-helix-loop-helix-orange (bHLH-O) transcriptional repressor. This is the zebrafish ortholog of the human *HES4* gene and, unlike other members of the Hairy-related family, does not function downstream of Notch-Delta signaling. Her9 has been shown to act downstream of Nodal expression, inhibiting notochord development and in the promotion of floor plate specification (Latimer et al., 2005). Her9 has also been shown to be expressed in the CMZ of the Medaka fish, where it represses *rx2* expression and inhibits stem-cell proliferation (Reinhardt et al., 2015). Previous research has shown an upregulation of *her9* during rod photoreceptor degeneration (Morris et al., 2011), suggesting Her9 plays a role during rod photoreceptor degeneration/regeneration. Still, little is known about the precise function of Her9 in this process. Initial characterization work on *her9* expression during retinal development was begun by Dr. Stephen G. Wilson (Wilson et al., 2016). To understand the role of Her9 during retinal development and to determine the regulatory networks involved in controlling Her9 expression, Dr. Wilson generated and established a *her9* CRISPR mutant line. In Chapters 3 and 4 of my dissertation, I will describe my studies to continue the work of understanding the role of Her9 during retinal development and regeneration as well as to identify the regulators of *her9* expression in the retina.

1.10 Specific Aims

The specific aims of this dissertation were directed towards understanding the function of both *Capn5* and *Her9* during vertebrate development and retinal regeneration. A combination of molecular, genetic and behavior assays were used to elucidate *Capn5* and *Her9* function. This work is organized as follows:

- I. Characterize the expression of *capn5* during zebrafish development and regeneration.
 - a. Use in situ hybridization and immunohistochemistry to characterize expression during significant stages of retinal development.
 - b. Use in situ hybridization and immunohistochemistry to characterize expression in response to rod photoreceptor degeneration and acute light damage

- II. Generate *capn5* knockout lines using CRISPR/Cas9 genome editing technology.
 - a. Characterize genome lesions and find germline transmitted *capn5* mutant alleles.
 - b. Characterize the *capn5* mutant phenotype.

- III. Elucidate the role of *Her9* during retinal development
 - a. Characterize the expression of *her9* during retinal development
 - b. Characterization of the *her9* mutant phenotype
 - c. Determine if *her9* is regulated by RA in the retina and what the downstream targets are.

- IV. Determine whether loss of *her9* affects neural crest cell development
 - a. Characterize the NCC phenotype present in the *her9* mutant

Aims I and II are addressed in Chapter 2 and the Appendix, respectively.

Aim III is addressed in Chapter 3

Aim IV is addressed in Chapter 4

Cagney E. Coomer and Ann C. Morris

Department of Biology, University of Kentucky, Lexington, Kentucky 40506

Key words: zebrafish, Capn5, ADNIV, regeneration

Adapted from: Investigative Ophthalmology & Visual Science , Vol.59, 3643-3654. (doi: <https://doi.org/10.1167/iovs.18-24278>) Coomer CE and Morris AC. Capn5 expression in the healthy and regenerating retina, pages 3643-3654, July 2018.

N.B. For this dissertation, figure numbers, headings, and text were modified to match dissertation style.

2.1 Abstract

Autosomal dominant neovascular inflammatory vitreoretinopathy (ADNIV) is a devastating inherited autoimmune disease of the eye that displays features commonly seen in other eye diseases, such as retinitis pigmentosa and diabetic retinopathy. ADNIV is caused by a gain of function mutation in Calpain-5 (*CAPN5*), a calcium dependent cysteine protease. Very little is known about the normal function of Capn5 in the adult retina, and there are conflicting results regarding its role during mammalian embryonic development. The zebrafish (*Danio rerio*) is an excellent animal model for studying vertebrate development and tissue regeneration and represents a novel model to explore the function of Capn5 in the eye. We characterized the expression of Capn5 in the developing zebrafish central nervous system (CNS) and retina, in the adult zebrafish retina, and in response to photoreceptor degeneration and regeneration using whole mount in situ hybridization, fluorescent in situ hybridization (FISH), and immunohistochemistry. In zebrafish, *capn5* is strongly expressed in the developing embryonic brain, early optic vesicles, and in newly differentiated retinal photoreceptors. We found that expression of *capn5* co-localized with cone specific markers in the adult zebrafish retina. We observed an increase in expression of Capn5 in a zebrafish model of chronic rod photoreceptor degeneration and regeneration. Acute light damage to the zebrafish retina, was accompanied by an increase in expression of Capn5 in the surviving cones and in a subset of Müller glia. These

studies suggest that Capn5 may play a role in CNS development, photoreceptor maintenance, and photoreceptor regeneration.

2.2 Introduction

Calpains are a family of calcium-dependent, non-lysosomal cysteine proteases that include at least 15 family members in humans (Tan et al., 2006). Calpains share similarity in their protease and calcium binding domains, and are unique to other proteases because they are localized to the cytosol or nucleus instead of the lysosome. Activated by influxes of calcium, calpains do not degrade their protein substrates, but rather modify the activity of their targets through proteolytic processing. Calpains have been implicated in numerous cellular processes, including cell death, signal transduction, intracellular signaling, and sex determination (Perche et al., 2009). Hyperactivation of calpains is associated with the pathogenesis of several diseases, including Alzheimer's, Parkinson's, cardiovascular, and autoimmune diseases, as well as neurodegeneration following traumatic brain injury (TBI) (Huang and Wang, 2001). Calpains have also been implicated in many eye and retinal diseases, such as retinitis pigmentosa, retinal detachment, and glaucoma. (Paquet-Durand et al., 2006). Although calpains have been the subject of extensive research, their functions and substrates are not fully defined. Moreover, while the majority of studies have focused on the ubiquitously expressed classical calpains CAPN1 (μ -calpain) and CAPN2 (m-calpain), the functions of the non-classical calpains in health and disease are much less well understood.

Capn5 is grouped with the non-classical calpains because it contains a C2-like domain instead of a penta-EF hand domain (domain 4) at its C-terminus. Capn5 is considered the vertebrate homolog of *C. elegans* *TRA3*, which plays a role in sex determination and mediates a necrotic pathway in neurons. (Aggad et al., 2014). Capn5 has been shown to be the second most abundantly expressed calpain in the mammalian central nervous system (CNS) (Singh et al., 2014). Expression of Capn5 has also been demonstrated in the mammalian retina, where it is found in the outer plexiform layer (OPL) and outer nuclear layer (ONL), specifically the inner and outer segments and synapses of the rod and cone photoreceptors, some ganglion cells and the inner plexiform layer (Schaefer et al., 2016). Within cells, Capn5 has been shown to be

associated with promyelocytic leukemia protein bodies (PML) in the nucleus, which have been implicated in cellular stress response, apoptosis, cellular senescence, and protein degradation (Singh et al., 2014).

Mutations in *CAPN5* are associated with the devastating retinal degenerative disease autosomal dominant neovascular inflammatory vitreoretinopathy (ADNIV) (Wert et al., 2015). ADNIV is a hereditary autoimmune disease of the eye that is characterized by abnormal retinal pigmentation, retinal neovascularization, photoreceptor degeneration, vitreous hemorrhage, intraocular fibrosis, and tractional retinal detachment. As the disease progresses it phenocopies more commonly known ocular diseases such as non-infectious uveitis, glaucoma, diabetic retinopathy and retinitis pigmentosa. (Wert et al., 2015). The three point mutations that have been identified in ADNIV patients (p.Arg243Leu, p.Leu244Pro, and p.Lys250Asn) are located in the calcium-sensitive domain 2 near the active site and are thought to cause the mislocalization of CAPN5 from the cell membrane to the cytosol (Mahajan et al., 2012). Thus, ADNIV is thought to result from gain-of-function mutations in *CAPN5* that lower its threshold for activation by calcium (Wert et al., 2015). However, the precise mechanism whereby mutant CAPN5 causes ADNIV is not well understood. Elucidating the role of CAPN5 in the retina could reveal the underlying pathogenetic mechanisms of ADNIV as well as other retinal degenerative diseases that display similarities to ADNIV.

The normal function of Capn5 during development and in the adult retina is not well understood. Previous studies using two different *Capn5* mutant mouse models yielded conflicting results. In one study, *Capn5* null mice (*Capn5 trn1Nde*) were born viable and fertile, but some mutant offspring were runted and died two months after birth (Franz et al., 2004). In another study, the *Capn5*^{-/-} null mutation (*Capn5 trn1Dgen*) was pre-implantation embryonic lethal (Franz et al., 2004). These conflicting results highlight a need for additional animal models to study Capn5 function. Zebrafish are an ideal model for developmental studies due to their strong genetic homology to humans, completely sequenced genome, and rapid, transparent, external development. Furthermore, unlike mammals, the zebrafish is capable of regenerating all classes of retinal neurons in response to injury or genetic insult. This regenerative response relies on the retinal Müller glia, which are stimulated to dedifferentiate, re-enter the cell cycle, and generate retinal progenitor cells to replace the cells that have been lost (Hitchcock and Raymond, 2004).

In this study, we examined the expression profile of *capn5* during embryonic development and in the adult retina of the zebrafish. The zebrafish has two orthologs of *Capn5* (*capn5a* and *capn5b*; <http://zfin.org/>) and we demonstrate that both are expressed in the CNS and the retina during zebrafish development. We also demonstrate that *Capn5* is expressed in the adult zebrafish retina in a similar pattern to that described for the mammalian retina, however we find that expression of *Capn5* is specific to cone, but not rod, photoreceptors. Finally, we show that *Capn5* is upregulated in response to photoreceptor degeneration and is expressed in the Müller glia following acute light exposure, suggesting that *Capn5* could be playing a role in the regenerative process to retinal damage.

2.3 Materials and methods

2.3.1 Zebrafish lines and maintenance

All zebrafish lines were bred, housed, and maintained at 28.5°C on a 14 hour light:10 hour dark cycle, except where indicated for the light damage experiments. The Tg(XRho:gap43-mCFP) q13 transgenic line (hereafter called XOPS:mCFP) has been previously described (Gross and Perkins, 2008; Morris et al., 2011; Morris et al., 2005). The Tg(3.2TαC:EGFP) transgenic line (TαC:EGFP) has been previously described, (Kennedy et al., 2001) and was generously provided by Susan Brockerhoff (University of Washington, Seattle, WA). The Tg(XIRho:EGFP) transgenic line (hereafter called XOPS:GFP) has been previously described (Fadool, 2003) and was obtained from James Fadool (Florida State University, Tallahassee, FL). Zebrafish were bred, raised and maintained in accordance with established protocols for zebrafish husbandry (Postlethwait et al., 1998). Embryos were anaesthetized with Ethyl 3-aminobenzoate methanesulfonate salt (MS-222, Tricaine, Sigma-Aldrich, St. Louis, MO) and adults were euthanized by rapid cooling as previously described (Wilson et al., 2016). All animal procedures were carried out in accordance with guidelines established by the University of Kentucky Institutional Animal Care and Use Committee (IACUC) and the ARVO Statement for the Use of Animals in Ophthalmic and Vision Research.

2.3.2 RNA extraction, RT-PCR and Real-time quantitative PCR (qPCR)

Total RNA was extracted from whole embryos at selected developmental time points or from the dissected retinas of adult zebrafish using TRIzol reagent (Invitrogen, Grand Island, NY) according to the manufacturer's protocol. The samples were treated with RNase-free DNase I (Roche, Indianapolis, IN) and purified using a chloroform/phenol extraction. The GoScript Reverse Transcriptase System (Promega, Madison, WI) was used to synthesize first strand cDNA from 1µg of the extracted RNA. PCR primers were designed to amplify unique regions of the *capn5a*, *capn5b*, and *atp5h* cDNAs (Eurofins Genomics; www.eurofinsgenomics.com; **Table 2.1**). Faststart Essential DNA Green Master mix (Roche) was used to perform qPCR on a Lightcycler 96 Real-Time PCR System (Roche). The relative transcript abundance was normalized to *atp5h* expression as the housekeeping gene control (Wen et al., 2015) and was calculated as fold-change relative to 4 hours post fertilization (hpf) for developmental expression, and fold-change relative to wild type, untreated adult fish (WT) for the XOPs:mCFP and light damage experiments. RT-PCR and qPCR experiments were performed with three biological replicates and three technical replicates. RT-PCR was performed on a Mastercycler Pro thermocycler (Eppendorf, Westbury, NY). PCR products were visualized on a 1% agarose gel. The sequences for the primers used to produce the PCR products are listed in **Table 2.1**.

2.3.3 Tissue sectioning

Whole embryos and adult retinas were collected as described above and fixed in 4% paraformaldehyde (PFA) at 4°C overnight. Fixed embryos or retinas were cryoprotected in 10% sucrose for a minimum of 8 hours, followed by 30% sucrose overnight at 4°C. Samples were placed into OTC medium (Ted Pella, Redding, CA) and frozen at -80°C for 2 hours. Ten micron-thick tissue sections were cut on a cryostat (Leica CM 1850, Leica Biosystems, Buffalo Grove, IL) and the sections were mounted on gelatin-coated or Superfrost Plus slides (VWR, Randor, PA) and air-dried overnight at room temperature.

2.3.4 Riboprobe synthesis

PCR products from the unique regions of *capn5a* and *capn5b* were cloned into the pGEMT-easy vector (Promega, Madison, WI). Plasmids were linearized using either SpeI or SacII restriction enzymes (NEB, Ipswich, MA). Riboprobes were synthesized from the plasmids by in vitro transcription using either T7 or Sp6 polymerase and a digoxigenin (DIG) labeling kit (Roche Applied Science, Indianapolis, IN). The sequences for the primers used to produce the PCR products are listed in **Table 2.1**.

2.3.5 Fluorescent in situ hybridization (FISH)

FISH was performed essentially as previously described (Forbes-Osborne et al., 2013). Briefly, embryos or adult retinas were fixed and sectioned as described above. Sections were post-fixed in 1% PFA and rehydrated in PBST. All solutions were prepared with diethyl pyrocarbonate (DEPC)-treated water. Hydrated sections were permeabilized for 10 minutes with 1µg/ml proteinase K, then acetylated in triethanolamine buffer containing 0.25% acetic anhydride (Sigma-Aldrich, Saint Louis, MO) and rinsed in DEPC treated water. Sections were incubated with DIG-labeled riboprobes (final concentration of 3 ng/µl) in hybridization buffer at 65°C in a sealed humidified chamber for at least 16 hours. After hybridization the sections were rinsed in 5x SSC followed by a 30 min 1xSSC/ 50% formamide wash. 1% H₂O₂ was used to quench the peroxidase activity and the sections were blocked using 0.5% PE blocking solution (Perkin Elmer Inc, Waltham, MA) for a minimum of 1 hour. Sections were incubated with anti-DIG-POD fab fragment (Roche, Indianapolis, IN) at 4°C overnight. The TSA plus Cy3 Kit (Perkin Elmer Inc, Waltham, MA) was used for probe detection. The sections were counterstained with 4', 6-diamidino-2-phenylindole (DAPI, 1:10,000 dilution, Sigma-Aldrich), mounted in 60% glycerol, and imaged on an inverted fluorescent microscope (Nikon Eclipse Ti-U, Nikon instruments, Melville, NY) using a 20x or 40x objective or a Leica SP8 DLS confocal/digital light sheet system (Leica Biosystems, Nussloch, Germany) using a 40x or 60x objective. At least 3 retinas or 6 embryos and a minimum of 6 sections were analyzed for each timepoint and probe.

2.3.6 Whole-mount in situ hybridization

Embryos were manually dechorionated, collected at selected developmental time points (18, 24, 48 hpf, 72 hpf and 120 hpf) and fixed as described above. WISH was performed as previously described (Forbes-Osborne et al., 2013). DIG-labeled riboprobes (3 ng/ μ l) were hybridized to the samples overnight at 60°C in hybridization buffer. After washing and blocking, samples were incubated overnight at 4°C with an anti-DIG-AP antibody (Roche, diluted 1:2000 in blocking solution). The next day, the embryos were washed and equilibrated in NTMT buffer followed by coloration with 4-nitro blue tetrazolium (NBT, Roche) and 5-bromo-4chloro-3-indolyl-phosphate, 4-toluidine salt (BCIP, Roche) in NTMT buffer. A stop solution (PBS pH 5.5, 1mM EDTA) was used to end the coloration reaction and embryos were placed in 40% glycerol for imaging on a dissecting microscope (Digital Sight Ds-Fi2, Nikon instruments). Six embryos were analyzed per time point for each probe.

2.3.7 Immunohistochemistry

Immunohistochemistry was performed as previously described (Forbes-Osborne et al., 2013). Primary antibodies used in this paper are described in **Table 2.2**. Alexa Fluor 488 goat anti-mouse, 488 goat anti-rabbit, 546 goat anti-rabbit, and 546 goat anti-mouse secondary antibodies (Molecular Probes, Invitrogen) were all used at 1:200 dilution. Nuclei were visualized by counterstaining with DAPI (1:10,000 dilution). Samples were mounted in 60% glycerol in PBS. Images were taken at 20x and 40x on an inverted fluorescent microscope (Eclipse Ti-U, Nikon instruments). At least six sections were analyzed on each slide and for each antibody.

2.3.8 Light damage experiment

Acute light damage (LD) was performed essentially as previously described (Vihtelic and Hyde, 2000b). Briefly, 18 month old, albino zebrafish were dark adapted for 14 days. Fish were

then placed in a 2.8 liter clear plastic tank surrounded by four 250W halogen bulbs placed 7 inches away, which collectively produced 20,000 lux of light. A bubbler, cooling fan, and water circulatory system were used to maintain the water level and keep the temperature under 32°C. The fish were maintained in constant light for 3 days, at which point they were returned to normal lighting conditions. Fish were collected at various time points during and after light damage (LD), and the left eyes were dissected for cryosectioning and in situ hybridization, whereas the right eyes were dissected and processed for RNA extraction followed by RT-PCR and qPCR. The fish were collected at 3 days LD, and at 2 and 7 days post LD. The light damage experiment was repeated three times, and three fish were collected for each time point.

2.3.9 Quantification and statistical analysis

For comparisons between groups, statistical significance was determined using the Student's t-test with $p < 0.05$ considered as significant. For all graphs, data are represented as the mean +/- the standard deviation (s.d.).

2.4 Results

2.4.1 Developmental expression of zebrafish *capn5* orthologs

While some studies have examined the expression and function of *Capn1* and *Capn2* orthologs in zebrafish (Lepage and Bruce, 2008) the developmental expression pattern of *Capn5* has not previously been reported. Through BLAST searches of zebrafish genome databases we identified two, full-length cDNA sequences with significant sequence similarity to human *CAPN5*. Due to an ancient genome duplication that occurred during the evolution of teleost fishes (Amores et al., 1998), zebrafish often possess two orthologs of single-copy mammalian genes. The two zebrafish orthologs of *CAPN5*, hereafter referred to as *capn5a* and *capn5b*, are located on zebrafish chromosomes 18 and 21, respectively. The predicted zebrafish *Capn5a* protein is 68% identical and 81% similar to human *CAPN5*, whereas zebrafish *Capn5b* is 71% identical and

83% similar. We identified unique regions of each cDNA sequence and designed PCR primers. We extracted RNA from embryos at selected developmental time points (4, 18, 24, 48, 72, and 120 hours post fertilization), and performed RT-PCR followed by agarose gel electrophoresis to detect expression of *capn5a* and *capn5b*. Expression of both genes was detectable starting at 4 hours post fertilization (hpf), indicating *capn5* is maternally deposited, and both *capn5a* and *capn5b* were expressed at every subsequent developmental timepoint tested (**Figure 2.1A**). To quantify the expression of *capn5a* and *capn5b*, we performed quantitative real-time RT-PCR (qPCR). For both *capn5a* and *capn5b*, we observed a gradual increase in expression as development progressed (**Figure 2.1B**). With the exception of 4 hpf, expression of *capn5a* was consistently higher than *capn5b* (**Figure 2.1B**). From these data, we conclude that *capn5a* and *capn5b* are expressed during zebrafish embryonic development and that *capn5a* is expressed more strongly during development than *capn5b*.

In the adult mouse, *Capn5* expression has been identified in many tissues including the brain, eye, uterus, and prostate (Arthur et al., 2000; Dear and Boehm, 1999; Dear and Boehm, 2001; Singh et al., 2014; Waghray et al., 2004); however, less is known about the expression pattern of *Capn5* during vertebrate embryonic development. To address this question, we performed whole-mount in situ hybridization (WISH) with unique probes for *capn5a* and *capn5b* at selected developmental timepoints in the zebrafish. At 18 hpf, *capn5a* expression was detected in the optic vesicles, developing diencephalon, mesencephalon and hindbrain (**Figure 2.1C-C'**). *Capn5b* expression was present in the diencephalon, mesencephalon, and hindbrain, but was not detected in the optic vesicles at 18 hpf (**Figure 2.1E**). At 24 hpf, expression of *capn5a* and *capn5b* is was observed in the developing zebrafish brain, more specifically the tectum, hindbrain, cerebellum and floor-plate. Expression of *capn5a* was also observed in the hatching gland (**Figure 2.1D-F**). We did not detect expression of *capn5a* or *capn5b* in the developing eye at 24, 36 or 48 hpf (data not shown). We conclude that *capn5a/b* are expressed in the developing zebrafish brain and in the optic vesicle prior to its invagination to form the bi-layered optic cup.

Figure 2. 1 *capn5a* and *capn5b* are expressed in the developing CNS of the zebrafish

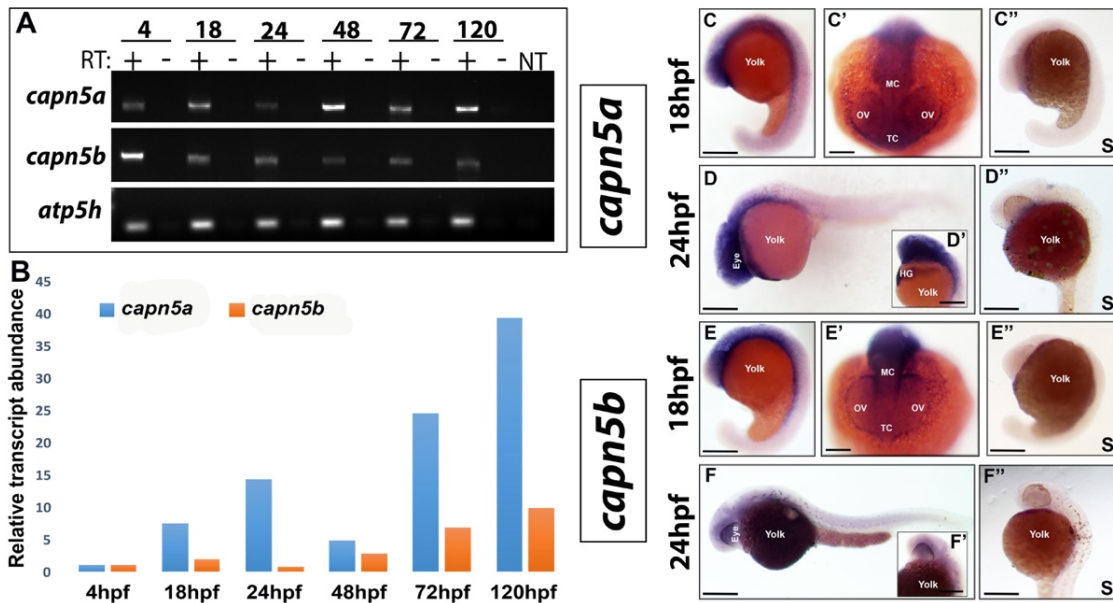


Figure 2.1 *capn5a* and *capn5b* are expressed in the developing brain of zebrafish. A) RT-PCR for *capn5a* and *capn5b* expression during development (24, 48, 72, and 120 hpf). *atp5h* expression is shown as housekeeping gene control. RT, reverse transcriptase; NT, no template. B) qPCR representation of fold-change in mRNA expression relative to 24 hpf. C-C'') Whole-mount in situ hybridization (WISH) of *capn5a* at 18hpf. Strong *capn5a* expression was observed in the optic vesicles and brain. WISH with a control sense probe is shown C'. D-D'') WISH for *capn5a* at 24hpf. Strong expression of *capn5a* was detected in the brain and hatching gland. Control sense probe is shown D'' E-E'') WISH for *capn5b* at 18hpf. Expression was observed in parts of the developing brain but not the optic vesicles. Sense probe shown in E''. F-F'') WISH for *capn5b* at 24 hpf. Modest expression of *capn5b* was observed in the brain. (OV, optic vesicle; fp, floor plate; T, Telencephalon; mc, mesencephalon; c, cerebellum; HG, hatching gland; H, hindbrain; r, retina. Scale bars = 50µm.)

Figure 2. 2 Capn5 is expressed in differentiated PR of the larval zebrafish retina

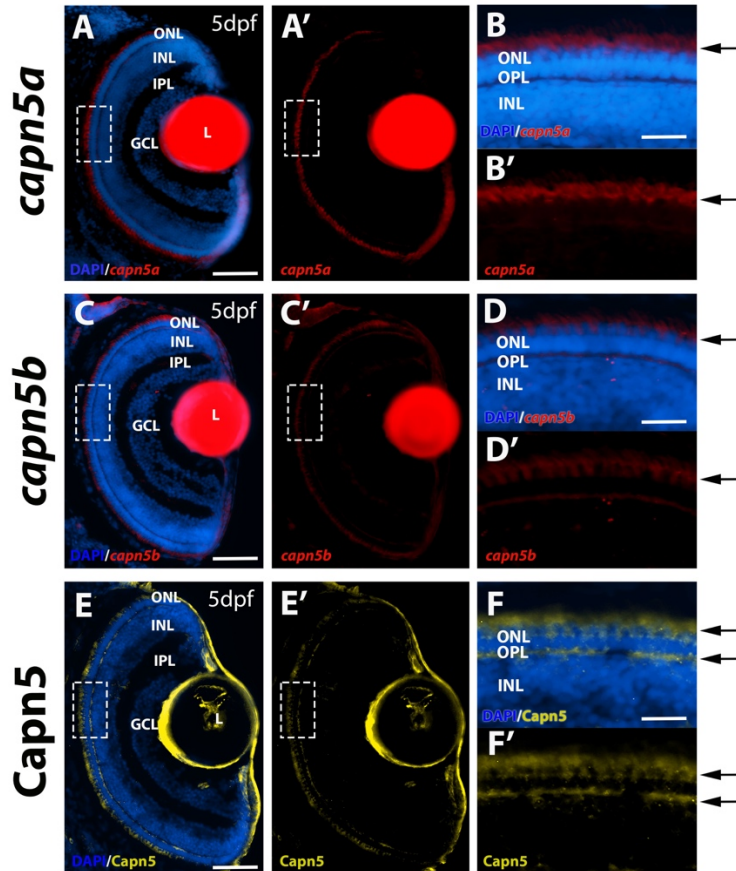


Figure 2.2 Capn5 is expressed in differentiated photoreceptors of the larval zebrafish retina. A-B') Fluorescent in situ hybridization (FISH) showing expression of *capn5a* in the zebrafish retina at 5 dpf. Expression was detected in the outer nuclear layer (arrows). B-B' show an enlarged image of the boxed area in A-A'. C-D') FISH for expression of *capn5b* in the 5 dpf zebrafish retina. Expression was also detected in the outer nuclear layer (arrows). D-D' show an enlarged image of the boxed area in C-C'. E-F') Immunohistochemistry (IHC) showing expression of Capn5 in the outer plexiform layer and inner segments of the zebrafish photoreceptors at 5 dpf (arrows). F-F' show an enlarged image of the boxed region in E-E'. L, lens (The red fluorescence in the Lens is non-specific autofluorescence); INL, inner nuclear layer; OPL, outer plexiform layer; GCL, ganglion cell layer; ONL, outer nuclear layer. Scale bars = 50 μ m in A,C and E and 100 μ m in B,D and F.

To further investigate the expression of *capn5a* and *capn5b* in the zebrafish retina, we used fluorescent in situ hybridization (FISH) with *capn5a/b* probes on cryosections of zebrafish larvae at 120 hpf (5 days post fertilization, dpf). At 5 dpf, all of the retinal cell types have differentiated and zebrafish larvae display visually evoked behaviors. At this timepoint expression of both *capn5a* and *capn5b* was detected across the photoreceptor cell layer, in the region of the photoreceptor inner segments (**Figure 2.2A-D'**). In a previous study, Schaefer et al. demonstrated CAPN5 antibody localization to photoreceptor inner segments and synaptic terminals in adult mouse retinal sections (Schaefer et al., 2016). We used the same CAPN5 antibody for immunohistochemistry (IHC) on 5 dpf zebrafish retinal sections. This antibody should detect both Capn5a and Capn5b proteins. Similar to the previous study in mouse retina, we detected Capn5a/b protein expression in the photoreceptor inner segments and the outer plexiform layer (OPL) where the photoreceptor synaptic terminals are located. (**Figure 2.2E-F'**). We detected a similar pattern of expression of *capn5a/b* across the photoreceptor cell layer of the retina as early as 3 dpf (when the cone photoreceptors have largely finished differentiating), but not prior to this time point (data not shown). Therefore, we conclude that Capn5a/b is expressed in differentiated photoreceptors in the zebrafish retina. Furthermore, the lack of expression of *capn5a/b* in the retina prior to 3 dpf suggests that Capn5 plays a role in photoreceptor cell maintenance rather than development or specification.

2.4.2 Capn5 expression is cone specific in the adult zebrafish retina

To further analyze the expression of *capn5a/b* in the adult zebrafish retina we performed FISH with *capn5a/b* probes on sections of adult wild type zebrafish retina. Expression of *capn5a* and *capn5b* was again observed in the photoreceptor inner segments (**Figure 2.3**). The rod and cone photoreceptors in the adult zebrafish retina are highly tiered and morphologically distinguishable, such that (moving from the vitreal to scleral direction), the round rod nuclei are located most proximal to the OPL, followed by the UV and blue cones, then the ellipsoid red/green double cone nuclei interspersed with rod inner segments, the red/green cone outer segments, and finally the rod outer segments located most proximal to the RPE (Fadool, 2003). Interestingly, the FISH expression pattern for *capn5a/b* appeared to localize

primarily to the cone, but not rod inner segments. To determine whether this was the case, we used the T2C-GFP transgenic line, in which GFP is expressed specifically in the cones (Kennedy et al., 2001) and performed FISH for *capn5a* in combination with IHC for GFP. We observed a perfect co-localization of GFP and *capn5a* expression (**Figure 2.3D-D''**). We then performed the same experiment using the XOPS:GFP transgenic line, which expresses GFP specifically in the rods (Fadool, 2003). We did not observe any co-localization of the rod GFP signal and *capn5a* expression (**Figure 2.3E-E''**), which we confirmed using confocal microscopy (**Figure 2.3F-F''**). *Capn5b* displayed the same co-localization pattern as *capn5a* (not shown). We confirmed the expression of Capn5 protein in the adult retina using the CAPN5 antibody (**Figure 3C-C''**). Capn5 expression was observed in the cone inner segments, outer segments and in the synaptic terminals of the adult retina. Taken together, these results suggest that, similar to mammals, zebrafish Capn5 is expressed in retinal photoreceptors. However, zebrafish Capn5 expression appears to be cone-specific, which has not been reported for Capn5 in the mammalian retina.

Figure 2. 3 Capn5 is expressed specifically in the cone PR of the adult zebrafish retina

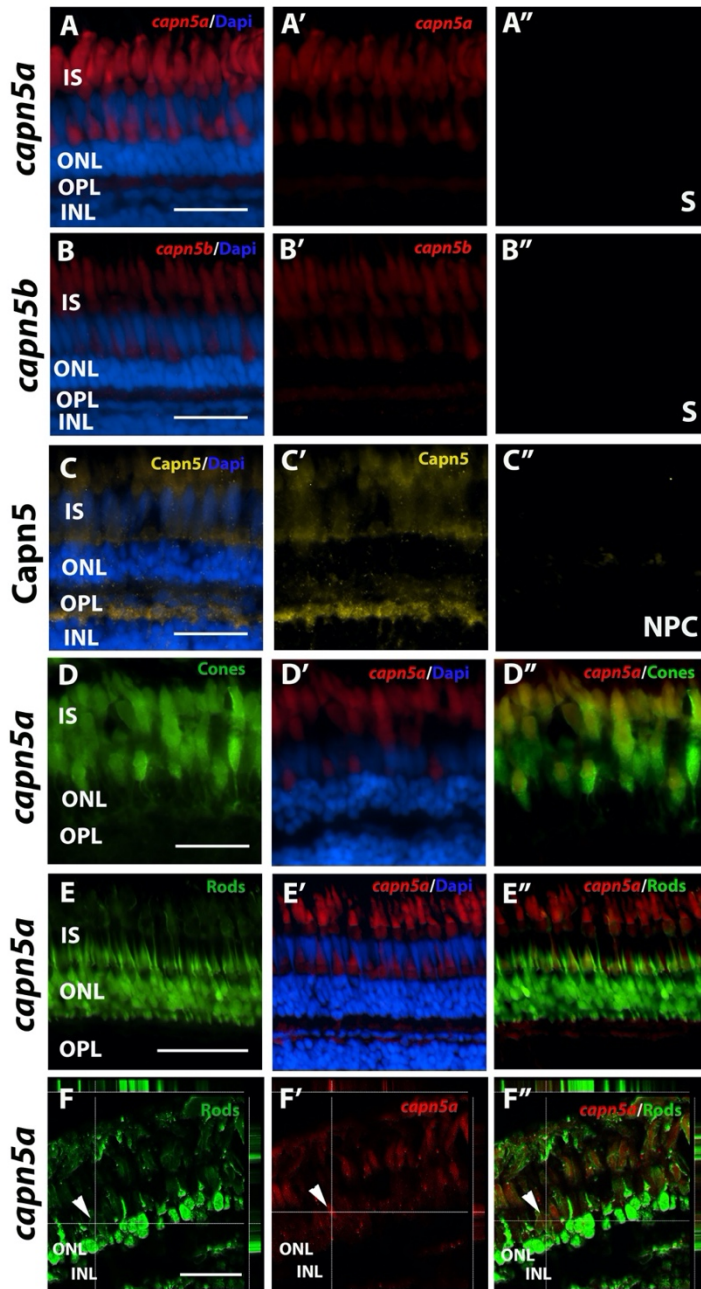


Figure 2.3 Capn5 is expressed specifically in the cone photoreceptors of the adult zebrafish retina. A-B'') Fluorescent in situ hybridization (FISH) showing expression of *capn5a* and *capn5b* in the adult (WT) retina; expression was seen in the inner segments of the cones. A'' and B'' show sense probe controls. C-C'') Immunohistochemistry (IHC) for Capn5 (both Capn5a and Capn5b). Expression was observed in the photoreceptor inner segments and in the outer plexiform layer. C'' shows control image with no primary antibody. D-D'') Co-localization of *capn5a* with a cone-specific marker. Combined FISH for *capn5a* and IHC for GFP on the TαC:GFP transgenic background demonstrates strong co-localization of *capn5a* expression with cone-specific GFP expression. E-E'') Combined FISH for *capn5a* and IHC for GFP on the XOPS:GFP transgenic background demonstrates a lack of co-localization of *capn5a* expression with rod-specific GFP expression. F-F'') Confocal microscopy imaging of combined FISH for *capn5a* and IHC for GFP on the XOPS:GFP transgenic background; the orthogonal view confirms there is no co-localization of rod specific GFP and *capn5a* expression. INL, inner nuclear layer; OPL, outer plexiform layer; ONL, outer nuclear layer; IS, inner segments; S, sense probe; NPC, no primary antibody control). Scale bars, 50 μm in E and 100 μm in A-D and F.

2.4.3 Capn5a expression is increased in response to rod photoreceptor degeneration

Figure 2. 4 Expression of Capn5 is elevated in the adult XOPS:mCFP retina

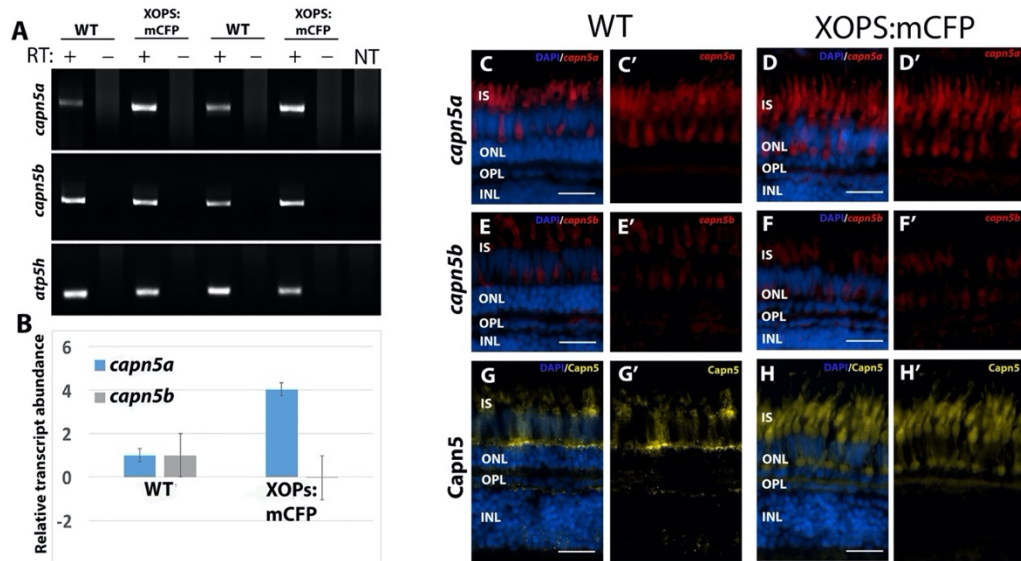


Figure 2.4 Expression of Capn5 is elevated in the adult XOPS:mCFP retina. A) RT-PCR for *capn5a* and *capn5b* expression in wild type (WT) and XOPS:mCFP retinas. *Capn5a* and *capn5b* are both expressed in the adult WT retina and *capn5a* levels are increased in the XOPS:mCFP retina. RT, reverse transcriptase; NT, no template control. B) qPCR for *capn5a* and *capn5b* in WT and XOPS:mCFP adult retina; a 4-fold increase of *capn5a* expression was observed in the XOPS:mCFP retina compared to WT. C-C') Fluorescent in situ hybridization (FISH) showing expression of *capn5a* in the adult (WT) retina; expression was seen in the inner segments of the cones. D-D') FISH showing expression of *capn5a* in the XOPS:mCFP retina; expression in the cone inner segments appears to be more intense than in WT. E-E') FISH for *capn5b* in the adult WT retina; modest expression was detected in the inner segments. F-F') FISH for *capn5b* in the XOPS:mCFP retina; expression levels appears similar to WT. G-G') Immunohistochemistry (IHC) for Capn5 (a and b) in the WT adult retina; expression was detected in the outer plexiform layer (OPL) and in the cone inner segments (IS). H-H') IHC for Capn5 in the XOPS:mCFP retina; increased expression was detected in the OPL and IS. INL, Inner nuclear layer; OPL, outer plexiform layer; ONL, outer nuclear layer; IS, photoreceptor inner segments. Scale bars, 100 μ m.

As described above, gain of function mutations in *CAPN5* have been associated with ADNIV, an autosomal dominant disease that eventually leads to the photoreceptor degeneration and retinal detachment (Bassuk et al., 2015; Mahajan et al., 2012; Mahajan et al., 2010; Singh et al., 2014; Wert et al., 2014). Moreover, other members of the calpain family have been implicated in apoptosis, necrosis, and photoreceptor degeneration (Azuma and Shearer, 2008; Mizukoshi et al., 2010; Paquet-Durand et al., 2006). To determine whether Capn5 expression is altered in response to photoreceptor degeneration in zebrafish, we evaluated the expression of *capn5a* and *capn5b* in the XOPs:mCFP transgenic line, which displays continual degeneration and regeneration of rod (but not cone) photoreceptor cells (Morris et al., 2005). RT-PCR and qPCR were performed on mRNA prepared from dissected wild type (WT) and XOPs:mCFP retinas. In both experiments, we observed elevated expression of *capn5a* in the XOP:mCFP retinas compared to WT, whereas *capn5b* expression levels remained unchanged (**Figure 2.4A-B**). Next, we performed FISH on retinal cryosections from WT and XOPs:mCFP zebrafish with *capn5a/b* probes. We found that the expression patterns for both *capn5a* and *capn5b* were similar in the WT and the XOPs:mCFP retina; however, the signal for *capn5a* was stronger in XOPs:mCFP cones than in WT, whereas *capn5b* expression levels did not change (**Figure 4C-H'**). These results indicate that the cone-specific expression of *capn5a* is upregulated in response to rod photoreceptor degeneration in zebrafish.

2.4.4 Capn5 expression increases in response to acute light damage

Our results indicate that cone-specific expression of Capn5 is induced in the XOPs:mCFP transgenic line. However, in the XOPs:mCFP retina, rod photoreceptor degeneration does not result in any secondary degeneration of the cones (Morris et al., 2011; Morris et al., 2005). This led us to ask whether upregulation of Capn5 in cones serves a cell-autonomous protective function, or whether it plays a non-cell autonomous role in promoting rod degeneration or regeneration. To begin to address this question, we used an acute light damage approach, which allowed us to temporally separate photoreceptor degeneration and regeneration. We adopted the light damage protocol described by Vithelic and Hyde, (Vithelic and Hyde, 2000b) in which

dark adapted albino zebrafish are exposed to 20,000 lux of constant light for three days, followed by 7 days of recovery in normal lighting conditions. The acute light exposure causes almost total ablation of the rods and extensive damage to the cones in the dorsal retina, and less severe damage to rods and cones in the ventral retina (Vihtelic et al., 2006). This is accompanied by de-differentiation and proliferation of a subset of the Müller glia, which produce retinal progenitor cells that migrate to the ONL to replace the degenerated photoreceptors. Zebrafish were collected prior to the start of the acute light damage, on the third day of light damage (LD), two days post-LD, and seven days post-LD, and the retinas were dissected and processed as described above for RT-PCR, qPCR, FISH and IHC.

RT-PCR and qPCR revealed a 12-fold upregulation of *capn5a* expression during photoreceptor degeneration (LD) followed by a return to WT levels by 7 days post-LD; we saw no change in *capn5b* expression during the entire light damage experiment (**Figure 2.5A-B**). To determine whether other calpains are also upregulated in response to retinal light damage, we analyzed the expression of *capn1* and *capn2* by RT-PCR (data not shown) and qPCR. We observed no significant increase in expression of *capn1a/b* or *capn2a/b* during light damage. *Capn1a/b* expression also did not change at either time point post-LD. However, we did observe a 3.5-fold increase in expression of *capn2a/b* at two and seven days post-LD (**Figure S2.1**). Thus, the increase in expression observed during light damage is specific to *capn5a*.

We performed FISH to characterize the expression pattern of *capn5a/b* in the retina during and following light damage. After three days of LD, the ONL was severely disrupted, with a significant reduction in the number of rod and cone nuclei. This was accompanied by novel expression of *capn5a* in the inner nuclear layer (INL) and increased expression in the remaining cone photoreceptors (**Figure 2.5D-D'**). By 7 days post-LD, the number of rod and cone nuclei had increased and the ONL appeared more organized. At this time point, expression began to return to the ONL only (data not shown) and by 7dpLD expression of *capn5a* was no longer observed in the INL and the photoreceptor expression resembled the pre-LD pattern (**Figure 2.5E-E'**). Expression of *capn5b* was restricted to the photoreceptor layer throughout the light damage experiment (**Figure 2.5F-H'**). Taken together, we conclude that *capn5a* expression increases during photoreceptor degeneration in response to acute light damage, with the novel INL expression unique to *capn5a*. Meanwhile, *capn5b* expression does not change in response to light-induced photoreceptor degeneration and regeneration.

Figure 2.5 Capn5a expression is induced in response to acute light damage

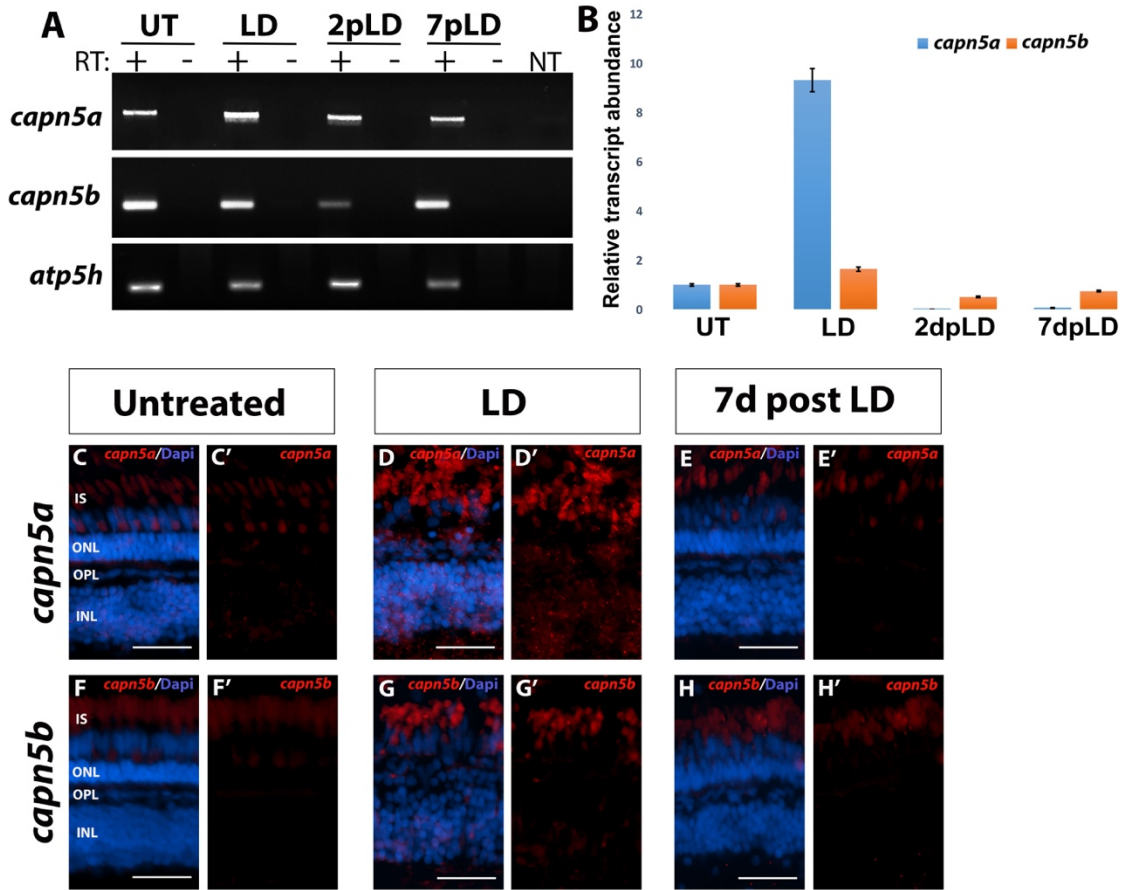


Figure 2.5 Capn5a expression is induced in response to acute light damage. A) RT-PCR of *capn5a* and *capn5b* expression during and following acute light damage. A significant increase in expression of *capn5a* was observed after 3 days of LD (LD) which returned to WT levels by 2dpLD. *Capn5b* expression did not change during LD. RT, reverse transcriptase; NT, no template control. B) qPCR qPCR for *capn5a* and *capn5b* during and following light damage. A 12-fold increase in *capn5a* expression was observed in the LD retina compared to untreated retina, followed by a significant decrease in expression post LD. *Capn5b* expression did not change during or after LD. C-E') Fluorescent in situ hybridization (FISH) for *capn5a* in untreated retina (UT), during light damage (LD), and post light damage (7dpLD). Whereas *capn5a* expression in the UT retina was confined to the outer plexiform layer (OPL) and cone inner segments (IS), *capn5a* expression in the LD retina was seen in the inner nuclear layer (INL) as well as the OPL and IS. F-H') FISH for *capn5b* in the UT, LD, 7dpLD retina. The *capn5b* expression pattern did not change during or after LD. INL, inner nuclear layer; OPL, outer plexiform layer; ONL, outer nuclear layer; IS, photoreceptor inner segments. Scale bars, 50 μ m.

2.4.5 Expression levels of Capn5 correlates with the extent of photoreceptor degeneration

As mentioned above, acute light damage results in greater photoreceptor degeneration in the dorsal versus the ventral retina (Vihtelic et al., 2006). This regional difference allowed us to determine whether the extent of Capn5 expression is correlated with the level of photoreceptor damage. Using the Capn5 antibody (which detects both Capn5a and Capn5b), we compared Capn5 protein expression in the dorsal and ventral retina by IHC prior to LD, at 3 days of LD, and at 7 days post-LD. IHC for cone and rod specific markers was used to assess the amount of damage induced in the retina. In untreated retinas, as we observed previously, Capn5 was expressed in the cone photoreceptor inner segments and synaptic terminals (**Figure 2.6A-F'**). Capn5 expression appeared to be stronger in the dorsal retina than in the ventral retina (**Figure 2.6E-F'**). After three days of LD rod photoreceptors were completely ablated and cone photoreceptors were reduced and severely truncated in the dorsal retina (**Figure 2.6G-I'**). In the dorsal region, Capn5 expression was upregulated not only in the photoreceptor cell layer, but also in a subset of cells in the INL with a morphology suggestive of Müller glia (**Figure 2.6K-K'**). In contrast, in the ventral retina the rods were reduced and severely distorted, but the cones were much less damaged. In this region, Capn5 expression remained strong in the photoreceptor layer but was much weaker in the INL (**Figure 2.6H-L'**)

Finally, at 7 days post-LD, both rods and cones reappeared in the dorsal retina, and were very abundant in the ventral retina (**Figure 2.6M-P'**). This was accompanied by a disappearance of Capn5 expression from the INL and a decrease in expression in the photoreceptor layer in the dorsal retina (**Figure 2.6Q-Q'**), as well as a return to pre-LD expression levels in the ventral retina (**Figure 2.6R-R'**).

We conclude that photoreceptor degeneration caused by acute light damage induces Capn5 expression in proportion to the level of damage inflicted. Moreover, when photoreceptor degeneration is severe, Capn5 expression is upregulated in a subset of cells with a Müller glia morphology as well as in the ONL.

Figure 2. 6 Increase in Capn5 expression correlates with the magnitude of retinal damage

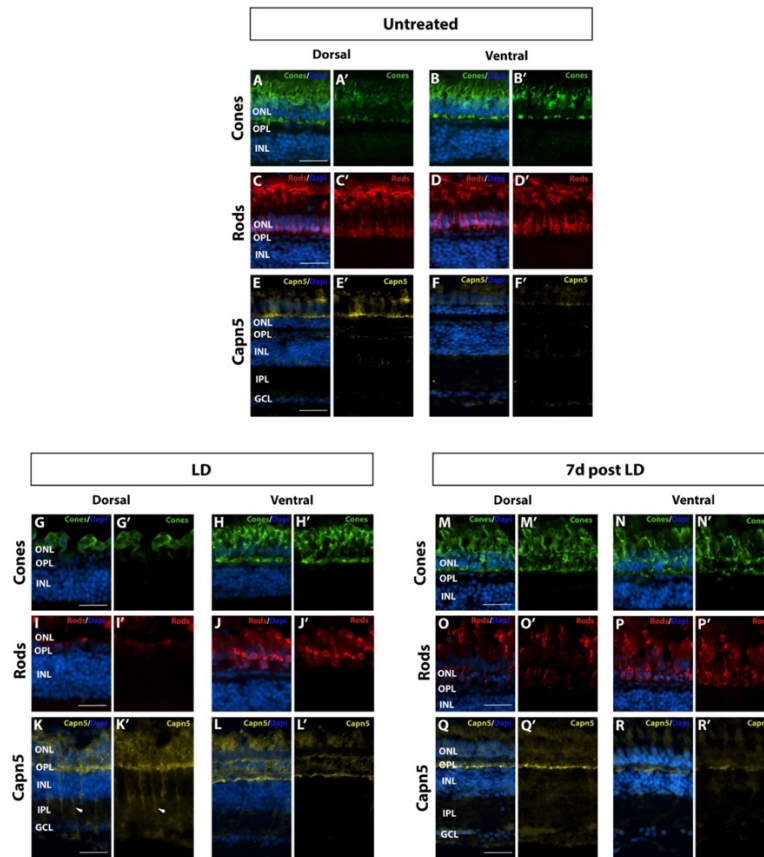


Figure 2.6 Increase in Capn5 expression correlates with magnitude of retinal damage. A-B') Dorsal and ventral expression of cone specific marker Zpr-1 in undamaged (UT) retina. C-D') Dorsal and ventral expression of rod specific marker 4C12 in the UT retina. E-F') IHC for dorsal and ventral Capn5 expression in the UT retina; Capn5 expression is stronger in the dorsal retina (E-E') compared to the ventral retina (F-F'). G-H') Dorsal and ventral cone damage after acute light exposure. There is a significant decrease in the amount of cone photoreceptors in the dorsal retina compared to the ventral retina. (I-J') Dorsal and ventral rod damage after acute light exposure. Rods are almost totally ablated in the dorsal retina, with more moderate damage observed in the ventral retina. (K-L') IHC for Capn5 expression in the LD retina. Capn5 is strongly upregulated in the inner nuclear layer and surviving cones in the dorsal retina, and more modestly upregulated in the ventral retina. (M-N') Dorsal and ventral cones have mostly recovered by 7 days post LD. O-P') At 7 days post LD rods are regenerating, with an more rods observed in the ventral compared to the dorsal retina. Q-R') IHC for Capn5 expression in the 7dpLD retina. Expression of Capn5 is similar to that of the undamaged retina. GCL, ganglion cell layer; INL, inner nuclear layer; OPL, outer plexiform layer; ONL, outer nuclear layer; Scale bars = 50 μ m.

2.4.6 Photoreceptor degeneration induces the expression of *capn5* in the Müller Glia

Finally, to confirm the identity of the Capn5-expressing cells in the INL of light damaged retinas, we performed co-localization experiments with the Capn5 antibody and the Zrf-1 antibody, which labels the processes of the Müller glia. In untreated retinas, we were unable to detect Capn5 expression in the INL and there was no co-localization of Capn5 expression with the Müller glia marker (**Figure 2.7A'-C'**). In contrast, after three days of LD, we observed an upregulation of Capn5 in the INL, and an increase in Zrf-1 staining indicative of the reactive gliosis that occurs in response to acute retinal damage (Bernardos et al., 2005a). Moreover, we observed strong co-localization of the Capn5 signal with Zrf-1 (**Figure 2.7D-F'**). These results demonstrate that Capn5 is induced in Müller glia in response to photoreceptor degeneration.

Figure 2. 7 *Capn5a* is expressed in the Müller Glia in response to acute light damage

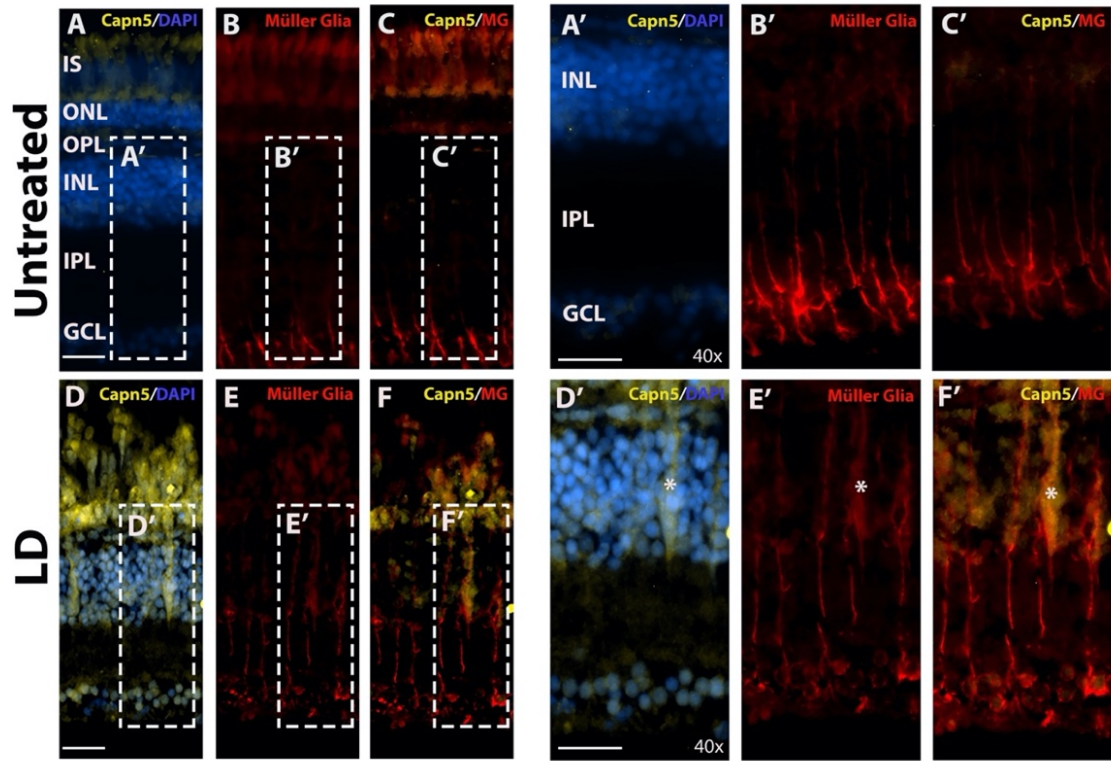


Figure 2.7 *capn5a* is expressed in the Müller glia in response to acute light damage. (A-C') Immunohistochemistry (IHC) for Capn5 expression (A) and the Müller glial marker Zrf-1 (B) in the undamaged (UT) adult retina. No co-localization of Capn5 and Müller cells is observed. A'-C' show an enlarged image of the boxed regions in A-C. D-F) IHC for Capn5 and Müller glia in the LD retina. Capn5 expressed in induced in the INL, where is co-localizes with reactive Müller glia (asterisk). D'-F' show enlarged images of the boxed regions in E-F. GCL, Ganglion cell layer; IPL, inner plexiform layer; INL, inner nuclear layer; OPL, outer plexiform layer; ONL, outer nuclear layer; IS, photoreceptor inner segments. Scale bars, 100 μ m in A-F and 500 μ m in A'-F'.

2.5 Discussion

Although mutations in CAPN5 are associated with a severe retinal degenerative disease, very few studies have described the developmental expression pattern of *Capn5*. In the mouse, developmental expression of *Capn5* was suggested to be relatively low (Dear and Boehm, 1999), with specific sites of expression noted in the developing thymus and the neurons of the sympathetic and dorsal root ganglia (Dear and Boehm, 1999; Nehls et al., 1996). Further in situ hybridization studies on embryonic tissue sections revealed *Capn5* expression in the developing mouse brain and in epithelial cells surrounding several tissues (Dear and Boehm, 2001; Franz et al., 2004). In our study, we found that *Capn5* is expressed in the developing brain at 18 hpf, and its expression increases throughout embryogenesis. We detected expression of *Capn5* in the mesencephalon, telencephalon and optic vesicles at 18 hpf, and the hindbrain and cerebellum at later stages. This expression pattern supports a role for *Capn5* during vertebrate brain development.

Cell death is a common and often essential process throughout embryonic development (Jacobson et al., 1997), and calpains have been implicated in mediating cell death pathways. Calpain 1 has been shown to cleave procaspase-12, activating caspase-12, and initiating cell death (Nakagawa and Yuan, 2000). In another study, calpain 2 was shown to mediate the cleavage of Atg5 switching the cell death pathway from autophagy to apoptosis (Dutt et al., 2006; Huang and Wang, 2001). Given that calpains are thought to modify a wide variety of target substrates, we hypothesize that *Capn5* plays a role in mediating cell death pathways in the nervous system during embryonic development.

To our knowledge, there are no published studies analyzing the expression of *Capn5* during retinal development. Since mutations in *Capn5* have been shown to cause the retinal degenerative disease ADNIV (Bassuk et al., 2015), elucidating the expression of *Capn5* during retinal development is imperative. Our data reveal that in the zebrafish retinal expression of *Capn5* is detectable in photoreceptors at 72 hpf, a time point at which the majority of cells have exited the cell cycle and differentiated. This indicates that *Capn5* is not needed for the development or specification of photoreceptors, but rather that *Capn5* is important for mature photoreceptor function or maintenance.

Previous studies have analyzed the expression of Capn5 in the adult human and rat retina, identifying protein expression in the outer nuclear layer, the outer plexiform layer, and the inner segments of the photoreceptors, as well as lower expression in some ganglion cells and the inner plexiform layer (Singh et al., 2014). Co-localization of Capn5 in the outer plexiform layer (OPL) with PSD95 expression, a marker for neural synaptic densities, coupled with the detection of Capn5 in the synaptic membrane by Western blot, indicated that Capn5 is expressed in the photoreceptor synapses. More specifically, expression was identified in both the outer segment and synaptic fractions of rod photoreceptors from mouse retina (Schaefer et al., 2016). In our study, we found that Capn5 is also expressed in mature photoreceptors in the wild type adult zebrafish retina, however its expression appears to be cone specific. We observed *capn5* mRNA expression in the inner segments of the cone photoreceptors, and analysis of protein expression by immunohistochemistry identified expression in the inner segments and the photoreceptor synaptic terminals, which is consistent with the mammalian expression pattern retina (Schaefer et al., 2016).

Previous studies of Capn5 expression in the mouse and human retina did not report whether Capn5 expression was associated with a specific photoreceptor subtype. The zebrafish possesses a cone-rich retina with each of the four spectral subtypes having distinct morphologies, making them easily identifiable in tissue sections. We found, using both FISH and immunohistochemical analyses, that Capn5 is not expressed in the rod photoreceptors of the zebrafish. It will be interesting to determine whether mammalian Capn5 is also expressed primarily in cones, or whether there are species-specific differences in its localization.

Using a genetic model of rod-specific degeneration and regeneration (Morris et al., 2005), we found that the cone-specific expression of Capn5 increases in response to rod degeneration. This is intriguing because the cone photoreceptors in the XOPs-mCFP zebrafish do not degenerate secondary to the rod degeneration, as is typically observed in other photoreceptor degeneration and disease models (Morris et al., 2005). This raises the question: Is Capn5 playing an anti-apoptotic role in the cone photoreceptors and protecting them from the residual effects of the rod degeneration?

Using an acute light-damage paradigm, which results in almost total rod photoreceptor loss and some cone photoreceptor damage, we found that there is a large increase in Capn5 expression during the acute light damage phase that correlates with the amount of

photoreceptor damage produced. In the zebrafish retina, the cones are much more resistant to the toxic effects of acute light exposure. Therefore, induction of Capn5 in cones in response to acute light damage could indicate a protective role for this protein during photoreceptor degeneration.

How do our data fit into the context of previously described functions of calpains? The role of calpains in regulating cell death pathways such as apoptosis, programmed cell death and necrosis has been extensively explored (Lu et al., 2002), with a focus on their function as either pro- or anti-apoptotic proteases. It has been shown that calpains play a pro-apoptotic role in the presence of a wide variety of stimuli. For example, in fibroblasts overexpression of Calpastatin, the endogenous calpain inhibitor, protected cells from okadaic acid induced apoptosis (Chi et al., 1999). Depletion of calpastatin in neutrophils promoted cell death during cycloheximide induced apoptosis (Squier et al., 1999). Evidence has also been presented that calpains play a pro-apoptotic role during cell death induced by hydrogen peroxide, ultra-violet light, and serum starvation through the PI3-kinase/Akt survival pathway (Arthur et al., 2000; Tan et al., 2006). Overexpression of Capn2 in CHO cells resulted in sensitivity to ER stress induced cell death (Lu et al., 2002). In contrast, anti-apoptotic roles for calpains have also been demonstrated in the presence of some stimuli. For example, Capn1 cleaves p53 which protects the cell from DNA damage induced apoptosis. (Wood and Newcomb, 1999). Given that no Capn5-specific substrates have been identified yet, it is possible that Capn5 plays an apoptotic or anti-apoptotic role, depending on the context. As mentioned above, our data indicate a possible protective role for Capn5 in the cones in response to rod photoreceptor degeneration. Future studies could test this hypothesis by creating a cone-specific Capn5 knockout and inducing photoreceptor cell death using acute light damage. If loss of Capn5 in cone photoreceptors results in a lower light threshold to induce cone cell death and/or an increase in the amount of cone damage caused by acute light exposure, this would support a protective function of Capn5 in cones.

Finally, one of the most intriguing results from our study is that, in addition to upregulation of Capn5 expression in the cones in response to acute light damage, we also observed induction of Capn5 in a subset of Müller glia. It should be noted that this Müller glia expression was not observed in the wild type or XOPs-mCFP zebrafish models, and has not been observed in the wild type mammalian retina. In teleosts, Müller glia are the source of retinal stem and progenitor cells for injury-induced regeneration, and they also phagocytose cell debris

to clean up the retina in the initial response to damage (Goldman, 2014). Therefore, the upregulation of Capn5 in Müller glia in response to acute light damage suggests a potential role for this calpain in photoreceptor regeneration as well.

In summary, this body of work lays the foundation for understanding the physiological function of Capn5 in the developing retina and in response to photoreceptor degeneration. As one of the few calpains that is not tightly associated with its inhibitor, understanding the function of Capn5 provides an opportunity to investigate calpain protease function in the absence of endogenous inhibition. Further investigation has the potential to shed light on the importance of proteolytic proteases in degeneration and regeneration, and possibly unlock the underlying mechanism associated with ADNIV.

Acknowledgments

We are grateful to Charles Mashburn, Vimala Bondada, and James Geddes at the University of Kentucky Spinal Cord and Brain Injury Research Center for technical assistance and helpful discussions. The authors would also like to thank Sara Perkins and Chris Mitchell for zebrafish care, and Kayla Titilii for editorial assistance.

Funding

This work was supported by a grant from the National Institutes of Health (R01EY021769, A.C.M.) and the University of Kentucky Lyman T. Johnson fellowship (C.E.C).

2.6 Chapter 2 tables

Table 2. 1 Primer sequences

Gene	Forward Primer	Reverse Primer	Product Size	
<i>capn1a</i>	CTGGAGGATGAGGAAGAAA	TATCTAGAGTGAGGTTACAGCAGGA	637 bp	RT-PCR and Riboprobes
<i>capn1b</i>	CAGAAAGGCGAGTGGGTA	GAGCATCAGGAGTGAGGTTG	610 bp	RT-PCR and Riboprobes
<i>capn2a</i>	GCGAACGATTTCAACA	CACATTTACACATTCCTGG	556 bp	RT-PCR and Riboprobes
<i>capn2b</i>	ACTTCTGCCTGCGTGCTTTC	ATTCTAGATTGAGTGCTGTGCTTTGA	650 bp	RT-PCR and Riboprobes
<i>capn5a</i>	TCCATCAGAGCCACAACCTCAG	AGATGGAGCTGCCCACTGAT	652 bp	RT-PCR and Riboprobes
<i>capn5b</i>	CGCAGAGCTACTCCAAGGAG	ACCCAGGAAGGTGTCAACAAT	558 bp	RT-PCR and Riboprobes
<i>capn1a</i>	GATAAAGATGGGAGCGACG	CTGATTCTACAGCGAGACGCA	148 bp	qPCR primers
<i>capn1b</i>	AGAAGGACAGAGCAACATTTTC	ATAAAGGTCTCGGAGCGTGC	148 bp	qPCR primers
<i>capn2a</i>	GCTCTGTTGGGATGCTCCAT	GCACTCGGACCAGCTTTTCT	148 bp	qPCR primers
<i>capn2b</i>	AGCTCGGGAACCATAAGCAC	TCAGGCAGGACACGAAGTTG	148 bp	qPCR primers
<i>capn5a</i>	TGCCATCTCAGCAAACTTG	CACAGGCTCAGGAACAGTCA	132 bp	qPCR primers
<i>capn5b</i>	TGTTTACAGCAGGCAGGACAA	ATGGAGCTGCCCACTGATTT	108 bp	qPCR primers
<i>atp5h</i>	TTTGAGGGGCAGCATTACTCC	CCCCTGGTAGAAGAGCGAATC	200 bp	RT-PCR and Riboprobes

Table 2. 2 IHC antibodies

Antibody	Labels	Raised in	Dilution	Acquired from
Zpr-1	red/green cones	mouse	1:20	ZIRC
4C12	rods	mouse	1:100	James Fadool FSU, Tallahassee, FL
Zrf-1	Müller glia	mouse	1:5000	ZIRC
N1C1	Capn5	rabbit	1:100	GeneTex
GFP	GFP	rabbit	1:1000	abcam

2.7 Supplemental Figures

Figure S2. 1 Expression of *capn1* and *capn2* in response to acute light damage

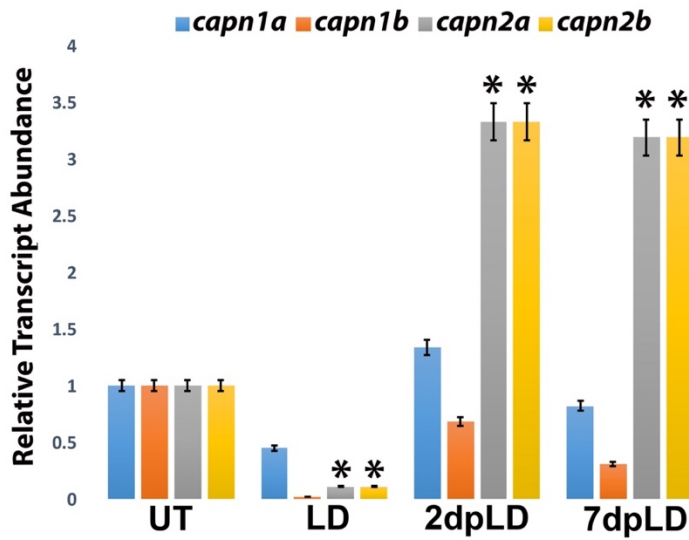


Figure S2.1 Expression of *capn1* and *capn2* in response to acute light damage. qPCR for *capn1a/b* and *capn2a/b* during and following light damage. A significant decrease in expression of *capn2a/b* was observed during light damage and a significant increase was observed after light damage. *Capn1a/b* expression did not change during LD. RT, reverse transcriptase; NT, no template control.

CHAPTER 3. HER9/HES4 IS REQUIRED FOR PHOTORECEPTOR DEVELOPMENT, MAINTENANCE AND SURVIVAL

Cagney E. Coomer, Stephen G. Wilson, Kayla F. Titalii-Torres, Jessica D. Bills, Laura A. Krueger, Rebecca A. Petersen, Evelyn M. Turnbaugh, Eden L. Janesch and Ann C. Morris

Department of Biology, University of Kentucky, Lexington, Kentucky 40506

Key words: zebrafish, Capn5, ADNIV, regeneration

Adapted from: Scientific Reports, (DOI : 10.1038/s41598-020-68172-2

b8e7677e-db82-4a73-8ce3-c54c355c5a3e) Cagney E. Coomer, Stephen G. Wilson, Kayla F. Titalii-Torres, Jessica D. Bills, Laura A. Krueger, Rebecca A. Petersen, Evelyn M. Turnbaugh, Eden L. Janesch and Ann C. Morris. Her9/Hes4 is required for retinal photoreceptor development, maintenance, and survival.

N.B. For this dissertation, figure numbers, headings, and text were modified to match dissertation style.

3.1 Abstract

The intrinsic and extrinsic factors that regulate vertebrate photoreceptor specification and differentiation are complex, and our understanding of all the players is far from complete. Her9, the zebrafish ortholog of human HES4, is a basic helix-loop-helix-orange (bHLH-O) transcriptional repressor that regulates neurogenesis in several developmental contexts. We have previously shown that *her9* is upregulated during chronic rod photoreceptor degeneration and regeneration in adult zebrafish, but little is known about the role of *her9* during retinal development. To better understand the function of Her9 in the retina, we generated zebrafish *her9* CRISPR mutants. *Her9* homozygous mutants displayed striking retinal phenotypes, including decreased numbers of rods and red/green cones, whereas blue and UV cones were relatively unaffected. The reduction in rods and red/green cones correlated with defects in photoreceptor subtype lineage specification. The remaining rods and double cones displayed abnormally truncated outer segments, and elevated levels of apoptosis. In addition to the

photoreceptor defects, *her9* mutants also possessed a reduced proliferative ciliary marginal zone, and decreased and disorganized Müller glia. Mutation of *her9* was larval lethal, with no mutants surviving past 13 days post fertilization. Our results reveal a previously undescribed role for Her9/Hes4 in photoreceptor differentiation, maintenance, and survival.

Keywords: Her9, Hes4, photoreceptor, retina, zebrafish, retinoic acid, CRISPR

3.2 Introduction

The vertebrate retina is a highly conserved tissue of the central nervous system (CNS) that captures and converts light into an electrical signal. The neural retina is composed of three layers; the ganglion cell layer (GCL), inner nuclear layer (INL) and outer nuclear layer (ONL); the light-sensitive rod and cone photoreceptors reside in the ONL. The six classes of retinal neurons and single glial cell type in the retina all differentiate from a single pool of multipotent retinal progenitor cells (RPCs). Across all vertebrates studied to date, specification and differentiation of retinal cell types occurs in a synchronized and largely conserved manner. The ganglion cells are born first and the rods, bipolar cells, and Müller glia differentiate last (Livesey and Cepko, 2001). Cone photoreceptor differentiation generally occurs before the rods. The development of photoreceptor cell identity is influenced by many factors, both intrinsic and extrinsic. Cone and rod photoreceptor specification, cell cycle exit, and differentiation are accompanied by the expression of photoreceptor-specific transcription factors such as *otx2* (which drives retinal progenitors towards a photoreceptor lineage) and *crx*, then rod or cone-specific factors such as *Nr2e3* and *trβ2* (Farre et al., 2019; Il et al., 2010). Photoreceptor differentiation is also regulated extrinsically by Hedgehog (Hh), thyroid hormone (TH), Notch, Wnt, retinoic acid (RA), and fibroblast growth factor (FGF) signaling pathways, to name a few (Doerre and Malicki, 2002). Our knowledge of the precise molecular determinants of photoreceptor subtype differentiation is far from complete. Understanding how photoreceptor cell development is regulated is essential for understanding the pathogenesis of blinding retinal degenerative diseases such as retinitis pigmentosa and macular degeneration. Several approaches have been developed to understand retinal development, one of the most prominent being the generation and characterization of genetic mutants. Due to its conserved retinal structure and function, as well

as the extensive genetic homology with humans, zebrafish have become an appealing model for interrogating the role of specific genes in retinal cell type differentiation.

In this study, we examine the role of the transcription factor *Hairy and enhancer of split related 9* (Her9) in retinal development. Her genes belong to a family of basic-Helix-Loop-Helix-Orange (bHLH-O) DNA binding proteins (Muller et al., 1996), and are homologs of the *Hairy* and *Enhancer-of-split* genes in *Drosophila* and of *Hes/Hey* genes in mammals. The zebrafish genome contains 19 *hairy-related* (*her*) genes which have been shown to play essential roles in developmental processes such as somitogenesis, neural tube and nervous system development, floor plate development, cell cycle exit, and apoptosis (Liu et al., 2015; Takke et al., 1999). Her proteins often function as downstream effectors of the Notch-Delta signaling pathway and mediate cross-talk between Notch and other pathways (Delidakis et al., 2014). A variety of members in the three *hairy* classes are also regulated by Hh, VEGF, Nodal, FGF, and RA signaling (Holzschuh et al., 2005a; Holzschuh et al., 2005b; Latimer et al., 2005; Morrow et al., 2009; Radosevic et al., 2011b).

Zebrafish Her9 shares homology with mouse and human Hes1 (Radosevic et al., 2011b), but is more closely related by sequence comparison and synteny analysis to human HES4 (El Yakoubi et al., 2012). As Hes4 is absent from the mouse and rat genomes, zebrafish provide a unique opportunity to explore the function of this transcription factor during retinal development. In zebrafish, *her9* is expressed in ectodermal tissues (Leve et al., 2001) and in inter-pro-neural domains during embryonic development (Bae et al., 2005b), where morpholino knockdown suggested it acts downstream of Bmp signaling. Recent studies have also shown that Her9 functions during inner ear development, where it defines the posterolateral non-neurogenic field downstream of *tbx1* expression and RA signaling (Radosevic et al., 2011b). Interestingly, *her9* expression was shown to be independent of Notch-Delta signaling in several developmental contexts (Bae et al., 2005b; Leve et al., 2001), suggesting that it does not function as a classical Notch effector gene. In the post-embryonic Medaka and *Xenopus* retina, Her9 regulates proliferation of retinal stem cells in the peripheral ciliary marginal zone (CMZ) (El Yakoubi et al., 2012; Reinhardt et al., 2015). Finally, *her9* expression is upregulated during the specific degeneration and regeneration of rod photoreceptors in the zebrafish retina, suggesting a role for this transcription factor in retinal regeneration (Morris et al., 2011). Although these studies strongly implicate *her9* in regulating continual neurogenesis and injury-induced

regeneration in the post-embryonic retina, the function of *her9* during embryonic retinal development has not been thoroughly investigated.

In this study, we generated *her9* mutants using the CRISPR/Cas9 system to determine whether *her9* has a required role in retinal development. Here, we demonstrate that loss of Her9 causes a significant decrease in rod photoreceptors, subsets of cone photoreceptors, Müller glia cells, and CMZ size. We also find that *her9* mutant photoreceptors have abnormal outer segments and undergo apoptosis. Finally, we show that *her9* expression in the retina is regulated by RA signaling, but RA responsiveness is not completely lost in *her9* mutants. Taken together, our study confirms the requirement for Her9/HES4 in retinal stem cell proliferation and identifies Her9/HES4 as a novel regulator of photoreceptor specification, maintenance, and survival

3.3 Materials and methods

3.3.1 Zebrafish line maintenance

All zebrafish lines were bred, housed, and maintained at 28.5°C on a 14 hour light: 10-hour dark cycle, in accordance with established protocols for zebrafish husbandry (Akimenko et al., 1995). The Tg(3.2TαC: EGFP) transgenic line (hereafter called TαC:EGFP) has been previously described (Kennedy et al., 2001), and was generously provided by Susan Brockerhoff (University of Washington, Seattle, WA). The Tg(gfap: GFP)mi2001 line (hereafter referred to as GFAP:GFP), was previously described (Bernardos and Raymond, 2006) and was obtained from the Zebrafish International Resource Center (ZIRC, Eugene, OR). The Tg(XIRho: EGFP) transgenic line (hereafter called XOPs:GFP) has been previously described (Fadool, 2003), and was obtained from James Fadool (Florida State University, Tallahassee, FL). The Tg(fli1a: EGFP)y1Tg transgenic line, (hereafter called fli1:GFP) has been previously described (Lawson and Weinstein, 2002a), and was obtained from ZIRC. The Tg(ato7:GFP) transgenic line, (hereafter called ath5:GFP) has been previously described (Masai et al., 2003) and was obtained from ZIRC. Embryos were anesthetized with Ethyl 3-aminobenzoate methanesulfonate salt (MS-222, Tricaine, Sigma-Aldrich, St. Louis, MO) and adults were euthanized by rapid cooling as previously described (Wilson et al., 2016). All animal procedures and experimental protocols were approved and carried out in accordance with guidelines established by the University of Kentucky Institutional

Animal Care and Use Committee (IACUC), the University of Kentucky Institutional Biosafety Committee, and the ARVO Statement for the Use of Animals in Ophthalmic and Vision Research.

3.3.2 Generation of *her9* mutant zebrafish by CRISPR/Cas9

The *her9* target sites and single strand DNA oligonucleotides used to generate the guide RNAs were selected using the ZiFit online tool (<http://zifit.partners.org/ZiFiT/>). The target sites for CRISPR/Cas9 genome editing were selected within the first and third exons of the *her9* gene. The first target site is 54 bp 3' of the translation start site and 46 bp upstream of the beginning of the BHLH domain, while the second target site is immediately after the region corresponding to the Orange domain (sequences listed in **Table S3.2**).

The pT3TS-nls-zCas9-nls (Addgene: 46757) expression vector was used to produce Cas9 mRNA. This vector contains a zebrafish codon-optimized Cas9 coding sequence flanked by the nuclear localization sequence. The plasmid was linearized using XbaI (NEB: R0145S) and purified by phenol:chloroform extraction and ethanol precipitation. Cas9 mRNA was generated using Ambion mMACHINE T3 Transcription Kit (Life Technologies: AM1304) and purified by phenol:chloroform extraction and ethanol precipitation.

Screening for mutations in *her9* was performed by high resolution melting analysis (HRMA). Genomic DNA was collected from 24 hpf embryos as described below. HRMA was performed using the LightCycler 480 High-Resolution Melting Master (Roche) kit according to the manufacturer's instructions on a LightCycler 96 Real-Time PCR System (Roche).

3.3.3 Restriction fragment length polymorphism (RFLP)

The mutant *her9* allele carrying a 1 bp deletion was identified by RFLP analysis due to the introduction of a BsaJI restriction site (NEB: R0563S). The mutant *her9* allele carrying a 1 bp insertion was identified by RFLP due to the introduction of a Bfal restriction site (NEB: R0568S). Genomic DNA from whole embryos or from tail clips was extracted and amplified by PCR as described above, then subjected to restriction digest. The restriction digests were visualized on a 2% agarose gel.

3.3.4 mRNA synthesis and microinjection

The coding region of *her9* was amplified by RT-PCR and the cDNA was cloned into a pGEMT-easy plasmid (Promega, Madison, WI). Capped mRNA was synthesized using the mMessage T7 kit (Ambion, Austin, TX) according to the manufacturer's instructions and purified by phenol-chloroform extraction and ethanol precipitation. The mRNA was injected at a volume of 4.18 nl/embryo (1.5 ng) in buffered solution with 0.025% Dextran red into the yolk of 1-cell stage zebrafish.

3.3.5 Western blot

Protein lysate was extracted from 20 heads of 3 dpf *her9* wildtype and mutant larvae. Protein was quantified by Bradford Assay (BIO-Rad), and 30 µg was diluted 1:3 in gel loading buffer (NEB), sonicated, spun down, then separated by SDS-PAGE on Mini-PROTEAN TGX Precast Gels (BIO-Rad). Following gel electrophoresis, separated proteins were transferred to a nitrocellulose membrane. The membrane was blocked with 5% non-fat milk/PBST for 30 minutes at room temperature then incubated in anti-HES4 (rabbit polyclonal, 1:500, Thermo Fisher) or anti-β actin (mouse monoclonal, 1:1000, Santa Cruz)/PBST solution overnight at 4°C. Membranes were washed in PBST then incubated in secondary antibody for one hour at room temperature, developed with HRP Development Reagent (BIO-Rad) for 1 minute, and imaged with a Chemidoc Bioimager (BIO-Rad).

3.3.6 RNA isolation and riboprobe synthesis

RNA was isolated from whole embryos at indicated developmental time points. RNA was extracted from pools of embryos using TRIzol Reagent (Life Technologies, Invitrogen), following the manufacturer's protocol, then treated with RNase-Free DNase I (Roche, Indianapolis, IN) to remove genomic DNA as previously described (Wilson et al., 2009). For riboprobes, PCR products from the unique regions of *her9* were cloned into the pGEMT-easy vector (Promega, Madison, WI). Plasmids were linearized using either NcoI and SpeI restriction enzymes (NEB, Ipswich, MA). Riboprobes were synthesized from the plasmids by in vitro transcription using either T7 or Sp6 polymerase and a digoxigenin (DIG) labeling kit (Roche Applied Science, Indianapolis, IN). The primer sequences used for riboprobe preparation are given in **Table S3.1**.

3.3.7 RT-PCR and real-time quantitative RT-PCR (qPCR)

The GoScript Reverse Transcriptase System (Promega, Madison, WI) was used to synthesize the first strand cDNA from 1µg of the extracted RNA. PCR primers were designed to amplify unique regions of the *her9* and *atp5h* cDNAs (Eurofins Genomics; www.eurofinsgenomics.com; **Table S3.1**). Faststart Essential DNA Green Master mix (Roche) was used to perform qPCR on a Lightcycler 96 Real-Time PCR System (Roche). The relative transcript abundance was normalized to *atp5h* expression as the housekeeping gene control (Wen et al., 2015), and was calculated as fold-change relative to 36 hours post fertilization (hpf) for developmental expression, and fold-change relative to wild type siblings, untreated, or uninjected embryos for the mRNA rescue and RA experiments. RT-PCR and qPCR experiments were performed with three biological replicates and three technical replicates. RT-PCR was performed on a Mastercycler Pro thermocycler (Eppendorf, Westbury, NY). PCR products were visualized on a 1% agarose gel.

3.3.8 Visually mediated background adaptation assay (VBA)

The VBA assay was adapted from previously described protocols (Mueller and Neuhaus, 2014; Viringipurampeer et al., 2014). Embryos at 5 dpf were incubated in the dark for 2 hours and the dorsal cranial pigment was immediately imaged after removal from the dark. The embryos were then placed under ambient light for 30 minutes. The dorsal cranial pigment was imaged immediately following light exposure. Images of the heads of the embryos were scored by naïve observers as either "Light" or "Dark". All imaged embryos were then genotyped by RFLP analysis. The assay was performed a minimum of three times. In each assay, 10 embryos were screened. Results were analyzed by Chi-square test.

3.3.9 Optokinetic Response assay (OKR)

Embryos were collected at 5 dpf and mounted in a 35-mm petri dish filled with 5% methylcellulose. The embryos were mounted near the surface of the methylcellulose, dorsal side up. The petri dish was then placed inside of a rotating drum containing illuminated vertical stripes. The drum was rotated clockwise for 30 seconds (s) at 8 rpm then 30 s counterclockwise at 8 rpm and finally clockwise for another 30 s. Embryos were scored "responders" if they displayed smooth saccade eye movements in response to the drum rotation in the direction of rotation for at least two of the 30 second intervals. Embryos were scored as "non-responders" if they displayed no eye movement in any of the 30 s intervals. After scoring, the embryos were collected in 1x Thermopol buffer for gDNA extraction and genotyping using RFLP analysis as described above. The OKR assay was performed a minimum of three times, and at least 10 embryos were scored each time.

3.3.10 Mobility assay

Single 5 dpf zebrafish larvae were filmed for 1 minute in a 96-well plate to assess their swimming behavior. Each larva was subsequently screened for the *her9* 1bp insertion via PCR amplification and a restriction digest with Bfal (NEB: R0568S). The videos were linked to the appropriate genotype and analyzed using EthoVision software (www.noldus.com/animal-

[behavior-research/products/ethovision-xt](#)). EthoVision analysis produced individual tracks for each larva, a compiled heat map of movement by genotype, and comparisons of total velocity and distance traveled.

3.3.11 Whole-mount and fluorescent in situ hybridization

Embryos were manually dechorionated, collected at selected developmental time points (18, 24, 48, 72, and 120 hpf) and fixed as described above. WISH was performed as previously described (Forbes-Osborne et al., 2013). Solutions were prepared with diethyl pyrocarbonate (DEPC)-treated water. DIG-labeled riboprobes (3 ng/ μ l) were hybridized to the samples overnight at 60°C in hybridization buffer. After washing and blocking, samples were incubated overnight at 4°C with an anti-DIG-AP antibody (Roche, diluted 1:2000 in blocking solution). The next day, the embryos were washed and equilibrated in NTMT buffer followed by coloration with 4-nitro blue tetrazolium (NBT, Roche) and 5-Bromo-4chloro-3-indolyl-phosphate, 4-toluidine salt (BCIP, Roche) in NTMT buffer. A stop solution (PBS pH 5.5, 1mM EDTA) was used to end the coloration reaction and embryos were placed in 40% glycerol for imaging.

FISH was performed as previously described (Pillai-Kastoori et al., 2014). Embryos were fixed and sectioned as previously described⁴⁹. Sections were post-fixed in 1% PFA and rehydrated in PBST. The TSA plus Cy3 Kit (Perkin Elmer Inc, Waltham, MA) was used for probe detection. The sections were counterstained with 4', 6-diamidino-2-phenylindole (DAPI, 1:10,000 dilution, Sigma-Aldrich), mounted in 60% glycerol, and imaged on an inverted fluorescent microscope (Nikon Eclipse Ti-U, Nikon Instruments, Melville, NY) using a 20x or 40x objective and a Leica SP8 DLS confocal/digital light sheet system (Leica Biosystems, Nussloch, Germany) using a 40x or 63x objective. At least 10 embryos and 10 sections were analyzed for each time point and probe.

3.3.12 Immunohistochemistry

Immunohistochemistry was performed as previously described (Coomer and Morris, 2018). The following primary antibodies were used: 4C12 (mouse, 1:100) generously provided by J. Fadool (Florida State University, Tallahassee, FL), which labels rod photoreceptor cell

bodies; 1D1 (mouse, 1:100, J. Fadool, FSU, Tallahassee, FL), which recognizes rhodopsin; Zpr-1 (mouse, 1:20, ZIRC), which labels red-green double cones; HuC/D (mouse, 1:20, Invitrogen, Grand Island, NY), which recognizes retinal ganglion cells and amacrine cells; Prox1 (rabbit, 1:2000, Millipore, Billerica, MA), which recognizes horizontal cells; anti-PCNA (mouse, 1:100, Santa Cruz Biotechnology, Dallas, TX), which labels proliferating cells; Zpr-3 (rabbit, 1:1000, ZIRC), which labels double cone and rod photoreceptor outer segments; and anti-Blue, -green, and -UV Opsin (rabbit, 1:1,000), generously provided by D. Hyde (University of Notre Dame) which labels the blue, green, and UV cones, respectively. Alexa Fluor 488 goat anti-mouse, 488 goat anti-rabbit, 546 goat anti-rabbit, and 546 goat anti-mouse secondary antibodies (Molecular Probes, Invitrogen) were all used at 1:200 dilution. Nuclei were visualized by counterstaining with DAPI (1:10,000 dilution). Samples were mounted in 60% glycerol in PBS. Images were taken at 20x and 40x on an inverted fluorescent microscope and a Leica SP8 DLS confocal/digital light sheet system using a 40x or 63x objective. Ten sections were analyzed on each slide and for each antibody.

3.3.13 TUNEL staining

Terminal deoxynucleotide transferase (TdT)-mediated dUTP nick end labeling (TUNEL) was performed on frozen retinal cryosections using the ApopTag Fluorescein Direct In Situ Apoptosis Detection Kit (Millipore, Billerica, MA). TUNEL staining was performed according to the manufacturer's protocol. Images were taken at 20x and 40x on an inverted fluorescent microscope (Eclipse Ti-U, Nikon instruments). Ten sections were analyzed on each slide.

3.3.14 RA treatment

Stocks of all-trans-RA in dimethyl-sulfoxide (DMSO) were thawed before use and diluted to 1 μ M retinoic acid with 0.3% DMSO in embryo medium, 100 μ M of the RA signaling inhibitor diethylaminobenzaldehyde (DEAB) in 0.3% DMSO in embryo medium or 0.3% DMSO alone as the carrier control. Fli1:EGFP embryos and embryos from *her9* heterozygous incrosses were immersed in the RA solution starting at 24 hpf and were incubated for 12 hours in complete

darkness. At 36 hpf the embryos were rinsed in artificial fish water for 10 min and processed for immunohistochemistry, or the heads were removed and processed for qPCR.

To observe effects of RA on rod and cone photoreceptors, embryos from wild type or *her9* heterozygous incrosses were incubated in 0.3 μ M RA solution starting at 48 hpf and the solution was refreshed every 24 hpf. The embryos were collected at 72 hpf for analysis of rods, and at 120 hpf for analysis of cones. The heads were removed and sectioned for IHC and imaging.

3.3.15 Cell counts

For comparing and counting retinal cells, retinal cryo-sections containing the optic nerve as a landmark and the same 100 μ m sections adjacent to the optic nerve of at least 10 wild-type, heterozygous or mutant embryos. The counts were then normalized to the average eye size (# of cells/ (eye size/100)) for each genotype to take into account variability in embryo size.

3.3.16 Statistical analysis

Statistical analysis was performed using a Student's t-test or Chi-square test with GraphPad Prism software (www.graphpad.com). For comparing the number of retinal cell types and other phenotypic features 10 wild type and 10 mutant animals were examined. All graph data are represented as the mean \pm the standard deviation (s.d.).

3.4 Results

3.4.1 *Her9* expression during retinal development

Previous studies in zebrafish have described *her9* expression patterns in the early embryo (Bae et al., 2005b; Latimer et al., 2005; Leve et al., 2001) and *her9* expression has also been documented in the CMZ of the post-embryonic medaka retina (Reinhardt et al., 2015). We investigated the expression of *her9* during the critical stages of retina development. We used fluorescent in situ hybridization (FISH) to detect *her9* mRNA in the developing zebrafish retina between 24 and 72 hpf, a time period which encompasses the progression from a pseudostratified proliferative retinal neuro-epithelium to a fully laminated, functional retina containing all retinal cell types. At 24 hpf, *her9* was expressed throughout the lens and retina, but most predominately in the ventral portion of the retina, and in a ring around the lens (**Figure 3.1A-A''**). At 48 hpf, *her9* expression became restricted to the undifferentiated peripheral retina, the expression in the lens in auto-fluorescent artifact (**Figure 3.1B-B''**). By 72 hpf, *her9* expression was only detected in a small patch of cells within the persistently neurogenic CMZ, the expression in the lens in auto-fluorescent artifact (**Figure 3.1C-D''**). Taken together, the expression of *her9* throughout the undifferentiated embryonic retina and in the proliferative CMZ suggests that it functions in retinal progenitor cells and potentially plays a role in retinal stem cell proliferation or maintenance.

Figure 3. 1 *Her9* expression in the developing retina

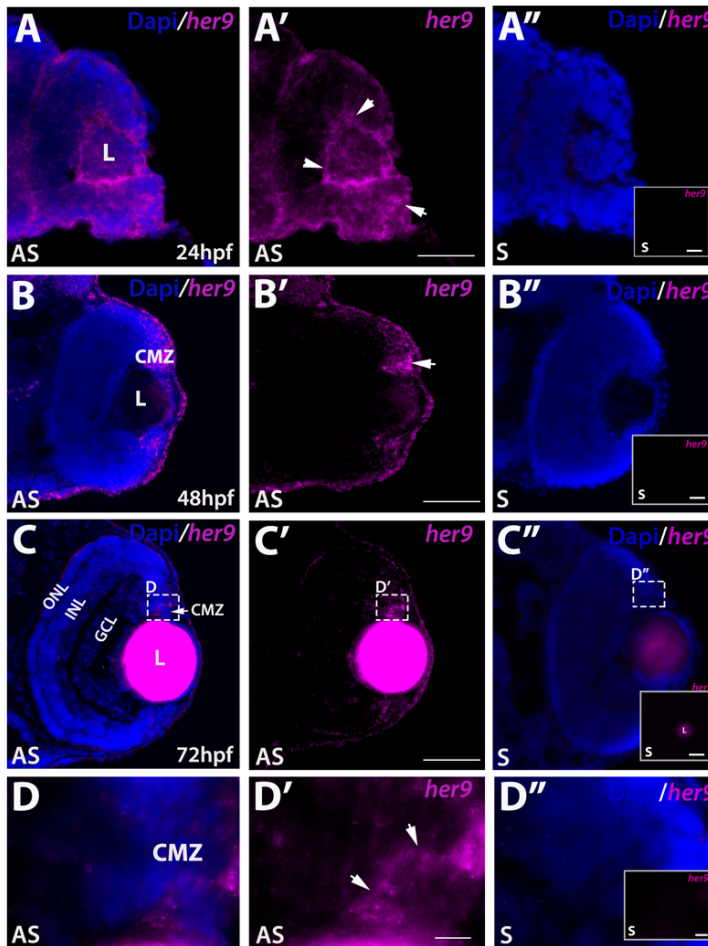


Figure 3.1 *Her9* expression in the developing retina. Fluorescent in situ hybridization (FISH) showing *her9* mRNA expression at 24 (A-A'), 48 (B-B'), and 72 (C-C') hpf in the developing retina. (D-D') 100x magnification of boxed area in C-C' showing *her9* expression in the CMZ. *her9* sense probes at 24, 48, and 72 hpf are shown in (A'', B'', C'', D''). Panels in A''-D'' display *her9* S probe without the Dapi staining. L, lens (expression in the lens is auto-fluorescent artifact); CMZ, ciliary marginal zone; NR, neural retina; ONL, outer nuclear layer; INL, inner nuclear layer; GCL, ganglion cell layer. Scale bar = 50 μ m and 100 μ m.

3.4.2 Generation of *her9* mutant using CRISPR/Cas9

To explore the role of *her9* during retinal development, we used the CRISPR/Cas9 system to introduce mutations in the *her9* gene, targeting a region of exon 1 upstream of the bHLH domain (Figure S3.1A). We recovered two *her9* mutant alleles, one carrying a 1-bp deletion and the other a 1-bp insertion at the target site (Figure S3.1B). Both mutations cause a frameshift resulting in a premature stop codon. Both mutations introduced novel restriction sites, allowing for genotyping by RFLP analysis (Figure S3.1C). We used qPCR to investigate *her9* expression in *her9*^{-/-} zebrafish, and observed a significant reduction in *her9* mRNA levels,

suggesting that the mutations resulted in nonsense-mediated decay (**Figure S3.1D**). We also used a HES4 antibody to detect Her9 protein, which confirmed a significant decrease in expression in *her9* mutants (**Figure S3.1E**). These results indicate that the CRISPR-generated genetic lesion in *her9* is a loss of function mutation. Both mutant alleles presented similar phenotypes so here we present data collected from the 1bp insertion mutant (**Figure S3.1F-G**).

Figure 3. 2 *Her9* mutant phenotype

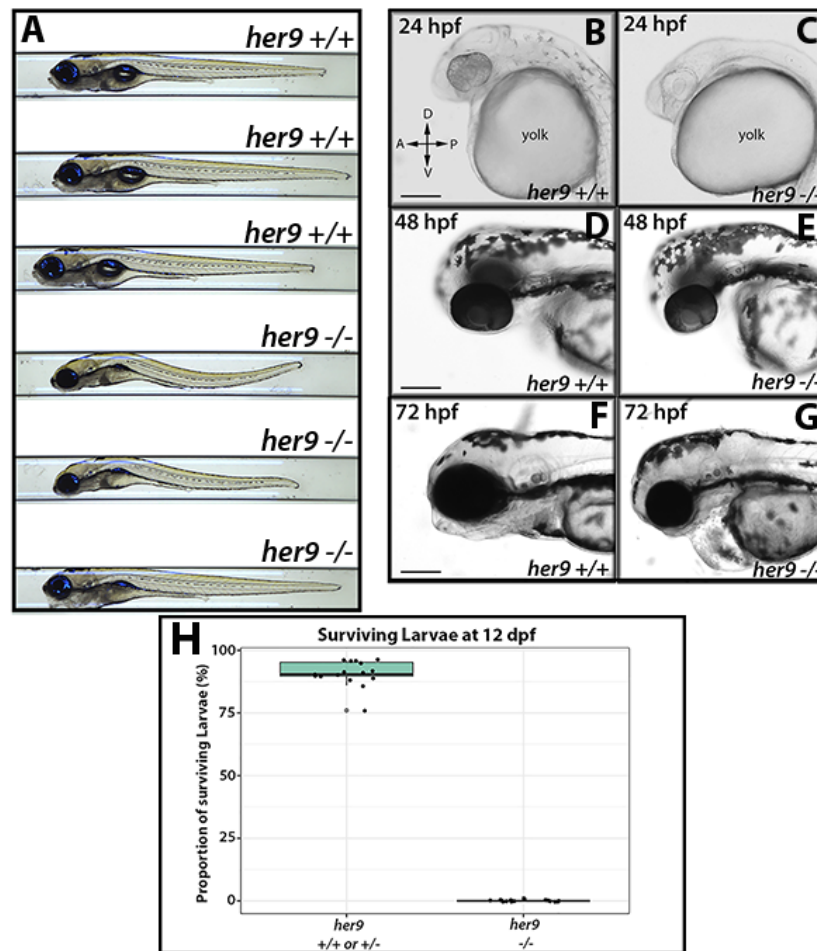


Figure 3.2 *Her9* mutant phenotype. (A) Gross morphology of WT and *her9* mutants at 5 dpf. (B-G) Gross morphology of WT and *her9* mutants at 24, 48, and 72 hpf. (H) Proportion of surviving larvae at 12 dpf; each point represents a separate cross. Scale bar= 50 μ m and 100 μ m.

3.4.3 Characterization of *her9* mutant phenotype

We first characterized the progeny of *her9* heterozygous in-crosses by light microscopy. At 24 hpf, *her9* mutants appeared somewhat developmentally delayed with lighter pigmentation and a smaller body size when compared to wild type (WT) and heterozygous siblings (**Figure 3.2B-C**). The mutants also displayed delayed development of the midbrain and hindbrain ventricles (**Figure 3.2B**), which appeared around 36 hpf (**Figure S3.3A-C**). At 48 hpf, mutant embryos were smaller in body size, microphthalmic, and some displayed pericardial edema (**Figure 3.2D-E**). At 72 hpf, homozygous mutants displayed a phenotypic range from mild to severe, where some mutant embryos looked fairly normal, and others displayed the same defects seen at earlier time points (**Figure 3.2F-G**). In wild type (WT) and *her9* heterozygotes, the swim bladder was fully developed by 5 dpf (**Figure 3.2A**). In contrast, *her9* homozygous mutant larvae did not develop a swim bladder and displayed an abnormal swimming pattern (**Figure 3.2A, Figure S3.2**). Other mutant phenotypes observed at 5 dpf included an enlarged liver, curved body, and craniofacial defects (**Figure 3.2A**). At 12 days post fertilization (dpf) we noticed a significant decrease in larval survival with approximately 29% mortality. None of the *her9*^{-/-} larvae survived beyond 13 dpf, indicating that loss of Her9 results in larval lethality (**Figure 3.2H**).

To rule out off-target contributions to the mutant phenotype, we performed a *her9* mRNA rescue experiment. Full-length *her9* mRNA was microinjected into one-cell stage embryos from *her9* heterozygous in-crosses, then the embryos were imaged and scored for the earliest visible mutant phenotype, which was lack of a clearly defined midbrain-hindbrain boundary and a missing midcerebral vein (MeCV) at 24 hpf (imaged by fluorescence microscopy of the *fli1*:GFP transgene; Fig. S3A-C). Whereas only 5.9% of uninjected *her9* homozygous mutant larvae had a detectable MeCV at 24 hpf, 80% of the *her9* mutant embryos that received *her9* mRNA had a MeCV (**Figure S3.3C-D**). We also observed a significant increase in the vasculature around the eye and heart in mRNA-injected mutant embryos (**Figure S3.3B-C**). As further confirmation that the phenotypes observed are specific to loss of Her9, the 1bp insertion heterozygotes were crossed with the 1bp deletion heterozygotes and the resulting phenotype in compound heterozygotes was equivalent to that seen in the individual mutants (**Figure S3.1F-G**).

Combined, these results indicate that the phenotypes described herein are specifically due to the mutation of *her9*, and also that Her9 may be required for proper vasculature development.

Figure 3. 3 *Her9* mutants lack a VBA response and display abnormal visual behavior (OKR)

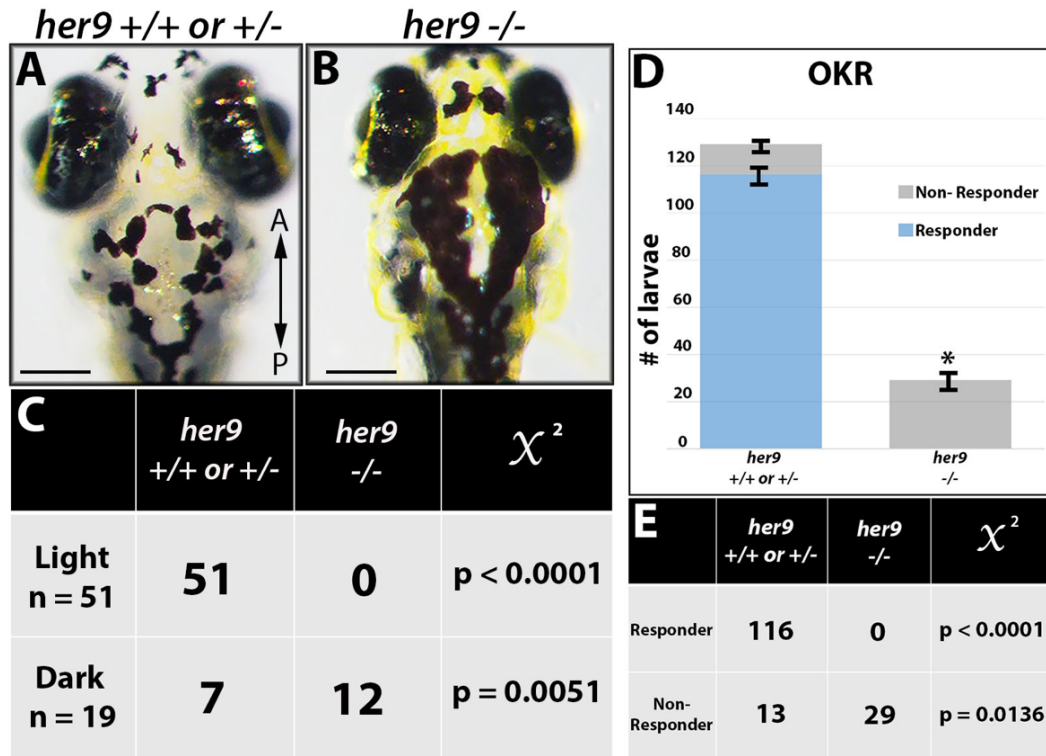


Figure 3. Her9 mutants lack a VBA response and display abnormal visual behavior (OKR). (A-B) Images displaying *her9* mutant with significantly darker pigmentation at 5 dpf (C) Genotyping of the “dark” and “light” larvae revealed that out of 51 individuals classified as “light”, zero were *her9*^{-/-} (p-value<0.0001, Chi-square analysis). Conversely, 12 out of 19 individuals classified as “dark” were *her9*^{-/-} (p-value=0.0051). (D) Number of responders and non-responders in the optokinetic response (OKR) assay. (E) Genotyping after OKR revealed that zero of the *her9*^{-/-} embryos displayed saccades in the OKR (p<0.0001). Scale bar= 50 μ m.

3.4.4 *Her9* mutants lack a visual mediated adaption response and display visual dysfunction

We observed that at 5 dpf, a significant number of the progeny of *her9*^{-/-} incrosses (~27%) appeared more darkly pigmented after prolonged light exposure when compared to their siblings. This suggested that *her9* mutants may lack a visually mediated background adaptation (VBA) response, a neuroendocrine camouflage response that allows zebrafish to manipulate their melanin granules in response to light exposure to match their background. Several previous studies have shown that the VBA response depends on retinal input (Mueller and Neuhauss, 2014; Neuhauss et al., 1999; Viringipurampeer et al., 2014), thus an absent VBA response can indicate visual impairment.

To determine whether the lack of a VBA response was associated with the *her9* mutant genotype, we first dark-adapted the larvae for two hours, then placed them in ambient light for 30 minutes, imaged and scored them as dark or light, then extracted genomic DNA for genotyping. After light exposure, 51 out of 70 larvae were scored as light and 100% of those embryos genotyped as WT or heterozygous ($p < 0.0001$; **Figure 3.3A and C**). In contrast, 19 of the larvae scored as dark, 63% of which genotyped as homozygous mutants ($p = 0.0051$; **Figure 3.3B-C**). From these data, we conclude that *her9* mutants lack a normal VBA response, which could suggest visual impairment and possible retinal defects.

Given their lack of VBA response, we wondered whether the *her9* mutants had any functional visual deficit. To investigate this, we used the optokinetic response (OKR) assay, which is a behavioral test that measures the larvae's ability to perform a combination of smooth pursuit and rapid saccade eye movements in response to a moving pattern of alternating black and white vertical stripes (Brockhoff, 2006). Individual larvae from a *her9* heterozygous incross were screened at 5 dpf over three 30-sec trials ($n = 159$), and then genotyped after screening. Whereas 116 out of 129 WT and heterozygous larvae displayed a positive OKR response, none of the *her9* mutants responded with saccadic movements in the OKR assay (0 out of 29 tested; $p < 0.0001$; **Figure 3.3D-E**). We conclude from these data that the loss of Her9 causes impaired visual responses at 5 dpf.

Figure 3. 4 *Her9* mutants have fewer rods with shorter outer segments

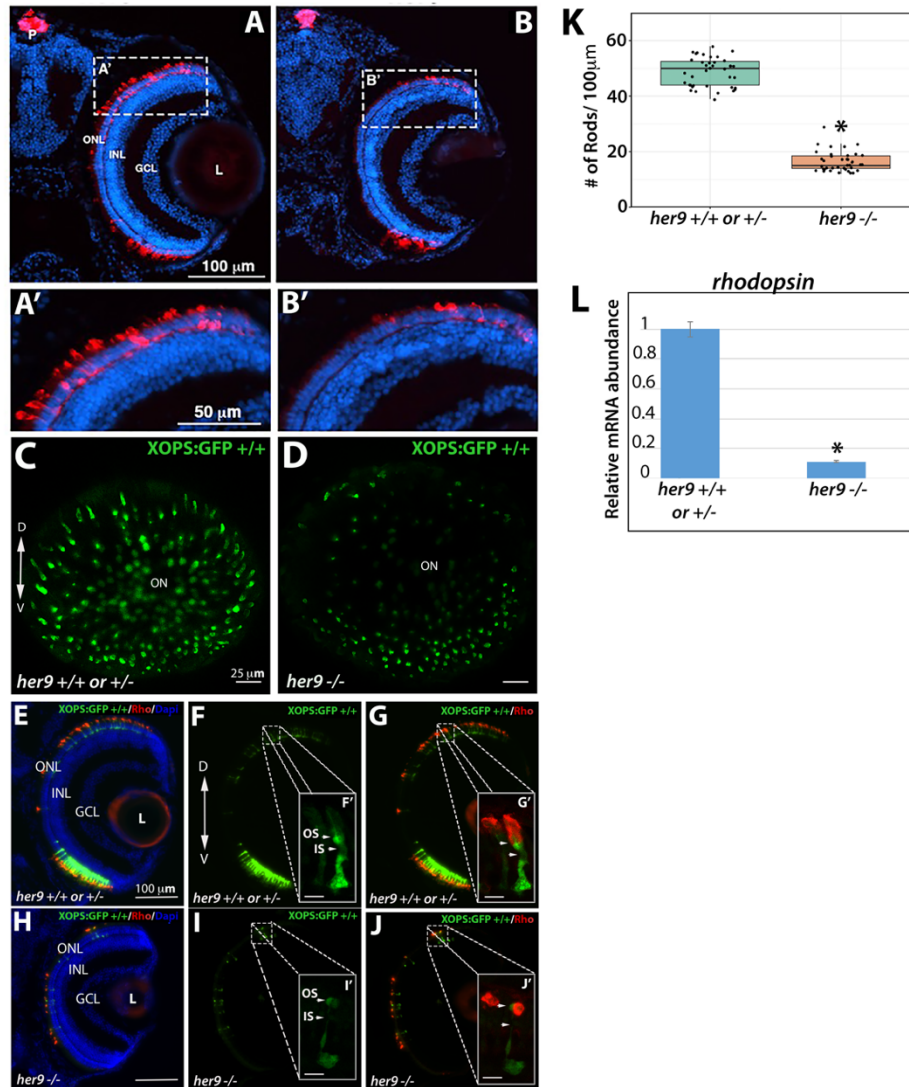


Figure 3.4 *Her9* mutants have fewer rods with shorter outer segments.

Immunohistochemistry with a rod antibody (4C12) in *her9*^{+/+ or +/-} (A, A') and *her9*^{-/-} (B, B') retinal sections. (C-D) Confocal images of whole eyes from *her9* heterozygous in cross progeny on the XOPS:GFP background. (E-G) Immunohistochemistry with an antibody that labels rhodopsin (1D1) on retinal cryosections of XOPS:GFP WT and heterozygous (E-G) or *her9* mutant (H-J) larvae. (K) Rod cell counts in *her9*^{-/-} larvae and their WT and heterozygous siblings (#of cells/ (eye size/100)). (L) qPCR analysis of *rhodopsin* expression at 8 dpf (fold change relative to *Ef1α*). ONL, outer nuclear layer; OPL, outer plexiform layer; INL, inner nuclear layer; GCL, ganglion cell layer; L, lens; ON, optic nerve; P, pineal gland. Scale bar= 50 µm and 100 µm.

3.4.5 *Her9* mutants display a decrease in rod photoreceptors and rod outer segment defects

Next, we used immunohistochemistry (IHC) on retinal tissue sections to examine the number and morphology of various retinal cell types in WT and *her9* mutant larvae, starting with the rod photoreceptors. Using a rod photoreceptor specific antibody (4C12), we observed numerous rod photoreceptors in the dorsal and ventral portions of the WT retina at 12 dpf (**Figure 3.4A**). At higher magnification the rod outer segments were easily detected (**Figure 3.4A'**). In contrast, *her9* mutant retinas displayed a significant decrease in rod photoreceptors which was especially apparent in the dorsal retina (**Figure 3.4B**). At higher magnification we also noticed that the outer segments of the remaining *her9* mutant rods looked shorter and distorted compared to those in the WT retina.

To more thoroughly examine the effects of the *her9* mutation on rod photoreceptor number and morphology, *her9* heterozygotes were crossed onto the XOPs:GFP transgenic background, which fluorescently labels rod photoreceptors (Fadool, 2003). The *her9* heterozygotes on the XOPs:GFP background were in-crossed, and whole eyes were removed from larvae at 5 dpf and imaged by confocal microscopy, while the rest of the body was used for genotyping. Using this approach, we observed a significant decrease in GFP⁺ rod photoreceptors across the entire *her9* mutant retina when compared to the WT (**Figure 3.4C-D**), confirming our previous results.

The remaining heads were pooled together based on genotype and cryo-sectioned, followed by counting of GFP⁺ cells. We observed a 69% reduction in the number of GFP⁺ rods in *her9* mutant larvae compared to WT (avg. 18 per 100 μm^2 in *her9* mutants vs. 58 per 100 μm^2 in WT), which was confirmed via qPCR for *rhodopsin* (**Figure 3.4K-L**). Finally, we used the 1D1 antibody to label the rod outer segments in WT and *her9* mutant retinal cryosections. In the *her9* mutant embryos the rod outer segments appeared severely truncated compared to the outer segments of the WT embryos (**Figure 3.4E-G' and 3.4H-J'**). Taken together, these data demonstrate that loss of Her9 causes a large decrease in rod photoreceptor number and defects in rod photoreceptor outer segment morphology.

Figure 3.5 Cone outer segments are truncated in *her9* mutants

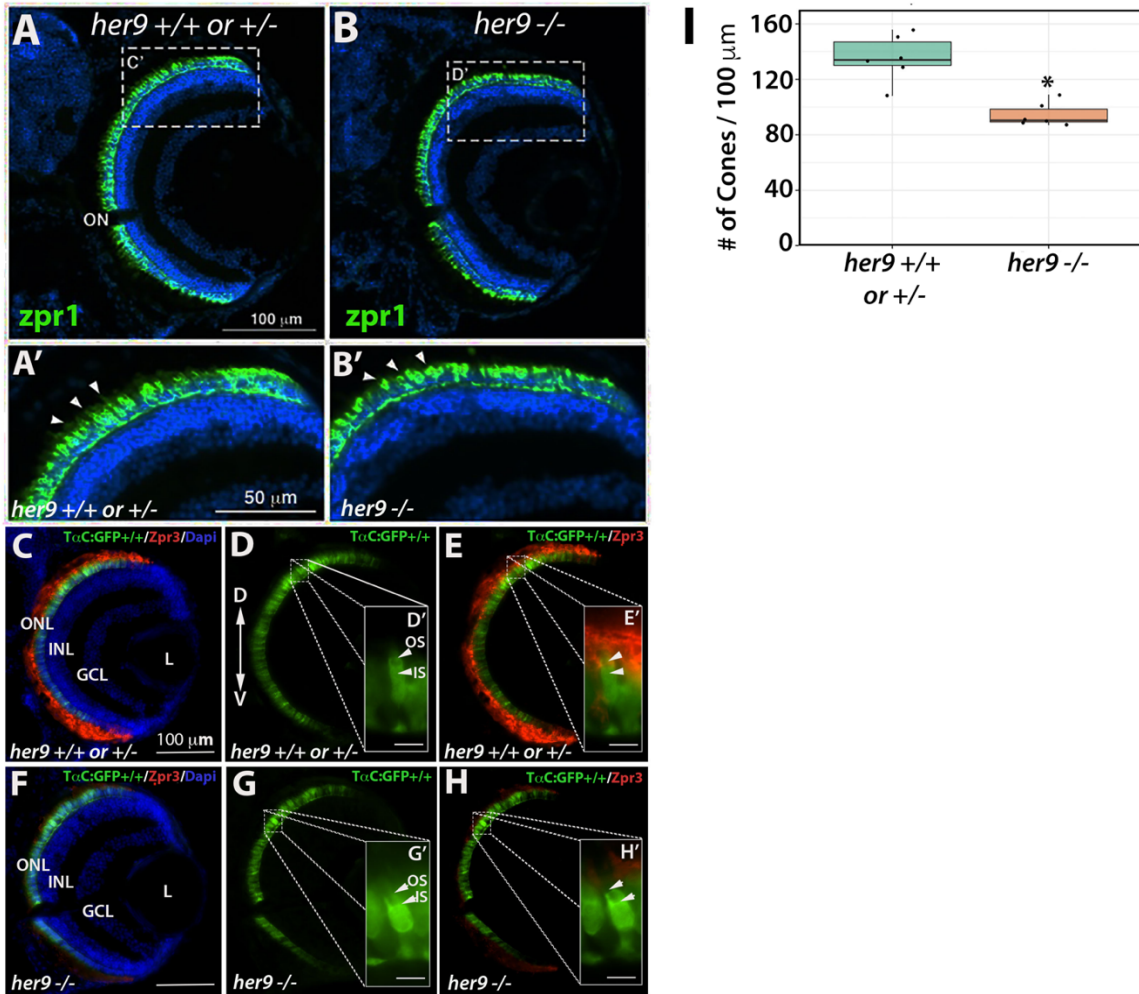


Figure 3.5 Cone outer segments are truncated in *her9* mutants. Immunohistochemistry with a red-green cone antibody (*Zpr1*) in *her9*^{+/+} or *her9*^{+/-} (A, A') and *her9*^{-/-} (B, B') retinal sections. Arrowheads indicate outer segments. (C-H) Immunohistochemistry with an antibody that labels rod and double cone outer segments (*Zpr3*) on retinal cryosections of *TαC:GFP*^{+/+}; *her9*^{+/+} or *her9*^{+/-} (C-E) or *TαC:GFP*^{+/+}; *her9*^{-/-} mutant (F-H) larvae. (I) Cone cell counts in *her9*^{-/-} mutant larvae and their WT and heterozygous siblings (# of cells/ (eye size/100)). ONL, outer nuclear layer; OPL, outer plexiform layer; INL, inner nuclear layer; GCL, ganglion cell layer; L, lens; ON, optic nerve; OS, outer segment; IS, inner segment. Scale bar= 100 μm

3.4.6 Cone outer segments are truncated in *her9* mutants

We used the Zpr1 antibody to detect the red-green double cones in WT and *her9* mutant retinas. At 12 dpf, we initially did not observe an obvious decrease in cone number in the *her9* mutant retina (**Figure 3.5A-B**). However, at higher magnification, we detected gaps in the spacing of the double cones, as well as truncated cone outer segments, in *her9* mutant retinas (**Figure 3.5A'-B'**). To examine this further, we crossed the *her9* mutation onto the T2C:GFP transgenic background, which fluorescently labels all cone photoreceptor subtypes (Kennedy et al., 2001). There was a significant decrease in the number of cone photoreceptors in the *her9* mutants compared to WT (**Figure 3.5I**). We used the Zpr3 antibody to label the outer segments of the double cones and rods, and found that these were missing or truncated in *her9* mutant retinas (**Figure 3.5C-H**). These results demonstrate that the loss of Her9 causes a decrease in the number of double cones, and has profound effects on red and green cone outer segment morphology.

Figure 3. 6 Her9 mutants display cone subtype-specific phenotypes

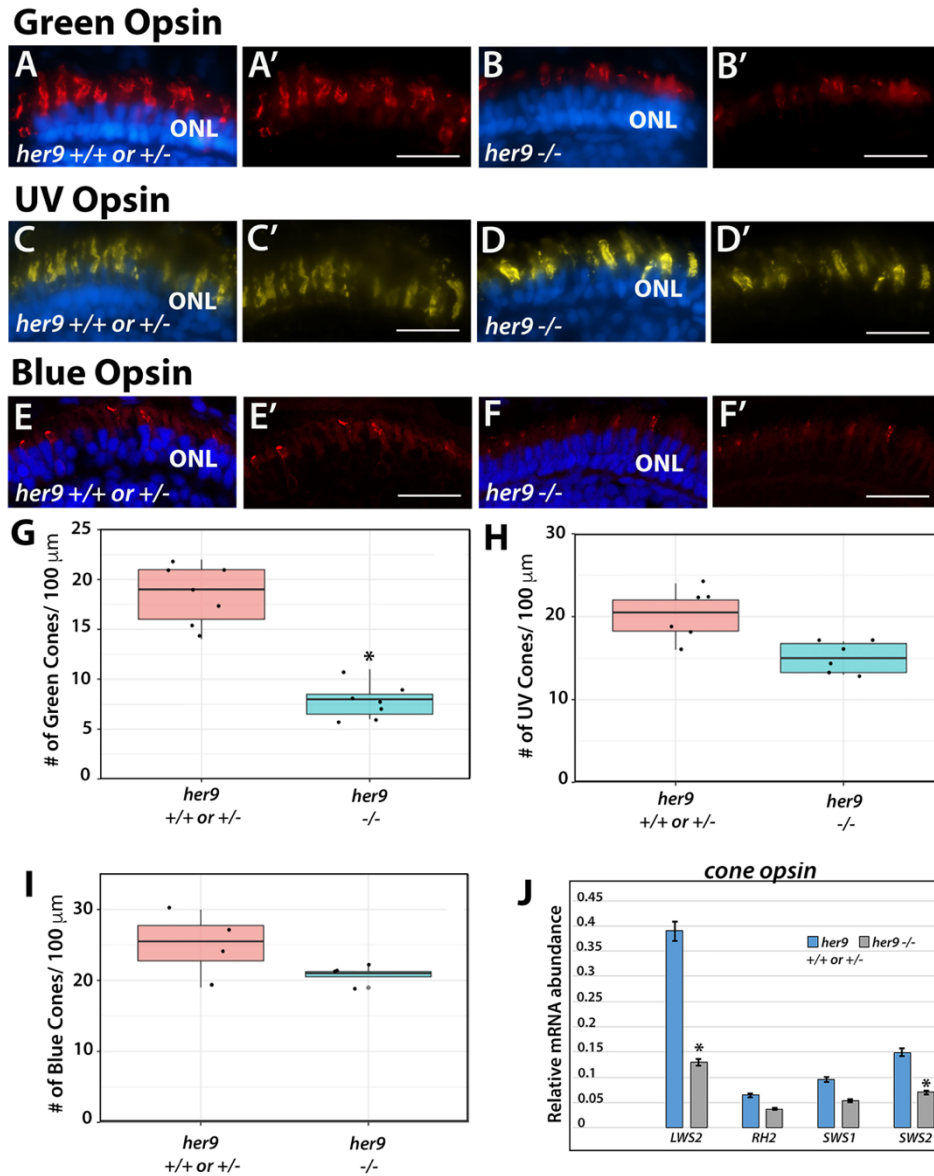


Figure 3.6 *Her9* mutants display cone subtype-specific phenotypes. Immunohistochemistry using a green (A-B'), UV (C-D'), or blue (E-F') cone opsin antibody on WT and *her9* mutant retinal cryosections. (G-I) Cell counts of opsin expressing cells in *her9* mutant retinas compared to their siblings (# of cells/ (eye size/100)). (J) qPCR analysis of the different cone opsins at 8 dpf (fold change relative to *Ef1α*). ONL, outer nuclear layer. Scale bar = 50 μm.

3.4.7 Her9 mutants display cone subtype-specific phenotypes

We next investigated whether all cone subtypes were equally affected by the loss of Her9, using cone opsin-specific antibodies to perform IHCs on retinal cryosections as described above. We again observed a significant reduction (42%) in the number of green cone photoreceptors and truncated green cone outer segments in the *her9* mutant retinas compared to their WT siblings (**Figure 3.6A-B, G**). Interestingly, IHC with the UV- and blue-cone opsin antibodies revealed a much smaller decrease in number for those cone subtypes in *her9* mutant retinas compared to the decrease in green cones (6.6% and 5%, respectively; **Figure 3.6C-F', H and I**) and we did not detect truncation in the blue and UV cone outer segments (**Figure 3.6D'-F'**). qPCR for long-, medium- and short-wavelength opsins confirmed a small decrease in UV- and blue- cone opsin expression and a large decrease in red cone opsin expression (**Figure 3.6J**). Green cone opsin expression was also modestly reduced by qPCR. The results of these experiments suggest that loss of Her9 causes variable reductions in all cone photoreceptors and defects in outer segments that are specific to red/green cones and rods.

Figure 3. 7 Loss of Her9 causes a decrease in Müller Glia number and distorts their organization

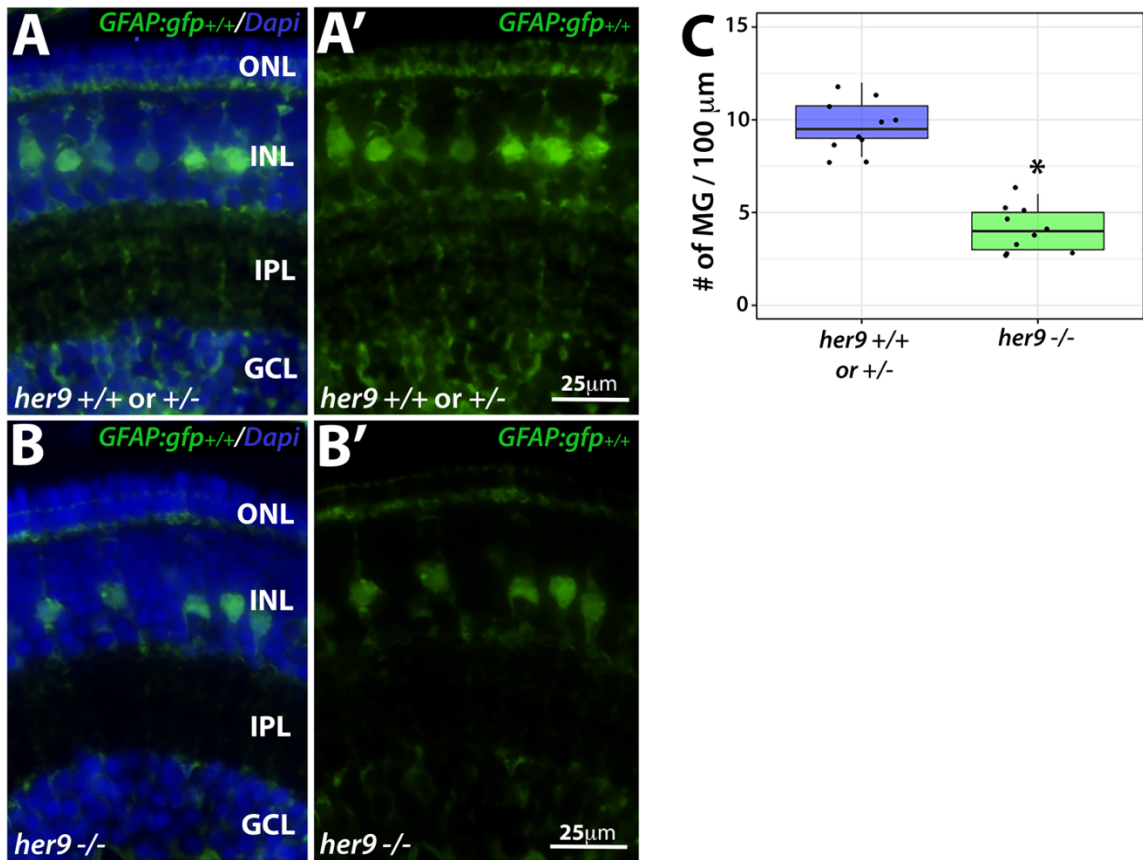


Figure 3.7 Loss of *her9* causes a decrease in Müller glia number and distorts their organization. Cryosections of WT and heterozygous (A-A') or *her9* mutant (B-B') retinas at 5 dpf on the *gfap:GFP* transgenic background. (C) Cell counts of GFP+ Müller glial cells in *her9* mutant retinas compared to their WT siblings (#of cells/ (eye size/100)).

3.4.8 Müller Glia abnormalities in *her9* mutants

To determine whether loss of Her9 affects other late-born cell types, we crossed the *her9* mutation onto the *gfap:GFP* transgenic background, which fluorescently labels retinal Müller glia (Li et al., 2015). At 5 dpf, *her9* homozygous mutants showed a significant reduction of GFP+ Müller glia compared to their WT and heterozygous siblings ($p < 0.0001$; **Figure 3.7A-C**). We also observed a decrease in GFP+ glial cells across the entire *her9* mutant embryo (brain and enteric nervous system) at this stage (**Figure S3.4A-D'**). In addition, the GFP+ Müller glia that were present in *her9* mutant retinas displayed a disorganized pattern, with their cell bodies located at various depths of the INL layer, rather than forming a uniform row as in the WT retinas (**Figure 3.7A' and B'**). We also observed a lack of processes from the Müller glia spanning the retina in the *her9* mutants compared to their WT siblings. These data indicate that the loss of Her9 not only causes a reduction in the number of Müller glia, but also distorts the morphology, organization and patterning of the Müller glial cells that do develop.

3.4.9 Loss of Her9 has minimal effects on other retinal cell types

Does the loss of Her9 disrupt development of all retinal cell types? To address this question, we used transgenic lines or IHC with cell-type specific antibodies for ganglion cells, amacrine cells, and horizontal cells. First, we crossed *her9* heterozygous zebrafish onto the *ath5:GFP* transgenic background (Masai et al., 2003) which fluorescently labels ganglion cells and the optic nerve (**Figure 3.8A-B**). We observed a modest decrease in GFP expression in the *her9* mutant retinas compared to WT and somewhat thinner optic nerves (**Figure 3.8B; arrow**). We followed this up with IHC using the HuC/D antibody, which labels both ganglion cells and amacrine cells. We observed a significant decrease in the number of ganglion cells in *her9* mutant retinas compared to the WT and heterozygous siblings (**Figure 3.8C-F, K**; $p < 0.0001$). However, the number of amacrine cells was not significantly different in the WT versus *her9* mutant retinas at 5 dpf (not shown).

The Prox1 antibody was then used to assess horizontal cells in the retinas of *her9*^{+/-} in-cross progeny (**Figure 3.8G-J'**). There were no morphological differences in the horizontal cells

of *her9* mutants compared to WT (**Figure 3.8H' and J'**). A small decrease in the number of horizontal cells was observed in mutant retinas compared to WT, but it was not statistically significant when normalized to the smaller mutant eye size (**Figure 3.8L**). These results demonstrate that loss of Her9 causes a mild decrease in ganglion cell number, but does not alter the numbers of amacrine or horizontal cells, and does not disrupt the morphology of these retinal cell types. This indicates that the morphological defects due to loss of Her9 are specific to photoreceptors and the Müller glia.

Figure 3. 8 Loss of Her9 minimal effects on other retinal cell types

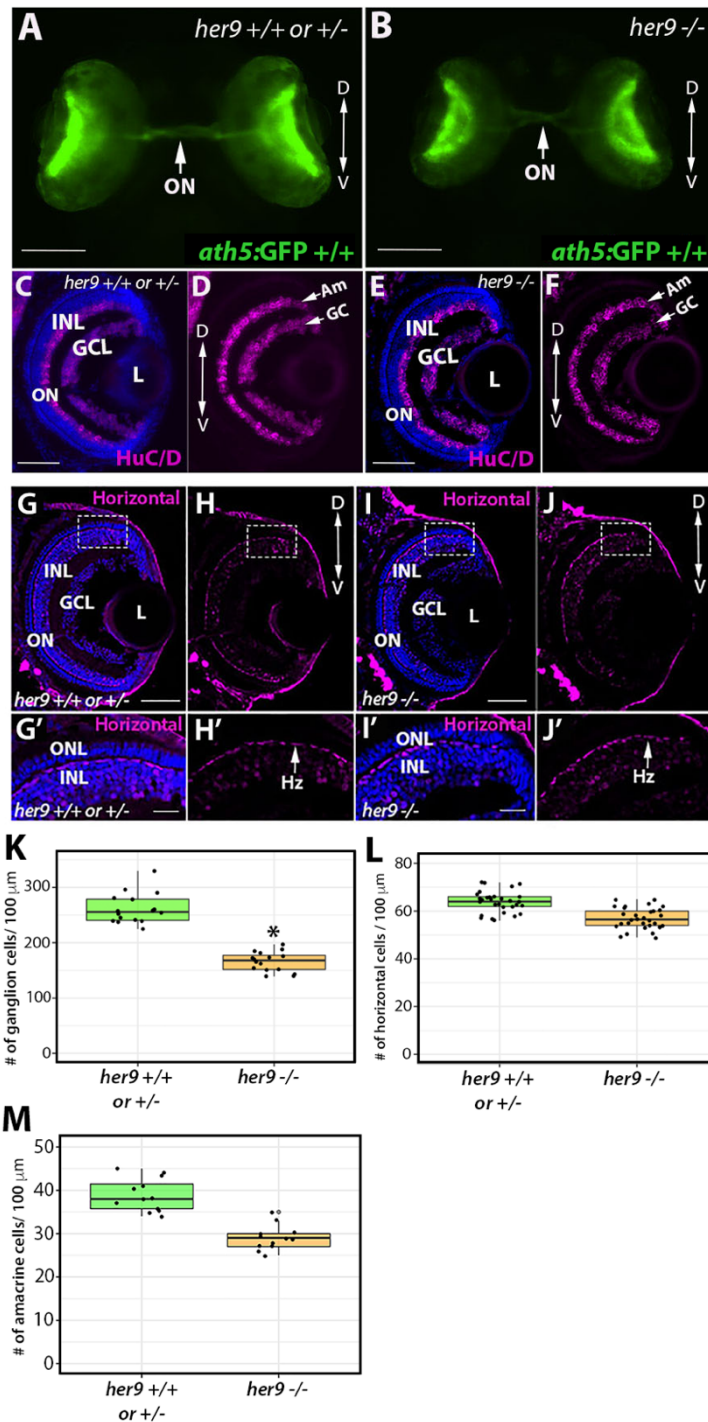


Figure 3.8 Loss of *her9* has minimal effects on other retinal cell types. Whole eye images of WT and heterozygous embryos (A) or *her9* mutant embryos (B) on the *Ath5:GFP* transgenic background at 5 dpf. Immunohistochemistry for ganglion and amacrine cells (HuC/D antibody) in cryosections from WT and heterozygous retinas (C-D) or *her9* mutant retinas (E-F). (G-H') Immunohistochemistry with the Prox1 antibody labels horizontal cells in cryosections of WT and heterozygous (G-H') or *her9* mutant (I-J') retinas. Cell counts reveal a decrease in the number of ganglion cells in the mutant retinas (K) but no significant difference in the number of horizontal cells (L; #of cells/ (eye size/100)). Am, Amacrine cells; GC, Ganglion cells; Hz, Horizontal cells; ONL, outer nuclear layer; INL, inner nuclear layer; ON, optic nerve; L, Lens. Scale bar= 50 μm and 100 μm.

3.4.10 Loss of Her9 causes a progressive collapse of the CMZ

Previous studies of the post-embryonic Medaka and *Xenopus* retina showed that *her9* regulates the proliferation of the retinal stem cells in the CMZ (Reinhardt et al., 2015). Therefore, we wanted to investigate whether germline mutation of zebrafish *her9* would affect the establishment of the CMZ during retinal development. We collected zebrafish larvae at 72 hpf, then prepared retinal sections for PCNA immunolabeling, which detects cells in S-phase (**Figure 3.9A-A'**). We observed a significant decrease in the number of PCNA+ cells in the CMZ of mutant retinas in comparison to their WT and heterozygous siblings. To determine whether the *her9* mutant CMZ could recover to a normal size later in development, we immunolabeled 5 dpf retinal sections with the PCNA antibody. We again observed significantly fewer PCNA+ cells in the CMZ of 5 dpf *her9* mutant retinas compared to their WT and heterozygous siblings (**Figure 3.9B-B'**). Quantification of both the PCNA-labeled CMZ area and fluorescence intensity confirmed a significant decrease in the *her9* mutants compared to WT and heterozygous siblings (**Figure 3.9C-D**). The area and fluorescent intensity was procured using the NIS-Elements software (Nikon Eclipse Ti-U, Nikon Instruments, Melville, NY). Interestingly, the lack of proliferating cells in the CMZ became more severe from 72 hpf to 5 dpf in *her9* mutants, indicating that there is a decrease in the number of proliferating cells in the mutant CMZ over time. Our results confirm that Her9 regulates the proliferation of stem cells in the CMZ. Moreover, as we also observed a decrease in pockets of stem cells in the *her9* mutant brain (**Figure S3.4A-D'**), this suggests that Her9 has a general role in regulating stem cell proliferation or maintenance throughout the developing central nervous system.

Figure 3.9 CMZ defects in *her9* mutants

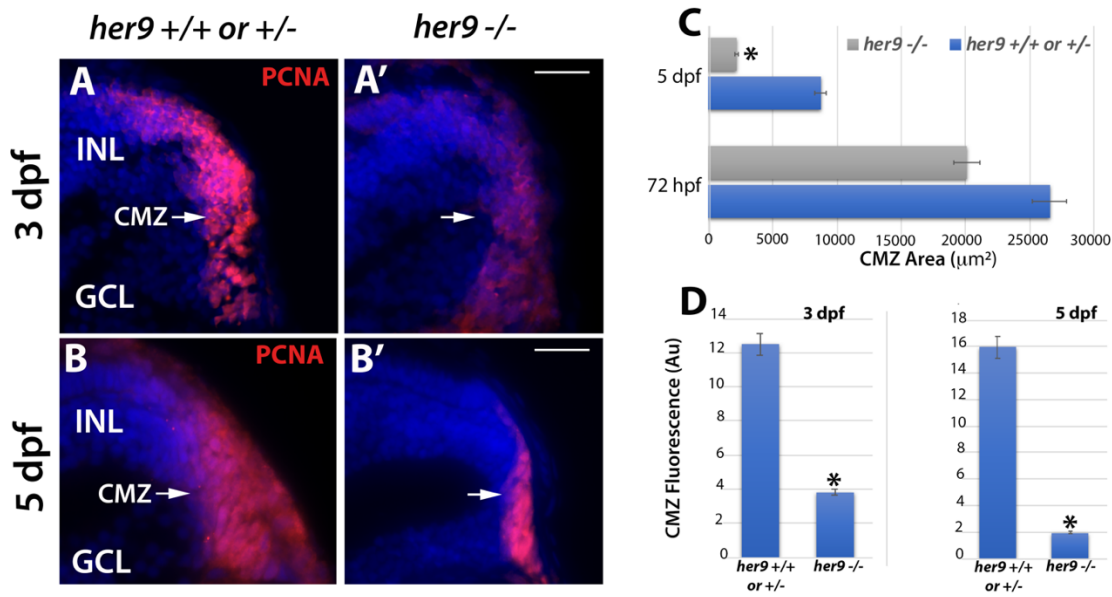


Figure 3.9 CMZ defects in *her9* mutants. Immunostaining for PCNA in WT or heterozygous (A, B) and *her9* mutant (A', B') retinal sections at 72 hpf and 5 dpf; a decrease in the size and fluorescence intensity of the CMZ is apparent in *her9* mutants. Area of CMZ calculated at 72 hpf and 5 dpf (C). *Her9* mutants have significantly fewer PCNA-positive cells in the peripheral retina. CMZ fluorescence intensity at 72 hpf and 5 dpf (D). GCL, ganglion cell layer; INL, inner nuclear layer; CMZ, ciliary marginal zone. Scale bar = 50 µm.

3.4.11 Her9 mutants display abnormal expression of photoreceptor lineage genes

To begin to address the mechanism underlying the photoreceptor phenotypes of *her9* mutant retinas, we first examined whether loss of *her9* affects the specification of retinal progenitor cells towards rod and cone lineages. Crx is a transcription factor that plays a critical role in the specification of all photoreceptor subtypes (Rath et al., 2007). We used FISH on

retinal cryosections to examine the expression of *crx* at 48 and 72 hpf. Starting at 48 hpf, the expression of *crx* spreads across the WT retina in a ventral to dorsal fan-like manner (**Figure 3.10A-A'**). In *her9* mutant retinas we observed a similar expression pattern of *crx*, albeit with reduced signal intensity (**Figure 3.10B-B'**); by 72 hpf, *crx* expression in *her9* mutant retinas was not significantly different from WT (**Figure S3.5A-B'**). Control sense probes showed no signal (**Figure 3.10C and F**). Therefore, we conclude that loss of Her9 does not perturb specification of photoreceptor progenitors.

Next, we examined expression of photoreceptor subtype-specific transcription factors. Nr2e3 is responsible for the activation of rod photoreceptor genes and repression of cone genes in photoreceptor progenitors (Chen et al., 2005). At 48 hpf in the WT retina, we observed robust expression of *Nr2e3* throughout the ONL of the retina (**Figure 3.10D-D'**). In contrast, in *her9* mutants, there was significantly less *Nr2e3* expression within the ONL in comparison to the WT (**Figure 3.10E-E'**). At 72 hpf the expression of *Nr2e3* in the *her9* mutant retina had increased relative to 48 hpf, but the expression pattern remained disorganized relative to WT (**Figure S3.5C-D'**). Taken together, this result indicates that the rod photoreceptors in *her9* mutants are specified but their differentiation is abnormal.

Figure 3. 10 *Her9* mutants display abnormal expression of PR lineage genes

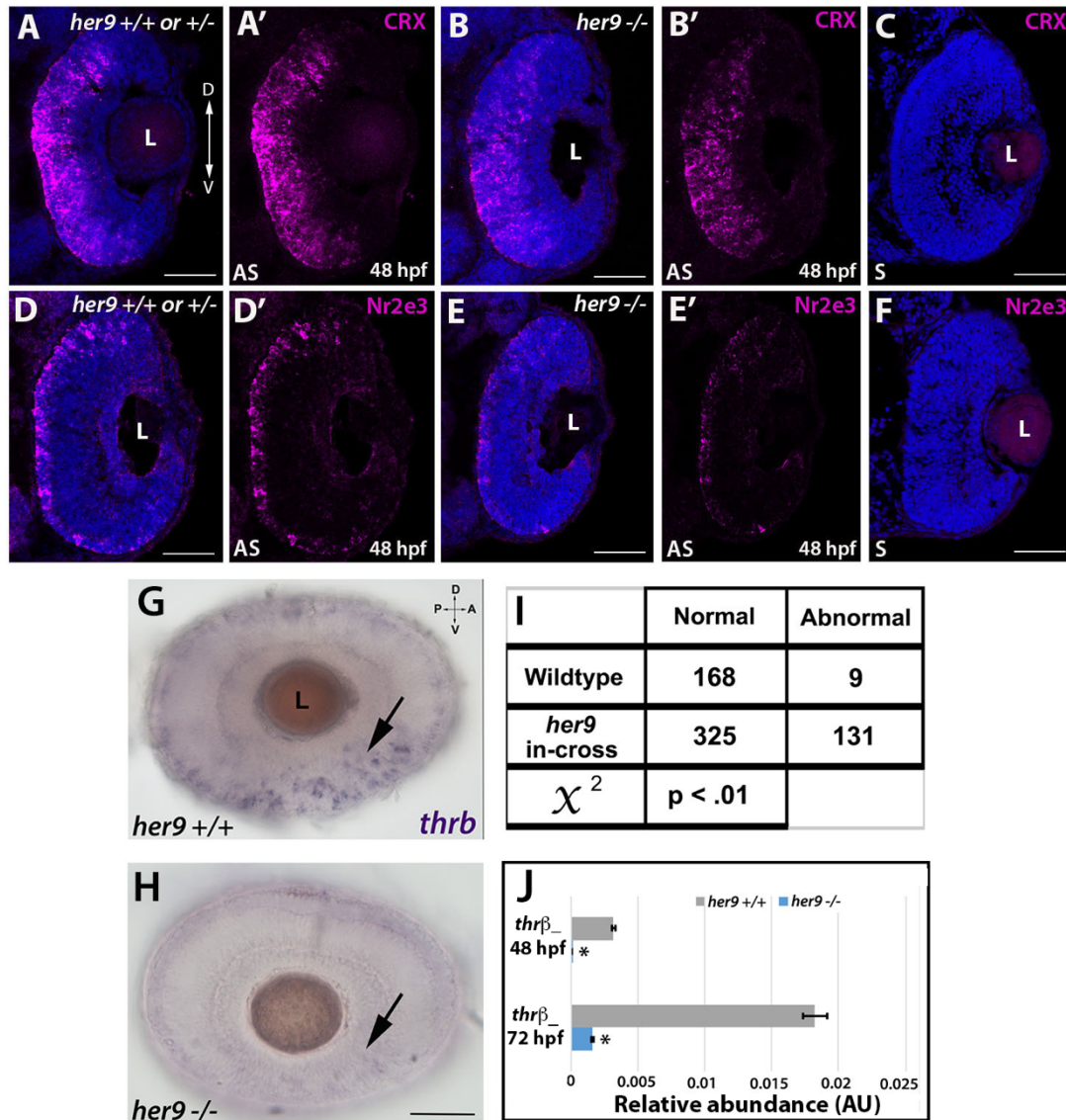


Figure 10. *Her9* mutants display abnormal expression of photoreceptor lineage genes. (A-B') Fluorescent in situ hybridization (FISH) for *crx* at 48 hpf in WT and mutant neural retina. **(C)** *Crx* sense probe. **(D-E')** Decreased expression of *Nr2e3* in the mutant retina compared to the wildtype. **(F)** *Nr2e3* sense probe. **(G-H)**. Whole mount in situ hybridization (WISH) for *thrβ* expression at 48 hpf in WT and *her9* mutant retina. **(H)** displaying a decreased and patchy or abnormal expression pattern across the circumference of the mutant retina. **(I)** Chi-square analysis comparing WT incross and *her9* heterozygous incross expression pattern. **(J)** qPCR for *thrβ* at 48 and 72 hpf. L, lens. Scale bar= 50μm

3.4.12 Her9 mutant photoreceptors undergo apoptosis

In addition to abnormal specification, the reduced numbers of rods and double cones in *her9* mutants could reflect a decrease in survival of differentiated photoreceptors. To determine whether this was the case, we performed TUNEL labeling on retinal cryosections from WT and *her9* mutant retinas from 24 hpf to 5 dpf to identify apoptotic cells. At 24 hpf, we observed a slight increase in TUNEL+ cells in the lens of *her9* mutants compared to WT, but no cell death in the retina (**Figure 3.11A-A' and E**). At 48 hpf, there was no difference in TUNEL+ cells between WT and *her9* mutant retinas (**Figure 3.11B-B' and E**). However, at 72 hpf we observed a significant increase in TUNEL+ cells in the GCL, INL, ONL, and CMZ of *her9* mutant retinas compared to the WT (**Figure 3.11C-C' and E-F**). Interestingly, we observed a noticeable cluster of TUNEL+ cells in the dorsal peripheral retina adjacent to the CMZ (**Figure 3.11C'**). Additionally, some of the TUNEL+ cells in the INL had the morphology of Müller glia, which could indicate the Müller glia were dying, but could also be due to Müller glia phagocytosis of other dying cells (**Figure 3.11C'**). By 5 dpf, apoptosis in *her9* mutants remained elevated in the ONL, CMZ, and INL relative to WT retinas (**Figure 3.11D-D' and G**). These data indicate that Her9 is required for the survival of post-embryonic retinal progenitor cells, photoreceptors, and possibly cells in the INL.

Figure 3. 11 Her9 mutant retinas display increased apoptosis beginning at 72 hpf

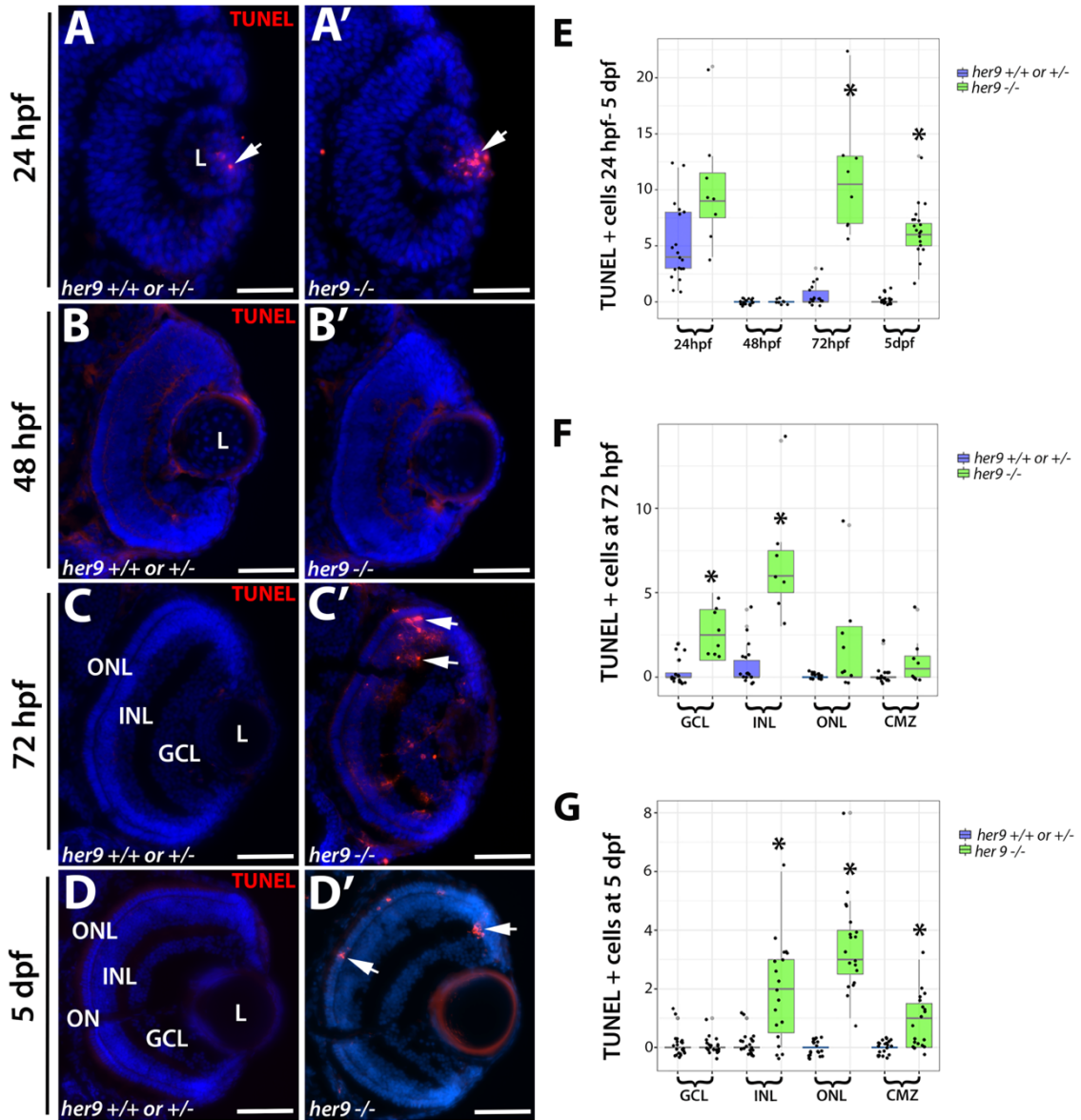


Figure 3.11 Her9 mutant retinas display increased apoptosis beginning at 72 hpf. (A-D')TUNEL staining on cryosections of WT and *her9* mutant retinas. *Her9* mutant embryos show no significant increase in cell death in the retina at 24 and 48 hpf compared to WT siblings (A-B'). At 72hpf, *her9* mutant larvae display increased apoptosis in the GCL, INL, ONL and CMZ (C-C') that remains elevated in the ONL at 5 dpf (D-D'). Cell counts of TUNEL+ cells (E-G). ****cell count data points below to 0 axis to not indicate negative numbers but are an attempt by the R software to display all the data points. **** ONL, outer nuclear layer; INL, inner nuclear layer; GCL, ganglion cell layer; L, lens. Scale bar = 50 μ m

3.4.13 RA regulates *her9* expression in the retina but Her9 is not required for RA's effects on opsin expression

What regulates Her9 activity in the retina? Several previous studies have demonstrated that unlike many Hes/Hey/Her family members, Her9 does not respond to Notch signaling (Latimer et al., 2005; Leve et al., 2001; Reinhardt et al., 2015). However, it has been shown that Her9 is downstream of RA signaling in the developing inner ear (Radosevic et al., 2011b). Given that RA signaling is critical for eye development (Hyatt et al., 1996a; Hyatt et al., 1996b) and has demonstrated effects on photoreceptor differentiation and opsin expression (Mitchell et al., 2015; Stenkamp et al., 2014; Stevens et al., 2011), we hypothesized that Her9 functions downstream of RA to regulate opsin expression and photoreceptor survival. We used in situ hybridization and qPCR on 36 hpf embryos to determine whether *her9* expression in the retina is altered by manipulation of the RA signaling pathway. Zebrafish embryos were treated in the dark from 24 to 36 hpf with 1 μ M RA, 100 μ M of the RA signaling inhibitor diethylaminobenzaldehyde (DEAB), or 0.3% DMSO alone as a carrier control. Embryos were then processed for WISH or qPCR to detect *her9* expression. In control embryos, *her9* expression was observed in the peripheral CMZ and around the lens and choroid fissure as described above (**Figure 3.12A**). We observed a noticeable decrease in *her9* expression in the retina when embryos were treated with DEAB (**Figure 3.12A'**). In contrast, there was a significant increase in the expression of *her9* all across the retina when embryos were exposed to RA (**Figure 3.12A''**). qPCR analysis for *her9* expression confirmed the decrease and increase in *her9* expression following DEAB and RA treatments, respectively (**Figure 3.12B**). From these data, we conclude that *her9* expression in the retina is regulated by RA signaling.

Previous work demonstrated that exposure to exogenous RA between 2 and 5 dpf resulted in increased rhodopsin expression and decreased red, UV, and blue cone opsin expression in zebrafish (Prabhudesai et al., 2005). To test the hypothesis that Her9 is required to mediate the effects of RA signaling on photoreceptor opsin expression, we treated WT and *her9* mutant zebrafish with RA from 24-48 hpf (for rods) or 24 hpf-5 dpf (for cones), and then examined XOPS:GFP or T α C:GFP transgene and cone opsin expression by IHC. In WT zebrafish, RA treatment resulted in a significant increase in GFP+ rhodopsin expressing cells dorsally and ventrally compared to the untreated retinas, and a significant decrease in UV and green cone

opsin expression, as expected (**Figure 3.12 and Figure S3.6**). Surprisingly, an increase in GFP+ rhodopsin expressing cells and a decrease in UV and green cone opsin expressing cells were also observed in RA-treated *her9* mutants when compared to control treated mutants (**Figure 3.12 and Figure S3.6**). Taken together, these data suggest that although *her9* expression in the retina is downstream of RA signaling, Her9 is not strictly required for the effects of RA on rod and cone opsin expression.

Figure 3. 12 RA regulates *her9* expression but Her9 is not required for the effects of RA on opsin expression

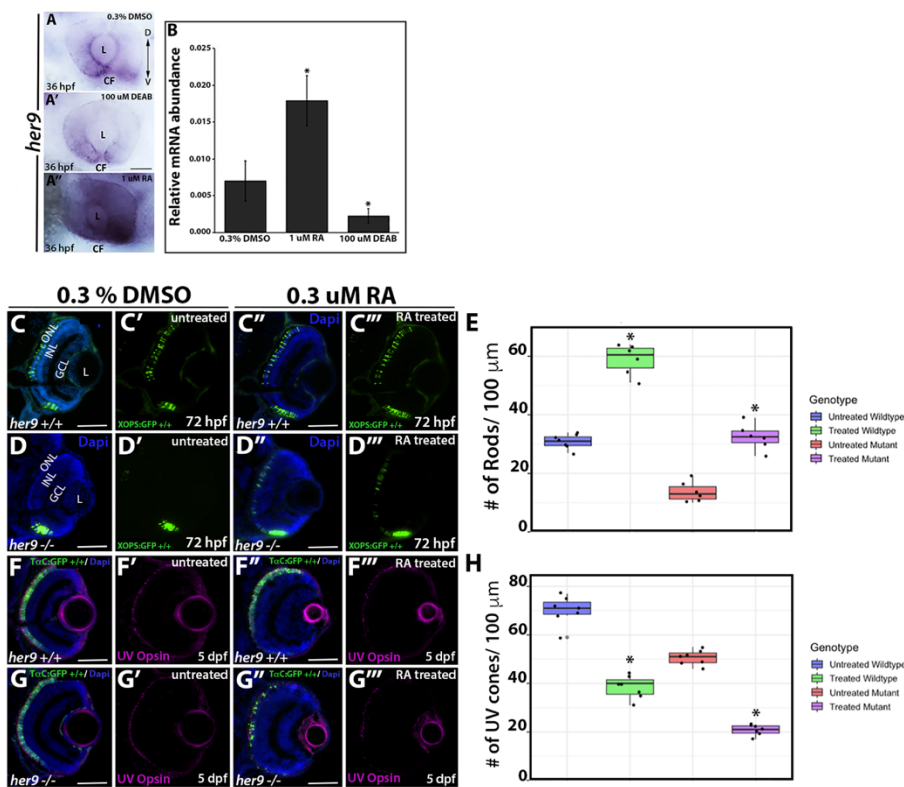


Figure 3.12 RA regulates *her9* expression but Her9 is not required for the effects of RA on opsin expression. WISH for *her9* expression at 36 hpf in control treated (**A**), DEAB treated (**A'**) and RA treated (**A''**) retinas. (**B**) qPCR for *her9* expression in heads of 36 hpf zebrafish embryos following drug treatments. N=20 heads per biological replicate, 3 biological replicates per drug treatment. *p<0.05. GFP expression in control treated vs. RA-treated XOPs:GFP;*her9*^{+/+} (**C-C''**) or XOPs:GFP;*her9*^{-/-} (**D-D''**) retinas. (**E**) Cell counts comparing rhodopsin expressing cells in the untreated and treated retinas. (**F-F''**) IHC for UV opsin in control vs. RA-treated TαC:GFP;*her9*^{+/+} (**F-F''**) or TαC:GFP;*her9*^{-/-} (**G-G''**) retinas. (**H**) Cell counts comparing UV opsin expressing cells in the untreated and treated retinas (# of cells/ (eye size/100)). CF, choroid fissure; ONL, outer nuclear layer; INL, inner nuclear layer; GCL, ganglion cell layer; L, lens; Scale bar= 50μm

3.5 Discussion

The zebrafish *her9* gene is the ortholog of the human *HES4* gene and is one of the least studied bHLH-O transcription factors. This is largely due to the fact that a Hes4 homolog is absent from the mouse and rat genomes (El Yakoubi et al., 2012). Since *HES4* is expressed in humans and has been shown to play critical roles in the development of several vertebrate tissues, further investigations of Her9 function are needed. To our knowledge, ours is the first study to describe a germline loss of function mutation of *her9*, which we believe will be a powerful resource for elucidating its role in several developmental contexts.

In this study, we focused on the role of Her9 during retinal development. We observed *her9* expression predominantly in the ventral most portion of the developing retina at 24 hpf, which localized to the ciliary marginal zone (CMZ) around 36 hpf until at least 5 dpf (**Figure 3.1**). This expression pattern is consistent with what has previously been described for *her9* in *Xenopus* and *Medaka* (El Yakoubi et al., 2012; Reinhardt et al., 2015), suggesting a conserved mode of action in the developing retina at least across fish and amphibians.

To characterize the role of Her9 in zebrafish development, we used CRISPR/Cas to generate null mutations in *her9*. The mutations caused frame-shifts, and early termination codons, leading to nonsense-mediated decay of *her9* mRNA, which is supported by our sequencing, qPCR and Western blot data. The *her9* mutants appear developmentally delayed at around 20 hpf but by 72 hpf many *her9* mutant larvae look similar to their WT siblings. The relatively mild embryonic phenotype could be due to the buffering effects of maternally deposited WT *her9* mRNA. Nevertheless, by 5 dpf the mutants have not developed a swim bladder, display craniofacial and gastrointestinal defects, darker pigmentation, and abnormal swimming patterns. The *her9* mutants do not survive past 12 dpf, which may be due to problems with feeding and digestion.

One of the most striking phenotypes in the *her9* mutant consists of a significant decrease in rod and double cone photoreceptors, which is associated with elevated levels of apoptosis in the ONL and dysmorphic and truncated outer segments in the surviving rods and red/green cones. Intriguingly, this defect does not seem to affect the short wavelength (blue and UV) photoreceptor subtypes. The rod-cone dystrophy observed in *her9* mutants suggests that Her9 is required for rod and cone maintenance and survival. The degeneration of the rod

photoreceptors seems more severe than the cones, supporting a rod-cone progression in degeneration. Given that we did not observe expression of *her9* in mature photoreceptors, this suggests that Her9 acts non-cell autonomously to maintain rods and double cones. It is unlikely that the RPE contributes to the photoreceptor phenotypes, since we did not observe *her9* expression in the RPE, nor were there any obvious RPE structural defects in *her9* mutants. One possibility is that one of the functions of Her9 in the peripheral retina is to influence gradients of retinoic acid or thyroid hormone signaling, which are known to be important for photoreceptor maintenance (see below). In any case, the truncation of the cone outer segments could explain the lack of VBA and OKR responses in the *her9* mutants, although we cannot rule out the possibility that the absent OKR response is due to defects in other tissues outside the retina. Given that we observed a significant decrease in rod and cone opsin expression, it is also possible that other phototransduction proteins are downregulated as well. Future electrophysiological and ultrastructural studies could help to resolve the functional consequences of Her9 loss to the photoreceptor outer segments.

The process of photoreceptor development has been extensively studied and important transcription factors that regulate photoreceptor specification have been identified, such as *Crx*, *Nr2e3*, and *thrβ*, among many others. In our investigations of whether Her9 is required for rod and/or cone lineage specification, we saw no significant changes in *crx* expression in *her9* mutant retinas, indicating that Her9 is not required at this stage of photoreceptor specification. However, we did observe a significant decrease in expression of *Nr2e3* and *thrβ* in *her9* mutants, indicating that Her9 may be required for the specification of some photoreceptor subtypes once progenitors have chosen a specific photoreceptor lineage.

The reduction in *thrβ* expression in *her9* mutants may contribute to additional phenotypes outside of the retina. Lui and Chan (Liu and Chan, 2002) showed that thyroid hormones are important for the embryonic to larval transition in zebrafish. Inhibition of *Thrβ* produced a missing swim bladder, defects in the gastrointestinal tract, and craniofacial defects. These phenotypes resemble those observed in the *her9* mutants where we also see a loss of swim bladder, gastrointestinal tract defects, and craniofacial abnormalities in addition to the photoreceptor defects. Furthermore, given that there is a direct link between *thrβ* expression and cone development and differentiation (Suzuki et al., 2013), our data suggest that Her9 could be directly or indirectly required for *thrβ* expression. This theory could be tested by exposing

mutant embryos to L- thyroxine (T4) and 3,5,3' –L-triiodothyronine (T3) to see whether we can rescue any components of the *her9* mutant phenotype.

In addition to decreases in photoreceptors, we also observed significant decreases in the number of Müller glia, ganglion cells, and in proliferating cells in the CMZ of *her9* mutants. Investigation into the role of Her9/Hes4 in both Medaka and *Xenopus* have demonstrated expression of *her9* in the CMZ of the developing and post-embryonic retina (El Yakoubi et al., 2012; Reinhardt et al., 2015). Consistent with those data, we also observed the expression of *her9* localized to the CMZ starting at 36 hpf. We observed a significant decrease in the proliferating cells of the CMZ of *her9* mutants that became more severe over time. This indicates that Her9 is required for the maintenance of proliferating retinal progenitor cells. Morpholino knockdown of Hes4 in *Xenopus* produced dose-dependent eye defects from small eyes to animals with no eyes at all (El Yakoubi et al., 2012). In our zebrafish *her9* mutants, we observed a variable degree of microphthalmia but never complete loss of eyes. This difference in phenotypic severity could be due to species-specific requirements for Her9 during oculogenesis, or to differences in experimental approach. In addition to a decrease in retinal cells, previous studies in *Xenopus* have shown that the loss of Hes4 leads to a significant increase in apoptosis in the retina (Nagatomo and Hashimoto, 2007; Nichane et al., 2008a; Nichane et al., 2008b). In our model, we also observe a significant increase in apoptosis in the retina and brain of our *her9* mutant which leads us to conclude that Her9 plays a role in cellular proliferation early on in retinal development and then cell survival later.

Radosevic et al. (Radosevic et al., 2011a) demonstrated that Her9 is downstream of the Retinoic acid (RA) signaling pathway in the neural patterning that underlies the development of the otic vesicle. With these data in mind, we wanted to determine whether Her9 is also downstream of RA signaling in the developing retina. Accordingly, we observed an increase in *her9* expression in the retina following exogenous treatment with RA, and blocking RA signaling with DEAB resulted in a decrease in *her9* expression. These data demonstrate that *her9* expression is regulated by RA signaling in the developing zebrafish retina. Taken together with the outer segment defects and decreased opsin expression in *her9* mutants, as well as previous studies demonstrating that opsin expression is regulated by RA signaling (Hyatt et al., 1996a; Hyatt et al., 1996b; Mitchell et al., 2015), we hypothesized that loss of Her9 was directly disrupting opsin expression downstream of RA signaling. However, when we exposed *her9*

mutants to exogenous RA, we observed similar modulations in opsin expression to those observed on their WT siblings. This suggests that Her9 is not acting directly on opsin expression and may instead be acting downstream of RA to indirectly regulate photoreceptor differentiation and opsin expression. Future studies will include determining whether Her9 is interacting with other components of the RA pathway such as retinoic acid receptors, retinoid X receptors, or retinoic acid synthesis or degradation enzymes.

In summary, we have characterized a novel role for Her9 in photoreceptor development, maintenance, outer segment morphology and opsin expression. Given that the *her9* mutant displays such significant defects in rod and cone photoreceptors our results implicate Her9/HES4 as an important component of the gene regulatory network that regulates photoreceptor differentiation and survival. Based on the data collected we cannot determine how much each component (differentiation, maintenance or survival) is contributing the retinal phenotype and further experimentation will be required. Future studies of Her9/HES4 could add to our understanding of its role in regulating retinal stem cell proliferation at the ciliary margin and determine how its loss leads to photoreceptor degeneration.

3.6 Supplemental Tables

Table S3. 1 Primer sequences

Primers	Sequences	Use
<i>her9</i> F	CCTGACGGAGAACTGAACACAAGACACACA	RT-PCR/ISH
<i>her9</i> R	TTTCTCAATGGTACGGCGGGTGCTCTGGGC	RT-PCR/ISH
<i>atp5h</i> F	TGCCATCTCAGCAAAACTTG	RT-PCR/qPCR
<i>atp5h</i> R	CACAGGCTCAGGAACAGTCA	RT-PCR/qPCR
<i>her9</i> CR F	AAGCTTCCTGACGGAGAACTGAACACAAGACACACA	cDNA plasmid
<i>her9</i> CR R	GAATTCCTTCTCAATGGTACGGCGGGTGCTCTGGGC	cDNA plasmid
<i>her9</i> F	CTCAGCAAGTACCGCGCAGGAT	qPCR
<i>her9</i> R	TCCCATACAACCGGACAGGTGG	qPCR
<i>trβ2</i> F	ACAGGGGAGACTGTAGAGGTCTGA	ISH
<i>trβ2</i> R	TCAGTCTTCAAACACTTCCAGGAAG	ISH
<i>trβ2</i> F	AAGAGGGGCTCTGGCTCTTA	qPCR
<i>trβ2</i> R	GTTGTCCACAGACTCGCTGA	qPCR
<i>Nr2e3</i> F	CCAGCAGTGGGAAACACTAT	qPCR
<i>Nr2e3</i> R	ATGGGCTTTATCCACAGGAC	qPCR
<i>Nr2e3</i> F	ATCATCGCGGCCGCCACCATGGAGGATCCGATGTCAGAAATG	ISH
<i>Nr2e3</i> R	ACTACTAAGCTTATCAGTTTTGAACATGTCACACAAG	ISH
<i>crx</i> F	ATGCTGTGAACGGGTTAAC	qPCR
<i>crx</i> R	AAGCTTCCAGAATGTCCAG	qPCR
<i>rho</i> F	GCCTATGTCCAATGCCACCGG	qPCR
<i>rho</i> R	AGTTGACGGGGAAGCCGGTGA	qPCR
<i>LWS</i> F	GCGGAGGGGACGAAACAACA	qPCR
<i>LWS</i> R	CCATCGAGGGGCAATGTGGT	qPCR
<i>RH2</i> F	TCTACATCCCATGTCAAACAGGA	qPCR
<i>RH2</i> R	AGTCAGGACATTGATGGGAAATCC	qPCR
<i>SWS1</i> F	CGTTCAATTCGGAAATGCTTCC	qPCR
<i>SWS1</i> R	TGTGCCACGATAAATACAAAGCC	qPCR
<i>SWS2</i> F	AGCAAACGCCAGAACTGTTCTGA	qPCR
<i>SWS2</i> R	CATGAATACGCCACTGTGTCCCA	qPCR
<i>eEF1α</i> F	CTTCTCAGGCTGACTGTGC	qPCR
<i>eEF1α</i> R	CCGCTAGCATTACCCTCC	qPCR
<i>six7</i> F	ACCGGTTTACACGCGAATCT	qPCR
<i>six7</i> R	GCAGGGGGAATTCTTACGG	qPCR
<i>gdf6a</i> F	TATTGGTGGTCTACACGCGG	qPCR
<i>gdf6a</i> R	TAAGCGCAGTTCTCCGTCTG	qPCR
<i>vsx2</i> F	GAAGTGTGGGGTCGCAGTA	qPCR
<i>vsx2</i> R	GTGCATCCCTAGAAGCCAGG	qPCR

Table S3. 2 Oligo sequences

Oligo name	Oligo sequence	Use
<i>her9</i> F CRISPR1	GTGTTTGATCATGCCAGCCGAT	HRMA/sequencing
<i>her9</i> R CRISPR1	CCTTTCTATGCTCGCTGGCATT	HRMA/sequencing
<i>her9</i> F CRISPR2	CCACCTGTCCGGTTGTATGGG	HRMA/sequencing
<i>her9</i> R CRISPR2	GAGGCGCCGTTGATGGGTAAC	HRMA/sequencing
<i>her9</i> C1 F	ATCTATAAATACCGCTGGCGTGTGG	RFLP
<i>her9</i> C1 R	TCTCGTTGATTCTCGCTCTGCG	RFLP
CRISPR1 target site	GGAGTATGAGATCCACTGGC	<i>her9</i> target 1
CRISPR1 oligo-1	TAGGAGTATGAGATCCACTGGC	<i>her9</i> C1 oligo-1
CRISPR1 oligo-2	AAACGCCAGTGGATCTCATACT	<i>her9</i> C1 oligo-2
CRISPR2 target site	GGCAGGCTGAGGGTAGTTCA	<i>her9</i> target 2
CRISPR2 oligo-1	TAGGCAGGCTGAGGGTAGTTCA	<i>her9</i> C2 oligo-1
CRISPR2 oligo-2	AAACTGAACTACCCTCAGCCTG	<i>her9</i> C2 oligo-2

3.7 Supplemental figures

Figure S3. 1 Generation of *her9* mutants using CRISPR/Cas9

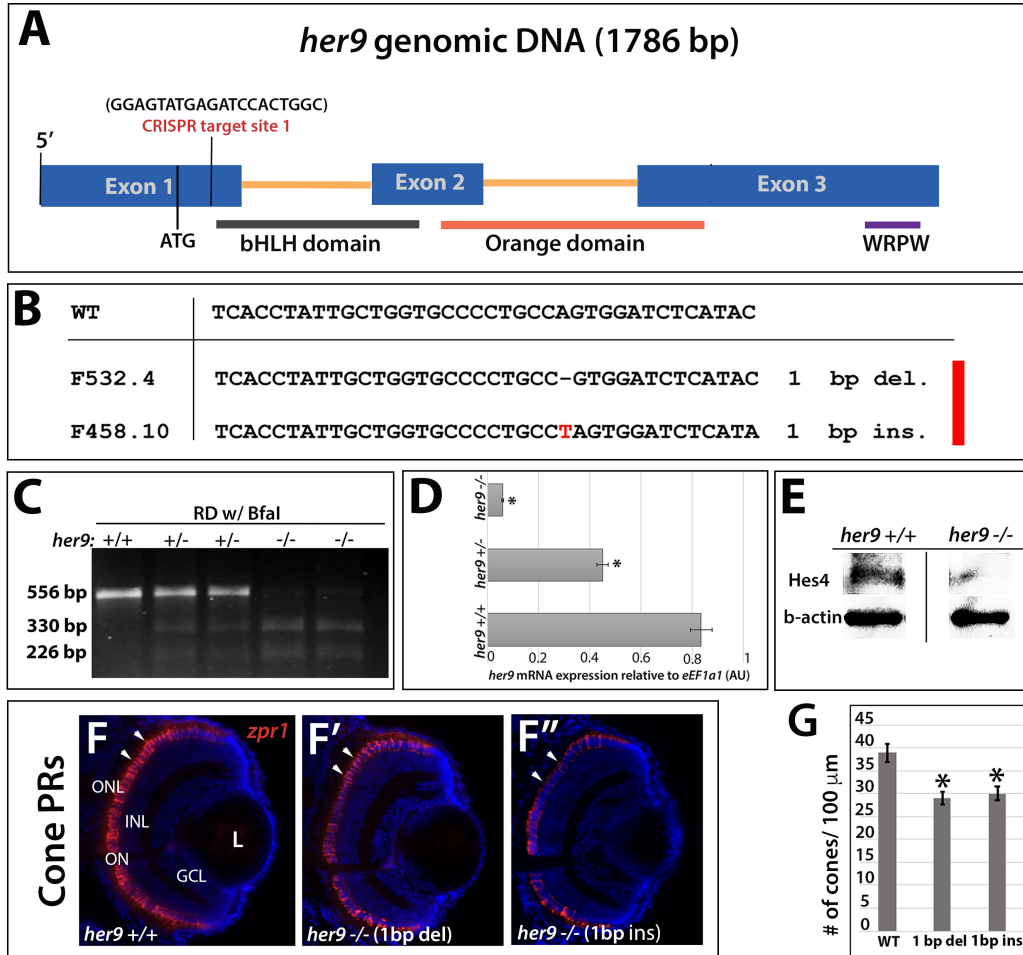


Figure S3.1 Generation of *her9* mutants using CRISPR/Cas9. (A) The *her9* locus contains 3 exons spanning 1786 bp on linkage group 23. The first CRISPR target site is 54 bp 3' of the translation start site, and 46 bp upstream of the beginning of the bHLH domain. (B) Comparison of WT *her9* sequence with 1bp deletion and 1bp insertion mutations. (C) RFLP analysis of WT, heterozygous and homozygous *her9* 1 bp insertion mutant cut with Bfal. (D) qPCR analysis of *her9* mRNA expression in WT, heterozygous and homozygous mutants at 48 hpf. (E) Western blot with a HES4 antibody, indicating the loss of Her9 protein in the *her9* mutants compared to WT siblings. Immunohistochemistry with a red-green cone antibody (Zpr1) in *her9*^{+/+} or *her9*^{+/-} and *her9*^{-/-} (1 bp ins and 1 bp del; F-F') retinal sections. (G) Cone cell counts in *her9*^{-/-} mutant larvae with 1 bp ins and 1 bp del and their WT siblings (# of cones/ 100 μ m; t-test ($p < .0001$)).

Figure S3. 2 Mobility assay of 5 dpf larvae

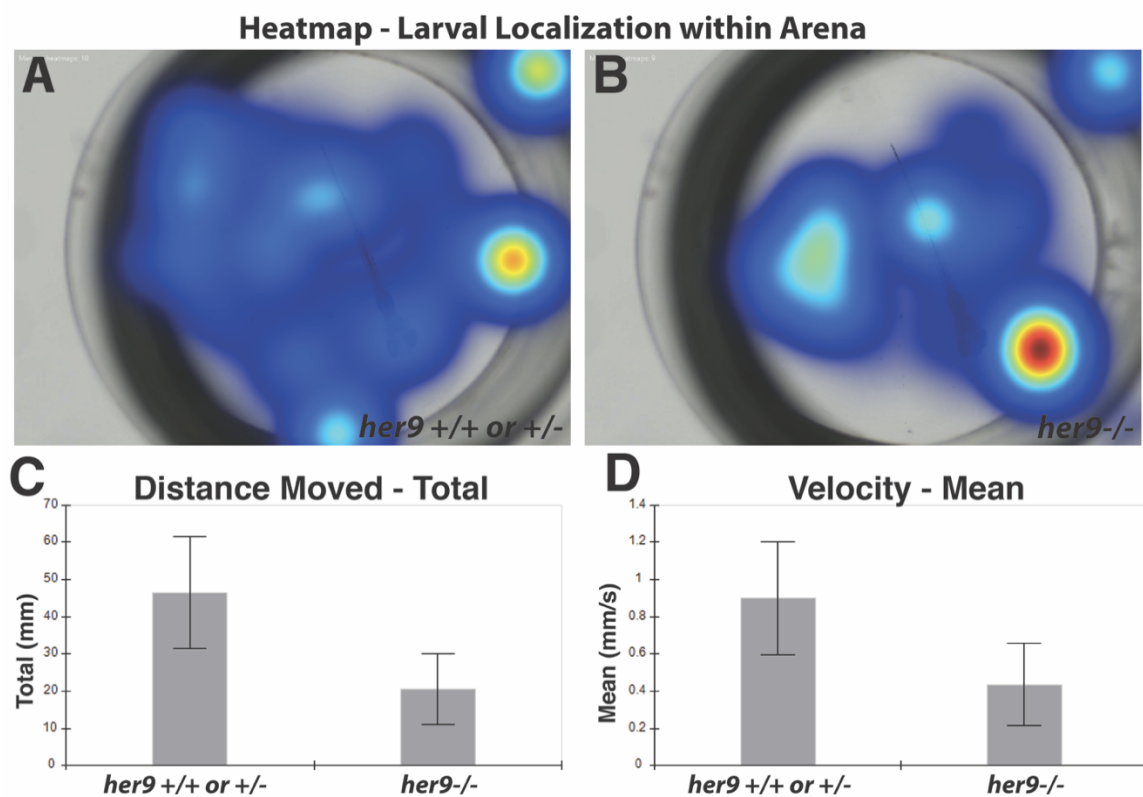


Figure S3.2 Mobility assay of 5 dpf larvae. (A) Heat map indicating the amount of time the WT or *her9*^{+/-} larva spends in different parts of the arena. **(B)** Heat map indicating the amount of time the *her9*^{-/-} larva spends in different parts of the arena. **(C)** Comparison of the average total distance travel by the larvae. The WT or *her9*^{+/-} average total distance traveled was 46.47±14.91 mm, the *her9*^{-/-} average total distance traveled was 20.59±9.59 mm. WT/Het= 10 embryos; Mut = 9; t-test (p=0.0824). **(D)** Comparison of the average velocity of larvae. The WT or *her9*^{+/-} average velocity was 0.901±0.302mm/s, the *her9*^{-/-} average velocity was 0.436±0.22 mm/s. WT/Het= 10 embryos; Mut = 9 embryos; t-test (p= 0.1162).

Figure S3. 3 Injection of *her9* mRNA rescues the *her9* mutant phenotype

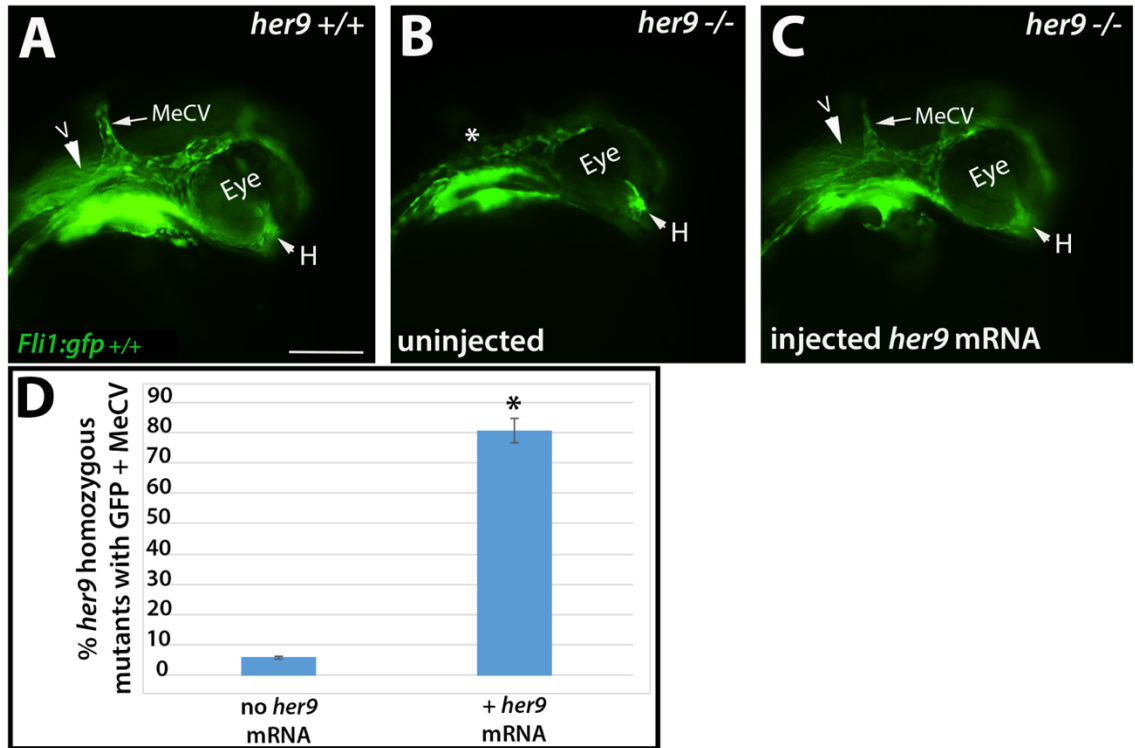


Figure S3.3 Injection of *her9* mRNA rescues the *her9* mutant phenotype. (A) Fli1:GFP+ midcerebral vein in WT embryos at 24 hpf. (B) Missing midcerebral vein in uninjected *her9* homozygous mutant embryos at 24 hpf (asterisk; n=193 embryos; WT=48, Het=101, Mut=44; MeCV+=160; MeCV-=33; $\chi^2 = p < .00001$). (C) In *her9* homozygous mutants injected with *her9* mRNA, the midcerebral vein is now visible at 24 hpf. (D) Quantification of rescue of *her9* mutant phenotype after *her9* mRNA injections (n=47 embryos; MeCV+=42; $\chi^2 = p < 0.000508$). MeCV, Midcerebral vein; H, hyaloid vein; V, ventricle. Scale bar= 50 μ m.

Figure S3. 4 *Her9* mutants display a decrease in glial cells in the brain and gut

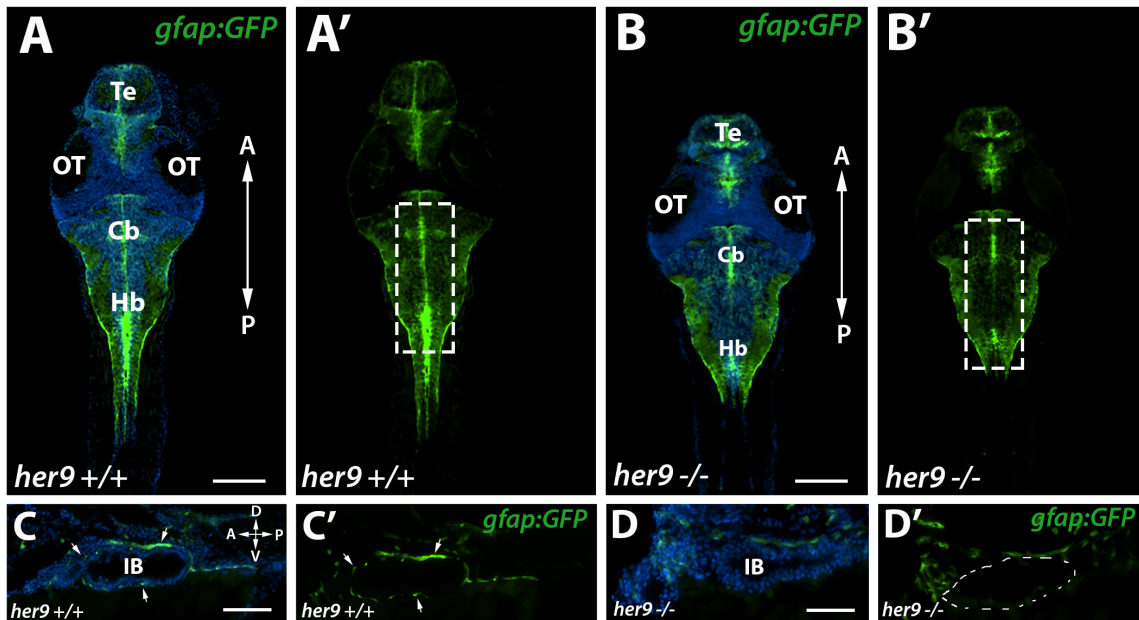


Figure S3.4 *Her9* mutants display decrease in glial cells in brain and gut. (A-B') Cryo-sections of *her9*^{-/-} mutant larvae and their WT siblings brain on *gfap:GFP* background (dash lined box highlights *gfap* expressing cells in Cb and Hb). (C-D') Cryo-sections of *her9*^{-/-} mutant larvae and their WT siblings brain on *gfap:GFP* background (Arrows indicate *gfap* expressing cells in Intestinal Bulb). Te, Telencephalon; OT, Optic tectum; Cb, Cerebellum; Hb, Hindbrain; IB, Intestinal Bulb. Scale bar= 50 μm

Figure S3. 5 Expression of *crx* and *Nr2e3* at 72 hpf

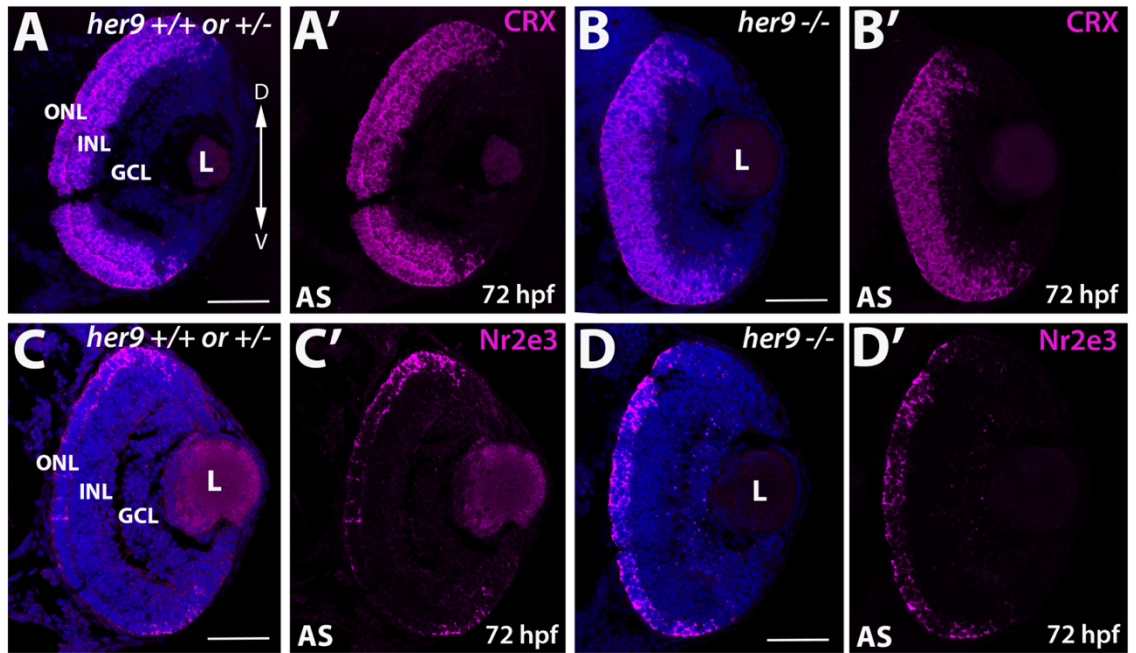


Figure S3.5 Expression of *crx* and *Nr2e3* at 72 hpf. (A-B) Fluorescent in situ hybridization (FISH). *Crx* expression at 72 hpf in WT and *her9* mutant retina. *Her9* mutants displayed similar expression to WT. (C-D') *Nr2e3* expression at 72 hpf in WT and *her9* mutant retina. Expression in the mutant ONL was distorted compared to the WT. L, lens; ON, optic nerve. Scale bar= 50 μ m

Figure S3.6 Her9 is not required for the effects of RA on opsin expression

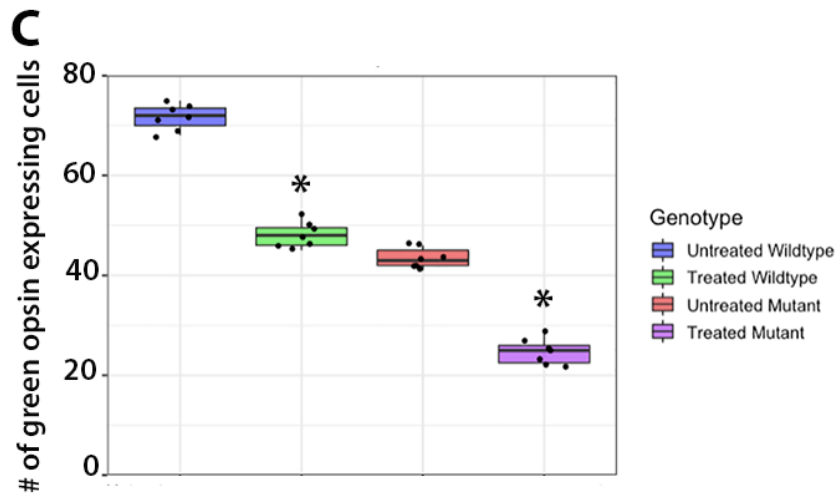
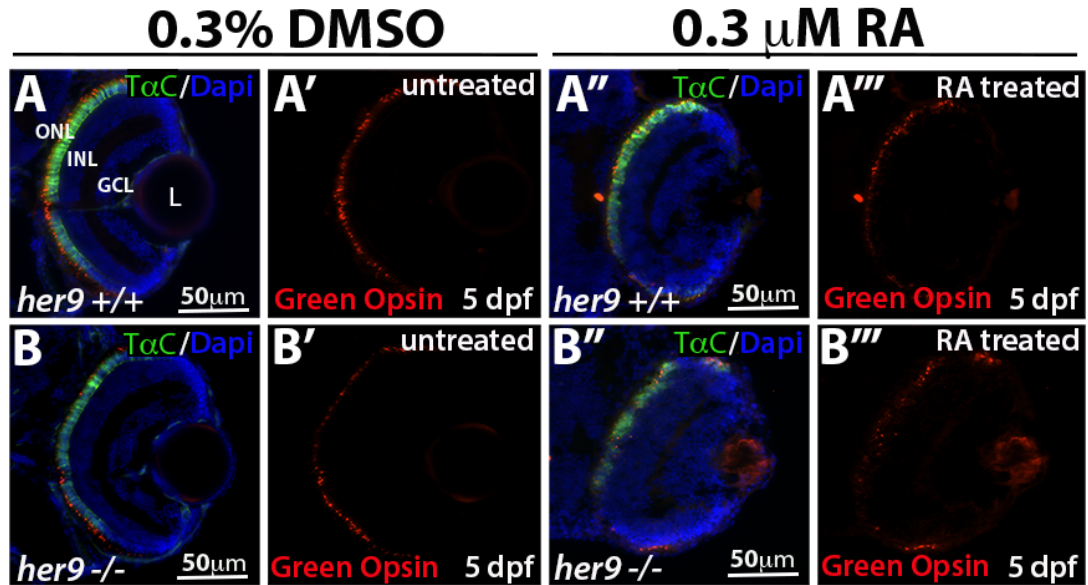


Figure S3.6 Her9 is not required for the effects of RA on opsin expression. (A-A''') IHC on TαC:GFP WT retinas comparing Green opsin expression after being treated with RA from 24-120 hpf. **(B-B''')** IHC on TαC:GFP mutant retinas comparing Green opsin expression after being treated with RA from 24-120 hpf. **(C)** Cell counts comparing Green opsin expressing cells in the untreated and treated retinas. WT/Het (untreated) = 10; WT/Het (treated) = 10; t-test ($p < .0001$). Mut (untreated) = 10; Mut (treated) = 10; t-test, $*p < .0001$. ONL, outer nuclear layer; INL, inner nuclear layer; GCL, ganglion cell layer; L, lens; Scale bar = 50 μm

Figure S3. 7 Western blot

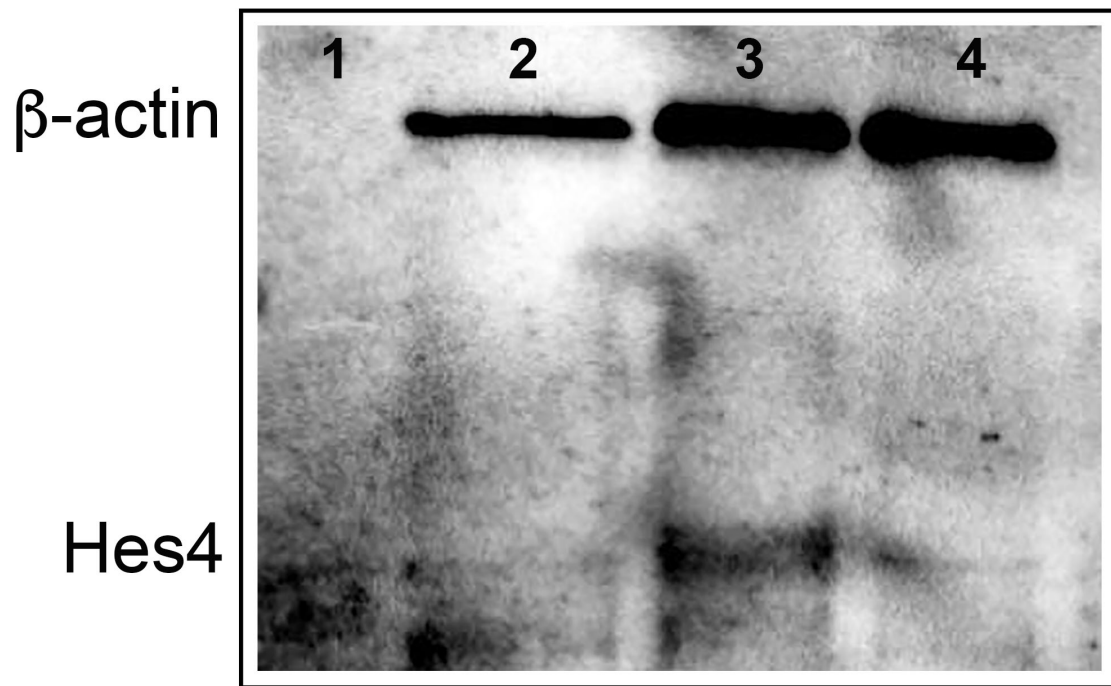


Figure S3.7 Western blot. (1) Ladder. (2) Adult zebrafish Pancreatic lysate (Positive control). (3) Her9 +/+ or +/- Lysate (Upper band β -actin; lower band Hes4). (4) Her9 -/- Lysate (Upper band β -actin; lower band Hes4). Small band in Mutant lane could be non-specific

Acknowledgments

The authors would like to thank Lucas Vieira Francisco for excellent zebrafish care. We also thank Dr. David Hyde (University of Notre Dame) for generously providing the zebrafish opsin antibodies.

Funding

This work was supported by a grant from the National Institutes of Health (R01EY021769, to A.C.M.) and the University of Kentucky Lyman T. Johnson graduate fellowship (to C.E.C).

Cagney E. Coomer, Evelyn Turnbaugh, Eden Janesch, and Ann C. Morris

Department of Biology, University of Kentucky, Lexington, Kentucky 40506

4.1 Abstract

Neural crest cells (NCC) are multipotent progenitor cells that arise from the neural plate border and go on to contribute to a wide variety of morphological structures such as the jaw and palate, enteric nervous system (ENS), and pigment cells. Defects in essential steps in neural crest cell development have been associated with a wide variety of congenital disorders, collectively referred to as neurocristopathies. Her9/Hes4 is a bHLH-O transcriptional repressor that has been shown to function in neural crest cell development in *Xenopus*. In this study, a line of CRISPR edited zebrafish harboring an inactivating mutation in *her9* was characterized for neural crest cell phenotypes. Here we show that Her9 is essential for the development of specific neural crest cell lineages. *Her9* mutants present a wide variety of NCC defects including craniofacial abnormalities, improper formation of the gut, and pigment cell defects. We also found that the loss of Her9 causes an upregulation in expression of BMP pathway genes and subsequent defects in neural crest cell specification, migration, differentiation, and survival. Furthermore, loss of Her9 leads to the downregulation of *foxd3*, a known NCC marker, and apoptosis. Our results suggest that Her9 functions in neural crest development by regulating members of the NCC gene regulatory network (GRN) to control specification, migration, differentiation and survival.

4.2 Introduction

Neural crest cells (NCC) are a population of multipotent migratory cells that give rise to a wide variety of cell types such as craniofacial cartilage, pigment, neuronal and glial cells (Rocha et al., 2020; Uribe and Bronner, 2015). Although all NCC arise from the neural tube they

are divided into subpopulations based on their region of origin. The subpopulations include the cranial (craniofacial skeleton, cranial ganglia and heart muscle), vagal (enteric and smooth muscle) and trunk (dorsal root and sympathetic ganglia) NCC, each of which display distinct migratory patterns and develop into multiple derivatives. NCC development takes place during late gastrulation and neurulation in a sequence of steps that begins with induction, where cranial neural crest cells (CNCC) are first induced at the interface between neural and non-neural ectoderm that is largely dependent on a BMP signaling gradient (Kelsh et al., 1996; Schumacher et al., 2011) The specification of NCC occurs on the dorsal side of the neural tube at the neural plate border (Meulemans and Bronner-Fraser, 2004; Simoes-Costa and Bronner, 2015). At this stage, transcription factors specific to NCC specification are expressed, including, but not limited to *sox10*, *snail1b*, *foxd3* and *twist* (Carney et al., 2006; Das and Crump, 2012; Thisse et al., 1995; Wang et al., 2011). Research has shown that these neural crest specific transcription factors are also required for the development of individual and overlapping NCC lineages. For instance, in the *colourless* mutant the loss of Sox10 results in defects in melanoblasts, neurons, and glia, but the cranial derivatives are unaffected (Dutton et al., 2001).

Following induction and specification, the NCCs go through an epithelial-to-mesenchymal transition (EMT; **Figure 4.1**), during which time they transition to migrating mesenchymal cells by changing their morphology, adhesion properties, polarity and behavior (Theveneau and Mayor, 2012b). Transcription factors such as *snail1b* and *twist1a/b* have been shown to be expressed during EMT, but their specific roles have yet to be discovered (Germanguz et al., 2007; Thisse et al., 1995). After the dynamic changes required for EMT, NCCs migrate along conserved pathways for long distances to reach their final destination, and differentiate into a wide variety of cell types (Bronner and Simoes-Costa, 2016). Cranial and trunk NCCs display very distinct modes of migration along different routes. Cranial NCC migration begins when a subset of cranial neural crest cells (CNCC) from the midbrain travels anteriorly between and around the eye towards the neurocranium (Knight and Schilling, 2006). CNCCs that are posterior to the midbrain/hindbrain migrate in streams ventrally to form the pharyngeal arches and viscerocranium (Schilling and Kimmel, 1994). Studies have shown that the major players influencing the migration of CNCC are semaphorins and their neuropilin receptors (Halloran and Berndt, 2003; Theveneau and Mayor, 2012a). *Sema3f* and *sema3g* are expressed in NCC free regions of the head and use the interaction with their receptors (*nrp2a* and *nrp2b*), which are expressed by NCC, to mediate the migration of CNCCs (Yu and Moens,

2005). Accompanying the repulsive cues in facilitating migration are chemoattractants such as *cxcr4a* (Theveneau and Mayor, 2012b). In contrast, trunk neural crest cells (TNCC) migrate in two specific pathways. First, they migrate between the neural tube and somites, then laterally between the somites and ectoderm (Raible et al., 1992). The first set of cells to migrate give rise to sympathetic and sensory neurons, Schwann cells, and pigment cells and the second set of cells produce only pigment cells (Raible and Eisen, 1994). The molecular basis of TNCC migration is not as well elucidated as CNCCs, but it's been shown that *MuSK* and *wnt11r* receptor play a major role in restricting TNCC migration to the center of each somite (Banerjee et al., 2011). The loss of *MuSK* leads to impaired migration stream formation.

Once migration is complete and NCCs reach their designated locations, the cells differentiate into specific NCC derivatives (**Figure 4.1**). Pigment cells derived from TNCC consist of 3 subtypes of cells: xanthophores, melanophores and iridophores. Transcription factors *mitfa*, *foxd3*, and *pax7* have been shown to play a central role in the differentiation of melanocytes. *Mitfa*^{-/-} mutants present with a lack of melanophores in larval and adult zebrafish (Lister et al., 1999), while the loss of *pax7a* and *pax7b* result in absence of xanthophores and an increase in melanophores (Nord et al., 2016). Chondrocytes give rise to a significant portion of the craniofacial skeleton in vertebrates such as the pharyngeal arches, the mandible, and most components of the jaw (Takahashi et al., 2001) and originate from CNCC. Specific factors have been identified and shown to be important for craniofacial development; some of those factors include *tbx1*, *vgll2* and *pitx2* (Arnold et al., 2006; Johnson et al., 2011). It has been demonstrated that *Vgll2* interacts with fibroblast growth factor (FGF) and retinoic acid (RA) to regulate NCC survival and craniofacial development, with the loss of *vgll2a* resulting in increased cell death and craniofacial defects (Johnson et al., 2011). The knockout of *pitx2* in mice is embryonic lethal and embryos display ocular, craniofacial, brain, heart, and body wall defects (Kitamura et al., 1999; Lin et al., 2009).

NCCs give rise to a multitude of neurogenic derivatives in the cranial region (cranial ganglia, Schwann and satellite cells) and in the trunk (dorsal root ganglia, autonomic sympathetic neurons, and Schwann cells (Kague et al., 2012; Raible and Eisen, 1994; Raible et al., 1992). *Sox10* has not only been shown to be a major contributor in pigment cell differentiation, but also in glia and neuronal lineages as well. *Sox10* deficient mutants display a reduction in dorsal root ganglia, satellite glia, and Schwann cells across the organism (Carney et

al., 2006; Kelsh and Eisen, 2000). The dorsal root ganglia phenotype is not directly affected by the loss of *sox10*, but instead the loss of its downstream target *neurog1*. This loss causes a switch in cell fate toward glia (McGraw et al., 2008).

The enteric nervous system (ENS) is comprised entirely of vagal neural crest (VNCC), VNCC are the cells that emerge from the hindbrain adjacent to somites 1-7 (Hutchins et al., 2018). Coined the “second brain”, the ENS is responsible for the innervation of the intestine that mediates the motility of the gut, secretions, and local blood flow (Ganz et al., 2016). All neural precursors express *crestin* which is downregulated immediately following differentiation (Olden et al., 2008), including the cells of the ENS. It has been shown that retinoic acid (RA), Meis3, and Ret act collaboratively to regulate the migration, survival, and subsequent differentiation of the enteric NCCs of the gut (Uribe and Bronner, 2015; Uribe et al., 2018). We have gained a great deal of insight on neural crest cells and their development but there is still much to discover about the mechanisms and missing components of their gene regulatory network.

Figure 4. 1 Diagram of the known NCC gene regulatory network

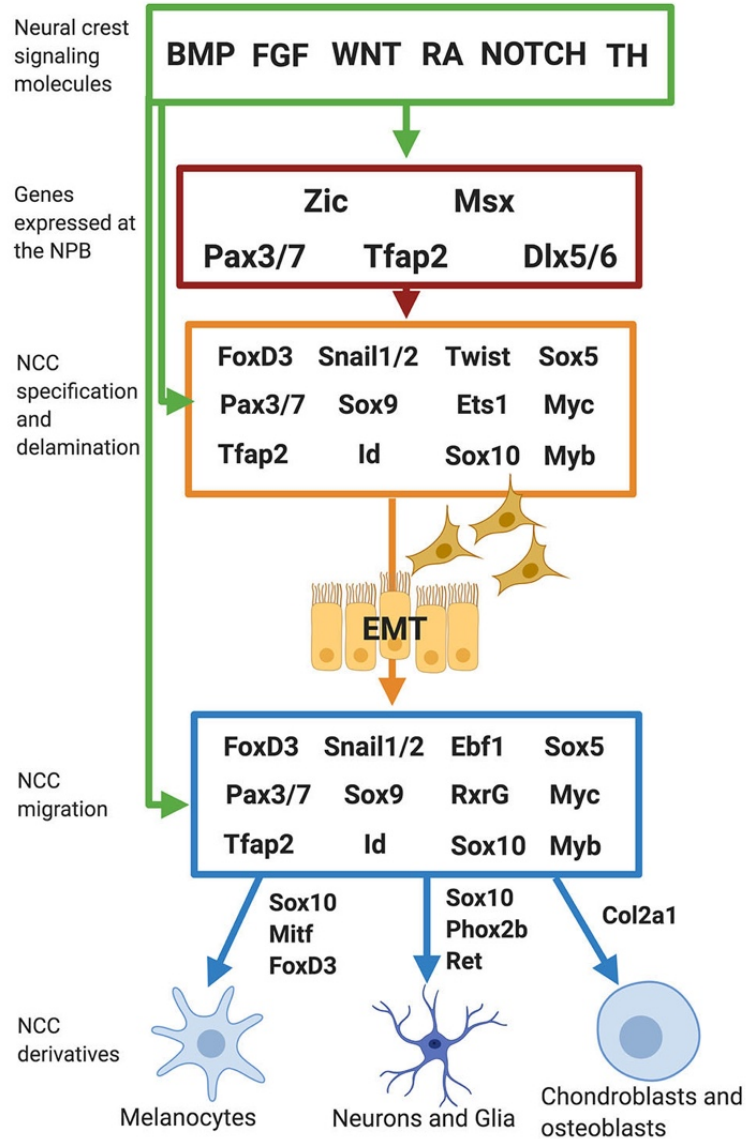


Figure 4.1 Diagram of the known NCC gene regulatory network. NPB, Neural plate border; NCC, neural crest cells; EMT, epithelia to mesenchymal transition.

Defects in NCC development at any of the steps discussed above leads to a number of developmental disorders and malformations called neurocristopathies (**Table 4.1**). Neurocristopathies encompass a wide range of disorders including cranioskeletal disorders, failed nervous system formation, loss of skin pigmentation, and cancer (Frisdal and Trainor, 2014) . As described above NCC developmental genes usually influence the development of multiple NCC derivatives. Because of this, neurocristopathies may preferentially affect one derivative but rarely exclusively (Etchevers et al., 2019). Hirschsprung disease (HSCR) is characterized by the lack of distal neuronal development in the rectum and colon which prevents normal defecation. Patients with HSCR also suffer from piebaldism (the congenital absence of melanocytes from areas of the skin) and/or hearing loss (Le Douarin et al., 2004; Steel and Barkway, 1989). The phenotypes associated with HSCR have been linked to quite a few genes such as *SOX10*, *PAX3*, *MITF*, and *SNAIL*. As described above, all of those genes have been shown to be involved in networks that control NCC development and migration (Edery et al., 1996; Etchevers et al., 2019). Interestingly, these genes have also been implicated in muscle, eye, brain and gonad formation (Simoës-Costa and Bronner, 2015).

Table 4. 1 Neurocristopathies and implicated genes

Neurocristopathy	Disease phenotypes	Implicated genes	References
Hirschsprung's disease	Megacolon, deafness, pigment defects	<i>Ret, Gdnf, Edn3</i>	Martucciello et al., 2000
Waardenburg Syndrome	hearing loss, pigment defects, bowel dysfunction	<i>Pax3, Mitf, Sox10</i>	Waardenburg, 1951
CHARGE syndrome	Coloboma, heart defects, retardation of growth	<i>Chd7</i>	Pagon et al., 1981
Piebaldism	pigment defects, gut defects	<i>Snail 1/2</i>	Giebel and Spritz, 1991
DiGeorge Syndrome	heart defects, developmental delay, cleft palate	<i>Tbx1</i>	Shprinten et al., 1978
Axenfeld-Rieger Syndrome	glaucoma, craniofacial defects, gut defects	<i>Pitx2, Foxc1</i>	Fitch and Kaback, 1978
Craniofrontonasal dysplasia	craniosynostosis, bifid nasal tip, facial asymmetry	<i>Efnb1</i>	Twigg et al., 2004
Central hypoventilation syndrome	respiratory defects, neuroblastoma, gut defects	<i>Phox2b</i>	Windisch et al., 2004
Congenital heart defects	heart defects, blue skin, poor weight gain	<i>Tbx1</i>	Srivastava, 2006
Multiple Sclerosis	neurological damage, blindness, muscle weakness	<i>Hla-a</i>	Berer and Krishnamoorthy, 2014

Proper migration, proliferation, differentiation and survival of NCCs are essential for both craniofacial and eye development. Genetic mutations in thyroid hormone signaling (TH) disrupt CNCC development, resulting in craniofacial, extraocular muscle, and ocular abnormalities which can be rescued with retinoic acid (Bohnsack et al., 2012; Bolande, 1997). *Her9/Hes4* (also referred to as *Xhair2* in *Xenopus*) has been shown to be a transcriptional repressor of *Xbmp4* during CNCC induction (Glavic et al., 2004a; Glavic et al., 2004b). Morpholino knockdown of *Xhair2* resulted in the repression of neural crest marker genes such as *slug* and *foxd3*, which in turn affected the proliferation and survival of some neural crest derivatives (cranial and pigment derivatives; (Glavic et al., 2004a). Interestingly, these embryos also displayed eye defects. Consistent with these data, in this chapter we characterize the neural crest defects present in our *her9* mutants. We observed craniofacial defects such as a shorter mandible, missing pharyngeal arches, and extended ethmoid plate. *Her9* mutants also display a fate switch in pigment cells towards xanthophores over melanophores and iridophores. *Her9* mutants have an underdeveloped gut with missing components of the ENS and increased cell death. Finally, *her9* mutants display an increase in *bmp4* expression over significant phases of NCC development, indicating that *Her9* may play a role in inhibiting *bmp4* expression during NCC induction and development.

4.3 Materials and methods

4.3.1 Zebrafish line maintenance

All zebrafish lines were bred, housed, and maintained at 28.5°C on a 14 hour light: 10-hour dark cycle, in accordance with established protocols for zebrafish husbandry (Westerfield; 1995). The Tg(*Sox10*:EGFP^{ba2}), Tg(*Sox10*:mRFP vu234), Tg(*pitx2*:EGFP), and Tg(*foxd3*:GFP) transgenic lines (hereafter called *sox10*:GFP, *sox10*:RFP, *pitx2*:GFP, *foxd3*:GFP) have been previously described in (Carney et al., 2006; Gilmour et al., 2002; Kucenas et al., 2008; Wolman et al., 2008), and were generously provided by Jakub Falmulski (University of Kentucky, Lexington, KY). The Tg(*gfap*:GFP)mi2001 line (hereafter referred to as GFAP:GFP), was previously described (Bernardos and Raymond, 2006) and was obtained from the Zebrafish International Resource Center (ZIRC, Eugene, OR). The Tg(*fli1a*:EGFP)y1Tg transgenic line, (hereafter called

fli1:GFP) has been previously described (Lawson and Weinstein, 2002b), and was obtained from ZIRC. Embryos were anesthetized with Ethyl 3-aminobenzoate methanesulfonate salt (MS-222, Tricaine, Sigma-Aldrich, St. Louis, MO) and adults were euthanized by rapid cooling as previously described (Wilson et al., 2016). All animal procedures and experimental protocols were approved and carried out in accordance with guidelines established by the University of Kentucky Institutional Animal Care and Use Committee (IACUC), the University of Kentucky Institutional Biosafety Committee, and the ARVO Statement for the Use of Animals in Ophthalmic and Vision Research.

4.3.2 Generation of *her9* mutant zebrafish by CRISPR

The *her9* target sites and single strand DNA oligonucleotides used to generate the guide RNAs were selected using the ZiFit online tool (<http://zifit.partners.org/ZiFiT/>) and the methods for generating the CRISPR mutant lines were previously described (Chapter 3).

4.3.3 Genomic DNA (gDNA) extraction and amplification

gDNA was extracted from whole embryos or from tail clips of adult fish. The embryos or tails were placed in 15 ul of 1x Thermopool buffer (NEB, Ipswich, MA) and 7 ul of Proteinase K (Pro K; Sigma-Aldrich, St. Louis, MO) was added to each and incubated at 55° C overnight. After at least 20 hours of digestion, tubes containing the digested tissue were incubated at 95° C for 15 min to deactivate the Pro K. The gDNA was then amplified using primers described in (Chapter 3).

4.3.4 Restriction fragment length polymorphism (RFLP)

The mutant *her9* allele carrying a 1 bp deletion was identified by RFLP analysis using BsaJI restriction enzyme (NEB: R0563S) and the mutant *her9* allele carrying a 1 bp insertion was identified by RFLP using Bfal restriction enzyme (NEB: R0568S) as described in (Coomer et al., 2020). Genomic DNA from whole embryos or from tail clips was extracted and amplified by PCR

as described above, then subjected to restriction digest. The restriction digests were visualized on a 2% agarose gel.

4.3.5 RT-PCR and real-time quantitative RT-PCR (qPCR)

The GoScript Reverse Transcriptase System (Promega, Madison, WI) was used to synthesize the first strand cDNA from 1 μ g of the extracted RNA. PCR primers were designed to amplify unique regions of the *her9*, *elf α* (Chapter 3), and each neural crest specific gene (**Table 4.2**; Eurofins Genomics; www.eurofinsgenomics.com; Coomer et al., 2020). Faststart Essential DNA Green Master mix (Roche) was used to perform qPCR on a Lightcycler 96 Real-Time PCR System (Roche). The relative transcript abundance was normalized to *elf α* expression as the housekeeping gene control (Wen et al., 2015), and was calculated as fold-change relative to 36 hours post fertilization (hpf) for developmental expression, or fold-change relative to wild type siblings, untreated. RT-PCR and qPCR experiments were performed with three biological replicates and three technical replicates. RT-PCR was performed on a Mastercycler Pro thermocycler (Eppendorf, Westbury, NY). PCR products were visualized on a 1% agarose gel.

Table 4. 2 Neural crest qPCR primers

Table 4.2 Neural crest qPCR primers

Gene	Forward Primer	Reverse Primer	Product size
<i>ets1</i>	ACAGACTCTGTACGTTTGAATGGACT	GTCCAGACTTTACTCGTCCGTGTC	122 bp
<i>sox10</i>	AAAACACTGGGGAAGCTGTG	CGACGTGGCTGGTACTTGT	130 bp
<i>foxd3</i>	TTGACGCTCAGTGGAATC	TCTTGACGAAGCAGTCGT	148 bp
<i>meis3</i>	GAGGAGTTGGTGCAGTACCC	ATGATATTGCAGCCTTTGCC	128 bp
<i>mitfa</i>	GACGACTGGTCAGTTCTTGC	GGTACTTCGAGGGGGTTCC	142 bp
<i>pax3a</i>	TACAGCCAATATGGGCAGAGC	ACCAATCCAAATGAAGCCCTTTT	101 bp
<i>pax7a</i>	TCAGAAACCTTCATGAGCCCG	TGCTGTTGTTTCATTGAGCGTC	137 bp
<i>pitx2</i>	CGAAGATTCGAACGATGACC	TGGGATGTTGAAAAACGAAA	146 bp
<i>bmp2a</i>	ACCGCCGCGCTAATGGTTCT	CCGAAGTTCAAACGCGTGCAG	120 bp
<i>bmp4</i>	GAGACGCCTCTGCGATTCGTT	GATGCAAACCATGGTCCCCTG	142 bp
<i>bmp7a</i>	TGGCTTGTTGGTGCAGTGTGC	TCTGCGCTCCTGGCTCTTCA	110 bp

4.3.6 Immunohistochemistry

Immunohistochemistry was performed as previously described (Pillai-Kastoori et al., 2014). The following primary antibodies were used: HuC/D (mouse, 1:20, Invitrogen, Grand Island, NY), which recognizes enteric neurons; α GFP (mouse, 1:1000, Santa Cruz biotechnology); Zrf-1, which recognizes glial cells (mouse, 1:5000, Santa Cruz biotechnology). Alexa Fluor 488 goat anti-mouse, 488 goat anti-rabbit, 546 goat anti-rabbit, and 546 goat anti-mouse secondary antibodies (Molecular Probes, Invitrogen) were all used at 1:200 dilution. Nuclei were visualized by counterstaining with DAPI (1:10,000 dilution). Samples were mounted in 60% glycerol in PBS. Images were taken at 20x and 40x on an inverted fluorescent microscope and a Leica SP8 DLS confocal/digital light sheet system using a 40x or 63x objective. Ten sections were analyzed on each slide and for each antibody.

4.3.7 TUNEL staining

Terminal deoxynucleotide transferase (TdT)-mediated dUTP nick end labeling (TUNEL) was performed on frozen retinal cryosections using the ApopTag Fluorescein Direct In Situ Apoptosis Detection Kit (Millipore, Billerica, MA). TUNEL staining was performed according to the manufacturer's protocol. Images were taken at 20x and 40x on an inverted fluorescent microscope (Eclipse Ti-U, Nikon instruments). Ten sections were analyzed on each slide.

4.3.8 H & E staining

To study the morphological features of the retina and zebrafish gut cryo sections were taken through a series of ETOH and H₂O washes and staining with Hematoxylin and Eosin was performed as described in Fischer et al., 2009.

4.3.9 Alcian blue staining

Zebrafish larvae (5 -7 dpf) were fixed in 4% paraformaldehyde (PFA) at 4°C overnight. The larvae were incubated in 'Alcian blue solution' (Alcian blue cationic dye; abcam.com) overnight at room temperature. The samples were washed in 100% ethanol (EtOH) and transferred through an ethanol series (90%, 80%, 70%) to 1X PBST. The embryos were digested in-100mg trypsin in 10 mL 30% saturated aqueous sodium borate. Specimens were bleached with Hydrogen peroxide (3% H₂O₂ in 1% KOH) until transparent and stored in 70% glycerol.

4.3.10 Feeding assay

To create the fluorescent tracker food, we mixed 100 mg of powdered larval feed (Gemma 75; Skretting) and 150 μ L of Fluosphere carboxylate modified microspheres supplied in 2% solid solution (Invitrogen, Carlsbad, CA, USA) in 50 μ L of deionized water. The mixture was combined into a paste and dried overnight, in the dark at room temperature. Once dry the flakes were stored at room temperature (Field et al., 2009). The fluorescent tracker food was mixed with 10 mL of artificial fish water and the feeding assay was conducted on 7 dpf embryos. Embryos were imaged prior to feeding and then placed in petri dishes containing food. After 10 min of feeding the embryos were screened for food in the gut and fish positive for food in the gut were isolated. The isolated fish were then imaged every 30 min for 2 hours to track the progression of the food through the digestive tract. After the feeding assay, the embryos were genotyped as described above.

4.3.11 Statistical analysis

Statistical analysis was performed using a Student's t-test or Chi-square test with GraphPad Prism software (www.graphpad.com). For comparing the number of neural crest cell and other phenotypic features 10 wild type and 10 mutant animals were examined. All graph data are represented as the mean \pm the standard deviation (s.d.)

4.4 Results

4.4.1 Her9 mutants display craniofacial defects

The retinal phenotype of *her9* homozygous CRISPR mutants was previously described (Chapter 4). In the course of characterizing *her9* mutant phenotypes, we noted that the mutants displayed a number of defects outside the retina. These phenotypes include, but are not limited to, lack of swim bladder (SB), craniofacial defects (CFD), curved body, and defects in

pigmentation. To further investigate how the loss of Her9 affects craniofacial development, we used light microscopy to document gross morphological changes within the facial structures of the *her9* mutants compared to their wild type siblings (**Figure 4.2 A-B**). *Her9* heterozygous incrosses were screened and 18% of the embryos had CFD and of those 94% genotyped as homozygous mutants (*her9*^{-/-}), while the other 6% genotyped as heterozygous, and 0 were homozygous wild type (**Figure 4.2 H**). To determine whether the mutant craniofacial phenotype was associated with cartilage malformation, we performed Alcian blue staining (**Figure 4.2 E-G'**) on 5 dpf embryos from a *her9*^{+/-} heterozygous incross. The cartilage of the wild type head skeleton contained two subdivisions, the neurocranium and viscerocranium, which included the ethmoid plate (e), trabeculae (tr), Meckel's cartilage (m), palatoquadrate (pq), ceratobranchial (cb 1-5), and ceratohyal (ch) (Liu et al., 2020, **Figure 4.2 D-E'**). Upon initial characterization of craniofacial defects in the *her9* homozygous mutants we observed two major phenotypic categories with respect to cb 1-5. In Phenotype 1 (60%), the ceratobranchial were present but appeared faint, smaller and abnormally shaped (**Figure 4.2 F-F'**), whereas in mutants with Phenotype 2 (20%), the ceratobranchial were missing (**Figure 4.2 G-G'**). Cranial width is often used as an indicator of craniofacial defects. To determine whether *her9* mutant embryos had smaller heads than their wild type siblings, we measured to distance between the eyes (**Figure 4.2 I-I'**) and observed a decrease in the distance in the *her9* mutants compared to their wildtype siblings (**Figure 4.2 J**). Taken together, these data indicate that the loss of Her9 causes craniofacial defects including loss of cb 1-5, and a smaller head

Figure 4. 2 Her9 mutants lack a swim bladder and display craniofacial defects

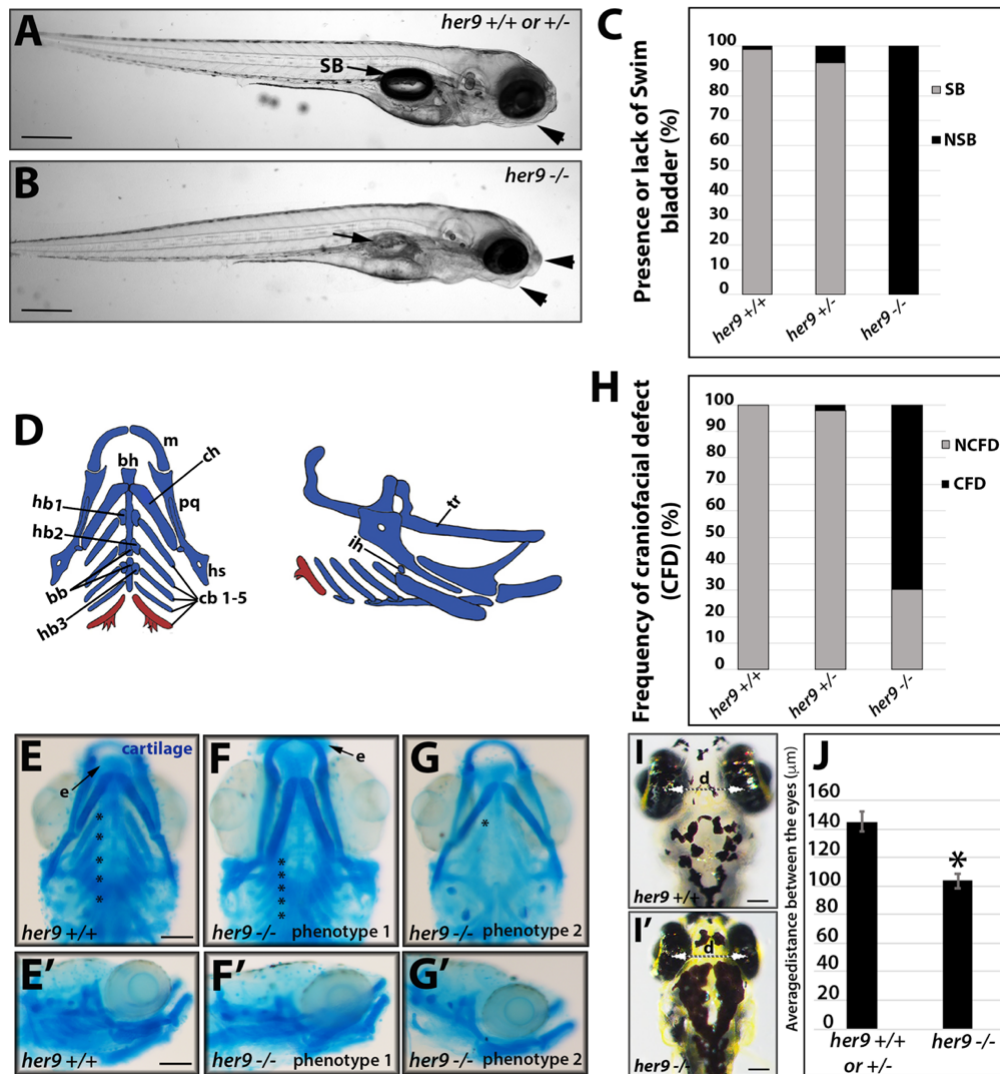


Figure 4.2 Her9 mutants lack a swim bladder and display craniofacial defects. A-B) Morphological phenotype of WT vs *her9* mutant. **C)** Percent of embryos that lack a swim bladder. **D)** Schematic of craniofacial structures. **E-G')** Variations in craniofacial defects visualized using Alcian blue staining. **H)** Frequency of craniofacial defects. **I-J)** Measurement of distance between the eyes of the WT and mutant embryos. Hs, hyosymplectic; bh, basihyal; ch, ceratohyal; m, Meckel's cartilage; pq, palatoquadrate; cb, ceratobranchial arches; hb, hinge bone; tr, trabeculae; ih, interhyoideus.

4.4.2 Loss of Her9 causes a decrease in sox10 expression and morphological defects in components of the viscerocranium

Craniofacial defects are usually attributed to defects in cranial neural crest cell (CNCC) development. Diseases such as Treacher Collins-syndrome and CHARGE syndrome (Asad et al., 2016; Sandell et al., 2014) have been linked to disruption in the migration, specification and/or maturation of CNCC (Okuno et al., 2017; Satoh and Ide, 1987; Serrano et al., 2019). To determine if the craniofacial defects present in *her9* mutants are linked to the disruption of CNCC development, we analyzed expression of *sox10*, a neural crest cell specific gene, using qPCR and observed a roughly 1.5-fold decrease in the expression of *sox10* in *her9* mutants at 48 hpf compared to their wildtype siblings (**Figure 4.3A**). To better understand the effects of the loss of Her9 on CNCC cell development we crossed the *her9* mutation onto the *sox10:RFP* transgenic background. After establishing a *sox10:RFP+/-; her9+/-* line, we took cryosections of zebrafish heads at 5 dpf, using the optic nerve as a landmark, and counted the number of RFP+ positive cells within the jaw/mouth area (**Figure 4.3B-C'**). We observed a significant decrease in the number of RFP+ cells within the jaw/mouth area of the *her9* mutants compared to their WT and heterozygous siblings (**Figure 4.3D**).

To further characterize the *her9* mutant craniofacial phenotypes originally observed by light microscopy, larvae from a *sox10:RFP+/-; her9+/-* in cross were screened for craniofacial defects, categorized based on severity, and genotyped. *Her9^{-/-}* embryos presented three phenotypic categories of severity in craniofacial defects (**Figure 4.3F**). “Mild” embryos looked similar to WT with cb 1-5 present, a protruding ethmoid plate (ep), and a narrow face (19%; **Figure 4.3G**), “Moderate” embryos were missing some but not all of cb 1-5, had a wider face, and the ceratohyal (ch) appeared longer (52%; **Figure 4.3H**). “Severe” embryos were completely missing cb 1-5, the ceratohyal appeared longer, Meckel’s cartilage and palatoquadrate fusion were disrupted, and they had a wider face (20%; **Figure 4.3I**). To quantify some of the craniofacial defects we measured significant features of the viscerocranium, (**Figure 4.3J**), and observed a significant increase in the length of the ceratohyal in *her9* mutants compared to the WT and heterozygous siblings. Next, we measured the length of the palatoquadrate (**Figure 4.3K**) which showed no significant changes in length. Length and width of the Meckel’s cartilage

were measured and there was a slight increase in both measurements in the *her9*^{-/-} larvae compared to their WT and heterozygous siblings (Figure 4.3L-M).

Taken together we conclude from these data that the loss of Her9 disrupts the expression of *sox10*, causing a decrease in *sox10* expressing cells in the jaw, ultimately causing a variable range of cartilage malformations. Specifically, the phenotypes include a longer protruding ceratohyal and missing pharyngeal arches (cb 1-5). While there is variation in jaw size, changes aren't significant.

Figure 4. 3 Loss of Her9 causes a decrease in *sox10* expression and morphological defects in components of the viscerocranium

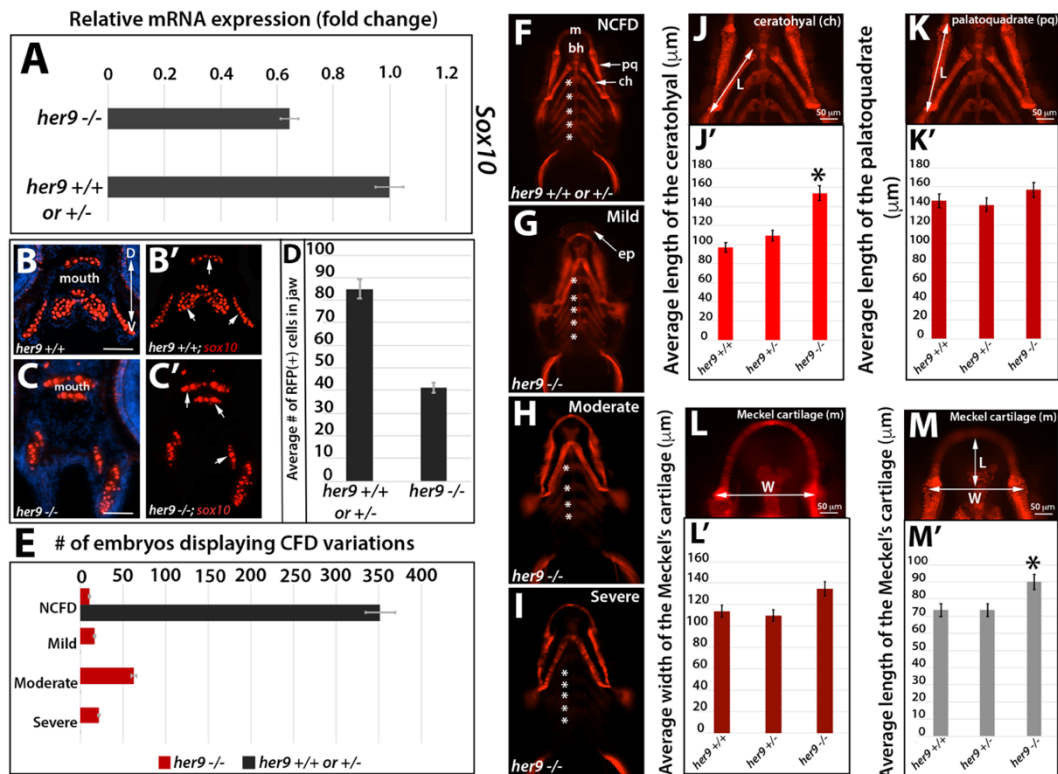


Figure 4.3 Loss of Her9 causes a decrease in *sox10* expression and morphological defects in components of the viscerocranium. A) qPCR expression of *sox10* in WT and mutant embryos at 48 hpf. A decrease in *sox10* expression is observed in the *her9* mutants but it is not statistically significant. B-B') *Sox10*:RFP expressing cells in craniofacial region of a WT embryo. C-C') *Sox10*:RFP expressing cells in craniofacial region of the mutant embryos. D) *Her9* mutants have a significant reduction in RFP+ cells of craniofacial region. E) Number of embryos displaying CFD variations. F-I) Craniofacial defect variations. J-M) Measurements of CF structures in the WT and mutant embryo. Ch, ceratohyal; pq, palatoquadrate.

4.4.3 Loss of Her9 results in defective segmentation of the branchial arches and an undeveloped ethmoid plate

Previous research has shown that pharyngeal arch development requires the segmentation of the pharyngeal endoderm into pouches (Piotrowski and Nusslein-Volhard, 2000). We observed a wide range of craniofacial defects in our *her9* mutants suggesting there may be disrupted branchial arch segmentation and/or pouch formation. To determine if this was the case, we imaged *her9^{+/+}*, *her9^{+/-}*, and *her9^{-/-}* embryos on the *sox10:RFP* background at 24 hpf, when all 4 pouches are distinguishable (**Figure 4.4A-B**). At 24 hpf, the *sox10:RFP⁺* cells in *her9* mutants had migrated into 3 branchial segments (**Figure 4.4B**), whereas the *sox10:RFP⁺* cells of their WT and heterozygous siblings had migrated into 5 distinct branchial segments (**Figure 4.4A**). Moreover, the WT and heterozygous embryos possessed 4 distinct pouches compared to 3 pouches observed in the *her9* mutants (**Figure 4.4A-B**).

To further examine the effects the loss of Her9 has on craniofacial development and CNCC migration, we imaged *her9^{+/+}*, *her9^{+/-}* and *her9^{-/-}* larvae on the *sox10:RFP* background at 72 hpf, and looked at Meckle's cartilage, the palatoquadrate, and the ethmoid plate (**Figure 4.4C-D'**). Meckle's cartilage and palatoquadrate of the WT and heterozygous embryos were longer but otherwise seemed similar to that of the *her9* mutants (**Figure 4.4C-D**). The ethmoid plate of the *her9* mutant was smaller than that of the WT and heterozygous embryos and there was a gap at the anterior end of the ethmoid plate forming a cleft (**Figure 4.4D'-C'**). *Ets-1* is a transcription factor that's been shown to be specifically expressed in CNCC and involved in CNCC migration (Simon et al., 2017) . Through qPCR analysis we observed a significant decrease in *ets-1* expression ($p = 0.0124$) in the *her9* mutants compared to their WT and heterozygous siblings (**Figure 4.4E**). Together, these data suggest that loss of Her9 affects the migration of CNCC into their branchial pouches and causes incomplete fusion of the ethmoid plate, disrupting CNCC differentiation.

Figure 4. 4 Loss of Her9 results in defective segmentation and an under-developed ethmoid plate

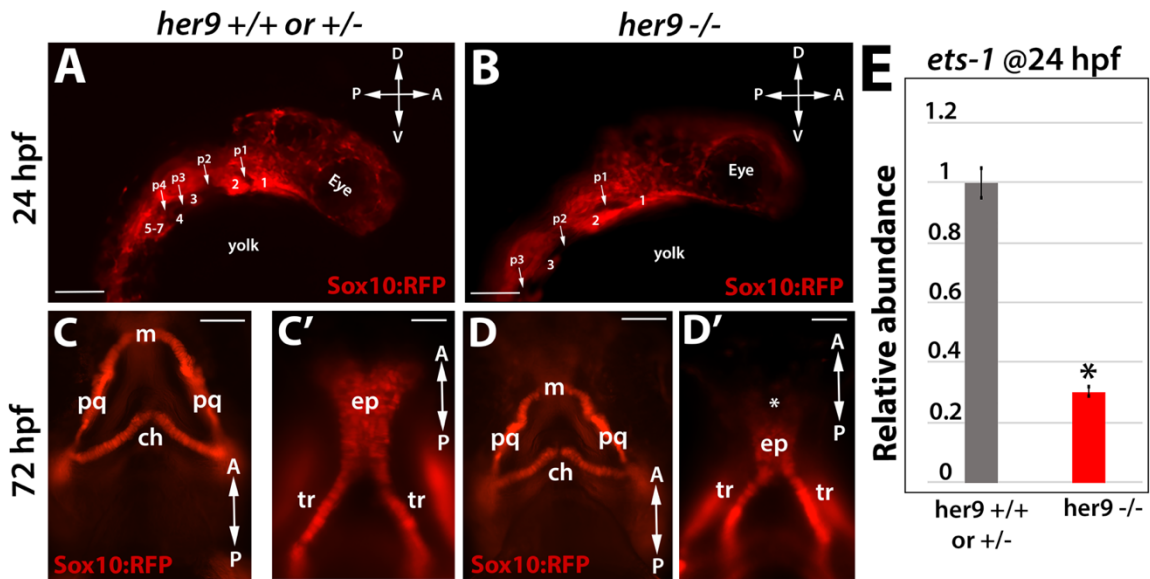


Figure 4.4 Loss of Her9 results in defective segmentation and an under-developed ethmoid plate. A-B) Comparison of *sox10*:RFP+ cells in the WT and *her9* mutants at 24 hpf. C) WT craniofacial structures at 72 hpf. C') WT ethmoid plate morphology at 72 hpf. D) Mutant craniofacial structures at 72 hpf. D') Mutant ethmoid plate morphology at 72 hpf. The ethmoid plate of the mutant had a gap and shorter facial structures. E) qPCR analysis of *ets-1* expression at 24 hpf. Her9 mutants display a significant decrease in *ets-1* compared to WT ($p = 0.124$). P1-P4, pouches 1-4; 1-7 branchial segments; pq, palatoquadrate; m, Meckel's cartilage, ep, ethmoid plate; tr, trabeculae; ch, ceratohyal.

4.4.4 Her9 mutants display pigment defects

To determine whether the loss of Her9 affected only the CNCC or other subtypes of NCCs, we first surveyed *her9* heterozygous embryo clutches for pigmentation defects. The pigment pattern displayed in larval zebrafish consists of three subtypes of vagal neural crest

cells (VNCC): melanophores (black), xanthophores (yellow) and iridophores (silver). These pigment subtypes are completely developed by 6 dpf (**Figure 4.5A**). Patterning of the melanin expressing melanophores consists of four longitudinal stripes: the dorsal and ventral stripe (extends from head to tail; black and blue arrows on **Figure 4.5A-B**), the yolk stripe (extends from under the heart to the anus; red arrows on **Figure 4.5A-B**), and the lateral stripe (extends through the myoseptum from somite 6 to 26; green arrows on **Figure 4.5A-B**; (Milos and Dingle, 1978). *Her9* mutants possess the same patterning as that observed in their WT and heterozygous siblings (**Figure 4.5A-B**). The dorsal stripe of the mutants contained less, but larger, pigment cells compared to WT and heterozygous siblings (**Figure 4.5A'-B and I-J**). The ventral stripe of the mutant was thinner in the head and region over the swim bladder but thicker towards the tail (**Figure 4.5A-B**). Additionally, the yolk and lateral stripes in the mutant appeared to have less melanophores (**Figure 4.5A-B**). Xanthophores have a yellow pigmentation to them and individual cells are hard to identify. These cells are predominantly located on the dorsal most portion of the zebrafish (**Figure 4.5E-F**; **purple arrows**) and the *her9* mutants appeared to have a darker yellow glow across the dorsal stripe (**Figure 4.5E-F**) compared to their WT and heterozygous siblings. Lastly, iridophores are silver under ambient light and are associated with the melanophores in the dorsal, lateral, yolk stripes and the eye (**Figure 4.5E-H'**; **asterisks**). We observed a decrease in iridophores in all of these regions (**Figure 4.5E-H'**).

The other pigmented cells of the zebrafish are the cells of the retina pigmented epithelium (RPE); the cells of RPE are not derived from NCCs. To determine whether the loss of *Her9* affected all pigmented cells or just NCC derived pigment cells, we imaged retinal sections of WT and mutant embryos at 6 dpf and observed no significant changes in the RPE (**Figure 4.5C-D**). To quantify, we measured the width of the RPE adjacent the optic nerve and observed no significant changes in the width (**Figure 4.5K**).

From these results we concluded that the loss of *Her9* causes a decrease in the VNCC derived melanophores and iridophores with an increase in xanthophores. These data also provide supporting evidence that the loss of *Her9* affects all NCCs and not just specific subtypes.

Figure 4. 5 Her9 mutants display pigmentation defects

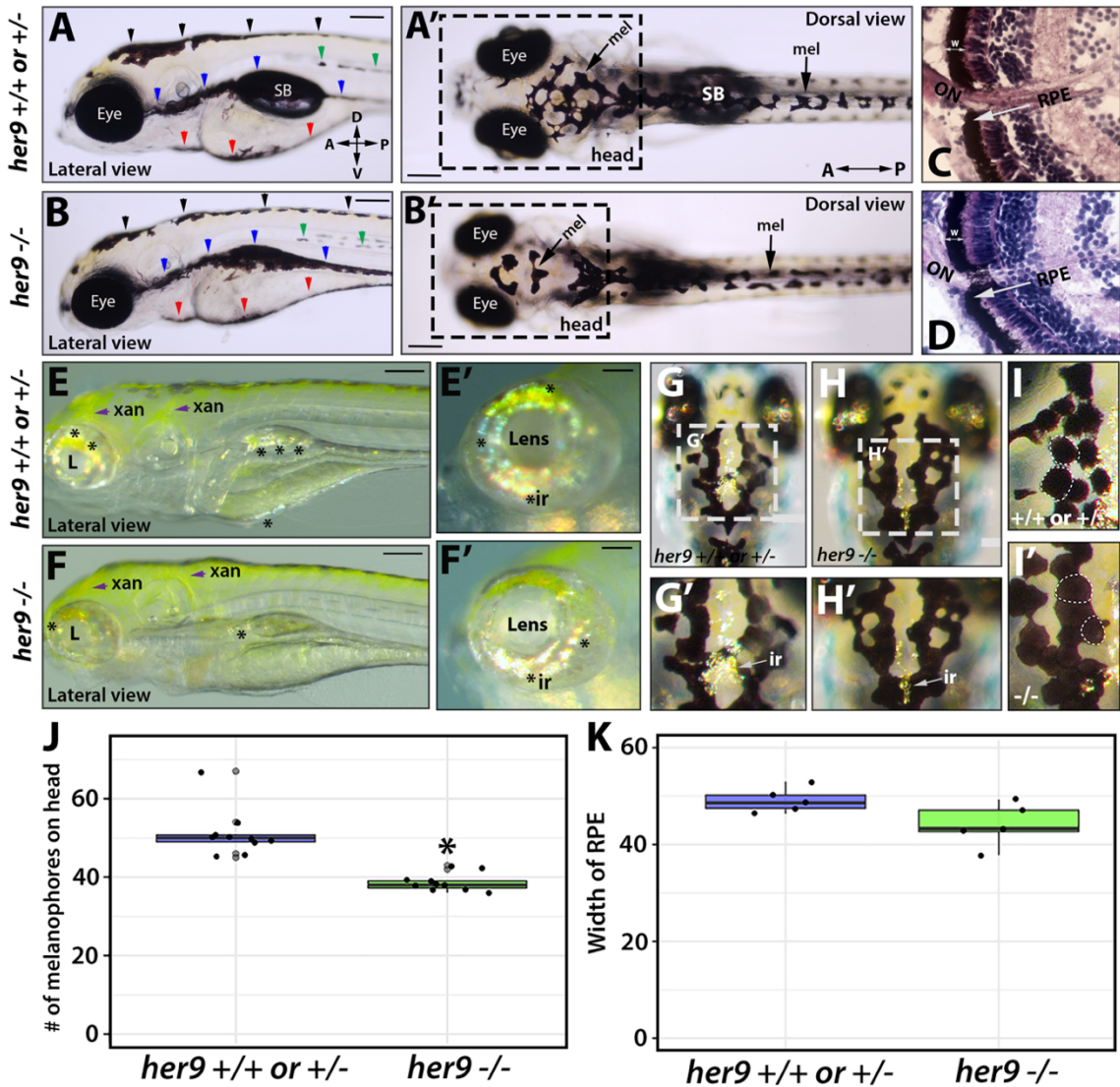


Figure 4.5 Her9 mutants display pigmentation defects. A-B) Morphological phenotypes of *her9* mutants compared to WT. A'-B') Comparison of melanophores on dorsal most portion of WT and mutant embryos. C-D) H&E staining of zebrafish retinas at 7 dpf to evaluate RPE. E-E') Xanthophore and iridophore phenotype of WT embryos. F-F') Xanthophore and Iridophore phenotype in *her9* mutant. *Her9* mutants have increased xanthophores and decreased iridophores. G-G') Analysis of iridophores on dorsal most region of WT embryos. H-H') Analysis of iridophores on dorsal most region of mutant embryos. I-I') Comparison of melanophore morphology. J) Number of melanophores on head. K) Width of RPE. Black arrow, dorsal stripe; green arrow, lateral stripe; blue arrow, ventral stripe; red arrow, yolk stripe; SB, swim bladder; mel, melanophore; xan, xanthophore; ir, iridophore; L, lens; RPE, retinal pigment epithelium.

4.4.5 Loss of Her9 results in the increase of xanthophores at the expense of melanophores and iridophores

To elucidate the roles of Her9 during neural crest cell differentiation and pigment cell development, we analyzed the expression patterns of neural crest cell markers specific for chromatophores at the beginning of their differentiation at 22 hpf and when chromatophore development is complete at 7 dpf (Budi et al., 2011; Rocha et al., 2020). *Foxd3* expression in NCCs has been shown to drive NCCs cells towards differentiation (Petratou et al., 2018), so we began by comparing *foxd3* expression at 22 hpf, before the first melanophore is present, and observed a decrease in *foxd3* expression in the mutants that was not statistically significant (**Figure 4.6A**). By 72 hpf, the chromatophores begin to differentiate and all lineages are present (xanthophores, melanophores and iridophores), so we analyzed the expression of 5 genes associated with their differentiation. Pax7 has been shown to be involved in the establishment of the xanthophore lineage, block melanophore lineage, and identified as a xanthophore specific gene (Minchin et al., 2008; Nord et al., 2016). We observed a 2-fold increase in the expression of both *pax3a* and *pax7a* in *her9* mutants compared to their WT and heterozygous siblings (**Figure 4.6B**). Sox10, Mitfa and Foxd3 have been shown to be key players in melanophore and iridophore lineage differentiation. Sox10 regulates the expression of *mitfa* and *mitfa* expression initiates the specification of melanocytes while Foxd3 blocks the expression of *mitfa* and initiates the specification of iridophores (Lister et al., 1999; Petratou et al., 2018). *Mitfa* and *foxd3* expression were slightly reduced in the *her9* mutants along with a reduction in *sox10* expression but none of these reductions were significant (**Figure 4.6C**).

Figure 4. 6 Loss of Her9 results in increased numbers of xanthophores at the expense of melanophores and Iridophores

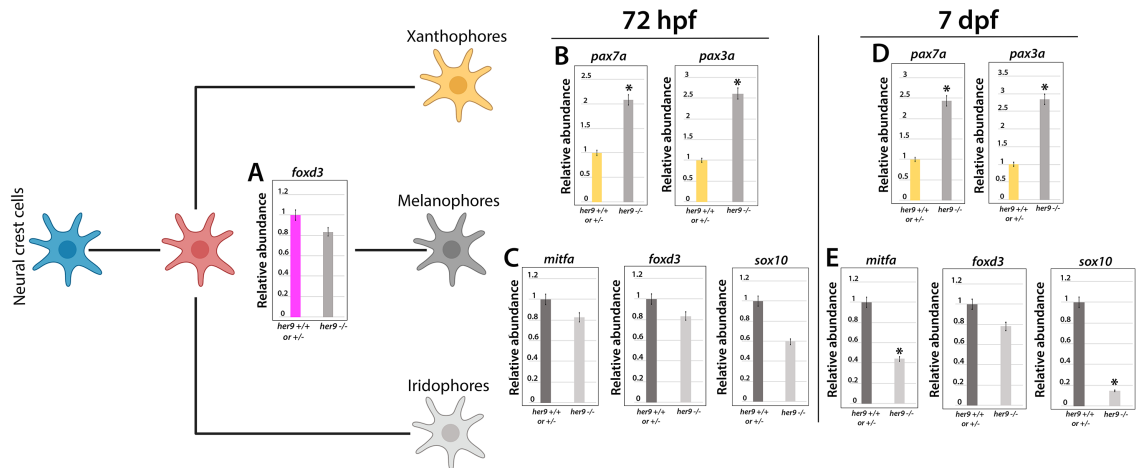


Figure 4.6 Loss of Her9 results in increased numbers of xanthophores at the expense of melanophores and iridophores. **A)** qPCR analysis of *foxd3* expression at 48 hpf. **B and D)** qPCR analysis of *pax 7* and *pax3* expression at 72 hpf and 7 dpf. *Her9* mutants show a significant upregulation in *pax3* and *pax7* expression ($p = 0.0009$ and $p = .00736$). **C and E)** qPCR analysis of *mitfa*, *foxd3* and *sox10* expression at 72 hpf and 7 dpf. *Her9* mutants show a downregulation in *mitfa*, *foxd3* and *sox10* expression but only *mitfa* and *sox10* are significantly decreased at 7 dpf ($p = 0.0267$ and $p = .0184$).

There was a consistent 2-fold increase in the expression of *pax3a* and *pax7a* in the *her9* mutant at 7 dpf, the point at which embryonic/larval chromatophores are fully developed (**Figure 4.6D**). Although decreased, *foxd3* expression remained the same at 7 dpf (**Figure 4.6E**), while *sox10* and *mitfa* expression were significantly decreased at 7 dpf (**Figure 4.6E**). The upregulation of *pax7* accompanied by the decrease in *mitfa* expression provide supporting data to the morphological phenotype and melanophore cells counts in *her9* mutants (**Figure 4.5**). These results suggest that loss of Her9 drives the specification of pigment neural crest cells towards xanthophore over melanophore and iridophore lineages.

4.4.6 Her9 mutants display morphological defects in the gut

Figure 4. 7 Her9 mutants display morphological defects in the gut

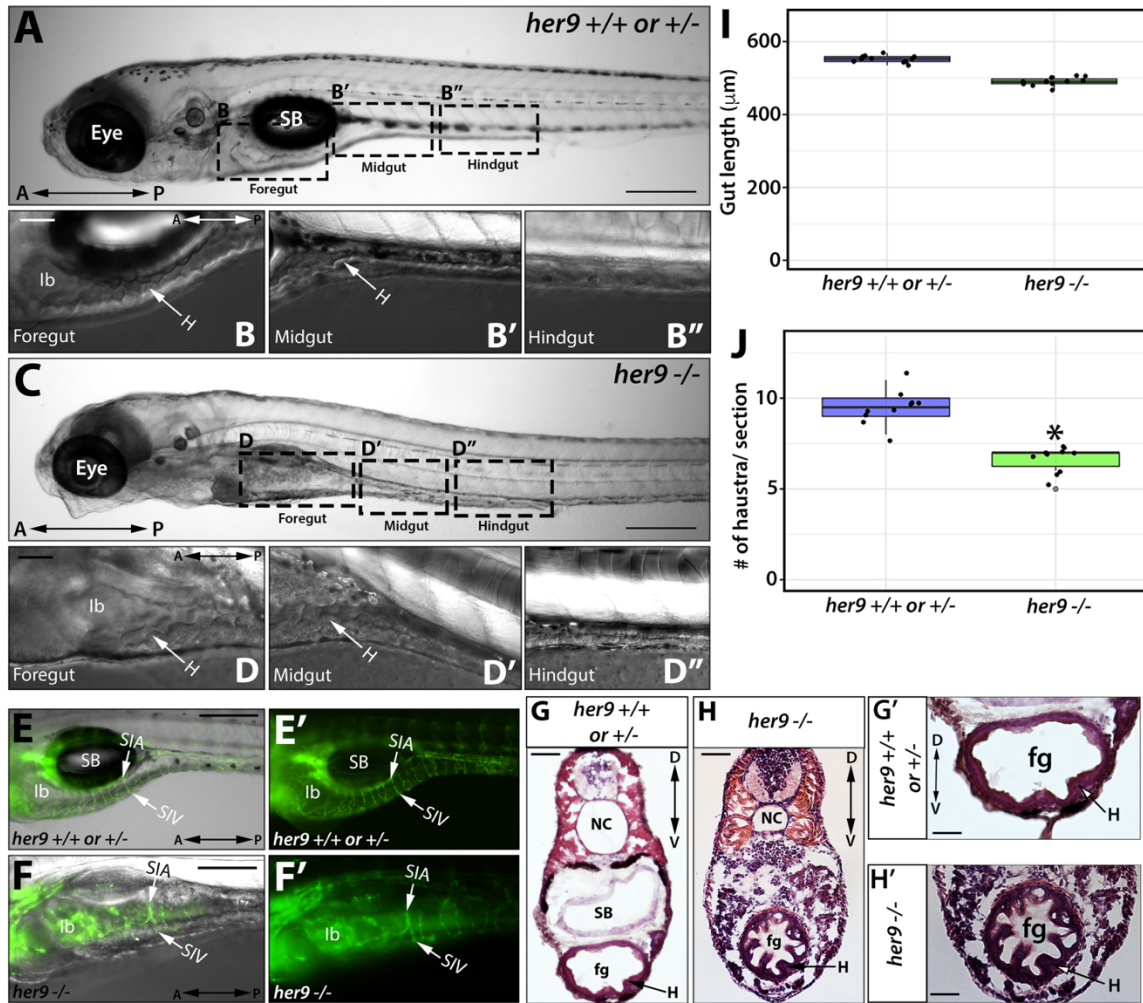


Figure 4.7 *her9* mutants display morphological defects in the gut. **A)** WT zebrafish at 5 dpf. **B-B'')** 40x magnification images of the WT foregut, midgut and hindgut. **C)** Mutant zebrafish at 5 dpf. **D-D'')** 40x magnification images of the mutant foregut, midgut and hindgut. *Her9* mutant gut has an abnormal shape and less haustra. **E-E')** WT embryo on *fli1*:GFP transgenic line. WT gut is intersected with vasculature. **F-F')** Mutant embryo on *fli1*:GFP transgenic line. Vasculature in mutant gut is disorganized and missing. **G-H)** transverse sections of WT and mutant guts after H&E staining. **G'-H')** 40x magnification of transverse sections after H&E staining. **I)** gut length measurements. **J)** haustra counts. SB, swim bladder; lb, intestinal bulb; SIA, supra-intestinal artery; SIV, sub-intestinal vein; fg, foregut; H, haustra; NC, notochord.

Next, we screened the *her9* mutants for gut defects using microscopy. Due to the loss of the swim bladder, the general shape of the gastrointestinal tract in *her9* mutants was altered compared to WT and heterozygous siblings (**Figure 4.7A and C**). The intestinal bulb (Ib), found at the anterior most portion of the foregut (fg), in the *her9* mutants had a thicker mucosa with less epithelial folding (haustra, H) and a smaller lumen (**Figure 4.7D**) compared to their WT counterparts (**Figure 4.7B**). Progressing along the gastrointestinal tract we continued to observe less haustra, and the folds we did observe were less defined in the midgut and hindgut (**Figure 4.7D'-D''**) compared to the WT and heterozygous digestive tract (**Figure 4.7B'-B''**). To determine whether the mutant gut is the same length as the WT or heterozygous gut we measured from foregut (at the tip of the intestinal bulb) to end of the hindgut. Although there was a decrease in the length of mutant gut, it was not considered significant compared to WT gut (data not shown). To analyze and compare haustra morphology and number, H&E staining was performed on sagittal sections of the mutant and WT gut. We observed abnormally shaped haustra and quantified the decrease by counting the haustra in sections along the foregut (**Figure 4.7E-G**); the decrease observed was significant (**Figure 4.7G**). Taken together, these data indicate that the loss of Her9 results in morphological defects in the gut, which include an abnormally shaped gut and decreased number of haustra.

4.4.7 Her9 mutants display decreased feeding habits and abnormal gut function

Do the morphological defects observed in the *her9* mutant gut affect its function? To answer this question, we utilized a fluorescent feeding assay described by Tang et al., 2009 (Tang et al., 2009). Once the fluorescent feed was prepared, the 7 dpf larvae (when the gut is completely developed and fully functioning) were fed and screened every 30 minutes while the food was processing through the gut (**Figure 4.8A**). We observed a significant decrease in the intake of food by the *her9* mutant larvae compared the WT and heterozygous larvae and we subsequently observed fewer mutant larvae with food in their gut (**Figure 4.8B**). The gastrointestinal tracts of all the larvae were imaged prior to first feeding (**Figure 4.8C-C'**). At 60 min post feeding (mpf), we observed significantly less food in the gut of the mutant larvae compared to the WT and heterozygous larvae (**Figure 4.8D-D'**). By 90 mpf, the food in the gut of WT and heterozygous larvae had processed through the foregut and into the midgut towards

the hindgut (**Figure 4.8E**). The food in *her9* mutants processed through the foregut into the midgut but stalled there and never passed into the hindgut (**Figure 4.8E'**). These data indicate that the loss of Her9 not only causes defects in gut morphology but also function, which results in decreased feeding and abnormal processing of food through the gastrointestinal tract.

Figure 4. 8 Her9 mutants display decreased feeding habits and abnormal gut function

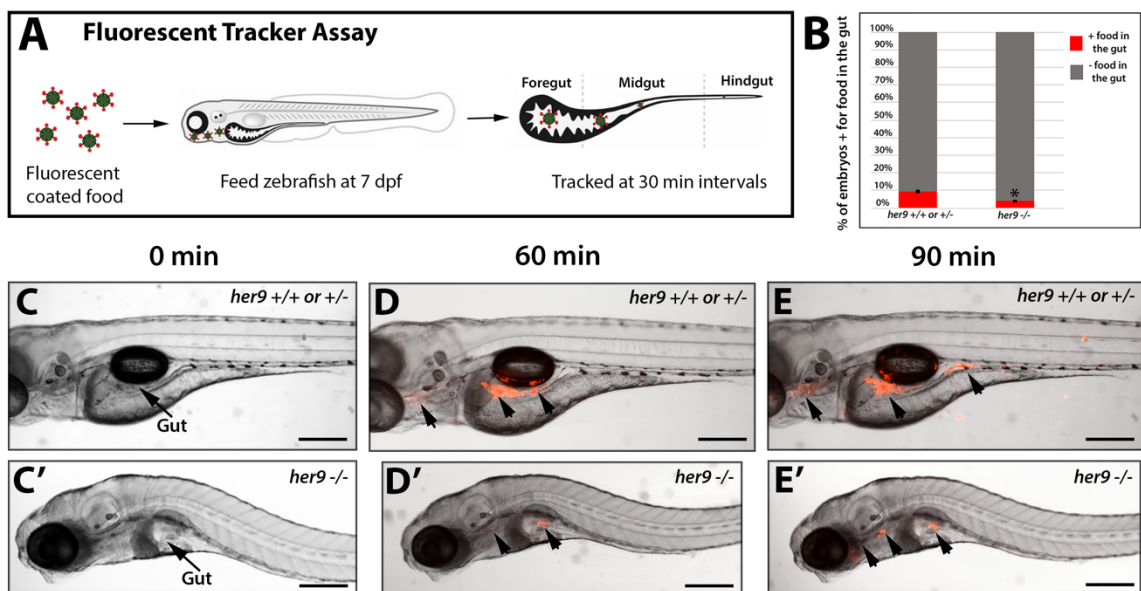


Figure 4.8 Her9 mutants display decreased food intake and abnormal gut function. A) Schematic of feeding assay. **B)** Percent of embryos that ingested the fluorescent food. **C-E)** Tracking of fluorescent food through WT gut at 0, 60, and 90 min. **C'-E')** Tracking of fluorescent food through mutant gut at 0, 60, and 90 min.

4.4.8 Her9 is required for the migration of NCCs into the gut and loss of Her9 results in improper differentiation of the glia and neurons

To further determine the extent of gut defects in the *her9* mutants we took transverse sections of *her9* WT, heterozygous and mutant guts. We sought to characterize *sox10*:RFP+ cells that had infiltrated the gut along the foregut, midgut and hindgut at 60 hpf, shortly before the completion of migration at 66 hpf (**Figure 4.9**). At 60 hpf, we observed the infiltration and migration of RFP+ cells in the foregut, midgut and hindgut of WT and heterozygous embryos (**Figure 4.9A-A''**), but when investigating the mutant gut we only observed RFP+ cells in the foregut (**Figure 4.9B-B''**). We also observed incomplete tube development in the hindgut of the mutants compared to their WT and heterozygous siblings (**Figure 4.9A'' and B''**). Differentiation of ENS neurons and glia starts around 55 hpf and by 96 hpf much of ENS development is complete. We used cryosections of 72 hpf larvae to look for *sox10*+ and Zrf-1+ (anti-GFAP) cells along the gastrointestinal tract of WT, heterozygous and *her9* mutant larvae (**Figure 4.9C-F**). In the gastrointestinal tract of the WT and heterozygous larvae, we observed *sox10*+ cells in the foregut, midgut and hindgut (**Figure 4.9C**) but we only observed *sox10*+ cells in the foregut and midgut of the *her9* mutant (**Figure 4.9D**). We observed a population of Zrf-1+ cells in the foregut, midgut and hindgut of the WT and heterozygous larvae. Interestingly, we observed Zrf-1+ cells in the foregut and midgut of the *her9* mutants, but we did not observe any Zrf-1+ cells in the intestinal bulb area (**Figure 4.9E-F**). Using cryosections of the zebrafish gut at 4 dpf, we investigated whether NCC of the ENS differentiate into neurons using HuCD staining (**Figure 4.9G-G' and I-I'**). We observed no HuCD+ cells in the *her9* mutant gut whereas we found HuCD+ cells along each section of WT and heterozygous gut (**Figure 4.9G-G' and I-I'**). To determine whether the loss of Her9 affects glial cell differentiation in the gut, we crossed our *her9* mutant line onto the GFAP:GFP background and used cryo-sections at 4 dpf to look for glia in the gut. We observed a gut completely populated with differentiated glia in the WT and heterozygous larvae, while *her9* mutant larvae completely lacked GFAP+ cells in the gut (**Figure 4.9H-H' and J-J'**). Lastly, Meis3 has been shown to be required for neural crest infiltration of gut (Uribe and Bronner, 2015). To determine whether the loss of Her9 may be affecting NCC gut infiltration, we used qPCR to look at the expression of *meis3* at 60 hpf and observed a significant decrease in

meis3 ($p = 0.0026$) in the *her9* mutant compared to WT and heterozygous siblings (**Figure 4.9K**). Taken together, these data demonstrate that the loss of Her9 affects NCC gut infiltration, migration, and differentiation.

Figure 4. 9 Her9 is required for the proper migration and differentiation of NCC in the gut

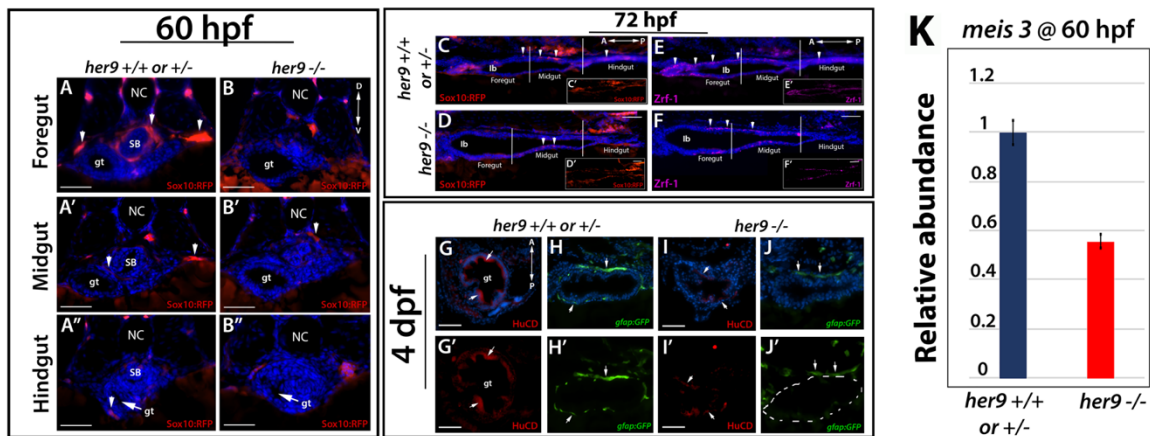


Figure 4.9 Her9 is required for the proper migration and differentiation of NCC in gut. A-A'' Transverse section of WT gut on the *sox10*:RFP background (Foregut, midgut and hindgut). **B-B''** Transverse section of mutant gut on the *sox10*:RFP background (Foregut, midgut and hindgut). *Her9* mutants lack RFP+ cells in midgut and hindgut. **C-D**) Cryosections of *her9*+/+ and -/- gastrointestinal tract at 72 hpf. *Her9* mutants lack RFP+ cells in the hindgut. **E-F**) Cryosections of *her9*+/+ and -/- gastrointestinal tract at 72 hpf. *Her9* mutants lack *zrf-1*+ cells in the intestinal bulb and hindgut. **G-G')** Transverse sections of WT gut at 4 dpf looking at HuCD+ cells. **H-H')** Transverse sections of WT gut at 4 dpf looking at GFAP+ cells. **I-I')** Transverse sections of mutant gut at 4 dpf looking at HuCD+ cells. *Her9* mutants lacked HuCD+ cells in the gut. **J-J')** Transverse sections of mutant gut at 4 dpf looking at GFAP+ cells. *Her9* mutants had significantly less GFAP+ cells in the gut (arrows indicate GFAP+ cells in the gut). **K**) qPCR analysis of *meis3* expression. *Meis3* is decreased in *her9* mutants but not significantly. SB, swim bladder; NC, notochord; gt, gut; lb, intestinal bulb.

4.4.9 The loss of Her9 has minimal effects on dorsal root ganglia development

Dorsal root ganglia (DRG) are the peripheral sensory ganglia and contain a subpopulation of neurons. To determine whether the loss of Her9 affects the development of the DRG population we performed IHC using HuCD on sagittal and transverse sections at 72 hpf, when the DRG have migrated from the neural tube to the middle of each body segment. The positioning of DRG in the *her9*^{-/-} larvae mirrored that seen in WT and heterozygous siblings. We observed a decrease in the number of DRG along the body axis of the mutants but when normalized to body size that decrease was not significant (**Figure 4.10A-B'' and E**). Using transverse sections of embryos on the *sox10*:RFP background, we observed DRG in the WT and mutant embryos that were positioned in the correct location with axons branching in dorsal and ventral sections (**Figure 4.10C-D'**). Taken together these data indicate that the loss of Her9 does not significantly alter DRG development.

Figure 4. 10 Loss of Her9 has minimal effect of DRG development

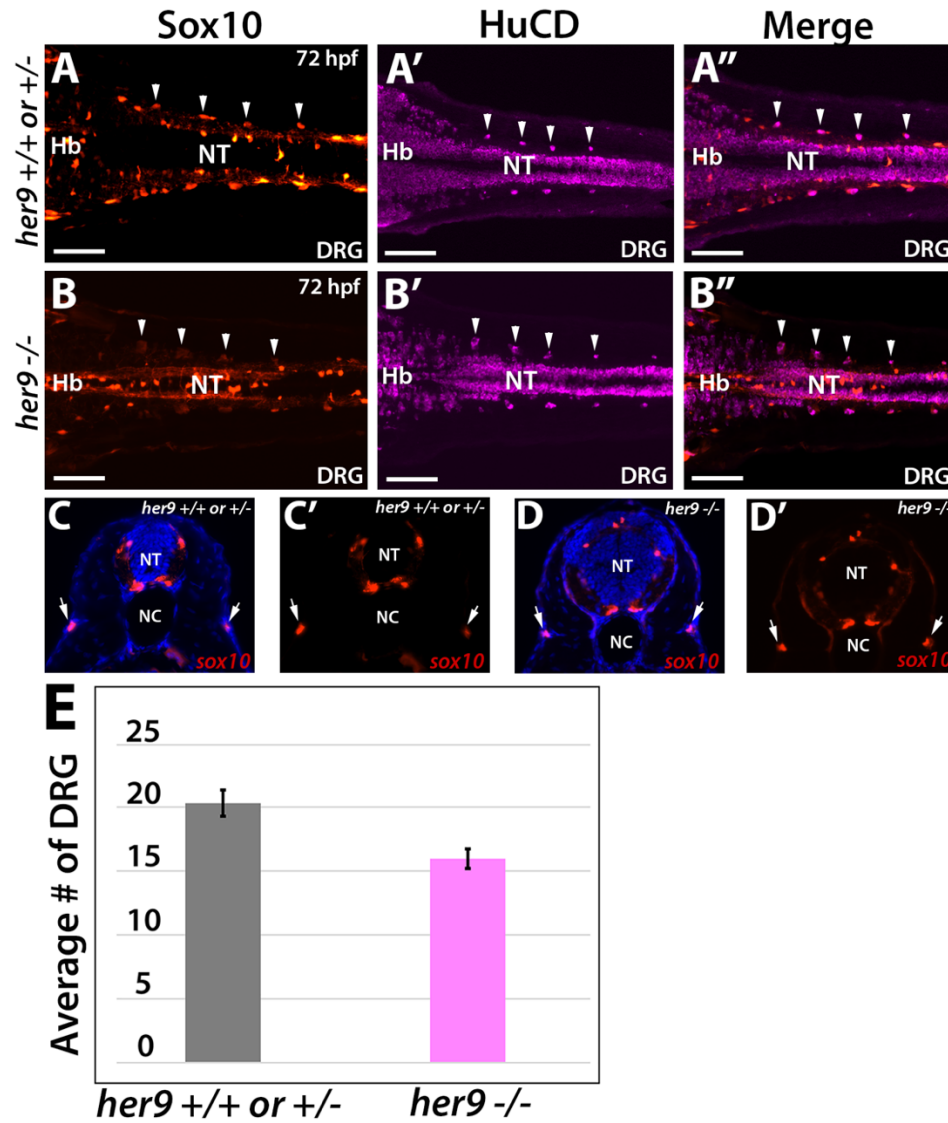


Figure 4.10 Loss of Her9 has minimal effects on DRG. **A)** Cryosection of WT embryo on *sox10*:RFP background. **A'-A'')** IHC staining using HuCD to label neurons. **B)** Cryosection of mutant embryo on *sox10*:RFP background. **B'-B'')** IHC staining using neurons to label HuCD to label neurons. **C-D')** transverse sections of *sox10*:RFP WT and mutant embryos. **E)** *Her9* mutants show a slight but not significant decrease in the number of neurons ($p = 0.837$). NT, Neural tube; NC, Notochord; Hb, hindbrain; DRG, dorsal root ganglia.

4.4.10 The loss Her9 during zebrafish development leads to a decrease in Foxd3-positive cells

Foxd3 is a forkhead box transcription factor that has been shown to be an important premigratory NCC gene, and when knocked down results in the reduction or loss of NCC derivatives such as jaw structures, glia, enteric neurons, and iridophore pigment cells (Lister et al., 2005). To determine whether loss of Her9 alters the expression of *foxd3*, we crossed our *her9* mutation onto the *foxd3*:GFP transgenic background (Curran et al., 2009) and imaged the WT, heterozygous, and mutant embryos at 24 hpf (**Figure 4.11**). We observed a decrease in the number of *foxd3*:GFP+ cells present in the *her9* mutant, specifically in the midbrain and posterior end of the hindbrain, compared to their WT and heterozygous siblings (**Figure 4.11A-D**). The GFP+ cells in the WT embryos were migrating and forming the branchial pouches, while fewer GFP+ cells had migrated in the *her9* mutants (**Figure 4.11A-D**). Upon closer observation at higher magnification, we also observed disorganization in the *foxd3*+ cells in the pineal gland in the *her9* mutants compared to WT (**Figure 4.11B' and D'**), as well as a decrease in *foxd3*+ cells at the midbrain hindbrain boundary (mhb; **Figure 4.11 B'' and D''**). To confirm that the changes in GFP+ cells reflected a change in endogenous *foxd3* expression qPCR was performed, from which we observed a significant decrease in *foxd3* expression at 24 hpf in *her9* mutants compared to the WT (**Figure 4.11E**). Taken together, these results suggest that Her9 may play a role in regulating *foxd3* and subsequent NCC specification, migration, and survival.

Figure 4. 11 Loss of Her9 leads to decreased *foxd3* expression

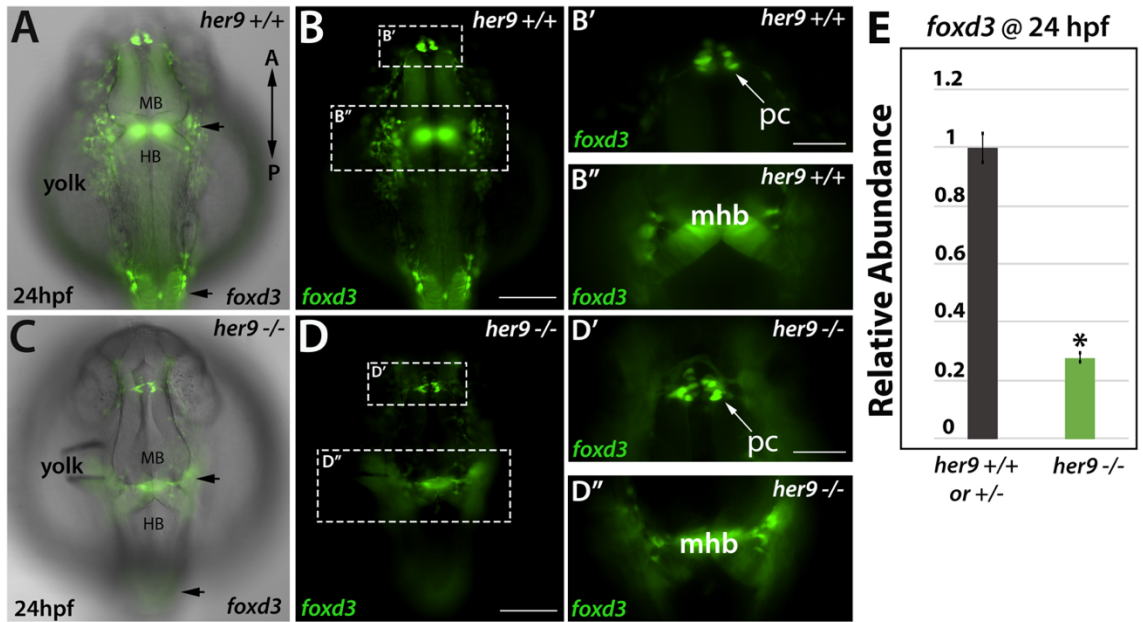


Figure 4.11 Loss of Her9 leads to decreased *foxd3* expression. **A-B)** *Foxd3*:GFP WT zebrafish embryos at 24 hpf. *Foxd3*⁺ cells are in the MB and HB as well as forming branchial pouches. **B'-B''**) 40x magnification of pineal complex and midbrain/hindbrain boundary. **C-D)** *Foxd3*:GFP mutant zebrafish at 24 hpf. A decrease in *foxd3*⁺ cells in the mutant. **D'-D''**) 40x magnification of pineal complex and midbrain/hindbrain boundary. **E)** qPCR expression of *foxd3* in the WT and Mutant. A decrease in *foxd3* expression in the mutant was observed. pc, pineal complex; mhb, midbrain/hindbrain boundary; MB; midbrain; HB hindbrain.

4.4.11 Her9 mutants have an altered Bmp gene expression during significant phases of NCC development

Bone Morphogenetic Protein (BMP) signaling along with other signaling molecules (FGF, Wnt, and Hh) have been implicated in the induction, migration and differentiation processes of NCC development (Schumacher et al., 2011). Morpholino knockdown of Her9/Hes4 in *Xenopus laevis* resulted in a significant increase in BMP4 signaling (Glavic et al., 2004a) leading researchers to believe Her9/Hes4 inhibits BMP expression. To determine whether BMP signaling was affected by the loss of Her9, we used qPCR to analyze the expression of *bmp2a*, *bmp4* and *bmp7* at 24, 48, 72 hpf and 5 dpf in *her9* wt and mutant embryos (**Figure 4.12**). By 24 hpf, NCC cell induction is complete and CNCC migration is in progress. At this time point we observed a decrease in the expression of *bmp4* in the mutant compared to their WT siblings, but this reduction was not statistically significant (**Figure 4.12A**), while *bmp2a* and *bmp7* expression was significantly decreased. At 48 hpf, during NCC migration, we observed an increase in the expression of *bmp2a*, *bmp4* and *bmp7*, but only *bmp7* was significantly increased in *her9* mutants (**Figure 4.12B**). Starting at 72 hpf, the VNCC that make up the ENS begin migration toward the posterior-most portion of the gastrointestinal tract. *Her9* mutants at this timepoint displayed an increase in *bmp2a*, *bmp4*, and *bmp7* expression, with *bmp4* being significantly increased (**Figure 4.12C**). By 5 dpf, most of the NCC derivatives have completed their migration and are differentiating. During this time point, in *her9* mutants, we observed an increase in *bmp2a*, *bmp4*, and *bmp7* and again only *bmp4* was significant (**Figure 4.12D**). The data presented here suggests that the loss of Her9 causes an upregulation in BMP ligand expression following NCC induction. We also conclude that upregulation of BMP signaling may be affecting the migration of NCC and subsequently, their differentiation.

Figure 4. 12 Her9 mutants have increased Bmp ligand expression during migration and differentiation of NCC

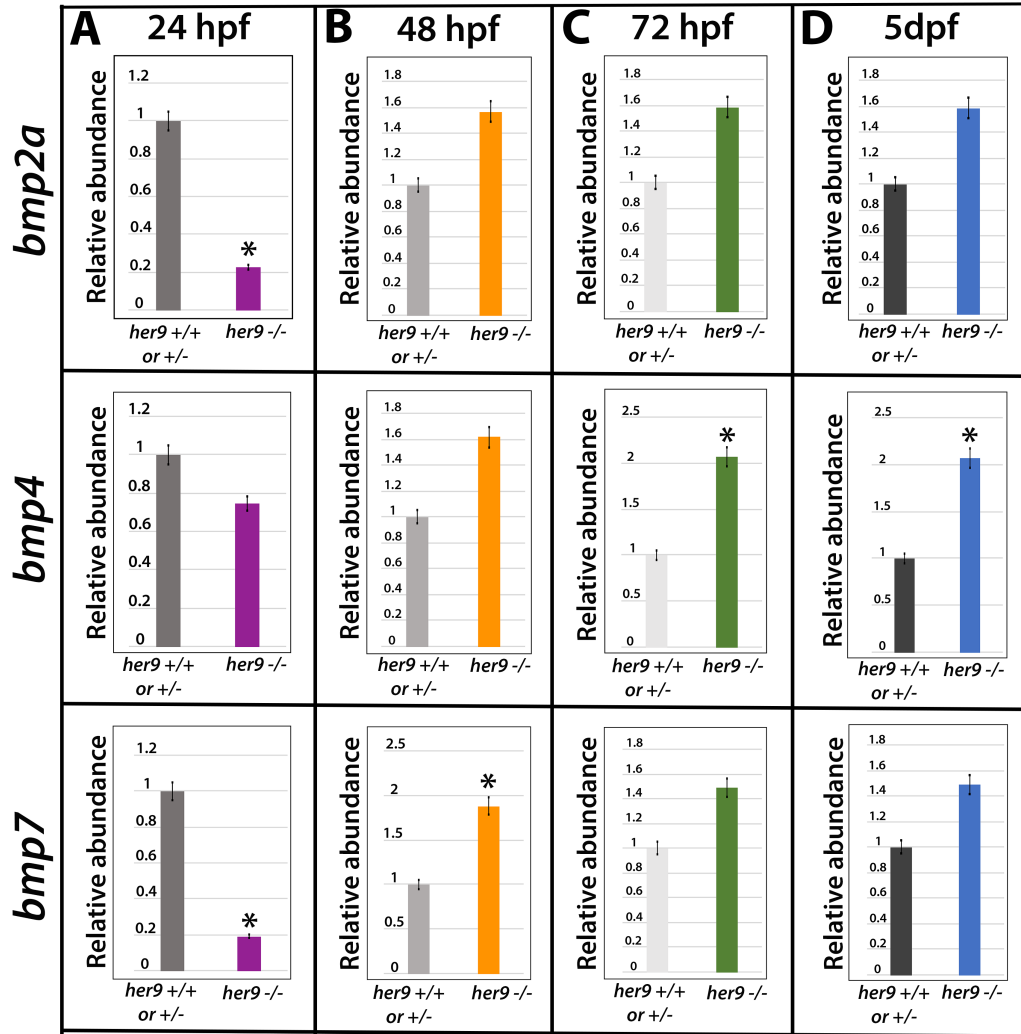


Figure 4.12 *Her9* mutants have increased Bmp ligand expression during migration and differentiation of NCC. qPCR was used to analyze the expression of *bmp2a*, *bmp4* and *bmp7* throughout NCC development. **A)** At 24 hpf, there was a significant decrease in *bmp2a* ($p = 0.0243$) and *bmp7* ($p = 0.345$). **B)** At 48 hpf, *bmp7* expression is the only expression significantly increased ($p = 0.0205$) although all Bmps are increased. **C-D)** At 72 hpf and 5 dpf, *bmp7* is significantly increased ($p = 0.0248$ and $p = 0.0251$).

4.4.12 Loss of Her9 function leads to CNCC and VNCC cell death

Disruption in expression of a number of the genes, such as *foxd3*, *bmp* ligands, and *vgll2a*, in the gene regulatory network (GRN) of NCCs have been shown to affect the survival of NCCs (Huang et al., 2016; Johnson et al., 2011; Stewart et al., 2006). To determine whether the loss of Her9 caused NCC death, we performed a TUNEL staining on cryosections from 5 and 7 dpf embryos. We did not observe any cell death in pigment cells, but we did observe a significant increase in TUNEL+ cells in the *her9* mutant mouth and jaw compared to the WT and heterozygous larvae (**Figure 4.13A-B'**). We also observed a significant increase in the number TUNEL+ cells in the gut of *her9* mutants compared to the WT and heterozygous larvae (**Figure 4.13C-D'**). This result suggests that the loss of Her9 leads to the death of CNCC and VNCC derivatives. Further, this supports that the loss of Her9 disrupts the expression of *foxd3*, *bmp*, and *ets-1*, and that Her9 is required for the survival of specific NCC derivatives.

Figure 4. 13 The Loss of Her9 causes the cell death of CNCC and VNCC

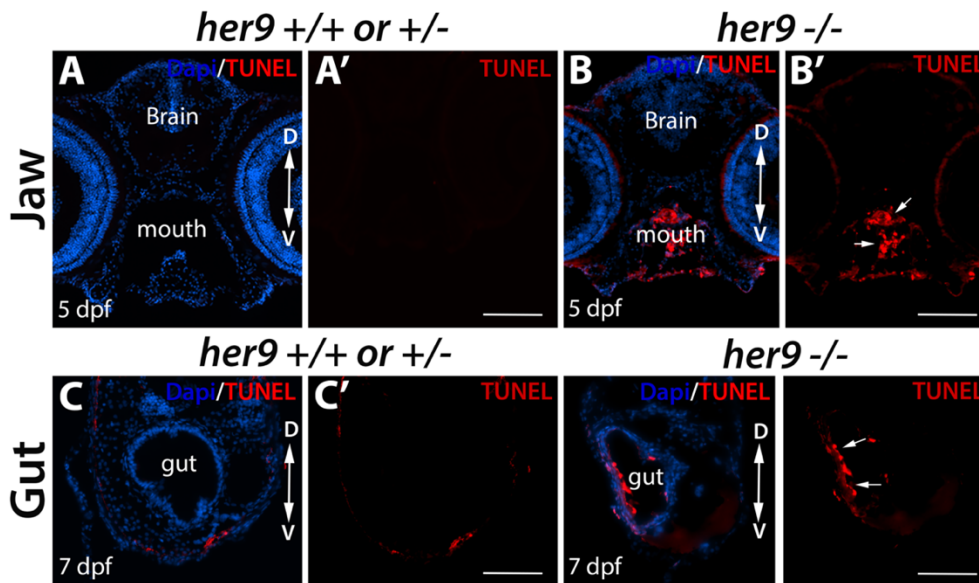


Figure 4.13 The loss of Her9 causes the cell death of CNCC and VNCC. A-A') TUNEL staining of WT embryos. **B-B')** TUNEL staining of *her9* mutants, showing an increase in the number of TUNEL+ cells. **C-C')** TUNEL staining of WT gastrointestinal tract. **D-D')** TUNEL staining of *her9* mutant gastrointestinal tract, showing an increase in TUNEL+ cells.

4.5 Discussion

In this study, we analyzed the NCC phenotypes present in the first described *her9* genetic mutant. Her9 is a bHLH-O transcription repressor and, like many other members of the Hairy/Hes family, is known to be involved in the regulation of neurogenesis. More specifically, it's been shown that Her9 regulates otic neurogenesis by defining the posterolateral non-neurogenic border (Radosevic et al., 2011b). The underlying mutation presented in this chapter is a 1 bp insertion that introduces an early stop codon, thus causing a loss of function mutation. We show that functional Her9 is involved in migration and differentiation of specific NCC derivatives. Our results indicate that Her9 functions by mediating expression of essential genes within the neural crest cell (NCC) gene regulatory network (GRN) such as *bmp*, *foxd3* and *sox10*.

4.5.1 Her9/Hes4 during early NCC development

An obvious question is whether Her9 is expressed in developing NCCs or whether it functions non-cell autonomously? Previous research has shown the *her9/hes4* is expressed at the neural plate border during the time of NCC induction (Nichane et al., 2008b) and suggest it is expressed in the NCC at induction (Nichane et al., 2008a). To confirm this, the *foxd3:GFP* line could be used in combination with Fluorescent in situ hybridization (FISH) for *her9* to determine whether *her9* co-localizes with NCC markers.

Bone morphogenetic protein (BMP) has been shown to act in coordination with noggin to create a gradient that allows for the specification of NCC at a specific concentration (Marchant et al., 1998). This gradient functions such that high levels of BMP activity induce epidermis, intermediate levels of BMP induce neural crest cells, and the lack of BMP is required for neural ectoderm formation (Schumacher et al., 2011). Supporting evidence for this theory was provided by experiments in zebrafish where BMP expression was manipulated using dorsomorphin. High concentrations of dorsomorphin result in low concentrations of BMP and the absence of neural crest cells. Low concentrations of dorsomorphin leads to increased BMP expression and an expansion of the NCC population (Kwon et al., 2010). In our *her9* mutant, there is a slight decrease in the expression of BMP at early timepoints then an increase at later

timepoints (Figure 4.12). The maternal *her9* mRNA present during at early timepoints may be enough to regulate BMP expression during this time. Using dorsomorphin to manipulate BMP in the *her9* mutant may be a way to rescue some of the mutant phenotypes and is a logical next step to help us determine whether Her9 is affecting NCC induction through the regulation of BMP expression. Changes in BMP alone are not sufficient to completely deplete the neural crest population though, so further investigation into specific genes associated with NCC cell induction and specification such as *crestin*, *tfap2* and *dlx5/6*, would help shed some light on the roles of *her9* during NCC induction and specification.

Our analysis of the *her9* mutant indicates that loss of Her9 may affect neural crest cell induction and specification but is not essential, because we do observe a differentiated NCC derived structures in *her9* mutants. Previous studies in frogs have shown that morpholino-knockdown of *her9/hes4* results in repression of specific NCC markers (*slug* and *foxd3*), leading to the decrease or depletion of specific NCC subpopulations (Stewart et al., 2006). It has also been shown that *foxd3* is not required for the induction of EMT of NCC but Foxd3 plays an early role in fate determination of specific NCC derivatives. The loss of *foxd3* results in a depletion of dorsal root ganglion and sympathetic and enteric neurons while melanocyte number is delayed but not significantly affected (Stewart et al., 2006). In this study we found that *her9* mutants presented with significant reduction of *foxd3* expression at 24 hpf, reduced number of *foxd3*:GFP positive cells, and gross morphological craniofacial and gut defects. The significant decrease in *foxd3* expression and decrease in the number of *foxd3* expressing cells could indicate a decrease in the premigratory NCC population. Additionally, the decreased expression of *sox10* and decreased number of *sox10* expressing cells in CNCC and ENS NCC populations indicate that there were fewer cells specified, implying Her9 is involved in induction and specification of NCCs.

Using HuCD staining, we did not identify a significant decrease in DRG number or any specific defects in DRG morphology. DRG have been shown to be downstream of Wnt and Hh signaling (Ungos et al., 2003; Won et al., 2011) but not BMP signaling during NCC development; this could explain why we did not see any significant affects to this particular NCC subpopulation. The HuCD antibody also limited our study to only the neuronal subpopulation. To circumvent this and better understand whether Her9 is affecting DRG development, crossing the *her9* mutation onto the *isl2b*:EGFP line (Won et al., 2011) which labels dorsal root and

Rohon-Beard neurons, would allow further investigation into the role of *her9* on DRG development. Future studies using RNAseq at significant timepoints before and during NCC induction, to look at changes in gene expression in the NCC gene regulatory network (GRN), would provide significant insight into whether Her9 regulates genes involved with NCC induction.

4.5.2 Her9 is necessary for the migration and differentiation of NCC lineages

When CNCC fail to properly migrate and differentiate, morphological defects in the face, neck and cardiovascular system arise (Hutson and Kirby, 2007; Tobin et al., 2008). The *her9* mutants display multiple craniofacial defects including missing pharyngeal arches, cleft palate and protruding mandible. CNCC migration begins with directed migration from the hindbrain along the dorsolateral pathway towards the branchial arch and finally entering and invading those arches (Kulesa et al., 2010). Improper development of branchial pouches and decreased expression of *ets-1* in the *her9* mutants are indicative of defects in NCC migration. To further analyze the role of Her9 in CNCC migration, live imaging of the *sox10:RFP* line is a necessary next step.

One of the most common congenital birth defects is a cleft palate, affecting 135,000 newborns worldwide, and is predominately associated with defects in CNCC migration and differentiation. Patients with a cleft palate usually have complications with feeding, speech and hearing. The formation of the palate begins with the elongation of palatal shelves and ends with fusion of the shelves, creating a separation between the oral and nasal cavity (Wu et al., 2008). Manipulation of *pax3* expression in mice has shown that persistent expression of *pax3* in CNCC leads to cleft palate, ocular defects, and prenatal lethality, while also mediating fate determination of pigment cells (Wu et al., 2008; Nord et al., 2016). Our results show that *her9* mutants display a visible cleft palate starting at 72 hpf, are not viable past larval stage, and, as described in the previous chapter, have ocular defects. Interestingly, we demonstrate a persistent increase (2-fold) in the expression of *pax3* over a significant period of time during development (at least from 3-7 dpf). Focusing on Pax3 related defects, we observed a significant decrease in the number of melanocytes. This could be the result of a fate switch, from melanophores and iridophores to xanthophores, indicating that the loss of Her9 affects pigment

cell number and fate determination. This fate switch is also accompanied by a consistent upregulation (2-fold) of *pax7*. These data provide supporting evidence that Her9 is not only affecting NCC migration but also differentiation.

Defects in the migration of NCC can lead to a wide range of developmental disorders such as Hirschsprung's disease, Axenfeld-Rieger syndrome, and CHARGE syndrome (Noisa and Raivio, 2014). Hirschsprung's disease is characterized by the lack of ganglia formation in the hindgut which in turn leads to decreased innervation, accumulation of digested food, and an enlarged and nonfunctional colon (Bergeron et al., 2013). The cells of the ENS are composed of VNCC and during migration the cells travel from the hindbrain and enter the gut. Once inside the gut the VNCC travel the entire length of the gut by 72 hpf (Olden et al., 2008). At 60 hpf, very few NCC can be identified in the gut of the *her9* mutant but by 72 hpf NCC can be isolated in the foregut and midgut of the mutant but there were still significantly less than WT. Consistent with the lack of NCC in the gut, we also observed less differentiated neurons and glia later in development of the mutant zebrafish. Due to these phenotypes, we tested digestive function via assays of feeding behavior in the *her9* mutant. Very few mutant larvae ate food to begin with (which could be a result of the craniofacial defects) and when they did, they were unable to process the food past the midgut causing a buildup of undigested food. These symptoms mimic those of the Hirschsprung's disease and indicate a defect in NCC migration, specifically in enteric NCC.

Enteric neural crest precursors maintain proliferation and inhibit differentiation as they migrate through the gut. Yakoubi et al. (2012) used morpholino knockdown of *hes4* in xenopus to show that Hes4 controls proliferative properties of neural stem cells during retinal development (2012), supporting the theory that the loss of Her9 could be disrupting proliferative capabilities in the NCC. Additionally, previous studies have shown that Meis3 plays a key role in migration and mediates proliferation of enteric neural crest cells during gut development (Uribe and Bonner, 2015). The loss of Meis3 during NCC development results in a significant decrease in the number of enteric neural crest precursors, indicating proliferation defects and delay in migration of VNCC towards and across the gut (Uribe and Bonner, 2015). Diminished expression of *meis3* in the *her9* mutant provides supporting evidence to the theory that loss of Her9 causes defects in NCC migration and differentiation. Time-lapse imaging and

tracking the migration of the enteric neural crest cells along the gut would allow a better understanding of any changes in migration patterns.

Finally, BMP signaling was shown to be upregulated in mice during the time of cardiac neural crest cell migration into the cardiac cushion (Kaartinen et al., 2012). During this developmental period, we also observe a significant increase in BMP ligand expression in our *her9* mutant zebrafish. Interestingly, we did not observe any obvious morphological cardiac defects in *her9* mutants, but further investigation into specific cardiac structures is necessary to rule out any effects of *her9* on heart development. Crossing the *her9* mutation onto the Tg(sox9b:EGFP) background, which labels CNCC, would allow for time-lapse imaging and tracking of the cardiac NCC (Hofsteen et al., 2013). Looking at the expression of genes such as *fgf8* and *GATA6* would also help us understand whether *her9* mutants have any heart defects.

The defects in migration and differentiation could be due to a decrease in the number of NCC available and subsequent morphological defects could be a consequence of Her9 playing a role early in NCC induction. It could also be that Her9 is playing dual roles within the GRN: one being an early role as described above and a later role where Her9 impacts the migration, differentiation, and survival of the remaining NCC of specific subpopulations (cranial and enteric NCC). Further investigation into the early phenotypes present in the *her9* mutants and analysis of specific gene expression across the GRN is necessary to answer these questions.

4.5.3 Her9 and NCC survival

Interestingly, *Xhair2*, or *Hes4*, has been described as being required for the proliferation and survival of neural crest cells (Nagatomo and Hashimoto, 2007) and in Chapter 3 we describe a decrease in glial cells in the hindbrain of *her9* mutants (Figure S3.). Further, in our *her9* mutant, we observed a significant increase in cell death in the pharyngeal arches and ENS. These could be a result of the misexpression of multiple transcription factors within the NCC GRN that are known to have dual roles in NCC development and apoptosis. For instance, disruption in the expression of *foxd3* in mice leads to the death of embryonic stem cells, a conserved feature of *Foxd3* in the regulation of cell death in stem cells (Hanna et al., 2002). It has been shown that the loss of *foxd3* expression also causes cell death in a subpopulation of NCC in the hindbrain

that contributes to neurons, glia, and pharyngeal arches (Stewart et al., 2005). The consistent downregulation of *foxd3* in the *her9* mutants could cause the significant cell death we observe in the cranial NCC as well as the neurons and glia of the ENS. While we surveyed cell death in the retina at several timepoints, we have not looked at all NCC populations at multiple timepoints. TUNEL assays to survey cell death at earlier time points would be necessary for determining when cell death in *her9* mutants begins, giving more insight into what genes might be involved in cell death.

4.5.4 Conclusion

Neurocristopathies are an expansive group of pathologies with a wide range of phenotypes ranging from craniofacial defects to abnormal eye morphology. In this study, we describe a *her9* mutant with a combination of NCC and retinal defects. The question remains if the defects in the retina and in NCC derivatives are both caused by dysregulation of a single pathway or gene, such as *gdf6a*. *Gdf6a* is a BMP ligand that has been shown to be involved in cone photoreceptor subtype differentiation (Duval et al., 2014), controls the transition from proliferation to differentiation by inhibiting RA signaling (Valdivia et al., 2016), and is essential for signal regulation between neural crest and the neural plate border (Reichert et al., 2013; Scille et al., 2016). Currently, most eye or retinal phenotypes associated with neurocristopathies are characterized by morphological and structural changes rather than cellular defects in the retina. This could very well be due to the extensive nature of some of the phenotypes in neurocristopathy patients, causing retinal cellular phenotypes to be overlooked and difficult to characterize. It is also possible that *Her9* is playing multiple roles through separate pathways, one in the retina and another in neural crest cells. Further exploration into the pathways that influence *her9* expression during NCC and retinal development would clarify some of these remaining questions and possibly provide key insight into less characterized retinal defects that could link them to neurocristopathies.

Acknowledgments

The authors would like to thank Lucas Vieira Francisco for excellent zebrafish care. We also thank Dr. Jakub Famulski (University of Kentucky) for generously providing the zebrafish lines.

Funding

This work was supported by a grant from the National Institutes of Health (R01EY021769, to A.C.M.) and the University of Kentucky Lyman T. Johnson graduate fellowship (to C.E.C).

Cagney E. Coomer

Department of Biology, University of Kentucky, Lexington, Kentucky 40506

5.1 Summary and Discussion

The senses are how organisms connect with their environment and for humans, vision is the most important of those senses. About 80% of the information we gather from our surroundings is acquired by the eyes and they serve as our best protection from danger. For correct visual function, a multitude of diverse cell types, tissue structures, and intricate interconnections must come together perfectly. An important component of this process is the retina, a thin layer of tissue at the back of the eye that is responsible for capturing light photons, converting them into a neural signal and sending those signals to the brain for interpretation into an image. Development of the retina requires the intricate coordination between regulatory networks and precise spatiotemporal gene expression. The retina is a complex structure and there are still many questions that remain concerning retinal development and regeneration in response to damage.

In many developed countries, visual disability is commonly associated with degeneration or cell death of retinal neurons such as photoreceptors or ganglion cells. This degeneration or cell death results in irreversible blindness, in part due to the fact that, in mammals, the Müller glia are mitotically inactive and become gliotic but do not reenter the cell cycle to repair retinal cell damage. Zebrafish on the other hand are highly visual organisms that are ideal for studying retinal development and regeneration as the Müller glia dedifferentiate and undergo asymmetric cell divisions to regenerate cells lost due to damage and integrate them into the retinal network to restore complete vision. With significant advances in our understanding of how some vertebrates are capable of regeneration on a molecular level, we can unlock regenerative potential in mammals to treat patients with visual disorders. Therapeutics like neuroprotective agents and antibody treatments are the current frontline

defense against retinal disorders. Unfortunately, our lack of knowledge creates significant barriers for developing and designing more impactful treatments. The challenge now lies in generating a better understanding of gene regulatory networks and cellular mechanisms involved in retinal development and regeneration, then using this understanding to better treat patients who suffer visual disorders and vision loss.

The goal of this dissertation was to determine the function of CAPN5 and Her9 during retinal development and regeneration. The roles of these two genes in retinal development and regeneration have not been previously described in zebrafish or mammals. The first gene, *capn5*, is a member of a group of calcium-dependent cysteine proteases (Sorimachi et al., 2011). These proteases have been implicated in signal transduction, mobility, cell cycle, apoptosis, and necrosis (Wells et al., 2005). *Capn5* has been shown to be ubiquitously expressed in humans, yet a gain of function mutation seems to only effect the retina, causing a disease called autosomal dominant neovascular inflammatory vitreoretinopathy (ADNIV; Randazzo et al., 2017; Wang et al., 2017). ADNIV is an ocular inflammatory disease that is characterized by progressive uveitis, cystoid macular edema (CME), neovascularization of the retina and iris, vitreous hemorrhage (VH), and tractional retinal detachment (TRD; Tang et al., 2020). The second gene, *her9*, is a member of the bHLH-O transcription factor hairy/hes/her family transcription factors shown to be involved in the regulation neural tube closure, floor plate development, progenitors in the cell cycle, and restricting the differentiation of cells. *Her9* was previously shown to be upregulated during chronic rod photoreceptor degeneration and the expression is concentrated to the proliferative areas of the retina (Davis and Turner, 2001; Kageyama et al., 2007; Yakoubi et al., 2012).

5.2 Calpain-5

The *C. elegans* homologue of *Capn5*, TRA-3, has been reported to be essential for necrotic neuronal cell death. *Capn5* has been linked to obesity, Huntington's disease, and polycystic ovarian syndrome in humans (Gonzalez et al., 2006; Saez et al., 2008; Wert et al., 2019). Moreover, the pathogenic activation of calpains results in the cleavage of essential substrates involved in neuronal survival mechanisms, leading to the initial hypothesis that *capn5* would be

expressed in all retinal neurons and play a role in regulating cell death mechanisms. The experiments described in Chapter 2 of this dissertation showed that *capn5* is expressed in the developing brain, optic vesicles, and newly differentiated photoreceptors. We did not observe *capn5* expression in the eye or retina during development which indicates that *capn5* does not have a role in development of retinal neurons. The first sign of expression of *capn5* was observed in the ONL starting at 72 hpf after the photoreceptors have differentiated leading us to conclude that *capn5* is involved in the maintenance of photoreceptors instead of the development. Additionally, this photoreceptor expression was shown to be cone specific and expressed in the inner and outer segments of the photoreceptor.

Is the cone photoreceptor specificity of *capn5* a zebrafish specific expression pattern? One explanation could be that *capn5* is expressed in the predominantly used photoreceptor subtype. Much of the previous research on *Capn5* has been in either the mouse or rat, which have rod dominant retinas compared to zebrafish's cone dominant retina. The expression of *capn5* in rat hasn't been connected to a specific photoreceptor subtype but it has been shown to be expressed in rod outer segments. Another explanation could be that the observed expression pattern is zebrafish specific and is more closely tied with the zebrafish's ability to regenerate. Expression of *capn5* in zebrafish Müller glia during photoreceptor regeneration provides supporting evidence for this. To further explore this question additional experiments are needed. One approach would be a comparative analysis of *capn5* expression in the developing and adult retinas of the organisms including but not limited to mouse, frog and zebrafish to hash out whether the expression pattern of *capn5* displays species specific patterns. If the expression of *capn5* is rod specific in mice and other nocturnal animals, that could indicate that *capn5* is expressed in the dominant photoreceptor subtype. Another approach could be to develop a *capn5* reporter transgenic line. CRISPR-Cas9 knock in of a Flag or GFP tag to the *capn5* protein would allow us to observe *capn5* expression in real time and give us a better understanding of its expression pattern in photoreceptors.

Additional experiments in Chapter 2 indicate that *capn5* has a role in cell survival and regeneration. We also showed that *capn5* is upregulated in a zebrafish model of chronic rod photoreceptor degeneration (Coomer and Morris, 2018), but *capn5* expression was only observed in the cone photoreceptors, which are interestingly unaffected during the rod photoreceptor degeneration. This unaffected cone phenotype is not typical of retinal

degenerative diseases such as in Retinitis pigmentosa (RP), where cone photoreceptor degeneration is a secondary consequence of rod photoreceptor degeneration (Petters et al., 1997). This evidence suggests that *Capn5* could play a protective role in cone photoreceptors during zebrafish rod photoreceptor degeneration/regeneration and promote cell survival. Consistent with this idea, we observed an upregulation in the expression *capn5* in the surviving cone photoreceptors and in Müller glia following acute light damage.

The upregulation of *capn5* during chronic degeneration was not a surprise because *Capn5* has been linked to neuronal degeneration and ADNIV. What was unexpected was that we observed upregulation of *capn5* in the cones (which are not degenerating) and in the Müller glia, which are the source for retinal regeneration in zebrafish. Taking into account that cone photoreceptors have a higher threshold for damage before degeneration is triggered (Petters et al., 1997; Lin et al., 2009), it could be that *capn5* is playing a role in protecting the cone photoreceptors from the bystander effects of rod photoreceptor cell death, which has been shown to trigger cone degeneration following rod degeneration in other models (Ripps, 2002). To test whether or not *capn5* expression promotes cell survival, knockout of *calpain-5* using CRISPR/Cas9 could be used to determine whether *capn5* is required for photoreceptor maintenance, and whether the loss of *capn5* affects photoreceptor survival in response to damage. In an attempt to address these questions, we designed CRISPR/Cas9 constructs, injected, and began screening for *capn5* CRISPR mutants (see Appendix). This work is ongoing. Additionally, to better understand whether or not *capn5* is playing a protective role during degeneration and/or influencing cell survival, a tissue specific CRISPR knockout strategy like that outlined by J. Ablain et. al could be used. This CRISPR makes use of a single construct to ubiquitously express the sgRNA and to drive tissue-specific expression of Cas9 (Ablain et. al, 2015). Following knockdown of *capn5* expression in the cone photoreceptors for instance, we could expose the zebrafish to acute light damage and determine whether the threshold to trigger cone cell death has been lowered by loss of *capn5*.

Calpain-5 is a regulatory protease expressed in photoreceptors and thought to regulate the biological functions of its targets (Schaefer et al., 2016). Extensive research has gone into understanding the pathogenesis of ADNIV, caused by mutations that induce *Capn5* hyperactivity, but the underlining mechanisms of the disease are poorly understood. One of the major barriers is that the function and targets of *Capn5* are also poorly understood at the

moment. Proteomic analysis of ADNIV patients at different stages of the disease have identified many differentially expressed proteins such as upregulated VEGF and IL-6 (Velez et al., 2020). When categorized by cellular compartment, many of the proteins that were decreased in ADNIV patients were localized to the synapse of the cell (Velez et al., 2020). These studies provide clues into the function and targets of Capn5 under the disease state but there is still a major gap in our knowledge surrounding Capn5 protein-protein interactions and its direct targets.

To investigate direct protein-protein interactions or targets of Capn5, mouse cell lines such as 661W cells (Tan et al., 2006) could be used to conduct tandem affinity purification (TAP) assays to look for specific binding partners or targets of Capn5. Since we currently do not know the targets of Capn5, creating a fusion protein containing a TAP tag would allow for an unbiased screen of possible targets. Activated Capn5 and hyperactive Capn5 from mouse and rat have been isolated and could be used to create fusion proteins. The 661W cells exhibit processes characteristic of neuronal cells and express cone specific proteins such as blue and green cone pigments, transducin, and cone arrestin. This will allow us to look at Capn5 protein-protein interactions that are relevant to cone photoreceptor biology. Investigating the interactions this way will allow the use of Western blot and mass spectrometry to identify target proteins. Investigation of Capn5 protein-protein interactions under high calcium levels can also be accomplished by growing cells in a calcium rich media followed by a TAP assay. Once we have identified some specific targets of Capn5 protein-protein interactions, we can use the yeast-two hybrid system to provide supporting evidence of an interaction between Capn5 and each of the proteins identified. Using the *Gal4BD+bait* and *Gal4AD+prey* system we can use a reporter assay to investigate the interactions between these genes as well as use the reporter gene expression (LacZ) to analyze the strength of the interactions themselves. The proposed experiments would provide data about Capn5 targets, furthering our understanding of its function and the underlying mechanisms of ADNIV.

When and how does the expression of Capn5 turn from advantageous to deleterious? As a family of proteases, Calpains have been associated with eye-specific diseases including retinal degeneration, retinitis pigmentosa, and retinal detachment when their activity is upregulated. As is the case for ADNIV, *capn5* mutations lead to a decreased calcium threshold resulting in increased activity (Schaefer et al., 2016). Most patients who present severe phenotypes of ADNIV are typically in their fourth decade of life, but the mutation is genetic and

present at birth leaving one to question the lack of phenotype in younger patients. One theory could be that Capn5 activity is restricted under very specific spatiotemporal conditions and prolonged activity creates space for Capn5 to come in contact with potential substrates that it would usually not encounter; essentially, too much of a good thing. To better understand whether prolonged activity of Capn5 is an underlying contributor to the transition from advantageous to deleterious, an inducible TetON system could be used to manipulate *capn5* expression in the eye in the developing and adult zebrafish. Studying the effects of sustained *capn5* expression to determine whether prolonged activity of Capn5 is the contributor to the ADNIV pathogenesis is imperative in understanding the disease and identifying therapeutic targets.

Long term implications of this work include, but are not limited to, possible roles of gene therapy in patients who are experiencing various degrees of ADNIV and vision loss. The various data presented along with experiments proposed could allow researchers and medical professionals to obtain a better understanding of Capn5 during development and regeneration as well as the pathogenesis of ADNIV. For any of these ideas to become reality, a significant amount of research is needed to understand the roles of Capn5 during retinal development, the mechanistic workings of the protease, and its potential target substrates. In addition, a better understanding of how the function of Capn5 fits into the larger context of networks and pathways associated with regeneration is imperative in furthering the possibility of regenerative medicine.

5.3 Hairy-related 9

Previous research has shown that *her9* is upregulated during chronic rod degeneration in zebrafish (Wilson et al., 2016), downstream of RA signaling during retina development (Coomer et al., 2020), and is primarily expressed in proliferative zones (CMZ) of the embryonic and adult retina (Coomer et al., 2020). Translation blocking morpholino mediated knockdown of *her9* resulted in a decrease of endothelial cells in the retina. These data led to the hypothesis that *her9* plays a role in the maintenance of proliferating stem and progenitor cells of the retina and is involved in retinal vasculogenesis. A *her9* mutant line containing a 1bp deletion and one containing a 1 bp insertion were generated using CRISPR/Cas9 to further investigate this

hypothesis. When zebrafish heterozygous for a mutant frame-shift allele of *her9* were in-crossed, and the subsequent generation raised to adulthood, *her9* *-/-* zebrafish were never recovered. Subsequent analysis showed that the homozygous *her9* mutant larvae died before 14 dpf and possessed a wide range of phenotypic abnormalities.

The experiments featured in Chapter 3 show that *her9* is downstream of RA signaling, and that loss of *her9* results in a reduction in specific photoreceptor subtypes and increased apoptosis in the retina. *Her9* homozygous CRISPR mutants characterized in this chapter also had a reduced CMZ and decreased and disorganized Müller glia. These results are consistent with the idea that *her9* plays a role in the maintenance of proliferating stem and progenitor cell populations. The decreased and disorganized Müller glia phenotype could also be linked to the decrease in rod photoreceptors, considering that a subset of Müller glia are responsible for contributing to post-embryonic rod photoreceptor development [ref]. A possible mechanism is that *her9* regulates extrinsic and/or intrinsic cues involved in Müller glia mediated generation of specific rod progenitor pools. Her9 could also play a role significantly earlier during retinal development to regulate retinal progenitor proliferation or specification.

In addition to the retinal phenotypes described in Chapter 3, *her9* *-/-* mutants also display decreased vasculature in the brain, trunk, and around the eye which can be rescued with *her9* mRNA. This evidence supports our hypothesis that *her9* has a previously undescribed role in vasculogenesis.

Unlike other members of the bHLH-O transcription factor family, *her9* is not downstream of Notch-Delta signaling (Radosevic et al., 2011). In fact, *her9* has been shown to be an effector of many distinct signaling pathways and regulatory networks in a tissue specific manner. For example, *her9* is downstream of Bmp signaling, involved in pre-patterning of the early neuroectoderm, and functions downstream of midline Nodal signaling during notochord development (Bae et al., 2005a; Latimer et al., 2005). Additional experiments in Chapter 3 show that manipulation of retinoic acid signaling alter the expression of *her9* in the developing retina. Further, analysis of the presumptive upstream cis-regulatory elements of *her9* show multiple retinoic acid responsive elements (RAREs), including several RAREs within the coding region of the gene as well. This suggests that *her9* is downstream of RA signaling in the retina. Interestingly, RA signaling has been shown to extrinsically regulate photoreceptor development and differentiation in collaboration with other signaling pathways such a thyroid hormone (TH)

(Cossette and Drysdale, 2004). Drug screens used to transiently activate and inhibit the TH signaling pathway also resulted in modulation of *her9* expression, although the data is only preliminary (data not shown). Thyroid hormone has been shown to be involved in tissue remodeling, cell proliferation, differentiation, and survival (Harpavat and Cepko, 2003; Yang et al., 2018). Furthermore, thyroid hormone receptors have been shown to dimerize with retinoid x receptors and current thought is that this heterodimer forms its most effective configuration of thyroid receptor for transcriptional regulation (Feher 2012). Taking this into account, and the fact that exogenous application of RA was not sufficient to rescue the *her9* retinal phenotypes while recapitulating previously known effects of increased RA signaling in the retina, I think *her9* could be mediating crosstalk between multiple signaling pathways.

To further investigate this, the *her9* coding region and cis-regulatory regions should be analyzed for thyroid hormone response elements. Identification and testing of these response elements could directly link *her9* to the TH signaling pathway and provide further evidence to theory that it regulates pathway crosstalk. Analysis of different retinoid x receptors and thyroid hormone receptors in the *her9* mutant compared to the wildtype could provide further clues about where in these pathways *her9* is acting. Additionally, using drug screens to manipulate the expression of RA and TH in the *her9* mutant could unlock whether the loss of *her9* is disrupting both pathways, which subsequently results in the retinal phenotypes. Interestingly, the loss of thyroid hormone receptor beta has been shown to result in the loss of long wave-length photoreceptors (Ng et al., 2001; Ng et al., 2010), mirroring the loss of long wave-length photoreceptors in the *her9* mutant. Further investigation into whether TH alone can rescue the mutant phenotype would be necessary to further understand the proposed relationship.

As discussed in Chapter 4, we hypothesize that maternally deposited *her9* mRNA is sufficient to permit survival of *her9* homozygous mutant embryos at least to the 5 dpf larval stage. However, as the reservoir of *her9* is depleted, and no endogenous wildtype *her9* is generated to replace it, numerous morphological phenotypes arise including defects in pigment cells, gut, and craniofacial structures, all of which are derivatives of NCC. We demonstrate that a loss of *her9* results in an increase of xanthophores, at the expense of melanophores and iridophores, and link this phenotype to BMP regulation of pigment specific NCC genes. Specifically, we show that a loss of *her9* results in the upregulation of BMP ligands, and subsequent expression changes of specific BMP target genes such as *pax7* and *foxd3*. These

unexpected NCC phenotypes support previous research in *Xenopus* that used morpholinos to knockdown Her9/Hes4. This study showed increased BMP signaling in Her9/Hes4 knockdown, placing Her9/Hes4 upstream of BMP signaling, and showed defects in the specification, migration, and survival of specific NCC subtypes. Deep sequencing of NCC populations from *her9* mutants compared to the wild type would get us a better understanding of what genes in the NCC GRN are affected by the loss of *her9* and help us better determine where *her9* acts in the NCC development pathway.

In Chapter 4, we show that the loss of *her9* results in craniofacial defects that could be a result of defects in both NCC migration and differentiation. This phenotype is interesting because it has been shown that coordinated interactions between TH and RA signaling pathways are required for proper craniofacial and ocular development. Alterations in TH signaling result in disruptions in CNCC migration, proliferation, and survival leading to defects in craniofacial, extraocular muscle (EOM), and ocular development defects. The craniofacial defects present in the *her9* mutant include missing pharyngeal arches, cleft palate, and an extended mandible. The missing pharyngeal arches were correlated with disrupted expression of *ets-1* and *vgl12a* in this dissertation, but a more extensive understanding of whether the loss of *her9* disrupts TH and RA signaling during craniofacial development is necessary. One approach to acquiring a better understanding would be to survey the expression of deiodinase enzymes (*dio1*, *dio2* and *dio3*). These enzymes have been shown to be involved in the synthesis and degradation of TH and an understanding of their expression after the loss of *her9* could provide insight into whether *her9* is involved in TH metabolism.

Beyond craniofacial defects, as discussed in Chapter 3 the *her9* mutants demonstrate a failed optokinetic response (OKR) which could be linked to the photoreceptor phenotypes described. An alternative explanation for the lack of an OKR could be that the loss of *her9* causes defects in extra ocular muscle (EOM) development. Taking into account that the ethmoid plate is a necessary component of the orbital cavity structure, and the EOM is housed within that cavity, it would not be a surprise if the defects in ethmoid plate development also perturb EOM development, further connecting *her9* to the cross talk between TH and RA signaling. To determine whether there are any defects in EOM development, cryosections of *her9* mutants stained with H&E could be used to analyze or search for morphological defects in the EOM. Additionally, analysis of genes specific to EOM development should be analyzed. Further

analysis to understand the relationship of *her9* with retinoid x receptors (RXR) and investigation into whether the loss of *her9* alters the expression patterns of RXRs will also be a significant component. Taken together, these data and the suggested future experiments would provide further insight into the relationship between *her9*, RA and TH as well as lay the foundation to understanding whether *her9* is involved in the regulating crosstalk between the two signaling pathways.

Additional experiments in Chapter 4 connect the loss of *her9* to the migration, differentiation, and survival of enteric neural crest cells. The *her9* mutant gut is missing this neural crest cell subpopulation in the hind gut and displays a lack of differentiated enteric neurons and glia. The mutant is incapable of correctly processing food through the gut, resulting in food buildup in the midgut. Taken together these phenotypes recapitulate Hirschsprung's disease. Interestingly, it has been shown that RA is critical for GDNF-induced enteric NCC migration, proliferation, and differentiation and recapitulates symptoms present in Hirschsprung's disease (Angrist et al., 1996). These data again raise questions about the relationship between *her9* and the RA signaling pathway. In fact, research has shown that both excessive RA signaling, and reduced RA synthesis can lead to abnormal ENS development (Fu et al., 2010). Members of the GDNF family have also been implicated in retinal development, indicating that the relationship between Her9, RA, and GDNF could be the underlying factor for the retinal and NCC phenotypes present in our *her9* mutants. Further analysis into GDNF as well as RA specific genes such as *raldh* and RA receptors in addition to TH receptors would provide further supporting evidence for a molecular relationship between RA and *her9*.

Given that NCC contribute to a multitude of structures during development and that no one gene in the NCC GRN has been linked to the development of any single subtype, it is no of no surprise that *her9* mutants contain multiple NCC phenotypes and that no subtype is significantly affected more than the others. The possibility of RA and TH signaling pathways being disrupted by the loss of *her9*, leading to defects in NCC development could be investigated by using drug screens to manipulate RA and TH and attempt to rescue the NCC phenotypes. Another possibility is that *her9* is involved in multiple steps during NCC development in a tissue specific manner, and the maternally deposited *her9* reserves are enough to get NCC cells through the initial induction phase but not the specification, migration, and differentiation phases of all subtypes. Because *her9* embryos homozygous for the mutation do not survive past

12 days, it eliminates the possibility of creating a maternal zygotic mutant and limits our ability to fully understand the effects of a complete loss of *her9*. Further investigation into the genes involved in the NCC GRN will be essential for determining the next steps. Currently there is no perfect solution for answering many of the remaining questions but injecting a translation blocking morpholino into a *her9* CRISPR mutant in-cross may help us better understand the role of *her9* during vertebrate development through near complete loss of function.

Hes/Her genes have shown to act as transcriptional repressors during the development of the CNS and inactivation of these Hes genes leads to an upregulation of proneural genes (Davis and Turner, 2001; Kageyama et al., 2008). Because Her9/Hes4 has not been as extensively studied as the other members of the Her/Hes family, not much is known about its targets. Based on previous research it seems as though *her9* has functional conservation with other members of the family and acts a transcriptional repressor (El Yakoubi et al., 2012) that has been shown to repress BMP4. Consistent with this data, we present in this dissertation data that suggests that Her9 represses *bmp2*, *bmp4* and *bmp7* as we see an upregulation in these genes in our *her9* mutants. BMP has been shown to play roles retinal development, NCC development and retinal regeneration (French et al., 2009; Marchant et al., 1998) and serves as an underlying connection between all of the phenotypes. One way to address the question of specific Her9 targets is to use FACS sorting to isolate rods, cones, and neural crest cells in the WT and *her9* ^{-/-} larvae and embryos, then use single cell RNAseq to analyze differentially expressed gene and determine some potential targets. Further research into *her9* and their potential targets will be essential for understanding the function of *her9* during retinal development.

The long-term implications of this work include, but are not limited to, possible use for gene therapy in human patients with visual defects, vision loss, and/or neurocristopathies. Her9/HES4 could also be implicated as a linking factor between neurocristopathies and retinal degenerative disease, which is currently something that hasn't been thoroughly investigated in neurocristopathy patients. One of the most commonly known terminal deletion syndromes is 1p36 deletion syndrome (Wu et al., 1999). Some of the major clinical features include craniofacial dysmorphism, gastrointestinal disorder, visual abnormalities, seizures, and behavioral disorders. Interestingly, the severity of the disease is dependent on the size of the deletion ((Rocha et al., 2016). HES4 is found on the chromosome, in the deleted region, which could also be an underlying connection in the seemingly distinct phenotypes observed in the

her9 mutants. Finally, overexpression of *her9* could possibly be used to rescue outer segment loss in patients with photoreceptor subtype specific defects and stimulate cell proliferation in the retina of patients with retinal degenerative diseases. There are still many missing components to our understanding of retinal development, regeneration, and NCC development. For any of these possibilities to become reality much research is still needed, particularly in a vertebrate model like the zebrafish, before attempting to unlock human regenerative capabilities and therapeutic targets.

The proposed model for Her9 during vertebrate development indicates that RA regulates Her9 during retinal development but we are currently not sure if it also regulates Her9 during NCC development. We also know that Her9 could possibly be acting through the BMP signaling pathway to disrupt NCC development while we are still unsure what the targets of Her9 are in the retina affecting photoreceptor development, maintenance and survival (**Figure 5.1**). There is still much research needed to unlock the unknowns of this model.

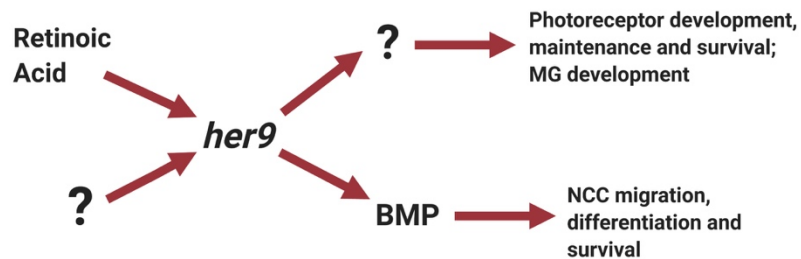


Figure 5.1 Schematic of possible Her9 pathways involved in both retinal and NCC development.

5.4 Conclusion

In conclusion, the projects described in this dissertation provide a detailed examination and description of novel functions of *capn5* and *her9* during development and regeneration of

the zebrafish retina as well as a role for *her9* in NCC development. Through molecular experiments, behavioral assays, and microscopy techniques, this dissertation provides detailed descriptions of the expression patterns for *capn5* and a possible role during regeneration as well as the knockout of *her9* and subsequent characterization of the mutant phenotype. I sincerely hope the studies presented here contribute to a greater understanding of development and regeneration of the visual system, leading to the development of therapies that could reverse vision loss or treat visual impairments in humans

APPENDIX

APPENDIX 1. PROGRESS TOWARDS GENERATING A ZEBRAFISH CAPN5 MUTANT USING CRISPR/CAS9

A1. Introduction

The only known inherited disease that has been linked to Calpain hyperactivity is Autosomal dominant neovascular inflammatory vitroretinopathy (ADNIV). As described in Chapter 1, ADNIV is characterized by recapitulation of the progression of more common retinal disorders such as proliferative diabetic retinopathy, retinitis pigmentosa, and retinal detachment. ADNIV is caused by mutations in *CAPN5*, a non-classical member of the calpain family (see Chapter 1 & 2 for more details). The expression pattern of *Capn5* in the developing mouse and zebrafish are the only clues we have into the function of Capn5 during vertebrate, and more specifically, retinal development. Data presented in this dissertation indicate that *capn5* is expressed in the developing embryonic brain, optic vessels, and in newly differentiated photoreceptors suggesting that Capn5 has a role CNS development and photoreceptor maintenance. We observed an increase in expression of Capn5 in a zebrafish model of chronic rod photoreceptor degeneration and regeneration. Additionally, acute light damage to the zebrafish retina was accompanied by an increase in expression of Capn5 in the surviving cones and in a subset of Müller glia, suggesting that Capn5 plays a role during regeneration. The severity of the ADNIV makes understanding the gene crucial for developing effective treatments, and the fact that ADNIV phenocopies so many other common eye diseases suggests that understanding the function of Capn5 may provide insight into common mechanisms associated with retinal degenerative diseases.

Currently therapies for patients with ADNIV focus on treating the symptoms of the disease but none are capable of treating every component. This leads scientists and physicians to believe that treatment for ADNIV will require the inhibition of the mutant Capn5 altogether. Due to gaps in knowledge about the function of Capn5 there is concern about what effects

inhibiting Capn5 will have on the eye and other parts of the body. To better understand the normal function of Capn5, animal models of Capn5 deficiency are needed. However, previous attempts at creating Capn5 knockout mice have generated debate over the whether or not Capn5 has an essential function. One study generated a Capn5 knockout (KO) mouse that produced viable embryos without any abnormal phenotype (they did report a small subset of stunted pups that died prematurely), but offspring were not carefully examined (Franz et al., 2004). A second study reported embryonic lethality in homozygous mutants by E3.5 (Jackson Laboratory: 005784; Mouse Genome Informatics [MGI]: 3604529). Given these results, I believe the zebrafish would be a good alternative model for using genome editing to knock out Capn5 and study its function during vertebrate development, with a focus on retinal development. As described in the previous chapters, zebrafish's small size, external development, optical transparency, genetic malleability, and sequenced genome make them a good alternative model for studying developmental roles of Capn5.

The CRISPR/Cas9 (Clustered Regularly Interspaced Short Palindromic Repeats) genome editing system was developed from the adaptive immune response of microbes. CRISPR/Cas9 relies on the incorporation of exogenous plasmid DNA and phage sequence into spacer regions of the bacterial genome flanked by short palindromic repeats which are cleaved and transcribed into CRISPR RNAs (crRNAs). crRNA sequences are complimentary to the target sequence on the invading phage. When the crRNAs form a complex with Cas DNA nucleases and the target DNA sequence, double stranded breaks (DSBs) are generated (Wiedenheft et al., 2012). Originating from *Streptococcus pyogenes*, the CRISPR/Cas9 system was adapted for use in eukaryotes in 2013 (Doudna and Charpentier, 2014). In this system, a dual-RNA structure consisting of a tracrRNA and crRNA duplex (gRNA) are designed to target a gene of interest as well as Cas9 mRNA synthesis. Following injection of the gRNA and Cas9 mRNA into an embryo, the gRNA recognizes and binds to the target sequence adjacent to the protospacer adjacent motif (PAM) site. After binding, the gRNA associates with Cas9 which results in DSBs usually 4-6 bp upstream of the PAM site (Jinek et al., 2012). The CRISPR/Cas9 genome editing system has been shown to work with very high efficiency and good specificity in a wide variety of organisms, including zebrafish. Libraries of zebrafish specific donor plasmids and zebrafish codon optimized Cas9 plasmids are available to the research community.

The following is a description of the progress I have made towards targeting *capn5a* and *capn5b* using the CRISPR/Cas9 system, in order to make stable *capn5* null mutant lines that will allow us to study the function of Capn5 during vertebrate development.

A.1.2 Materials and methods

A.1.2.1 Zebrafish line maintenance

All zebrafish lines were bred, housed, and maintained at 28.5°C on a 14 hour light:10 hour dark cycle, except where indicated for the light damage experiments. Zebrafish were bred, raised and maintained in accordance with established protocols for zebrafish husbandry (Westerfield, 1995) embryos were anaesthetized with Ethyl 3-aminobenzoate methanesulfonate salt (MS-222, Tricaine, Sigma-Aldrich, St. Louis, MO) and adults were euthanized by rapid cooling as previously described. (Wilson et al., 2016) All animal procedures were carried out in accordance with guidelines established by the University of Kentucky Institutional Animal Care and Use Committee (IACUC) and the ARVO Statement for the Use of Animals in Ophthalmic and Vision Research.

A.1.2.2 RNA extraction and RT-PCR

Total RNA was extracted from whole embryos at selected developmental time points or from the dissected retinas of adult zebrafish using TRIzol reagent (Invitrogen, Grand Island, NY) according to the manufacturer's protocol. The samples were treated with RNase-free DNase I (Roche, Indianapolis, IN) and purified using a chloroform/phenol extraction. The GoScript Reverse Transcriptase System (Promega, Madison, WI) was used to synthesize first strand cDNA from 1µg of the extracted RNA. PCR primers were designed to amplify unique regions of the *capn5a*, *capn5b*, and *atp5h* cDNAs (Eurofins Genomics; www.eurofinsgenomics.com; Table 1).

A.1.2.3 Generation of guide RNA oligonucleotides and Cas9

The two target sites for CRISPR/Cas9 based genome editing within the *capn5a* gene were selected using the CHOPCHOP tool for selecting target sites (<https://chopchop.cbu.uib.no/>). Target site one is located on exon 2 in Domain 1 and the second target site is in exon 5 in Domain 2b (Table A1.1). Oligos were annealed at a concentration of 100 μ M (5 minutes at 95-100°C, then slowly cooled to room temperature for 5 hours) and ligated into BsaI (NEB: R0535S) digested pDR274 vector (Addgene: 42250). Recombinant vectors containing the gRNA insert sequence were digested with DraI (NEB: R0129S) and the insert was amplified by PCR. The PCR product (QIAquick PCR purification kit) was in vitro transcribed using Ambion-MEGAscript T7 Transcription Kit (Life Technologies#AM1334) then purified by phenol:chloroform extraction followed by ethanol precipitation. A gRNA targeting the tyrosinase gene was used as a positive control for the study. pT7tyrgRNA (Addgene: 46761) plasmid was linearized using BamHI (NEB: R3136T) and in vitro transcribed using Ambion-MEGAscript T7 Transcription Kit (Life Technologies: AM1334) then purified by phenol:chloroform extraction followed by ethanol precipitation. Products were stored at -80C until ready for use. A ready for injection Cas9 protein was ordered from NEB (EnGen Spy Cas9 NLS; <https://www.neb.com/>).

Table A1. 1 gRNA target and primer sequences

Table A1.1 gRNA target and primer sequences

gRNA	Primer sequence	Exon	Target sequence
CSR1_FP	TGTGAAGACCCTCATCTGTTTG	Exon 2	CTGCCATAGGGCTTCTCTGGAGG
CSR1_RP	TTATAATGGAAGTCAATGGGGG	Exon 2	CTGCCATAGGGCTTCTCTGGAGG
CSR2_FP	AAGTTTGCTCAGGATGAAGAGG	Exon 5	TGATGAGGCCTCCTCTGTTGTGG
CSR2_RP	CATGCAAACCTCCACACAGAAAT	Exon 5	TGATGAGGCCTCCTCTGTTGTGG

Table A1.1 CRISPR primer and target sequences. *Capn5a* CSR1 targets exon 2 and CSR2 targets exon 5, creating a 1223 bp deletion. CSR1, CRISPR1; CSR2, CRISPR2; FP, forward primer; RP, reverse primer.

A.1.2.4 Microinjections

Cas9 mRNA and both gRNAs (injected together to create a larger deletion) were injected at 150-300 and 50-100 ng/embryo respectively at a volume of 4.18 nl/embryo in buffered solution with 0.025% dextran red (as an injection indicator) into the yolk of 1-cell stage zebrafish.

A.1.2.5 Screening for deletions

A set of primers were designed outside the CRISPR target regions to screen for the deletion (Table A1.1). gDNA was extracted from embryos and tail-clips of adults, and PCR was used to amplify the target region. The PCR products were run on a 2% gel and PCR bands were gel purified then transformed into a plasmid to screen for deletion via sequencing.

A.1.3 Results

A.1.3.1 Design and generation of gRNA constructs

For the use of CRISPR/Cas9 targeted genomic editing system to knockout *capn5*, I designed two single-stranded guide RNAs (gRNAs) that are complimentary to specific sequences within the *capn5a* coding region, hereafter referred to as *capn5a* CSR1 and *capn5a* CSR2 (**Table A1.1**). *Capn5a* is very large gene containing 13 small exons separated by large introns. This coupled with high sequence conservation amongst calpains made designing the gRNA's difficult but not impossible. Capn5a CSR1 was designed to target the end of exon 2 while capn5a CSR2 was designed to target the middle of exon 5 in an attempt to create a large deletion that cuts out domain 2a of the catalytic domain (**Figure A1.1**). The gRNAs were then synthesized using direct in vitro transcription (IVT) from a restriction digest fragment produced from a donor vector that contained the synthetic oligos.

Figure A1. 1 CRISPR targets in the *capn5a* genomic locus

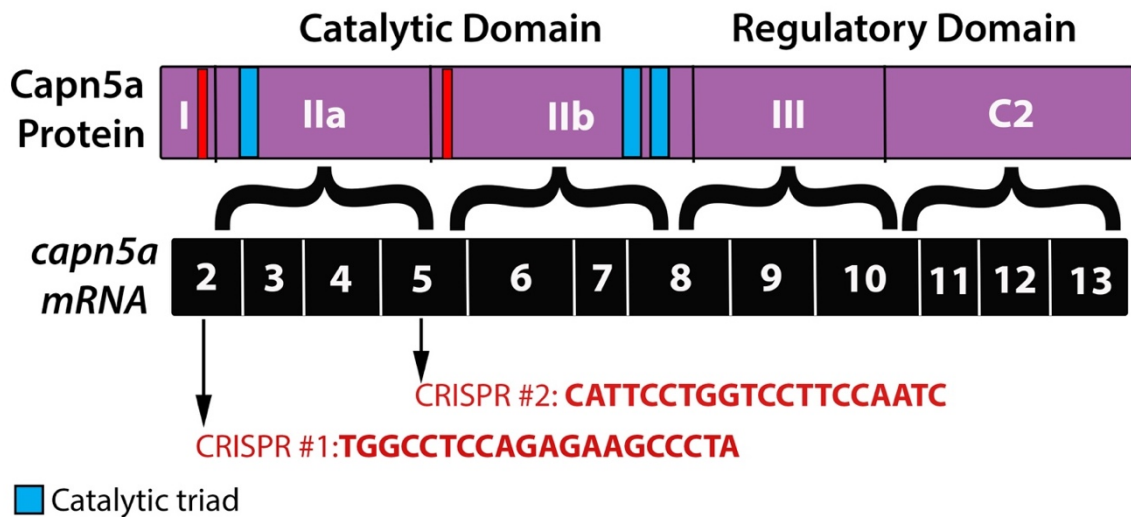


Figure A1.1 CRISPR targets in the *capn5a* genomic locus. The *capn5a* locus contains 12 exon. The first CRISPR target site is located on exon 2 in domain 1. The second CRISPR target site is located on exon 5 in domain 2b.

A.1.3.2 Injection of *capn5a* gRNA and Cas9 results in a variety of large deletions

CRISPR/Cas9 mutagenesis of *capn5a* should result in a combination of mutant and wildtype alleles in the mosaic F0 embryos regardless of whether the gRNAs are injected together or independently. To increase the chances of creating a null mutation, one cell stage embryos were injected with *capn5a* CSR1 and CSR2 which would produce an estimated deletion size of 1223 bp. Following injection, the embryos were screened at 24 hpf for Dextran red+ cells indicative of successful injection. gDNA was extracted from Dextran red+ embryos, PCR was used to amplify the region around the target sequence, and the product was run on a 2% gel to screen for deletions. 1041 embryos were injected with CSR1 and CSR2 and 746 of those

embryos tested positive for Dextran red. Of those, 58% presented some sort of deletion when screened (**Table A1.2**).

Table A1. 2 injected embryos

Table A1.2

# embryos injected	# of embryos Dex+	# of embryos with deletion	% of embryos with deletions
43	12	3	25%
221	176	74	42%
134	51	22	43%
97	81	56	69%
107	65	51	78%
312	268	179	66.4%
27	24	15	62.5%
100	87	46	52.8%

A.1.3.3 Screening for F0 founder fish

To determine if the CRISPR/Cas9 generated mutations in *capn5a* were heritable, injected embryos were raised to 1 month of age, tail-clipped, and the extracted genomic DNA was screened for mutations in *capn5a* (**Figure A1.2**). The PCR products were cloned into plasmids and sent for sequencing. Of 250 embryos that were injected with CSR1 and CSR2, 153 embryos were dextran red positive and reared to adulthood. Of the 153, 76 embryos survived to one month post fertilization and 12 have so far been successfully screened for deletions and sent off for sequencing. Sequencing results showed that these 12 fish contained large deletions in *capn5a* (between 300-1100 bp; **Figure A1.2**), but it appears that a significant portion of the

deletions are in introns and the portions that affected the exons did not cause any frameshift mutations or large deletions within the coding region (data not shown). Currently there is ongoing screening needed for the remainder of the potential Founder Fish (F0).

Figure A1. 2 CRISPR injection tail-clip screen

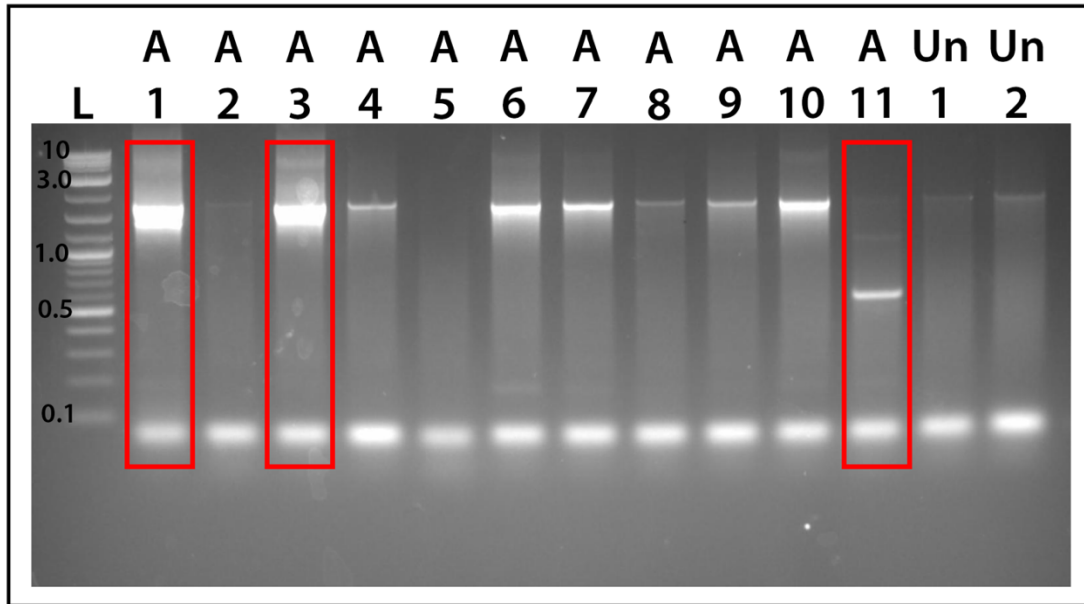


Figure A1.2 CRISPR injection tail clip screen. 2% electrophoresis gel used to screen injected embryos for deletions. A variety of deletions was observed ranging from 300-1100 bp. L, 2kb ladder; A, animal; Un, uninjected.

A.1.4 Conclusion

Capn5 is non-classical member of a family of non-lysosomal cysteine proteases and mutations create a hyperactive form of Capn5 that has been implicated in a devastating retinal degenerative disease called ADNIV. Currently very little is known about the normal

function of Capn5 or its role during development, creating barriers to treating patients suffering from ADNIV. Here I outline the steps I have taken to create and establish a *capn5a* CRISPR mutant line, through which I have produced 64 possible *capn5a* CRISPR F0 mutants ready for continued screening. The *capn5a* CSR1 and CSR2 gRNAs cut at a high rate of 60% on average with most deletions present being 300-1100 bp.

I predict that the loss of *capn5a* alone will not be embryonic lethal due to some redundancy and overlap with *capn5b* expression and function, but there will be significant defects in the CNS and photoreceptor survival. Generation of the *capn5b* CRISPR mutant is a necessary next step. If the mutations aren't lethal alone, and the embryos are viable, I predict crossing the two mutations to create *capn5a/capn5b* double mutant will be embryonic or larval lethal. The production of these lines will be invaluable to understanding the role of Capn5 during vertebrate development and developing effective treatments for ADNIV.

REFERENCES

- Aggad, D., Veriepe, J., Tauffenberger, A. and Parker, J. A.** (2014). TDP-43 Toxicity Proceeds via Calcium Dysregulation and Necrosis in Aging *Caenorhabditis elegans* Motor Neurons. *Journal of Neuroscience* **34**, 12093-12103.
- Akimenko, M. A., Johnson, S. L., Westerfield, M. and Ekker, M.** (1995). DIFFERENTIAL INDUCTION OF 4 MSX HOMEODOMAIN GENES DURING FIN DEVELOPMENT AND REGENERATION IN ZEBRAFISH. *Development* **121**, 347-357.
- Allen, R. S., Hanif, A. M., Gogniat, M. A., Prall, B. C., Haider, R., Aung, M. H., Prunty, M. C., Mees, L. M., Coulter, M. M., Motz, C. T., et al.** (2018). TrkB signalling pathway mediates the protective effects of exercise in the diabetic rat retina. *European Journal of Neuroscience* **47**, 1254-1265.
- Alvarez-Delfin, K., Morris, A. C., Snelson, C. D., Gamse, J. T., Gupta, T., Marlow, F. L., Mullins, M. C., Burgess, H. A., Granato, M. and Fadool, J. M.** (2009). Tbx2b is required for ultraviolet photoreceptor cell specification during zebrafish retinal development. *Proceedings of the National Academy of Sciences of the United States of America* **106**, 2023-2028.
- Amores, A., Force, A., Yan, Y. L., Joly, L., Amemiya, C., Fritz, A., Ho, R. K., Langeland, J., Prince, V., Wang, Y. L., et al.** (1998). Zebrafish hox clusters and vertebrate genome evolution. *Science* **282**, 1711-1714.
- Angrist, M., Bolk, S., Halushka, M., Lapchak, P. A. and Chakravarti, A.** (1996). Germline mutations in glial cell line-derived neurotrophic factor (GDNF) and RET in a hirschsprung disease patient. *Nature Genetics* **14**, 341-344.
- Angueyra, J. M. and Kindt, K. S.** (2018). Leveraging Zebrafish to Study Retinal Degenerations. *Frontiers in Cell and Developmental Biology* **6**.
- Applebury, M. L., Farhangfar, F., Glosmann, M., Hashimoto, K., Kage, K., Robbins, J. T., Shibusawa, N., Wondisford, F. E. and Zhang, H.** (2007). Transient expression of thyroid hormone nuclear receptor TR beta 2 sets S opsin patterning during cone photoreceptor genesis. *Developmental Dynamics* **236**, 1203-1212.
- Arnold, J. S., Werling, U., Braunstein, E. M., Liao, J., Nowotschin, S., Edelman, W., Hebert, J. M. and Morrow, B. E.** (2006). Inactivation of Tbx1 in the pharyngeal endoderm results in 22q11DS malformations. *Development* **133**, 977-987.

- Arthur, J. S. C., Elce, J. S., Hegadorn, C., Williams, K. and Greer, P. A.** (2000). Disruption of the murine calpain small subunit gene, *Capn4*: Calpain is essential for embryonic development but not for cell growth and division. *Molecular and Cellular Biology* **20**, 4474-4481.
- Asad, Z., Pandey, A., Babu, A., Sun, Y., Shevade, K., Kapoor, S., Ullah, I., Ranjan, S., Scaria, V., Bajpai, R., et al.** (2016). Rescue of neural crest-derived phenotypes in a zebrafish CHARGE model by Sox10 downregulation. *Human Molecular Genetics* **25**, 3539-3554.
- Azuma, M. and Shearer, T. R.** (2008). The role of calcium-activated protease calpain in experimental retinal pathology. *Survey of Ophthalmology* **53**, 150-163.
- Bae, Y.-K., Shimizu, T. and Hibi, M.** (2005a). Patterning of proneuronal and inter-proneuronal domains by hairy- and enhancer of split-related genes in zebrafish neuroectoderm. *Development (Cambridge, England)* **132**, 1375-1385.
- Bae, Y. K., Shimizu, T. and Hibi, M.** (2005b). Patterning of proneuronal and inter-proneuronal domains by hairy- and enhancer of split-related genes in zebrafish neuroectoderm. *Development* **132**, 1375-1385.
- Banerjee, S., Gordon, L., Donn, T. M., Berti, C., Moens, C. B., Burden, S. J. and Granato, M.** (2011). A novel role for MuSK and non-canonical Wnt signaling during segmental neural crest cell migration. *Development* **138**, 3287-3296.
- Bassuk, A. G., Yeh, S., Wu, S., Martin, D. F., Tsang, S. H., Gakhar, L. and Mahajan, V. B.** (2015). Structural Modeling of a Novel CAPN5 Mutation that Causes Uveitis and Neovascular Retinal Detachment. *Plos One* **10**, 11.
- Baumann, L., Ros, A., Rehberger, K., Neuhauss, S. C. F. and Segner, H.** (2016). Thyroid disruption in zebrafish (*Danio rerio*) larvae: Different molecular response patterns lead to impaired eye development and visual functions. *Aquatic Toxicology* **172**, 44-55.
- Bernal, J.** (2017). Thyroid hormone regulated genes in cerebral cortex development. *Journal of Endocrinology* **232**, R83-R97.
- Bernardos, R. L., Barthel, L. K., Meyers, J. R. and Raymond, P. A.** (2007). Late-stage neuronal progenitors in the retina are radial Muller glia that function as retinal stem cells. *Journal of Neuroscience* **27**, 7028-7040.
- Bernardos, R. L., Lentz, S. I., Wolfe, M. S. and Raymond, P. A.** (2005a). Notch-Delta signaling is required for spatial patterning and Muller glia differentiation in the zebrafish retina. *Developmental Biology* **278**, 381-395.

- (2005b). Notch-Delta signaling is required for spatial patterning and Müller glia differentiation in the zebrafish retina. *Developmental biology* **278**, 381-395.
- Bernardos, R. L. and Raymond, P. A.** (2006). GFAP transgenic zebrafish. *Gene expression patterns : GEP* **6**, 1007-1013.
- Bibliowicz, J., Tittle, R. K. and Gross, J. M.** (2011). Toward a Better Understanding of Human Eye Disease: Insights From the Zebrafish, *Danio rerio*. *Animal Models of Human Disease* **100**, 287-330.
- Bierich, J. R., Christie, M., Heinrich, J. J. and Martinez, A. S.** (1991). NEW OBSERVATIONS ON MIDLINE DEFECTS - COINCIDENCE OF ANOPHTHALMOS, MICROPHTHALMOS AND CRYPTOPHTHALMOS WITH HYPOTHALAMIC DISORDERS. *European Journal of Pediatrics* **150**, 246-249.
- Boatright, J. H., Stodulkova, E., Nguyen, H. T., Do, V. T. and Nickerson, J. M.** (2002). The effect of retinoids and butyrate on the expression of CRX and IRBP in retinoblastoma cells. *Investigative Ophthalmology & Visual Science* **43**, U1013-U1013.
- Bohnsack, B. L., Kasprick, D. S., Kish, P. E., Goldman, D. and Kahana, A.** (2012). A Zebrafish Model of Axenfeld-Rieger Syndrome Reveals That pitx2 Regulation by Retinoic Acid Is Essential for Ocular and Craniofacial Development. *Investigative Ophthalmology & Visual Science* **53**, 7-22.
- Bolande, R. P.** (1997). Neurocristopathy: Its growth and development in 20 years. *Pediatric Pathology & Laboratory Medicine* **17**, 1-25.
- Brockehoff, S. E.** (2006). Measuring the optokinetic response of zebrafish larvae. *Nature Protocols* **1**, 2448-2451.
- Brockehoff, S. E. and Fadool, J. M.** (2011). Genetics of photoreceptor degeneration and regeneration in zebrafish. *Cellular and Molecular Life Sciences* **68**, 651-659.
- Brockehoff, S. E., Hurley, J. B., Janssenbienhold, U., Neuhauss, S. C. F., Driever, W. and Dowling, J. E.** (1995). A BEHAVIORAL SCREEN FOR ISOLATING ZEBRAFISH MUTANTS WITH VISUAL-SYSTEM DEFECTS. *Proceedings of the National Academy of Sciences of the United States of America* **92**, 10545-10549.
- Bronner, M. E. and Simoes-Costa, M.** (2016). The Neural Crest Migrating into the Twenty-First Century. *Essays on Developmental Biology, Pt A* **116**, 115-+.

- Budi, E. H., Patterson, L. B. and Parichy, D. M.** (2011). Post-Embryonic Nerve-Associated Precursors to Adult Pigment Cells: Genetic Requirements and Dynamics of Morphogenesis and Differentiation. *Plos Genetics* **7**.
- Carney, T. J., Dutton, K. A., Greenhill, E., Delfino-Machin, M., Dufourcq, P., Blader, P. and Kelsh, R. N.** (2006). A direct role for Sox10 in specification of neural crest-derived sensory neurons. *Development* **133**, 4619-4630.
- Carterdawson, L. D. and Lavail, M. M.** (1979). RODS AND CONES IN THE MOUSE RETINA .1. STRUCTURAL-ANALYSIS USING LIGHT AND ELECTRON-MICROSCOPY. *Journal of Comparative Neurology* **188**, 245-262.
- Chen, J. C., Rattner, A. and Nathans, J.** (2005). The rod photoreceptor-specific nuclear receptor Nr2e3 represses transcription of multiple cone-specific genes. *Journal of Neuroscience* **25**, 118-129.
- Chi, X. J., Hiwasa, T., Maki, M., Sugaya, S., Nomura, J., Kita, K. and Suzuki, N.** (1999). Suppression of okadaic acid-induced apoptosis by overexpression of calpastatin in human UVR-1 cells. *Febs Letters* **459**, 391-394.
- Cideciyan, A. V.** (2010). Leber congenital amaurosis due to RPE65 mutations and its treatment with gene therapy. *Progress in Retinal and Eye Research* **29**, 398-427.
- Connaughton, V. P.** (2011). Bipolar cells in the zebrafish retina. *Vis Neurosci.* **28**, 77-93. Epub 2010 Nov 2016.
- Coomer, C. E. and Morris, A. C.** (2018). Capn5 Expression in the Healthy and Regenerating Zebrafish Retina. *Investigative Ophthalmology & Visual Science* **59**, 3643-3654.
- Couto, L. A., Narciso, M. S., Hokoc, J. N. and Martinez, A. M. B.** (2004). Calpain inhibitor 2 prevents axonal degeneration of opossum optic nerve fibers. *Journal of Neuroscience Research* **77**, 410-419.
- Curran, K., Raible, D. W. and Lister, J. A.** (2009). Foxd3 controls melanophore specification in the zebrafish neural crest by regulation of Mitf. *Developmental Biology* **332**, 408-417.
- Das, A. and Crump, J. G.** (2012). Bmps and Id2a Act Upstream of Twist1 To Restrict Ectomesenchyme Potential of the Cranial Neural Crest. *Plos Genetics* **8**.
- Das, A., Garner, D. P., Del Re, A. M., Woodward, J. J., Kumar, D. M., Agarwal, N., Banik, N. L. and Ray, S. K.** (2006). Calpeptin provides functional neuroprotection to rat retinal ganglion cells following Ca²⁺ influx. *Brain Research* **1084**, 146-157.

- Davis, R. L. and Turner, D. L.** (2001). Vertebrate hairy and Enhancer of split related proteins: transcriptional repressors regulating cellular differentiation and embryonic patterning. *Oncogene* **20**, 8342-8357.
- Dawson, S. R., Turner, D. L., Weintraub, H. and Parkhurst, S. M.** (1995). SPECIFICITY FOR THE HAIRY/ENHANCER OF SPLIT BASIC HELIX-LOOP-HELIX (BHLH) PROTEINS MAPS OUTSIDE THE BHLH DOMAIN AND SUGGESTS 2 SEPARABLE MODES OF TRANSCRIPTIONAL REPRESSION. *Molecular and Cellular Biology* **15**, 6923-6931.
- Dear, N., Matena, K., Vingron, M. and Boehm, T.** (1997). A new subfamily of vertebrate calpains lacking a calmodulin-like domain: Implications for calpain regulation and evolution. *Genomics* **45**, 175-184.
- Dear, T. N. and Boehm, T.** (1999). Diverse mRNA expression patterns of the mouse calpain genes Capn5, Capn6 and Capn11 during development. *Mechanisms of Development* **89**, 201-209.
- Dear, T. N. and Boehm, T.** (2001). Identification and characterization of two novel calpain large subunit genes. *Gene* **274**, 245-252.
- Delidakis, C., Monastirioti, M. and Magadi, S. S.** (2014). E(spl): Genetic, Developmental, and Evolutionary Aspects of a Group of Invertebrate Hes Proteins with Close Ties to Notch Signaling. In *Bhlh Transcription Factors in Development and Disease* (ed. R. Taneja), pp. 217-262. San Diego: Elsevier Academic Press Inc.
- Doerre, G. and Malicki, J.** (2002). Genetic analysis of photoreceptor cell development in the zebrafish retina. *Mechanisms of Development* **110**, 125-138.
- Doonan, F., Donovan, M. and Cotter, T. G.** (2005). Activation of multiple pathways during photoreceptor apoptosis in the rd mouse. *Investigative Ophthalmology & Visual Science* **46**, 3530-3538.
- Doudna, J. A. and Charpentier, E.** (2014). The new frontier of genome engineering with CRISPR-Cas9. *Science* **346**, 1077-+.
- Dowling, J. E. and Wald, G.** (1960). THE BIOLOGICAL FUNCTION OF VITAMIN-A ACID. *Proceedings of the National Academy of Sciences of the United States of America* **46**, 587-608.
- Dutt, P., Croall, D. E., Arthur, J. S. C., De Veyra, T., Williams, K., Elce, J. S. and Greer, P. A.** (2006). m-Calpain is required for preimplantation embryonic development in mice. *Bmc Developmental Biology* **6**, 11.

- Dutton, K. A., Pauliny, A., Lopes, S. S., Elworthy, S., Carney, T. J., Rauch, J., Geisler, R., Haffter, P. and Kelsh, R. N.** (2001). Zebrafish colourless encodes sox10 and specifies non-ectomesenchymal neural crest fates. *Development* **128**, 4113-4125.
- DuVal, M. G. and Allison, W. T.** (2018). Photoreceptor Progenitors Depend Upon Coordination of gdf6a, thr beta, and tbx2b to Generate Precise Populations of Cone Photoreceptor Subtypes. *Investigative Ophthalmology & Visual Science* **59**, 6089-6101.
- DuVal, M. G., Oel, A. P. and Allison, W. T.** (2014). gdf6a Is Required for Cone Photoreceptor Subtype Differentiation and for the Actions of tbx2b in Determining Rod Versus Cone Photoreceptor Fate. *Plos One* **9**, 15.
- Ederly, P., Attie, T., Amiel, J., Pelet, A., Eng, C., Hofstra, R. M. W., Martelli, H., Bidaud, C., Munnich, A. and Lyonnet, S.** (1996). Mutation of the endothelin-3 gene in the Waardenburg-Hirschsprung disease (Shah-Waardenburg syndrome). *Nature Genetics* **12**, 442-444.
- El Yakoubi, W., Borday, C., Hamdache, J., Parain, K., Tran, H. T., Vleminckx, K., Perron, M. and Locker, M.** (2012). Hes4 Controls Proliferative Properties of Neural Stem Cells During Retinal Ontogenesis. *Stem Cells* **30**, 2784-2795.
- Emori, Y., Kawasaki, H., Imajoh, S., Imahori, K. and Suzuki, K.** (1987). ENDOGENOUS INHIBITOR FOR CALCIUM-DEPENDENT CYSTEINE PROTEASE CONTAINS 4 INTERNAL REPEATS THAT COULD BE RESPONSIBLE FOR ITS MULTIPLE REACTIVE SITES. *Proceedings of the National Academy of Sciences of the United States of America* **84**, 3590-3594.
- Etchevers, H. C., Dupin, E. and Le Douarin, N. M.** (2019). The diverse neural crest: from embryology to human pathology. *Development* **146**.
- Fadool, J. M.** (2003). Development of a rod photoreceptor mosaic revealed in transgenic zebrafish. *Developmental Biology* **258**, 277-290.
- Farre, A., Mackin, R. and Stenkamp, D. L.** (2019). Thyroid hormone regulates the tandemly-quadruplicated rh2 cone opsin gene array in zebrafish. *Investigative Ophthalmology & Visual Science* **60**, 2.
- Fausett, B. V. and Goldman, D.** (2006). A role for alpha 1 tubulin-expressing Muller glia in regeneration of the injured zebrafish retina. *Journal of Neuroscience* **26**, 6303-6313.
- Fimbel, S. M., Montgomery, J. E., Burket, C. T. and Hyde, D. R.** (2007). Regeneration of inner retinal neurons after intravitreal injection of ouabain in zebrafish. *Journal of Neuroscience* **27**, 1712-1724.

- Fischer, A. and Gessler, M.** (2007). Delta–Notch—and then? Protein interactions and proposed modes of repression by Hes and Hey bHLH factors. *Nucleic Acids Research* **35**, 4583-4596.
- Fonseka, T. M., Wen, X. Y., Foster, J. A. and Kennedy, S. H.** (2016). Zebrafish Models of Major Depressive Disorders. *Journal of Neuroscience Research* **94**, 3-14.
- Forbes-Osborne, M. A., Wilson, S. G. and Morris, A. C.** (2013). Insulinoma-associated 1a (Insm1a) is required for photoreceptor differentiation in the zebrafish retina. *Developmental Biology* **380**, 157-171.
- Franz, T., Winckler, L., Boehm, T. and Dear, T. N.** (2004). Capn5 is expressed in a subset of T cells and is dispensable for development. *Molecular and Cellular Biology* **24**, 1649-1654.
- French, C. R., Erickson, T., French, D. V., Pilgrim, D. B. and Waskiewicz, A. J.** (2009). Gdf6a is required for the initiation of dorsal-ventral retinal patterning and lens development. *Developmental Biology* **333**, 37-47.
- Frisdal, A. and Trainor, P. A.** (2014). Development and evolution of the pharyngeal apparatus. *Wiley Interdisciplinary Reviews-Developmental Biology* **3**, 403-418.
- Fu, M., Sato, Y., Lyons-Warren, A., Zhang, B., Kane, M. A., Napoli, J. L. and Heuckeroth, R. O.** (2010). Vitamin A facilitates enteric nervous system precursor migration by reducing Pten accumulation. *Development* **137**, 631-640.
- FurutaniSeiki, M., Jiang, Y. J., Brand, M., Heisenberg, C. P., Houart, C., Beuchle, D., vanEeden, F. J. M., Granato, M., Haffter, P., Hammerschmidt, M., et al.** (1996). Neural degeneration mutants in the zebrafish, *Danio rerio*. *Development* **123**, 229-239.
- Gamborino, M. J., Sevilla-Romero, E., Munoz, A., Hernandez-Yago, J., Renau-Piqueras, J. and Pinazo-Duran, M. D.** (2001). Role of thyroid hormone in craniofacial and eye development using a rat model. *Ophthalmic Research* **33**, 283-291.
- Ganz, J., Melancon, E. and Eisen, J. S.** (2016). Zebrafish as a model for understanding enteric nervous system interactions in the developing intestinal tract. *Zebrafish: Cellular and Developmental Biology, Pt B: Developmental Biology* **134**, 139-164.
- Germanguz, I., Lev, D., Waisman, T., Kim, C. H. and Gitelman, I.** (2007). Four twist genes in zebrafish, four expression patterns. *Developmental Dynamics* **236**, 2615-2626.
- Gilmour, D. T., Maischein, H. M. and Nusslein-Volhard, C.** (2002). Migration and function of a glial subtype in the vertebrate peripheral nervous system. *Neuron* **34**, 577-588.
- Glass, A. S. and Dahm, R.** (2004). The zebrafish as a model organism for eye development. *Ophthalmic Research* **36**, 4-24.

- Glavic, A., Honore, S. M., Feijoo, C. G., Bastidas, F., Allende, M. L. and Mayor, R.** (2004a). Role of BMP signaling and the homeoprotein *iroquois* in the specification of the cranial placodal field. *Developmental Biology* **272**, 89-103.
- Glavic, A., Silva, F., Aybar, M. J., Bastidas, F. and Mayor, R.** (2004b). Interplay between Notch signaling and the homeoprotein *Xiro1* is required for neural crest induction in *Xenopus* embryos. *Development* **131**, 347-359.
- Goldman, D.** (2014). Muller glial cell reprogramming and retina regeneration. *Nature Reviews Neuroscience* **15**, 431-442.
- Gorsuch, R. A. and Hyde, D. R.** (2014). Regulation of Muller glial dependent neuronal regeneration in the damaged adult zebrafish retina. *Experimental Eye Research* **123**, 131-140.
- Gross, J. V. and Perkins, B. D.** (2008). Zebrafish mutants as models for congenital ocular disorders in humans. *Molecular Reproduction and Development* **75**, 547-555.
- Haider, N. B., Jacobson, S. G., Cideciyan, A. V., Swiderski, R., Streb, L. M., Searby, C., Beck, G., Hockey, R., Hanna, D. B., Gorman, S., et al.** (2000). Mutation of a nuclear receptor gene, *NR2E3*, causes enhanced S cone syndrome, a disorder of retinal cell fate. *Nature Genetics* **24**, 127-131.
- Halloran, M. C. and Berndt, J. D.** (2003). Current progress in neural crest cell motility and migration and future prospects for the zebrafish model system. *Developmental Dynamics* **228**, 497-513.
- Herberger, A. L. and Loretz, C. A.** (2013). Morpholino oligonucleotide knockdown of the extracellular calcium-sensing receptor impairs early skeletal development in zebrafish. *Comparative Biochemistry and Physiology a-Molecular & Integrative Physiology* **166**, 470-481.
- Hitchcock, P. F. and Cirenza, P.** (1994). SYNAPTIC ORGANIZATION OF REGENERATED RETINA IN THE GOLDFISH. *Journal of Comparative Neurology* **343**, 609-616.
- Hitchcock, P. F. and Raymond, P. A.** (2004). The Teleost Retina as a Model for Developmental and Regeneration Biology. *Zebrafish* **1**, 257-271.
- Hojo, M., Ohtsuka, T., Hashimoto, N., Gradwohl, G., Guillemot, F. and Kageyama, R.** (2000). Glial cell fate specification modulated by the bHLH gene *Hes5* in mouse retina. *Development* **127**, 2515-2522.

- Holzschuh, J., Wada, N., Wada, C., Schaffer, A., Javidan, Y., Tallafuss, A., Bally-Cuif, L. and Schillili, T. F.** (2005a). Requirements for endoderm and BMP signaling in sensory neurogenesis in zebrafish. *Development* **132**, 3731-3742.
- Holzschuh, J., Wada, N., Wada, C., Schaffer, A., Javidan, Y., Tallafuss, A., Bally-Cuif, L. and Schilling, T. F.** (2005b). Requirements for endoderm and BMP signaling in sensory neurogenesis in zebrafish. *Development (Cambridge, England)* **132**, 3731-3742.
- Howe, K., Clark, M. D., Torroja, C. F., Tarrance, J., Berthelot, C., Muffato, M., Collins, J. E., Humphray, S., McLaren, K., Matthews, L., et al.** (2013). The zebrafish reference genome sequence and its relationship to the human genome. *Nature* **496**, 498-503.
- Hsiao, C. D. and Tsai, H. J.** (2003). Transgenic zebrafish with fluorescent germ cell: a useful tool to visualize germ cell proliferation and juvenile hermaphroditism in vivo. *Developmental Biology* **262**, 313-323.
- Huang, M., Miller, M. L., McHenry, L. K., Zheng, T. N., Zhen, Q. Q., Ilkhanizadeh, S., Conklin, B. R., Bronner, M. E. and Weiss, W. A.** (2016). Generating trunk neural crest from human pluripotent stem cells. *Scientific Reports* **6**.
- Huang, Y. H. and Wang, K. K. W.** (2001). The calpain family and human disease. *Trends in Molecular Medicine* **7**, 355-362.
- Hutchins, E. J., Kunttas, E., Piacentino, M. L., Howard, A. G. A., Bronner, M. E. and Uribe, R. A.** (2018). Migration and diversification of the vagal neural crest. *Developmental Biology* **444**, S98-S109.
- Hyatt, G. A., Schmitt, E. A., Fadool, J. M. and Dowling, J. E.** (1996a). Retinoic acid alters photoreceptor development in vivo. *Proceedings of the National Academy of Sciences of the United States of America* **93**, 13298-13303.
- Hyatt, G. A., Schmitt, E. A., MarshArmstrong, N., McCaffery, P., Drager, U. C. and Dowling, J. E.** (1996b). Retinoic acid establishes ventral retinal characteristics. *Development* **122**, 195-204.
- Il, L. L. N., Alur, R. P., Boobalan, E., Sergeev, Y. V., Caruso, R. C., Stone, E. M., Swaroop, A., Johnson, M. A. and Brooks, B. P.** (2010). Two Novel CRX Mutant Proteins Causing Autosomal Dominant Leber Congenital Amaurosis Interact Differently With NRL. *Human Mutation* **31**, E1472-E1483.
- Jacobson, M. D., Weil, M. and Raff, M. C.** (1997). Programmed cell death in animal development. *Cell* **88**, 347-354.

- Jadhav, A. P., Roesch, K. and Cepko, C. L.** (2009). Development and neurogenic potential of Müller glial cells in the vertebrate retina. *Progress in retinal and eye research* **28**, 249-262.
- Jinek, M., Chylinski, K., Fonfara, I., Hauer, M., Doudna, J. A. and Charpentier, E.** (2012). A Programmable Dual-RNA-Guided DNA Endonuclease in Adaptive Bacterial Immunity. *Science* **337**, 816-821.
- Johnson, C. W., Hernandez-Lagunas, L., Feng, W. G., Melvin, V. S., Williams, T. and Artinger, K. B.** (2011). Vgll2a is required for neural crest cell survival during zebrafish craniofacial development. *Developmental Biology* **357**, 269-281.
- Kageyama, R., Ohtsuka, T. and Kobayashi, T.** (2007). The Hes gene family: repressors and oscillators that orchestrate embryogenesis. *Development* **134**, 1243-1251.
- Kageyama, R., Ohtsuka, T., and Kobayashi, T.** (2008). Roles of Hes genes in neural development. *Development Growth & Differentiation* **50**, S97-S103.
- Kague, E., Gallagher, M., Burke, S., Parsons, M., Franz-Odenaal, T. and Fisher, S.** (2012). Skeletogenic Fate of Zebrafish Cranial and Trunk Neural Crest. *Plos One* **7**.
- Kelley, M. W., Turner, J. K. and Reh, T. A.** (1994). RETINOIC ACID PROMOTES DIFFERENTIATION OF PHOTORECEPTORS IN-VITRO. *Development* **120**, 2091-2102.
- Kelsh, R. N., Brand, M., Jiang, Y. J., Heisenberg, C. P., Lin, S., Haffter, P., Odenthal, J., Mullins, M. C., vanEeden, F. J. M., FurutaniSeiki, M., et al.** (1996). Zebrafish pigmentation mutations and the processes of neural crest development. *Development* **123**, 369-389.
- Kelsh, R. N. and Eisen, J. S.** (2000). The zebrafish colourless gene regulates development of non-ectomesenchymal neural crest derivatives. *Development* **127**, 515-525.
- Kennedy, B. N., Vihtelic, T. S., Checkley, L., Vaughan, K. T. and Hyde, D. R.** (2001). Isolation of a zebrafish rod opsin promoter to generate a transgenic zebrafish line expressing enhanced green fluorescent protein in rod photoreceptors. *Journal of Biological Chemistry* **276**, 14037-14043.
- Kimmel, B. E., Heberlein, U. and Rubin, G. M.** (1990). THE HOMEODOMAIN PROTEIN ROUGH IS EXPRESSED IN A SUBSET OF CELLS IN THE DEVELOPING DROSOPHILA EYE WHERE IT CAN SPECIFY PHOTORECEPTOR CELL SUBTYPE. *Genes & Development* **4**, 712-727.
- Kimmel, C. B., Ballard, W. W., Kimmel, S. R., Ullmann, B. and Schilling, T. F.** (1995). STAGES OF EMBRYONIC-DEVELOPMENT OF THE ZEBRAFISH. *Developmental Dynamics* **203**, 253-310.
- Kitamura, K., Miura, H., Miyagawa-Tomita, S., Yanazawa, M., Katoh-Fukui, Y., Suzuki, R., Ohuchi, H., Suehiro, A., Motegi, Y., Nakahara, Y., et al.** (1999). Mouse Pitx2 deficiency

- leads to anomalies of the ventral body wall, heart, extra- and periocular mesoderm and right pulmonary isomerism. *Development* **126**, 5749-5758.
- Knight, R. D. and Schilling, T. F.** (2006). Cranial neural crest and development of the head skeleton. *Neural Crest Induction and Differentiation* **589**, 120-133.
- Kobayashi, M., Takezawa, S., Hara, K., Yu, R. T., Umesono, Y., Agata, K., Taniwaki, M., Yasuda, K. and Umesono, K.** (1999). Identification of a photoreceptor cell-specific nuclear receptor. *Proceedings of the National Academy of Sciences of the United States of America* **96**, 4814-4819.
- Kucenas, S., Takada, N., Park, H. C., Woodruff, E., Broadie, K. and Appel, B.** (2008). CNS-derived glia ensheath peripheral nerves and mediate motor root development. *Nature Neuroscience* **11**, 143-151.
- Kwon, H. J., Bhat, N., Sweet, E. M., Cornell, R. A. and Riley, B. B.** (2010). Identification of Early Requirements for Preplacodal Ectoderm and Sensory Organ Development. *Plos Genetics* **6**.
- Lamb, T. D., Collin, S. P. and Pugh, E. N.** (2007). Evolution of the vertebrate eye: opsins, photoreceptors, retina and eye cup. *Nature Reviews Neuroscience* **8**, 960-975.
- Lamb, T. D. and Pugh, E. N.** (2006). Phototransduction, dark adaptation, and rhodopsin regeneration - The Proctor Lecture. *Investigative Ophthalmology & Visual Science* **47**, 5138-5152.
- Latimer, A. J., Shin, J. and Appel, B.** (2005). her9 promotes floor plate development in zebrafish. *Developmental Dynamics* **232**, 1098-1104.
- Lawson, N. D. and Weinstein, B. M.** (2002a). In vivo imaging of embryonic vascular development using transgenic zebrafish. *Developmental biology* **248**, 307-318.
- Le Douarin, N. M., Creuzet, S., Couly, G. and Dupin, E.** (2004). Neural crest cell plasticity and its limits. *Development* **131**, 4637-4650.
- Lepage, S. E. and Bruce, A. E. E.** (2008). Characterization and comparative expression of zebrafish calpain system genes during early development. *Developmental Dynamics* **237**, 819-829.
- Leve, C., Gajewski, M., Rohr, K. B. and Tautz, D.** (2001). Homologues of c-hairy1 (her9) and lunatic fringe in zebrafish are expressed in the developing central nervous system, but not in the presomitic mesoderm. *Development Genes and Evolution* **211**, 493-500.

- Li, A. M., Zhu, X. M., Brown, B. and Craft, C. M.** (2003). Melatonin enhances retinoic acid induction of cone arrestin gene expression in retinoblastoma cells. *Retinal Degenerations: Mechanisms and Experimental Therapy* **533**, 361-368.
- Li, J., Zhang, B. B., Ren, Y. G., Gu, S. Y., Xiang, Y. H., Huang, C. and Du, J. L.** (2015). Intron targeting-mediated and endogenous gene integrity-maintaining knockin in zebrafish using the CRISPR/Cas9 system. *Cell Research* **25**, 634-637.
- Li, L. and Dowling, J. E.** (1997). A dominant form of inherited retinal degeneration caused by a non-photoreceptor cell-specific mutation. *Proceedings of the National Academy of Sciences of the United States of America* **94**, 11645-11650.
- Lin, H. Y., Liu, F., Zhang, C. S., Zhang, Z. Y., Guo, J. P., Ren, C. L. and Kong, Z. D.** (2009). Pluripotent Hair Follicle Neural Crest Stem-Cell-Derived Neurons and Schwann Cells Functionally Repair Sciatic Nerves in Rats. *Molecular Neurobiology* **40**, 216-223.
- Lister, J. A., Robertson, C. P., Lepage, T., Johnson, S. L. and Raible, D. W.** (1999). nacre encodes a zebrafish microphthalmia-related protein that regulates neural-crest-derived pigment cell fate. *Development* **126**, 3757-3767.
- Liu, Y. W. and Chan, W. K.** (2002). Thyroid hormones are important for embryonic to larval transitory phase in zebrafish. *Differentiation* **70**, 36-45.
- Liu, Z. H., Dai, X. M. and Du, B.** (2015). Hes1: a key role in stemness, metastasis and multidrug resistance. *Cancer Biology & Therapy* **16**, 353-359.
- Livesey, F. J. and Cepko, C. L.** (2001). Vertebrate neural cell-fate determination: Lessons from the retina. *Nature Reviews Neuroscience* **2**, 109-118.
- Lu, T., Xu, Y., Mericle, M. T. and Mellgren, R. L.** (2002). Participation of the conventional calpains in apoptosis. *Biochimica Et Biophysica Acta-Molecular Cell Research* **1590**, 16-26.
- Ma, W. X. and Wong, W. T.** (2016). Aging Changes in Retinal Microglia and their Relevance to Age-related Retinal Disease. *Retinal Degenerative Diseases: Mechanisms and Experimental Therapy* **854**, 73-78.
- Mahajan, V. B., Skeie, J. M., Bassuk, A. G., Fingert, J. H., Braun, T. A., Daggett, H. T., Folk, J. C., Sheffield, V. C. and Stone, E. M.** (2012). Calpain-5 Mutations Cause Autoimmune Uveitis, Retinal Neovascularization, and Photoreceptor Degeneration. *Plos Genetics* **8**.
- Mahajan, V. B., Vallone, J. G., Lin, J. H., Mullins, R. F., Ko, A. C., Folk, J. C. and Stone, E. M.** (2010). T-cell infiltration in autosomal dominant neovascular inflammatory vitreoretinopathy. *Molecular Vision* **16**, 1034-1040.

- Marchant, L., Linker, C., Ruiz, P., Guerrero, N. and Mayor, R.** (1998). The inductive properties of mesoderm suggest that the neural crest cells are specified by a BMP gradient. *Developmental Biology* **198**, 319-329.
- Marelli, F., Carra, S., Agostini, M., Cotelli, F., Peeters, R., Chatterjee, K. and Persani, L.** (2016). Patterns of thyroid hormone receptor expression in zebrafish and generation of a novel model of resistance to thyroid hormone action. *Molecular and Cellular Endocrinology* **424**, 102-117.
- Marsharmstrong, N., McCaffery, P., Gilbert, W., Dowling, J. E. and Drager, U. C.** (1994). RETINOIC ACID IS NECESSARY FOR DEVELOPMENT OF THE VENTRAL RETINA IN ZEBRAFISH. *Proceedings of the National Academy of Sciences of the United States of America* **91**, 7286-7290.
- Masai, I., Lele, Z., Yamaguchi, M., Komori, A., Nakata, A., Nishiwaki, Y., Wada, H., Tanaka, H., Nojima, Y., Hammerschmidt, M., et al.** (2003). N-cadherin mediates retinal lamination, maintenance of forebrain compartments and patterning of retinal neurites. *Development* **130**, 2479-2494.
- McGraw, H. F., Nechiporuk, A. and Raible, D. W.** (2008). Zebrafish Dorsal Root Ganglia Neural Precursor Cells Adopt a Glial Fate in the Absence of Neurogenin1. *Journal of Neuroscience* **28**, 12558-12569.
- Mears, A. J., Kondo, M., Swain, P. K., Takada, Y., Bush, R. A., Saunders, T. L., Sieving, P. A. and Swaroop, A.** (2001). Nrl is required for rod photoreceptor development. *Nature Genetics* **29**, 447-452.
- Meulemans, D. and Bronner-Fraser, M.** (2004). Gene-regulatory interactions in neural crest evolution and development. *Developmental Cell* **7**, 291-299.
- Michaelides, M., Aligianis, I. A., Ainsworth, J. R., Good, P., Mollon, J. D., Maher, E. R., Moore, A. T. and Hunt, D. M.** (2004). Progressive cone dystrophy associated with mutation in CNGB3. *Investigative Ophthalmology & Visual Science* **45**, 1975-1982.
- Milos, N. and Dingle, A. D.** (1978). DYNAMICS OF PIGMENT PATTERN FORMATION IN ZEBRAFISH, BRACHYDANIO-RERIO .1. ESTABLISHMENT AND REGULATION OF LATERAL LINE MELANOPHORE STRIPE DURING 1ST 8 DAYS OF DEVELOPMENT. *Journal of Experimental Zoology* **205**, 205-216.

- Miscevic, F., Rotstein, O. and Wen, X. Y.** (2012). Advances in Zebrafish High Content and High Throughput Technologies. *Combinatorial Chemistry & High Throughput Screening* **15**, 515-521.
- Mitchell, D. M., Stevens, C. B., Frey, R. A., Hunter, S. S., Ashino, R., Kawamura, S. and Stenkamp, D. L.** (2015). Retinoic Acid Signaling Regulates Differential Expression of the Tandemly-Duplicated Long Wavelength-Sensitive Cone Opsin Genes in Zebrafish. *Plos Genetics* **11**, 33.
- Mizukoshi, S., Nakazawa, M., Sato, K., Ozaki, T., Metoki, T. and Ishiguro, S.** (2010). Activation of mitochondrial calpain and release of apoptosis-inducing factor from mitochondria in RCS rat retinal degeneration. *Experimental Eye Research* **91**, 353-361.
- Morris, A. C. and Fadool, J. M.** (2005). Studying rod photoreceptor development in zebrafish. *Physiology & Behavior* **86**, 306-313.
- Morris, A. C., Forbes-Osborne, M. A., Pillai, L. S. and Fadool, J. M.** (2011). Microarray Analysis of XOPS-mCFP Zebrafish Retina Identifies Genes Associated with Rod Photoreceptor Degeneration and Regeneration. *Investigative Ophthalmology & Visual Science* **52**, 2255-2266.
- Morris, A. C., Scholz, T. and Fadool, J. M.** (2008). Rod progenitor cells in the mature zebrafish retina. *Adv Exp Med Biol* **613**, 361-368.
- Morris, A. C., Schroeter, E. H., Bilotta, J., Wong, R. O. L. and Fadool, J. M.** (2005). Cone survival despite rod degeneration in XOPS-mCFP transgenic zebrafish. *Investigative Ophthalmology & Visual Science* **46**, 4762-4771.
- Morrow, D., Cullen, J. P., Liu, W., Guha, S., Sweeney, C., Birney, Y. A., Collins, N., Walls, D., Redmond, E. M. and Cahill, P. A.** (2009). Sonic Hedgehog induces Notch target gene expression in vascular smooth muscle cells via VEGF-A. *Arteriosclerosis, thrombosis, and vascular biology* **29**, 1112-1118.
- Morrow, J. M., Lasic, S., Fox, M. D., Kuo, C., Schott, R. K., Gutierrez, E. D., Santini, F., Tropepe, V. and Chang, B. S. W.** (2017). A second visual rhodopsin gene, rh1-2, is expressed in zebrafish photoreceptors and found in other ray-finned fishes. *Journal of Experimental Biology* **220**, 294-303.
- Mueller, K. P. and Neuhauss, S. C. F.** (2014). Sunscreen for Fish: Co-Option of UV Light Protection for Camouflage. *Plos One* **9**, 5.

- Muller, M., vonWeizsacker, E. and CamposOrtega, J. A.** (1996). Expression domains of a zebrafish homologue of the *Drosophila* pair-rule gene hairy correspond to primordia of alternating somites. *Development* **122**, 2071-2078.
- Nagatomo, K. I. and Hashimoto, C.** (2007). *Xenopus* hairy2 functions in neural crest formation by maintaining cells in a mitotic and undifferentiated state. *Developmental Dynamics* **236**, 1475-1483.
- Nakagawa, T. and Yuan, J. Y.** (2000). Cross-talk between two cysteine protease families: Activation of caspase-12 by calpain in apoptosis. *Journal of Cell Biology* **150**, 887-894.
- Nakajima, T., Fukiage, C., Azuma, M., Ma, H. and Shearer, T. R.** (2001). Different expression patterns for ubiquitous calpains and Capn3 splice variants in monkey ocular tissues. *Biochimica Et Biophysica Acta-Gene Structure and Expression* **1519**, 55-64.
- Nasevicius, A. and Ekker, S. C.** (2000). Effective targeted gene 'knockdown' in zebrafish. *Nature Genetics* **26**, 216-220.
- Nathans, J.** (1992). RHODOPSIN - STRUCTURE, FUNCTION, AND GENETICS. *Biochemistry* **31**, 4923-4931.
- Nehls, M., Kyewski, B., Messerle, M., Waldschutz, R., Schuddekopf, K., Smith, A. J. H. and Boehm, T.** (1996). Two genetically separable steps in the differentiation of thymic epithelium. *Science* **272**, 886-889.
- Neuhauss, S. C. F., Biehlmaier, O., Seeliger, M. W., Das, T., Kohler, K., Harris, W. A. and Baier, H.** (1999). Genetic disorders of vision revealed by a behavioral screen of 400 essential loci in zebrafish. *Journal of Neuroscience* **19**, 8603-8615.
- Ng, L., Hurley, L. B., Dierks, B., Srinivas, M., Salto, C., Vennstrom, B., Reh, T. A. and Forrest, D.** (2001). A thyroid hormone receptor that is required for the development of green cone photoreceptors. *Nature Genetics* **27**, 94-98.
- Nichane, M., de Croze, N., Ren, X., Souopgui, J., Monsoro-Burq, A. H. and Bellefroid, E. J.** (2008a). Hairy2-I δ 3 interactions play an essential role in *Xenopus* neural crest progenitor specification. *Developmental Biology* **322**, 355-367.
- Nichane, M., Ren, X., Souopgui, J. and Bellefroid, E. J.** (2008b). Hairy2 functions through both DNA-binding and non DNA-binding mechanisms at the neural plate border in *Xenopus*. *Developmental Biology* **322**, 368-380.

- Nishida, A., Furukawa, A., Koike, C., Tano, Y., Aizawa, S., Matsuo, I. and Furukawa, T.** (2003). Otx2 homeobox gene controls retinal photoreceptor cell fate and pineal gland development. *Nature Neuroscience* **6**, 1255-1263.
- Nord, H., Dønnhag, N., Muck, J. and von Hofsten, J.** (2016). Pax7 is required for establishment of the xanthophore lineage in zebrafish embryos. *Molecular Biology of the Cell* **27**, 1853-1862.
- Ogawa, Y., Shiraki, T., Kojima, D. and Fukada, Y.** (2015). Homeobox transcription factor Six7 governs expression of green opsin genes in zebrafish. *Proceedings of the Royal Society B-Biological Sciences* **282**, 233-240.
- Ohsako, S., Hyer, J., Panganiban, G., Oliver, I. and Caudy, M.** (1994). HAIRY FUNCTION AS A DNA-BINDING HELIX-LOOP-HELIX REPRESSOR OF DROSOPHILA SENSORY ORGAN FORMATION. *Genes & Development* **8**, 2743-2755.
- Okuno, H., Mihara, F. R., Ohta, S., Fukuda, K., Kurosawa, K., Akamatsu, W., Sanosaka, T., Kohyama, J., Hayashi, K., Nakajima, K., et al.** (2017). CHARGE syndrome modeling using patient-iPSCs reveals defective migration of neural crest cells harboring CHD7 mutations. *Elife* **6**.
- Olden, T., Akhtar, T., Beckman, S. A. and Wallace, K. N.** (2008). Differentiation of the zebrafish enteric nervous system and intestinal smooth muscle. *Genesis* **46**, 484-498.
- Ono, Y., Kakinuma, K., Torii, F., Irie, A., Nakagawa, K., Labeit, S., Abe, K., Suzuki, K. and Sorimachi, H.** (2004). Possible regulation of the conventional calpain system by skeletal muscle-specific calpain, p94/calpain 3. *Journal of Biological Chemistry* **279**, 2761-2771.
- Paquet-Durand, F., Azadi, S., Hauck, S. M., Ueffing, M., van Veen, T. and Ekstrom, P.** (2006). Calpain is activated in degenerating photoreceptors in the rd1 mouse. *Journal of Neurochemistry* **96**, 802-814.
- Pearson, R. A., Gonzalez-Cordero, A., West, E. L., Ribeiro, J. R., Aghaizu, N., Goh, D., Sampson, R. D., Georgiadis, A., Waldron, P. V., Duran, Y., et al.** (2016). Donor and host photoreceptors engage in material transfer following transplantation of post-mitotic photoreceptor precursors. *Nature Communications* **7**.
- Peng, G. H., Ahmad, O., Ahmad, F., Liu, J. and Chen, S.** (2005). The photoreceptor-specific nuclear receptor Nr2e3 interacts with Crx and exerts opposing effects on the transcription of rod versus cone genes. *Human Molecular Genetics* **14**, 747-764.

- Perche, O., Doly, M. and Ranchon-Cole, I.** (2009). Calpains are activated by light but their inhibition has no neuroprotective effect against light-damage. *Experimental Eye Research* **89**, 989-994.
- Petratou, K., Subkhankulova, T., Lister, J. A., Rocco, A., Schwetlick, H. and Kelsh, R. N.** (2018). A systems biology approach uncovers the core gene regulatory network governing iridophore fate choice from the neural crest. *Plos Genetics* **14**.
- Pietrobon, D., Divirgilio, F. and Pozzan, T.** (1990). STRUCTURAL AND FUNCTIONAL-ASPECTS OF CALCIUM HOMEOSTASIS IN EUKARYOTIC CELLS. *European Journal of Biochemistry* **193**, 599-622.
- Pillai-Kastoori, L., Wen, W., Wilson, S. G., Strachan, E., Lo-Castro, A., Fichera, M., Musumeci, S. A., Lehmann, O. J. and Morris, A. C.** (2014). Sox11 Is Required to Maintain Proper Levels of Hedgehog Signaling during Vertebrate Ocular Morphogenesis. *Plos Genetics* **10**, 19.
- Piotrowski, T. and Nusslein-Volhard, C.** (2000). The endoderm plays an important role in patterning the segmented pharyngeal region in zebrafish (*Danio rerio*). *Developmental Biology* **225**, 339-356.
- Polok, B., Escber, P., Ambresin, A., Chouery, E., Bolay, S., Meunier, I., Nan, F., Hamel, C., Munier, F. L., Thilo, B., et al.** (2009). Mutations in CNNM4 Cause Recessive Cone-Rod Dystrophy with Amelogenesis Imperfecta. *American Journal of Human Genetics* **84**, 259-265.
- Postlethwait, J. H., Yan, Y. L., Gates, M. A., Horne, S., Amores, A., Brownlie, A., Donovan, A., Egan, E. S., Force, A., Gong, Z. Y., et al.** (1998). Vertebrate genome evolution and the zebrafish gene map (vol 18, pg 345, 1998). *Nature Genetics* **19**, 303-303.
- Prabhudesai, S. N., Cameron, D. A. and Stenkamp, D. L.** (2005). Targeted effects of retinoic acid signaling upon photoreceptor development in zebrafish. *Developmental Biology* **287**, 157-167.
- Radosevic, M., Robert-Moreno, A., Coolen, M., Bally-Cuif, L. and Alsina, B.** (2011a). Her9 represses neurogenic fate downstream of Tbx1 and retinoic acid signaling in the inner ear. *Development* **138**, 397-408.
- Radosevic, M., Robert-Moreno, A., Coolen, M., Bally-Cuif, L. and Alsina, B.** (2011b). Her9 represses neurogenic fate downstream of Tbx1 and retinoic acid signaling in the inner ear. *Development (Cambridge, England)* **138**, 397-408.
- Raible, D. W. and Eisen, J. S.** (1994). RESTRICTION OF NEURAL CREST CELL FATE IN THE TRUNK OF THE EMBRYONIC ZEBRAFISH. *Development* **120**, 495-503.

- Raible, D. W., Wood, A., Hodsdon, W., Henion, P. D., Weston, J. A. and Eisen, J. S. (1992).** SEGREGATION AND EARLY DISPERSAL OF NEURAL CREST CELLS IN THE EMBRYONIC ZEBRAFISH. *Developmental Dynamics* **195**, 29-42.
- Ramachandran, R., Fausett, B. V. and Goldman, D. (2015).** Ascl1a regulates Muller glia dedifferentiation and retinal regeneration through a Lin-28-dependent, let-7 microRNA signalling pathway (vol 12, pg 1101, 2010). *Nature Cell Biology* **17**, 532-532.
- Rath, M. F., Morin, F., Shi, Q., Klein, D. C. and Moller, M. (2007).** Ontogenetic expression of the Otx2 and Crx homeobox genes in the retina of the rat. *Experimental Eye Research* **85**, 65-73.
- Ray, S. K., Hogan, E. L. and Banik, N. L. (2003).** Calpain in the pathophysiology of spinal cord injury: neuroprotection with calpain inhibitors. *Brain Research Reviews* **42**, 169-185.
- Raymond, P. A. (1985).** Cytodifferentiation of photoreceptors in larval goldfish: delayed maturation of rods. *The Journal of comparative neurology* **236**, 90-105.
- Raymond, P. A., Barthel, L. K., Bernardos, R. L. and Perkowski, J. J. (2006).** Molecular characterization of retinal stem cells and their niches in adult zebrafish. *Bmc Developmental Biology* **6**.
- Raymond, P. A. and Rivlin, P. K. (1987).** Germinal cells in the goldfish retina that produce rod photoreceptors. *Developmental biology* **122**, 120-138.
- Reider, M. and Connaughton, V. P. (2014).** Effects of Low-Dose Embryonic Thyroid Disruption and Rearing Temperature on the Development of the Eye and Retina in Zebrafish. *Birth Defects Research Part B-Developmental and Reproductive Toxicology* **101**, 347-354.
- Reinhardt, R., Centanin, L., Tavhelidse, T., Inoue, D., Wittbrodt, B., Concordet, J. P., Martinez-Morales, J. R. and Wittbrodt, J. (2015).** Sox2, Tlx, Gli3, and Her9 converge on Rx2 to define retinal stem cells in vivo. *Embo Journal* **34**, 1572-1588.
- Rocha, C. F., Vasques, R. B., Santos, S. R. and Paiva, C. L. A. (2016).** Monosomy 1p36 syndrome: reviewing the correlation between deletion sizes and phenotypes. *Genetics and Molecular Research* **15**.
- Rocha, M., Singh, N., Ahsan, K., Beiriger, A. and Prince, V. E. (2020).** Neural crest development: insights from the zebrafish. *Developmental Dynamics* **249**, 88-111.
- Saatman, K. E., Abai, B., Grosvenor, T., Vorwerk, C. K., Smith, D. H. and Meaney, D. F. (2003).** Traumatic axonal injury results in biphasic calpain activation and retrograde transport impairment in mice. *Journal of Cerebral Blood Flow and Metabolism* **23**, 34-42.

- Sandell, L. L., Tjaden, N. E. B., Barlow, A. J. and Trainor, P. A.** (2014). Cochleovestibular nerve development is integrated with migratory neural crest cells. *Developmental Biology* **385**, 200-210.
- Sanquer, S. and Gilchrest, B. A.** (1994). CHARACTERIZATION OF HUMAN CELLULAR RETINOIC ACID-BINDING PROTEIN-I AND PROTEIN-II - LIGAND-BINDING AFFINITIES AND DISTRIBUTION IN SKIN. *Archives of Biochemistry and Biophysics* **311**, 86-94.
- Santos-Ferreira, T., Llonch, S., Borsch, O., Postel, K., Haas, J. and Ader, M.** (2016). Retinal transplantation of photoreceptors results in donor-host cytoplasmic exchange. *Nature Communications* **7**.
- Sasai, Y., Lu, B., Steinbeisser, H., Geisler, D., Gont, L. K. and Derobertis, E. M.** (1994). XENOPUS CHORDIN - A NOVEL DORSALIZING FACTOR-ACTIVATED BY ORGANIZER-SPECIFIC HOMEBOX GENES. *Cell* **79**, 779-790.
- Satoh, M. and Ide, H.** (1987). MELANOCYTE-STIMULATING HORMONE AFFECTS MELANOGENIC DIFFERENTIATION OF QUAIL NEURAL CREST CELLS-INVITRO. *Developmental Biology* **119**, 579-586.
- Satow, T., Bae, S. K., Inoue, T., Inoue, C., Miyoshi, G., Tomita, K., Bessho, Y., Hashimoto, N. and Kageyama, R.** (2001). The basic helix-loop-helix gene *hesr2* promotes gliogenesis in mouse retina. *Journal of Neuroscience* **21**, 1265-1273.
- Schaefer, K. A., Toral, M. A., Velez, G., Cox, A. J., Baker, S. A., Borcharding, N. C., Colgan, D. F., Bondada, V., Mashburn, C. B., Yu, C. G., et al.** (2016). Calpain-5 Expression in the Retina Localizes to Photoreceptor Synapses. *Investigative Ophthalmology & Visual Science* **57**, 2509-2521.
- Schier, A. F., Neuhauss, S. C. F., Harvey, M., Malicki, J., SolnicaKrezel, L., Stainier, D. Y. R., Zwartkuis, F., Abdelilah, S., Stemple, D. L., Rangini, Z., et al.** (1996). Mutations affecting the development of the embryonic zebrafish brain. *Development* **123**, 165-178.
- Schilling, T. F. and Kimmel, C. B.** (1994). SEGMENT AND CELL-TYPE LINEAGE RESTRICTIONS DURING PHARYNGEAL ARCH DEVELOPMENT IN THE ZEBRAFISH EMBRYO. *Development* **120**, 483-494.
- Schmitt, E. A. and Dowling, J. E.** (1999). Early retinal development in the zebrafish, *Danio rerio*: Light and electron microscopic analyses. *The Journal of comparative neurology* **404**, 515-536.

- Schumacher, J. A., Hashiguchi, M., Nguyen, V. H. and Mullins, M. C.** (2011). An Intermediate Level of BMP Signaling Directly Specifies Cranial Neural Crest Progenitor Cells in Zebrafish. *Plos One* **6**.
- Serrano, F., Bernard, W. G., Granata, A., Iyer, D., Steventon, B., Kim, M., Vallier, L., Gambardella, L. and Sinha, S.** (2019). A Novel Human Pluripotent Stem Cell-Derived Neural Crest Model of Treacher Collins Syndrome Shows Defects in Cell Death and Migration. *Stem Cells and Development* **28**, 81-100.
- Sharon, D., Sandberg, M. A., Caruso, R. C., Berson, E. L. and Dryja, T. P.** (2003). Shared mutations in NR2E3 in enhanced S-cone syndrome, Goldmann-Favre syndrome, and many cases of clumped pigmentary retinal degeneration. *Archives of Ophthalmology* **121**, 1316-1323.
- Simoës-Costa, M. and Bronner, M. E.** (2015). Establishing neural crest identity: a gene regulatory recipe. *Development* **142**, 242-257.
- Simon, E., Theze, N., Fedou, S., Thiebaud, P. and Faucheux, C.** (2017). Vestigial-like 3 is a novel Ets1 interacting partner and regulates trigeminal nerve formation and cranial neural crest migration. *Biology Open* **6**, 1528-1540.
- Singh, R., Brewer, M. K., Mashburn, C. B., Lou, D. Y., Bondada, V., Graham, B. and Geddes, J. W.** (2014). Calpain 5 Is Highly Expressed in the Central Nervous System (CNS), Carries Dual Nuclear Localization Signals, and Is Associated with Nuclear Promyelocytic Leukemia Protein Bodies. *Journal of Biological Chemistry* **289**, 19383-19394.
- Sjoberg, M., Vennstrom, B. and Forrest, D.** (1992). THYROID-HORMONE RECEPTORS IN CHICK RETINAL DEVELOPMENT - DIFFERENTIAL EXPRESSION OF MESSENGER-RNAS FOR ALPHA AND N-TERMINAL VARIANT BETA-RECEPTORS. *Development* **114**, 39-47.
- Sorimachi, H., Hata, S. and Ono, Y.** (2011). Calpain chronicle-an enzyme family under multidisciplinary characterization. *Proceedings of the Japan Academy Series B-Physical and Biological Sciences* **87**, 287-327.
- Squier, M. K. T., Sehnert, A. J., Sellins, K. S., Malkinson, A. M., Takano, E. and Cohen, J. J.** (1999). Calpain and calpastatin regulate neutrophil apoptosis. *Journal of Cellular Physiology* **178**, 311-319.
- Steel, K. P. and Barkway, C.** (1989). ANOTHER ROLE FOR MELANOCYTES - THEIR IMPORTANCE FOR NORMAL STRIA VASCULARIS DEVELOPMENT IN THE MAMMALIAN INNER-EAR. *Development* **107**, 453-463.

- Stenkamp, D. L.** (2007). Neurogenesis in the fish retina. *International Review of Cytology - a Survey of Cell Biology, Vol 259* **259**, 173-+.
- Stenkamp, D. L.** (2015). Development of the Vertebrate Eye and Retina. *Molecular Biology of Eye Disease* **134**, 397-414.
- Stenkamp, D. L. and Cameron, D. A.** (2002). Cellular pattern formation in the retina: retinal regeneration as a model system. *Molecular Vision* **8**, 280-293.
- Stenkamp, D. L., Gregory, J. K. and Adler, R.** (1993). RETINOID EFFECTS IN PURIFIED CULTURES OF CHICK-EMBRYO RETINA NEURONS AND PHOTORECEPTORS. *Investigative Ophthalmology & Visual Science* **34**, 2425-2436.
- Stenkamp, D. L., Stevens, C. B., Frey, R. A. and Kawamura, S.** (2014). Retinoic acid signaling regulates expression of the tandemly duplicated LWS1 and LWS2 genes in zebrafish. *Investigative Ophthalmology & Visual Science* **55**, 3.
- Stevens, C. B., Cameron, D. A. and Stenkamp, D. L.** (2011). Plasticity of photoreceptor-generating retinal progenitors revealed by prolonged retinoic acid exposure. *Bmc Developmental Biology* **11**, 25.
- Stewart, R. A., Arduini, B. L., Berghmans, S., George, R. E., Kanki, J. P., Henion, P. D. and Look, A. T.** (2006). Zebrafish foxd3 is selectively required for neural crest specification, migration and survival. *Developmental Biology* **292**, 174-188.
- Streichert, L. C., Birnbach, C. D. and Reh, T. A.** (1999). A diffusible factor from normal retinal cells promotes rod photoreceptor survival in an in vitro model of retinitis pigmentosa. *Journal of Neurobiology* **39**, 475-490.
- Streisinger, G., Walker, C., Dower, N., Knauber, D. and Singer, F.** (1981). PRODUCTION OF CLONES OF HOMOZYGOUS DIPLOID ZEBRA FISH (BRACHYDANIO-RERIO). *Nature* **291**, 293-296.
- Stuermer, C. A. O., Bastmeyer, M., Bahr, M., Strobel, G. and Paschke, K.** (1992). TRYING TO UNDERSTAND AXONAL REGENERATION IN THE CNS OF FISH. *Journal of Neurobiology* **23**, 537-550.
- Suzuki, K. and Sorimachi, H.** (1998). A novel aspect of calpain activation. *Febs Letters* **433**, 1-4.
- Suzuki, S. C., Bleckert, A., Williams, P. R., Takechi, M., Kawamura, S. and Wong, R. O. L.** (2013). Cone photoreceptor types in zebrafish are generated by symmetric terminal divisions of dedicated precursors. *Proceedings of the National Academy of Sciences of the United States of America* **110**, 15109-15114.

- Takahashi, K., Nuckolls, G. H., Takahashi, I., Nonaka, K., Nagata, M., Ikura, T., Slavkin, H. C. and Shum, L.** (2001). Msx2 is a repressor of chondrogenic differentiation in migratory cranial neural crest cells. *Developmental Dynamics* **222**, 252-262.
- Takke, C., Dornseifer, P., Von Weizsacker, E. and Campos-Ortega, J. A.** (1999). her4, a zebrafish homologue of the Drosophila neurogenic gene E(spl), is a target of NOTCH signalling. *Development* **126**, 1811-1821.
- Tamada, Y., Nakajima, E., Nakajima, T., Shearer, T. R. and Azuma, M.** (2005). Proteolysis of neuronal cytoskeletal proteins by calpain contributes to rat retinal cell death induced by hypoxia. *Brain Research* **1050**, 148-155.
- Tan, Y., Wu, C., De Veyra, T. and Greer, P. A.** (2006). Ubiquitous calpains promote both apoptosis and survival signals in response to different cell death stimuli. *Journal of Biological Chemistry* **281**, 17689-17698.
- Tang, Y. M., Forsyth, C. B., Farhadi, A., Rangan, J., Jakate, S., Shaikh, M., Banan, A., Fields, J. Z. and Keshavarzian, A.** (2009). Nitric Oxide-Mediated Intestinal Injury Is Required for Alcohol-Induced Gut Leakiness and Liver Damage. *Alcoholism-Clinical and Experimental Research* **33**, 1220-1230.
- Tappeiner, C., Gerber, S., Enzmann, V., Balmer, J., Jazwinska, A. and Tschopp, M.** (2012). Visual acuity and contrast sensitivity of adult zebrafish. *Frontiers in Zoology* **9**.
- Theveneau, E. and Mayor, R.** (2012a). Cadherins in collective cell migration of mesenchymal cells. *Current Opinion in Cell Biology* **24**, 677-684.
- Theveneau, E. and Mayor, R.** (2012b). Neural crest delamination and migration: From epithelium-to-mesenchyme transition to collective cell migration. *Developmental Biology* **366**, 34-54.
- Thisse, C., Thisse, B. and Postlethwait, J. H.** (1995). EXPRESSION OF SNAIL2, A 2ND MEMBER OF THE ZEBRAFISH SNAIL FAMILY, IN CEPHALIC MESENDODERM AND PRESUMPTIVE NEURAL CREST OF WILD-TYPE AND SPADETAIL MUTANT EMBRYOS. *Developmental Biology* **172**, 86-99.
- Thomas, J. L., Ranski, A. H., Morgan, G. W. and Thummel, R.** (2016). Reactive gliosis in the adult zebrafish retina. *Experimental Eye Research* **143**, 98-109.
- Tomita, K., Ishibashi, M., Nakahara, K., Ang, S. L., Nakanishi, S., Guillemot, F. and Kageyama, R.** (1996). Mammalian hairy and Enhancer of split homolog 1 regulates differentiation of retinal neurons and is essential for eye morphogenesis. *Neuron* **16**, 723-734.

- Trimarchi, J. M., Stadler, M. B. and Cepko, C. L.** (2008). Individual Retinal Progenitor Cells Display Extensive Heterogeneity of Gene Expression. *Plos One* **3**.
- Tsujikawa, M. and Malicki, J.** (2004). ovl is essential for differentiation and survival of vertebrate sensory neurons. *Investigative Ophthalmology & Visual Science* **45**, U382-U382.
- Tsung, P. K. and Lombardini, J. B.** (1985). IDENTIFICATION OF LOW-CA-2+ AND HIGH-CA-2+ REQUIRING NEUTRAL PROTEASES IN RAT RETINA. *Experimental Eye Research* **41**, 97-103.
- Turner, D. L. and Cepko, C. L.** (1987). A common progenitor for neurons and glia persists in rat retina late in development. *Nature* **328**, 131-136.
- Ungos, J. M., Karlstrom, R. O. and Raible, D. W.** (2003). Hedgehog signaling is directly required for the development of zebrafish dorsal root ganglia neurons. *Development* **130**, 5351-5362.
- Uribe, R. A. and Bronner, M. E.** (2015). Meis3 is required for neural crest invasion of the gut during zebrafish enteric nervous system development. *Molecular Biology of the Cell* **26**, 3728-3740.
- Uribe, R. A., Hong, S. S. and Bronner, M. E.** (2018). Retinoic acid temporally orchestrates colonization of the gut by vagal neural crest cells. *Developmental Biology* **433**, 17-32.
- Vancamp, P., Houbrechts, A. M. and Darras, V. M.** (2019). Insights from zebrafish deficiency models to understand the impact of local thyroid hormone regulator action on early development. *General and Comparative Endocrinology* **279**, 45-52.
- Velez, G., Sun, Y. J., Khan, S., Yang, J., Herrmann, J., Chemudupati, T., MacLaren, R. E., Gakhar, L., Wakatsuki, S., Bassuk, A. G., et al.** (2020). Structural Insights into the Unique Activation Mechanisms of a Non-classical Calpain and Its Disease-Causing Variants. *Cell Reports* **30**, 881-+.
- Vihtelic, T. S. and Hyde, D. R.** (2000a). Light-induced rod and cone cell death and regeneration in the adult albino zebrafish (*Danio rerio*) retina. *J Neurobiol.* **44**, 289-307.
- Vihtelic, T. S., Soverly, J. E., Kassen, S. C. and Hyde, D. R.** (2006). Retinal regional differences in photoreceptor cell death and regeneration in light-lesioned albino zebrafish. *Experimental Eye Research* **82**, 558-575.
- Viringipurampeer, I. A., Shan, X., Gregory-Evans, K., Zhang, J. P., Mohammadi, Z. and Gregory-Evans, C. Y.** (2014). Rip3 knockdown rescues photoreceptor cell death in blind pde6c zebrafish. *Cell Death and Differentiation* **21**, 665-675.

- Waghray, A., Wang, D. S., McKinsey, D., Hayes, R. L. and Wang, K. K. W.** (2004). Molecular cloning and characterization of rat and human calpain-5. *Biochemical and Biophysical Research Communications* **324**, 46-51.
- Wang, M. S., Davis, A. A., Culver, D. G., Wang, Q. B., Powers, J. C. and Glass, J. D.** (2004). Calpain inhibition protects against Taxol-induced sensory neuropathy. *Brain* **127**, 671-679.
- Wang, W. D., Melville, D. B., Montero-Balaguer, M., Hatzopoulos, A. K. and Knapik, E. W.** (2011). Tfp2a and Foxd3 regulate early steps in the development of the neural crest progenitor population. *Developmental Biology* **360**, 173-185.
- Wang, Y. B., Hersheson, J., Lopez, D., Hammer, M., Liu, Y., Lee, K. H., Pinto, V., Seinfeld, J., Wiethoff, S., Sun, J. D., et al.** (2016). Defects in the CAPN1 Gene Result in Alterations in Cerebellar Development and Cerebellar Ataxia in Mice and Humans. *Cell Reports* **16**, 79-91.
- Ward, A. C. and Lieschke, G. J.** (2002). The zebrafish as a model system for human disease. *Frontiers in Bioscience* **7**, D827-D833.
- Wen, W., Pillai-Kastoori, L., Wilson, S. G. and Morris, A. C.** (2015). Sox4 regulates choroid fissure closure by limiting Hedgehog signaling during ocular morphogenesis. *Developmental Biology* **399**, 139-153.
- Wert, K. J., Bassuk, A. G., Wu, W. H., Gakhar, L., Cogan, D., Mahajan, M., Wu, S., Yang, J., Lin, C. S., Tsang, S. H., et al.** (2015). CAPN5 mutation in hereditary uveitis: the R243L mutation increases calpain catalytic activity and triggers intraocular inflammation in a mouse model. *Human Molecular Genetics* **24**, 4584-4598.
- Wert, K. J., Skeie, J. M., Bassuk, A. G., Olivier, A. K., Tsang, S. H. and Mahajan, V. B.** (2014). Functional validation of a human CAPN5 exome variant by lentiviral transduction into mouse retina. *Human Molecular Genetics* **23**, 2665-2677.
- Westerfield M** (1995) *The Zebrafish Book: A guide for the Laboratory Use of Zebrafish (brachydanio rerio)*. University of Oregon Press, Eugene, OR.
- Wiedenheft, B., Sternberg, S. H. and Doudna, J. A.** (2012). RNA-guided genetic silencing systems in bacteria and archaea. *Nature* **482**, 331-338.
- Wilson, J. M., Bunte, R. M. and Carty, A. J.** (2009). Evaluation of Rapid Cooling and Tricaine Methanesulfonate (MS222) as Methods of Euthanasia in Zebrafish (*Danio rerio*). *Journal of the American Association for Laboratory Animal Science* **48**, 785-789.

- Wilson, S. G., Wen, W., Pillai-Kastoori, L. and Morris, A. C.** (2016). Tracking the fate of her4 expressing cells in the regenerating retina using her4:Kaede zebrafish. *Experimental Eye Research* **145**, 75-87.
- Wingrave, J. M., Schaecher, K. E., Sribnick, E. A., Wilford, G. G., Ray, S. K., Hazen-Martin, D. J., Hogan, E. L. and Banik, N. L.** (2003). Early induction of secondary injury factors causing activation of calpain and mitochondria-mediated neuronal apoptosis following spinal cord injury in rats. *Journal of Neuroscience Research* **73**, 95-104.
- Wolman, M. A., Sittaramane, V. K., Essner, J. J., Yost, H. J., Chandrasekhar, A. and Halloran, M. C.** (2008). Transient axonal glycoprotein-1 (TAG-1) and laminin-alpha 1 regulate dynamic growth cone behaviors and initial axon direction in vivo. *Neural Development* **3**.
- Won, Y. J., Ono, F. and Ikeda, S. R.** (2011). Identification and Modulation of Voltage-Gated Ca²⁺ Currents in Zebrafish Rohon-Beard Neurons. *Journal of Neurophysiology* **105**, 442-453.
- Wood, D. E. and Newcomb, E. W.** (1999). Caspase-dependent activation of calpain during drug-induced apoptosis. *Journal of Biological Chemistry* **274**, 8309-8315.
- Wu, Y. Q., Heilstedt, H. A., Bedell, J. A., May, K. M., Starkey, D. E., McPherson, J. D., Shapira, S. K. and Shaffer, L. G.** (1999). Molecular refinement of the 1p36 deletion syndrome reveals size diversity and a preponderance of maternally derived deletions. *Human Molecular Genetics* **8**, 313-321.
- Xie, B. B., Zhang, X. M., Hashimoto, T., Tien, A. H., Chen, A., Ge, J. and Yang, X. J.** (2014). Differentiation of Retinal Ganglion Cells and Photoreceptor Precursors from Mouse Induced Pluripotent Stem Cells Carrying an Atoh7/Math5 Lineage Reporter. *Plos One* **9**.
- Yoshimura, N., Tsukahara, I. and Murachi, T.** (1984). CALPAIN AND CALPASTATIN IN PORCINE RETINA - IDENTIFICATION AND ACTION ON MICROTUBULE-ASSOCIATED PROTEINS. *Biochemical Journal* **223**, 47-51.
- Yu, H. H. and Moens, C. B.** (2005). Semaphorin signaling guides cranial neural crest cell migration in zebrafish. *Developmental Biology* **280**, 373-385.
- Zupanc, G. K. H. and Sirbulescu, R. F.** (2011). Adult neurogenesis and neuronal regeneration in the central nervous system of teleost fish. *European Journal of Neuroscience* **34**, 917-929.

VITA

Cagney Elayna Coomer

Education

- 2006 – 2010 Virginia State University, Petersburg, Va., B.S. Biology
- 2011 – 2013 Bluegrass Community and Technical College, Lexington, Ky., AAS Biotechnology
- 2014 – 2020 University of Kentucky, Lexington, Ky., PhD Molecular Biology

Scholastic Honors

- 2015 – 2017 Lyman T. Johnson Graduate Fellowship recipient
- 2016 1st place, UAB NEURAL conference for oral and poster presentations
- 2016 Gordon Conference Carl Storm Travel Fellowship recipient
- 2016 UAB NEURAL Travel Fellowship recipient
- 2017 University of Kentucky Sullivan award recipient
- 2017 University of Kentucky Inclusive Excellence award
- 2018 3rd place, 4th Annual SOPS postdoc research symposium poster competition
- 2018 2nd place, UAB NEURAL conference oral presentation
- 2019 SDB Travel grant recipient
- 2019 Lyman T. Johnson Torch bearer award
- 2020 Inaugural SDB Trainee Science Communication award

Research publications

Coomer, C.E., Wilson, S.G., Titalii-Torres, K.F., Bills, J.D., Krueger, L.A., Petersen, R.A.,

Turnbaugh, E.M., Janesch, E.L., and Morris, A.C. (2019) "Her9/HES4 is required for retinal photoreceptor development, maintenance, and survival. BioRxiv [preprint]. doi:

<https://doi.org/10.1101/833301>

Coomer, C.E., Morris, A.C. (2018) Capn5 Expression in the Healthy and Regenerating Zebrafish Retina. IOVS. 59:3643-3654.

Cagney Elayna Coomer